Fire disturbance and functional dynamics of terrestrial ecosystems – A remote-sensing framework to analyze severity, recovery, and resilience

Bruno André Santos Marcos

Doctoral Program in Biodiversity, Genetics, and Evolution

Department of Biology

Faculty of Sciences, University of Porto

2021

Supervisor

João P. Honrado, Associate Professor, Faculty of Sciences, University of Porto

Co-supervisors

Domingo Alcaraz Segura, Associate Professor, Faculty of Sciences, University of Granada

Mário Cunha, Associate Professor, Faculty of Sciences, University of Porto

Foreword

In compliance with the no. 2 of article 4 of the General Regulation of the Third Cycles of the University of Porto, and with article 31 of the Decree-Law no. 74/2006 of 24 March, with the alteration introduced by the Decree-Law no. 230/2009 of 14 September, this thesis includes works already published or at the final stages of preparation to be submitted for publication in peer-review scientific journals, which were used and included in some of the chapters of this dissertation. Since these manuscripts result from collaborations with several co-authors, the candidate clarifies that, in all these works, he participated and contributed significantly in obtaining, analyzing, and discussing the results, as well as in the writing of the manuscripts.

This thesis was elaborated with the Research Center in Biodiversity and Genetic Resources – Research Network in the Research Network in Biodiversity and Evolutionary Biology, Associate Laboratory (CIBIO-InBIO) as the host institution, and supervised by Prof. João Pradinho Honrado (Faculty of Sciences and CIBIO-InBIO – University of Porto, Portugal), and co-supervised by Prof. Domingo Alcaraz Segura (Faculty of Sciences and IISTA – University of Granada, and CAESCG – University of Almería, Spain), and Prof. Mário Cunha (Faculty of Sciences and INESC-TEC – University of Porto, Portugal).

The candidate was financially supported by the National Foundation for Science and Technology (Fundação para a Ciência e Tecnologia – FCT, Portugal), through Ph.D. Studentship SFRH/BD/99469/2014, funded by the National Ministry of Science, Technology and Higher Education, through the Regional Operational Program North (POR-NORTE), and Portugal 2020.

Acknowledgements

As it might be expected, during my Ph.D., I have encountered many difficulties, of varied nature. Between moving house several times, going through a small surgery, and losing one of my greatest friends and dearest family members, facing such challenges would have not been – at all – possible without the help and support of others, to whom I would like to express my deepest gratitude.

First, I would like to thank my supervisor, **João Honrado**, for having received me in his research group all those years ago, and for all the support and contributions to my work since, both before and during the Ph.D. I would also like to thank **Domingo Alcaraz** and **Mário Cunha** for co-supervising this thesis, and for all the contributions towards its improvement.

My big thanks to the many people with which I have worked throughout the years. I would like to express my gratitude especially to all the former and current members of the **EcoChange** (formerly PRECOL, formerly BIOCON) research group within CIBIO, for all the (both scientific and non-scientific) discussions and conversations exchanged, which greatly contributed to my professional and personal growth. Particularly, I would like to thank my colleague and friend **João Gonçalves**, with whom I have started this academic journey almost twenty years ago, shared countless experiences, and learned immeasurably.

Finally, I would like to thank all my friends and family, for everything – especially my parents, **António** and **Olinda**, for their unconditional and eternal love and support. I would also like to acknowledge **Blok**, for having accompanied me for most of my adult life – and through many of its phases –, and for leaving such a positive and enduring mark on it – Thank you very much, and Goodbye.

Lastly, my biggest appreciation, as well as my infinite gratitude, goes to **Cristiana**, for – in addition to being the amazing person that she is –, being at my side through every single step of this journey, with admirable understanding and support. Without you, this would have never been possible!

Summary

Wildfires can pose a major threat to a wide range of social, economic, and environmental assets, modify the composition, structure, and functioning of ecosystems, and erode their resilience. There is therefore a growing need for more comprehensive sets of indicators to assess and monitor the impacts of wildfire disturbances and post-fire processes on ecosystems, based on **multiple dimensions of ecosystem functioning**, which is still lacking. To this end, remote sensing has been increasingly employed in fire-related applications, however usually without consistent frameworks that link ecological theory to remotely sensed observations, with the subsequent translation of spectral data into biologically meaningful and informative ecosystem variables. Such frameworks would allow for improved assessment and mapping of the multiple impacts of wildfire disturbances on ecosystems, and ecosystem responses and resilience to those disturbances. Hence, data-driven but theoretically grounded monitoring would represent a major asset for post-fire management and restoration, and risk prevention and governance.

The overarching goal of this thesis was to **improve the assessment and monitoring of wildfire disturbances**. This improvement was sought by proposing, developing, and showcasing a satellite-driven conceptual and experimental framework to evaluate the effects of wildfire disturbances on multiple key dimensions of the matter and energy fluxes on ecosystems and ecosystem responses to those disturbances. Overall, this thesis aimed to introduce the ecosystem functioning dimensions into fire ecology by clarifying and mainstreaming the links between ecological processes, fire disturbance, and remotely-sensed observations, in the pursuit of improving the comprehensiveness and cost-efficiency of monitoring systems. These goals were addressed throughout three studies where the following three research hypotheses were tackled using satellite image time-series of the long data record of the *Moderate Resolution Imaging Spectroradiometer* (MODIS) between 2000 and 2018 in the fire-prone region of northwestern Iberian Peninsula.

The first study addressed **Research Hypothesis 1** (H1) – *"The location, extension, and date of occurrence of wildfire disturbance events can be identified using indicators of multiple dimensions of ecosystem functioning, related to matter and energy exchanges, to enhance existing burned area maps and fill important gaps in fire databases"*. In this study, a generic conceptual and experimental framework was developed to compare, rank, and combine multiple remotely-sensed indicators of wildfire disturbances. As a result, the best

indicators to map annually burned areas and to estimate the dates of fire occurrence were selected. Multi-indicator consensuses improved the detection of wildfire disturbances in space and time and complemented preexisting fire databases by filling information gaps on the dates of fire occurrences. Indicators related to key aspects of ecosystem functioning – particularly the *Tasseled Cap* features of *Brightness*, *Greenness*, and *Wetness* (related to albedo, primary productivity, and vegetation water content, respectively) – performed the best. Overall, the results highlighted the advantage of adopting a multi-indicator consensus approach for mapping and detecting wildfire disturbances at a regional scale. This allowed profiting from multiple spectral indices that capture the Earth's surface dynamics through different electromagnetic wavelengths, informing on the multi-dimensional response of ecosystems to fire disturbance and contributing to filling information gaps in preexisting fire databases.

The second study partially addressed **Research Hypothesis 2** (H2) – *"The short-, medium-, and long-term effects of wildfires on ecosystem functioning, and ecosystem responses to those disturbances can be better estimated with the synergistic use of multiple indicators, enabling in-depth multi-dimensional and synoptic assessments of wildfire disturbance severity and post-fire recovery"*. In this study, a conceptual and experimental framework was developed, described, and showcased to support enhanced fire severity assessments, from short (i.e., the year of the fire) to medium term (i.e., up to the second year after the fire). A large set of descriptors – called *Ecosystem Functioning Attributes* (EFAs) – of the intra-annual dynamics of four essential dimensions of ecosystem functioning related to the carbon and water cycles, and the radiation and heat balances – i.e., primary productivity, vegetation water content, albedo, and sensible heat, respectively –, was compared at the regional scale. Assessment and ranking of the predictive importance of EFA deviations from the normal inter-annual variability allowed for the analysis of the main spatial and temporal patterns. The best performing EFAs were related to *quantity* metrics rather than to seasonality or timing metrics. Then, a parsimonious set of indicators was further used to analyze four individual burned patches. Important effects were observed for all four dimensions of ecosystem functioning, with different spatiotemporal patterns of wildfire severity. The results highlighted the importance of multi-dimensional approaches to analyze the effects of wildfire disturbances on multiple key aspects of ecosystem functioning at different timeframes.

Finally, the third and final study revisited H2 but also addressed **Research Hypothesis 3** (H3) – *"Indicators extracted from post-fire trajectories of remotely-sensed variables of ecosystem functioning allow for the identification and characterization of potential regime shifts after wildfires and, consequently, the assessment of (changes in)*

ecological resilience to those disturbances". This study developed, described, and showcased a conceptual and experimental framework for characterizing and classifying the resilience of ecosystems following wildfire disturbances. Satellite-derived indicators of the short-term and medium-to-long term responses to wildfire disturbances, across the same four dimensions addressed in the previous study, were used to assess fire severity and post-fire recovery and resilience for fires occurring in 2005. Post-fire effects were observed across all dimensions of ecosystem functioning, but particularly for those related to the removal of vegetation caused by wildfires. Post-fire trajectories were classified into main types of post-fire recovery and resilience, allowing for potential regime shifts to be identified in each of the four dimensions of ecosystem functioning. The overall strength-of-evidence for regime shifts in ecosystem functioning was evaluated based on a synthetic multi-dimensional indicator, which was showcased for six individual burned patches. This exercise highlighted key features of the underlying post-fire processes at different timeframes and ultimately upholding promising implications for post-fire ecosystem management.

Overall, the conceptual and experimental framework developed, implemented, and presented in this thesis allowed for successfully testing the above-mentioned research hypotheses and associated research goals. The proposed framework combines resilience theory and remote sensing of ecosystem functioning for an integrative assessment of wildfire patterns and impacts. Ultimately, this thesis contributed to the advancement of scientific knowledge in fire ecology, ecosystem functioning, and ecological resilience. In the future, the framework developed for this thesis could potentially be improved by capitalizing on a more diverse set of characteristics of remotely-sensed data in terms of spatial, temporal, and spectral resolutions, as well as the length of the historical archive available. Those improvements can be complemented with data collected in-field, and combined with further remotely-sensed data in consensus-based approaches or integrated for validation purposes. This thesis also opened numerous research and development pathways and challenges to be explored in the future, with promising developing technologies, resources, and methods presenting considerable potential. These pathways will enable further testing and improvement of the proposed framework integrating further dimensions, components, and temporal scales of wildfire effects on ecosystems, grounded on ecological theory and supported by remote sensing. Together with automated workflows and processing pipelines, the framework proposed in this thesis could be an invaluable asset to support the development of more ecologically-based fire data products, as well as web-based services, at regional, national, and even global scales.

Keywords

Wildfires, Fire Ecology, Post-fire trajectories, Ecosystem functioning, Indicators, Regime shifts, Satellite image time-series, MODIS, Iberian Peninsula.

Sumário (em Português)

Os **incêndios florestais** representam uma potencial ameaça a um largo conjunto de bens sociais, económicos e ambientais, podendo alterar a composição, estrutura e funcionamento dos ecossistemas, contribuir para a erosão da sua resiliência. Há, portanto, uma crescente necessidade de obter indicadores mais abrangentes para avaliar e monitorizar os impactes das perturbações por incêndio e os processos pós-fogo nos ecossistemas, baseados em **múltiplas dimensões do funcionamento dos ecossistemas**, os quais estão ainda em falta. Para este fim, a deteção remota tem sido cada vez mais utilizada em aplicações relacionadas com os incêndios florestais, embora normalmente sem estabelecer molduras (concetuais e experimentais) de análise que permitam ligar teoria ecológica a observações remotas, com a consequente tradução de índices espectrais em variáveis dos ecossistemas que tenham significado biológico e sejam informativas. Tais molduras de análise poderão permitir melhorar a avaliação e o mapeamento de múltiplos impactes das perturbações por incêndio nos ecossistemas e as respetivas respostas e resiliência. Neste sentido, uma monitorização guiada por dados, mas sólida do ponto de vista teórico, poderá representar um importante ativo para a gestão e restauro pós-fogo, bem como para a prevenção e governança do risco.

O objetivo global desta tese foi o **melhoramento da avaliação e da monitorização das perturbações por incêndio**. Para alcançar este objetivo, foi proposta, desenvolvida e demonstrada uma moldura concetual e experimental baseada em dados de satélite para avaliar os efeitos das perturbações por incêndio em múltiplas dimensões-chave dos fluxos de matéria e energia nos ecossistemas e respetivas respostas a essas perturbações. Globalmente, esta tese introduziu os conceitos de dimensões do funcionamento dos ecossistemas no campo da ecologia do fogo, procurando clarificar e integrar as ligações entre processos ecológicos, perturbação por fogo e observações por deteção remota, na busca pela melhoria da abrangência e da eficiência dos sistemas de monitorização. Para alcançar estes objetivos, as três hipóteses de investigação seguintes foram abordadas através de três estudos, onde foram utilizados dados do sensor de longo arquivo histórico *Moderate Resolution Imaging Spectroradiometer* (MODIS), entre 2000 e 2018, na região propícia a incêndios florestais do noroeste da Península Ibérica.

O primeiro estudo abordou a **Hipótese de Investigação 1** (H1) – *"A localização, extensão e data de ocorrência de eventos de perturbação por incêndio podem ser*

identificados com recurso a indicadores de múltiplas dimensões do funcionamento dos ecossistemas, relacionados com os fluxos de matéria e energia, para melhorar os mapas de áreas ardidas existentes e colmatar falhas importantes nas bases de dados de fogo". Neste estudo, foi desenvolvida uma moldura conceptual e experimental para a comparação, ordenação e combinação de múltiplos indicadores de perturbação por incêndios baseados em deteção remota. Como resultado, foram selecionados os melhores indicadores para mapear áreas ardidas anualmente e para estimar as respetivas datas de ocorrência. Consensos multi-indicador contribuíram para melhorar a deteção de perturbações por incêndio no espaço e no tempo e para complementar bases de dados pré-existentes colmatando falhas de informação nas datas de ocorrência. Indicadores relacionados com aspetos-chave do funcionamento dos ecossistemas – particularmente as variáveis *Tasseled Cap Brightness*, *Greenness* e *Wetness* (relacionados com o albedo, a produtividade primária e o teor de água da vegetação, respetivamente) – obtiveram um melhor desempenho. Globalmente, os resultados destacaram a vantagem em adotar abordagens de consenso multi-indicador para mapear e detetar perturbações por incêndio à escala regional, o que permitiu tirar partido de múltiplos índices espetrais que capturam as dinâmicas da superfície da Terra através de diferentes comprimentos de onda, fornecendo informação acerca da resposta multidimensional dos ecossistemas às perturbações por fogo e contribuindo para colmatar falhas de informação em bases de dados pré-existentes.

O segundo estudo abordou parcialmente a **Hipótese de Investigação 2** (H2) – *"É possível melhorar a estimativa dos efeitos a curto, médio e longo prazo dos incêndios florestais no funcionamento dos ecossistemas, bem como as respostas dos ecossistemas a essas perturbações, utilizando múltiplos indicadores sinergicamente, possibilitando avaliações multidimensionais e sinóticas aprofundadas da severidade dos incêndios e da recuperação pós-fogo"*. Neste estudo, foi desenvolvida, descrita e ilustrada uma moldura conceptual e experimental para suportar avaliações melhoradas da severidade dos incêndios, no curto (i.e., no ano do incêndio) e no médio (i.e., até ao segundo ano após o incêndio) prazo. Um largo conjunto de descritores – chamados de *Atributos do Funcionamento dos Ecossistemas* (EFAs) – das dinâmicas intra-anuais de quatro dimensões do funcionamento dos ecossistemas relacionados com os ciclos do carbono e da água e com os balanções radiativos e térmicos – i.e., produtividade primária, teor de água na vegetação, albedo e calor sensível –, for alvo de comparação à escala regional. A avaliação e ordenação da importância preditiva dos desvios dos EFAs à variabilidade intra-anual normal possibilitou a análise dos principais padrões espaciais e temporais. Os EFAs de quantidade foram aqueles que obtiveram melhor desempenho, em detrimento dos de

sazonalidade ou tempo. Seguidamente, um conjunto parcimonioso de indicadores foi utilizado para analisar quatro manchas ardidas individuais. Foram observados importantes efeitos em todas as quatro dimensões do funcionamento dos ecossistemas, associados a diferentes padrões espácio-temporais de severidade dos incêndios. Os resultados permitiram destacar a importância de abordagens multidimensionais para analisar os efeitos das perturbações por incêndio florestal em múltiplos aspetos-chave do funcionamento dos ecossistemas em diferentes períodos.

Por fim, o terceiro e último estudo revisitou a H2, mas também abordou a **Hipótese de Investigação 3** (H3) – *"Indicadores extraídos de trajetórias pós-fogo de variáveis do funcionamento dos ecossistemas, obtidas por deteção remota, possibilitam a identificação e a caracterização de potenciais alterações de regime após incêndios florestais e, consequentemente, a avaliação da (ou de alterações na) resiliência ecológica face a essas perturbações"*. Este estudo propôs, descreveu e ilustrou uma moldura concetual e experimental para a caraterizar e classificar a resiliência dos ecossistemas após perturbações por incêndios florestais. Foram utilizados indicadores das respostas a perturbações por incêndio a curto e médio prazo, derivados de dados de satélite, para as mesmas quatro dimensões abordadas no estudo anterior, no sentido de avaliar a severidade dos incêndios e a recuperação e resiliência pós-fogo face a incêndios florestais ocorridos em 2005. Foram também observados efeitos em todas as quatro dimensões do funcionamento dos ecossistemas, particularmente os que estão relacionados com a remoção de vegetação causada pelos incêndios. As trajetórias pós-fogo foram classificadas em tipos principais de recuperação e resiliência pós-fogo, o que permitiu a identificação de potenciais alterações de regime, para cada uma das quatro dimensões do funcionamento dos ecossistemas. Foi ainda avaliada a força-de-evidência global para alterações no regime do funcionamento dos ecossistemas, baseada num indicador multidimensional sintético, o qual foi ilustrado para seis manchas ardidas individuais. Este exercício permitiu destacar as principais características dos processos pós-fogo subjacentes, em diferentes períodos, evidenciando, em última análise, implicações promissoras para a gestão pós-fogo dos ecossistemas.

No geral, a moldura concetual e experimental que foi desenvolvida, implementada e apresentada nesta tese permitiu testar com sucesso as hipóteses e os objetivos de investigação supramencionados. A moldura de análise proposta combina teoria da resiliência com deteção remota do funcionamento dos ecossistemas, para uma avaliação integrativa dos padrões e impactes dos incêndios florestais. Em última análise, esta tese contribuiu para progresso do conhecimento científico nas áreas da ecologia do fogo, funcionamento dos ecossistemas resiliência ecológica. No futuro, a moldura de análise

desenvolvida no âmbito desta tese poderá vir a ser melhorada, capitalizando um conjunto diverso de características de dados de deteção remota, ao nível quer das resoluções espaciais, temporais e espetrais, quer da duração total dos arquivos históricos disponíveis. Estas melhorias poderão vir a ser complementadas por dados recolhidos em campo e combinados com dados adicionais de deteção remota em abordagens baseadas em consensos, ou integrados para fins de validação. Esta tese apontou, também, numerosos caminhos e desafios de investigação e desenvolvimento possíveis, com tecnologias em desenvolvimento, recursos e métodos promissores mostrando um potencial considerável. Estes caminhos poderão vir a possibilitar a realização de novos testes e melhorias à moldura de análise proposta, integrando dimensões, componentes e escalas temporais adicionais dos efeitos dos incêndios florestais nos ecossistemas, enraizados em teoria ecológica e suportados por deteção remota. Juntamente com fluxos de trabalho automatizados e cadeias de processamento, a moldura de análise proposta nesta tese poderá vir a constituir um ativo valioso no suporte ao desenvolvimento de produtos de dados de fogo mais baseados em conhecimento ecológico, bem como de serviços baseados na rede, a escalas regionais, nacionais ou até mesmo globais.

Palavras-chave

Incêndios, Ecologia do Fogo, Trajetórias pós-incêndio, Funcionamento dos Ecossistemas, Indicadores, Alterações de regime, Séries temporais de imagens de satélite, MODIS, Península Ibérica.

Table of contents

Foreword ..... **iii**

Acknowledgements ..... **v**

Summary ..... **vii**

Keywords x

Sumário (em Português) ..... **xi**

Palavras-chave xiv

Table of contents ..... **xv**

List of figures ..... **xxi**

List of supplementary figures ..... **xxvii**

List of tables ..... **xxix**

List of supplementary tables ..... **xxxiii**

List of abbreviations ..... **xxxv**

CHAPTER 1. General introduction **1**

1.1. The role of fire in terrestrial ecosystems **3**

1.1.1. Fire on an intrinsically flammable planet 3

The nature of (wild)fire *3*

Fire as an evolutionary driver *4*

1.1.2. The worldwide wildfire problem 5

Fire as a useful but unreliable tool *5*

The pyric transition *6*

1.1.3. The impacts and costs of wildfires 8

Ecological impacts *8*

Impacts on human assets *9*

1.2. Concepts and methods for wildfire disturbance assessment **11**

1.2.1. The science of wildfires 11

Wildfire events *11*

Fire intensity and severity *11*

Fire regimes *12*

1.2.2. Wildfires and the functioning of ecosystems 14

The multi-dimensional concept of biodiversity *14*
The ecosystem functioning aspect of biodiversity *15*
Ecosystem functioning and wildfire disturbances *16*
1.2.3. Remote sensing of wildfires and ecosystem functioning 17
Remotely sensed Earth observations *17*
Remote sensing and the electromagnetic spectrum *18*
Characteristics and advantages of remotely sensed images *20*
Remote sensing applications to wildfire science *21*
The ecosystem functioning approach to wildfire assessment *22*
1.3. Research goals and thesis structure 24
1.3.1. Research goals and hypotheses 24
Motivation *24*
Overarching research goals *25*
Research hypotheses *25*
1.3.2. Thesis structure 26
References 28

CHAPTER 2. Improving the detection of wildfire disturbances 45
Disclaimer 47
Abstract 49
Keywords 49
2.1. Introduction 50
2.2. Material and Methods 53
2.2.1. Study area and data description 53
Study area *53*
Spectral variables *54*
Reference fire datasets *54*
2.2.2. Methodology 56
Detection of wildfire disturbances *56*
Evaluation of indicators' performance *57*
2.3. Results and Discussion 59
2.3.1. Burned area mapping performance 59
2.3.2. Temporal estimates of wildfire disturbances 61
2.3.3. Complementing fire databases gaps 64
2.4. Conclusions 68
References 69
Supplementary material 75

CHAPTER 3. Expanding the assessment of wildfire disturbance severity 77
Disclaimer 79
Abstract 81
Keywords 81
3.1. Introduction 82
3.2. Materials and Methods 85
3.2.1. Generic framework 85
General workflow 85
Step 1 – Satellite time-series 85
Step 2 – Extraction of EFAs 86
Step 3 – Computation of EFA anomalies 86
Step 4 – EFA ranking and selection procedures 87
Step 5 – Translation into indicators of wildfire disturbance severity 88
3.2.2. Test case 88
Study area 88
Satellite data preprocessing 91
EFA anomalies computation 92
Ranking and selection of EFAs 94
Analysis of indicators of wildfire disturbance severity 95
3.3. Results 97
3.3.1. EFA ranking 97
3.3.2. Analysis of effects 98
3.3.3. Main patterns in EFA anomalies 99
3.3.4. Multi-dimensional assessment of wildfire disturbance severity 100
3.4. Discussion 103
3.4.1. Fire severity patterns in the NW Iberian Peninsula 103
Effects of wildfires across dimensions and components 103
Temporal effects of wildfires 104
General patterns 105
3.4.2. General considerations about the proposed framework 106
Satellite image time-series 106
Additional data sources 107
Applicability and future directions 107
3.5. Conclusions 109
References 110
Supplementary material 120

CHAPTER 4. Characterizing post-fire recovery and resilience 127
Disclaimer 129
Abstract 131
Keywords 131
4.1. Introduction 132
4.2. Materials and Methods 136
4.2.1. Generic framework 136
General workflow 136
Step 1 – Collect and preprocess satellite image time-series 136
Step 2 – Decompose time-series 137
Step 3 – Characterize post-fire resistance and recovery using indicators extracted from post-fire trajectories 138
Step 4 – Classify resilience to wildfire disturbances and identify potential regime shifts 140
4.2.2. Test case 141
Study area 141
Satellite data collection and preprocessing 142
Time-series decomposition and normalization 143
Characterization of post-fire trajectories 144
Identification of potential regime shifts 144
4.3. Results 146
4.3.1. General patterns of post-fire indicators 146
Statistical distributions 146
Pairwise correlations 147
4.3.2. Classifications of post-fire resilience 148
Main regional-scale patterns 148
Patterns in individual burned areas 150
4.4. Discussion 153
4.4.1. Patterns of resilience to wildfire disturbances in NW Iberian Peninsula 153
Primary productivity 153
Vegetation water content 155
Albedo 156
Sensible heat 157
General patterns across dimensions 157
4.4.2. General considerations about the proposed framework 159
Applicability 159

Future improvements *160*
4.5. Conclusions **162**
References **163**
Supplementary material **178**
CHAPTER 5. General discussion and conclusions **179**
Preamble **181**
5.1. Synthesis: a framework for the multi-dimensional assessment of wildfire disturbances **182**
5.1.1. Rationale 182
5.1.2. Implementation 183
Theoretical foundations: the multi-dimensionality of ecosystem functioning *183*
Input data: satellite image time-series *184*
Test case: regional-scale study area *185*
Technical implementation: open code-based workflows *185*
5.1.3. Summary of main findings and contributions 186
Improving the detection of wildfire disturbances *186*
Expanding the assessment of wildfire disturbance severity *187*
Characterizing post-fire recovery and resilience *188*
Post-fire assessments at multiple timeframes *189*
5.2. General conclusions and outlook **190**
5.2.1. General concluding remarks 190
Wildfire occurrence detection and severity assessment *190*
Post-fire recovery and resilience evaluation and monitoring *190*
Multi-dimensional and multi-timeframe approach *191*
Cost-efficiency and open principles *192*
5.2.2. Future directions 192
Additional input satellite data *192*
Other types of input data and validation *193*
Methodological improvements and dissemination of outputs *195*
Applications and contributions at the global scale *196*
References **197**
Appendix **209**
About the Author **211**
Biosketch 211
Selected works 212

List of figures

Figure 1.1. Dominant factors that influence fire at different scales: a flame, a single wildfire, and a fire regime. This is an extension of the traditional *fire triangle* concept, here including broad scales of space and time, the feedbacks that fire has on the controls themselves (small loops), as well as feedbacks between processes at different scales (arrows). [source: Moritz *et al.* 2005] 3

Figure 1.2. Qualitative schematic of global fire activity through time, based on the pre-Quaternary distribution of charcoal, Quaternary and Holocene charcoal records, and modern satellite observations, concerning the percentage of atmospheric O_2 content, parts per million (ppm) of CO_2, the appearance of certain vegetation types, and the presence of the genus Homo. Dotted lines indicate periods of uncertainty. [source: Bowman *et al.* 2009] 4

Figure 1.3. Summary of the available historical sources and palaeoecological proxies to reconstruct fire regimes, spanning the period from the advent of fire on Earth in deep time to the modern industrial period characterized by fossil fuel combustion. The spatial and temporal resolution of all these approaches varies and decays with increasing time depth, constraining our understanding of fire regimes, especially before the Industrial Revolution. [source: Bowman *et al.* 2011] 7

Figure 1.4. The six components of individual fire events and environmental factors controlling the properties of each component to defining the fire type. Ignition sources (lightning, anthropogenic) may affect the properties of each component rather than being a component itself. The fire regime arises from repeated patterns over time of the properties of the components for each fire. For a certain vegetation structure under a given climate, the fire regime is relatively predictable (as indicated by the circles) and selects for an adapted group of plants, microflora, and associated fauna. [source: He *et al.* 2019] 13

Figure 1.5. A diagrammatic representation of the hierarchy of biodiversity, composed of compositional, structural, and functional aspects of biodiversity, each encompassing multiple levels of organization. [adapted from Noss 1990].....15

Figure 1.6. The electromagnetic spectrum, which is divided into regions based on wavelengths, ranging from the very short wavelengths of the gamma-ray region to the long wavelengths of the radio region. [source: Purkis and Klemas 2011] 18

Figure 1.7. Illustration of the solar spectrum expressed in terms of energy per unit wavelength at the top of the Earth's atmosphere as compared with the black body curve for an emitter at 5800 K, together with the corresponding total and direct radiation received on a horizontal surface for typical clear-sky conditions. Also shown are the main absorption bands due to O_3, O_2, water vapor, and carbon dioxide. [source: Jones and Vaughan 2010] 19

Figure 1.8. Illustration of the main phases of wildfire management, with the term "crisis" referring to the wildfire event, from ignition to extinction. [source: Faour *et al.* 2004] 21

Figure 2.1. The study area (bottom), in the context of southern Europe (top), with a representation of fire occurrences in the decade of 2001–2010 (dots), which was extracted from the *European Forest Fire Information System* (EFFIS). .. 53

Figure 2.2. Dot chart representing the yearly burned area mapping accuracy measures for 2001–2016, for each one of the indicators used, as well as the MODIS burned area products MCD45 and MCD64 (as "mcd45_v51" and "mcd64_v6", respectively), compared to the national fire database. Bootstrapped estimates for *Kappa* are shown with their respective confidence intervals. 59

Figure 2.3. Temporal accuracies (a) and delays (i.e., errors) (b) of the estimates of wildfire occurrence date, compared to the Portuguese national fire database. The horizontal lines mark especially remarkable values for the mean absolute errors: 1 (dots), and 2 (dashes). Besides the estimates for the indicators, the comparison of the dates given by the MODIS Burned Area products MCD45 and MCD64, in comparison with the national database, is shown as "mcd45v51" and "mcd64v6", respectively. Additional information such as sample sizes is presented in **Table 2.3**. 62

Figure 2.4. Density distributions of dates from all the five datasets compared (i.e., reference – National fire DB, MCD45 and MCD64, and date estimates from the *Median* and *Best* indicators). For comparability purposes, only the dates available for the same polygons as the ones with date information on the national fire database were plotted. 65

Figure 2.5. Percentage of burned area polygons of the Portuguese national fire database (with an area above 100 ha) for which each indicator was considered the *best* (i.e., the top-ranked) indicator. For more information, including sample sizes, see **Table 2.4**. 65

Figure 3.1. General workflow of the proposed approach to assess wildfire disturbance severity using indicators based on Ecosystem Functioning Attributes (EFAs) derived from satellite image time-series (SITS). TCTB: Tasseled Cap Transformation Brightness feature; TCTG: Tasseled Cap Transformation Greenness feature; TCTW: Tasseled Cap Transformation Wetness feature; and LST: Land Surface Temperature.....85

Figure 3.2. The study area for the illustrative test case, with: (a) location of the overall study area, for regional-scale analyses, within the Iberian Peninsula; (b) size distribution of all fires; (c) distribution of the area burned, by day-of-the-year (DOY); and (d) location of the four individual burned patches selected for local-scale analyses (labels A–D), overlapped with the number of fires occurred. For these figures, all wildfires with an area > 100 ha which occurred between 2000 and 2018 (according to the MODIS MCD64A1 Burned Areas product) were considered. 89

Figure 3.3. Distributions of variable importance scores obtained from Random Forest models, to assess the effects of wildfire disturbances on four dimensions of ecosystem functioning: Primary productivity ("Productivity"), vegetation water content ("Water"), "Albedo", and Sensible heat ("Heat"), in the same year as the respective fire ("year 0"), and the two years after ("year +1" and "year +2"), for each of the three components considered: *quantity* (left); *seasonality* (center); and *timing* (right). (Note that the scale of the y-axis is logarithmic.) 98

Figure 3.4. Distributions of the anomalies of the 12 selected EFAs, in the same year as the respective fire (*year 0*), and the two years after (*year +1* and *year +2*), for each of the three components considered: (a) *quantity*; (b) *seasonality*; and (c) *timing*. The specific intra-annual metrics selected for each of the four dimensions of ecosystem functioning considered were the following: Primary productivity ("Productivity") – *Tasseled Cap Transformation* (TCT) *Greenness* feature minimum value (TCTG-min), standard deviation (TCTG-std), and time-of-the-year of the minimum value (TCTG-tmn); Vegetation water content ("Water") – TCT *Wetness* feature average value (TCTW-avg), standard deviation (TCTW-std), and time-of-the-year of the minimum value (TCTW-tmn); "Albedo" – TCT

Brightness feature average value (TCTB-avg), standard deviation (TCTB-std), and time-of-the-year of the maximum value (TCTB-tmx); and Sensible heat ("Heat") – *Land Surface Temperature* (LST) maximum value (LST-max), standard deviation (LST-std), and time-of-the-year of the maximum value (LST-tmx). 100

Figure 3.5. Profiles of wildfire disturbance severity on the four dimensions of ecosystem functioning: primary productivity ("Productivity"), vegetation water content ("Water"), "Albedo", and sensible heat ("Heat"), at short-to-medium term (i.e., between years 0 and +2 after the fire event), for four individual burned areas (letters A–D; see **Figure 3.2** for their location within the study area). Dots connected by thick lines represent median values across all pixels of each individual burned area, while shaded areas of the corresponding color represent ±0.5 × median absolute deviation. Values for the *Heat* dimension are scaled by a factor of 0.005, for visual comparability purposes. 101

Figure 3.6. Maps of wildfire severity on primary productivity ("Productivity"), vegetation water content ("Water"), "Albedo", and sensible heat ("Heat"), at short-to-medium term (i.e., between years 0 and +2 after the fire event), for four individual burned areas (letters A–D), based on indicators derived from inter-annual anomalies in quantity EFAs extracted from satellite image time-series. 102

Figure 4.1. General workflow of the proposed framework for characterizing and classifying post-fire trajectories of satellite image time-series related with the four key dimensions of ecosystem functioning of *primary productivity*, *vegetation water content*, *albedo*, and *sensible heat*, according to different attributes of their resilience (resistance and recovery) to wildfire disturbances. 136

Figure 4.2. Illustration of the indicators of post-fire resilience extracted from satellite-derived trajectories, used in this study. "S95" corresponds to the difference between the pre-fire median and the 95% percentile of the seasonally-adjusted values in the first moving window after the date of the wildfire event. "I1p", "RRp", and "REp" represent the post-fire points of: *inflection* in the trend component of the time-series, *return-to-reference*, and *return-to-equilibrium*, respectively. "I1T", "RRT", and "RET" represent the amount of time between the date of the fire occurrence and the dates of the I1p, RRp, and REp, respectively. 139

Figure 4.3. Illustration of the classification of post-fire recovery and resilience based on the *Time to Return-to-Reference* (RRT) and *Time to Return-to-Equilibrium* (RET)

indicators, which measure the duration of the periods between the date of the wildfire event and the date in which the post-fire trajectory crosses the pre-fire reference interval (i.e., the *Return-to-Reference* point, RRp), and the date when equilibrium is achieved (i.e., the *Return-to-Equilibrium* point, REp). 140

Figure 4.4. The burned areas analyzed in this study: (a) burned patches of fires that occurred in 2005, with the corresponding month of occurrence (letters A–F); (b) geographical context within the Iberian Peninsula; and (c) summary table of environmental characteristics of the six individual burned areas (letters A–F). 141

Figure 4.5. Distributions of the four MODIS-derived indicators extracted from post-fire trajectories, represented in combined box-violin plots, for all areas burned in 2005 (identified by the MODIS burned area product), in NW Iberian Peninsula, for each of the four dimensions of ecosystem functioning (i.e., primary productivity, vegetation water content, albedo, and sensible heat). (a) the S95 *fire severity/resistance* indicator, obtained as the difference between the pre-fire median and the 95% percentile of the seasonally adjusted time-series values within the first moving window immediately after a fire (note that the values for the *Heat* dimension presented are scaled by a factor of 0.01, for visual comparability purposes); (b) the *Time to Inflection* (I1T) indicator of *short-term recovery speed*, obtained as the duration of the period between the date of the fire event and the date of the first inflection in the trend component; (c) the *Time to Return-to-Reference* (RRT) indicator of *medium-to-long-term recovery and resilience*, obtained as the duration of the period between the date of the fire event and the date when the values of the trend component achieve the pre-fire reference interval; and (d) the *Time to Return-to-Equilibrium* (RET) indicator of *long-term recovery and resilience*, obtained as the duration of the period between the date of the fire event and the date when the trend component achieves equilibrium or a stable state. 147

Figure 4.6. Relative frequencies of the obtained classes of long-term post-fire recovery, for each of the four dimensions of ecosystem functioning considered (i.e., primary productivity, vegetation water content, albedo, and sensible heat), across all patches burned in 2005 in NW Iberian Peninsula, using satellite image time-series between 2000 and 2018. Numbers in bold correspond to percentages above 1%. 149

Figure 4.7. Maps of post-fire recovery and resilience classifications, for each of the four dimensions of ecosystem functioning – i.e., primary productivity (*Productivity*), vegetation water content (*Water*), *Albedo*, and sensible heat (*Heat*) – considered for the six selected individual burned areas (A–F). 151

Figure 4.8. Maps of the *Strength-of-Evidence* (SoE) of regime shifts, across the four dimensions of ecosystem functioning considered (i.e., primary productivity, vegetation water content, albedo, and sensible heat), for the six selected individual burned areas (A–F). 152

List of supplementary figures

Figure S3.1. Distributions of the variable importance scores of all individual predictive variables, extracted from *Random Forest* models for all 100 random samples. 120

Figure S3.2. Partial dependence plots of the 36 predictive variables of the *Random Forest* models, extracted from the 12 EFAs selected for regional-scale analyses...121

Figure S3.3. Distributions of the reference values (i.e. inter-annual median of values from unburned years) of the selected EFAs of *quantity* (a), *seasonality* (b), and *timing* (c), for pixels with zero (n_0 = 279,962), one (n_1 = 49,384), two (n_2 = 12,714), and three or more (n_{3+} = 3581) fires identified by the MODIS burned areas product, for the period of 2000–2018, in the study area.....123

Figure S3.4. Heatmap summarizing the maximum *Spearman* rank pairwise correlations between the 12 selected metrics.....124

Figure S3.5. Maps of local *Spearman* rank correlations across the selected wildfire severity indicators, at short-to-medium term (i.e. between years 0 and +2 after the fire event), for four individual burned areas (letters A–D; see Figure 2 for their location within the study area). 125

Figure S4.1. Examples of pixel-wise post-fire trajectory profiles (a–e), each corresponding to one of the classes of post-fire recovery and resilience obtained: *(not detected)* (a), *No equilibrium* (b), *Under-recovery* (c), *Return to pre-fire* (d), and *Over-recovery* (e); as well as the respective legend (f). 178

List of tables

Table 2.1. List of spectral indices used in this study to derive wildfire disturbance indicators. The b1, b2, b3, b4, b5, b6, and b7 correspond to MODIS bands 1–7, with bandwidth ranges at 620–670 nm, 841–876 nm, 459–479 nm, 545–565 nm, 1230–1250 nm, 1628–1652 nm, and 2105–2155 nm, respectively. 55

Table 2.2. Performance of burned area mapping, on an annual basis (2001–2016), for the selected indicators, compared to the Portuguese national fire polygons database. MODIS burned area products MCD45 and MCD64 were also compared, and their performance results are also presented (as “mcd45_v1” and “mcd64_v6”, respectively). Note that indicators here are presented with lower case, to denote the difference between each indicator and the index, indices, or product on which it was based (indicator names with underscore were based on ratios, as described in the text). Both estimates for Kappas and their respective confidence intervals (CI) were obtained by bootstrapping with 10,000 repetitions. 60

Table 2.3. Performance statistics of temporal delays, compared to the national reference dataset. The values are expressed in the number of 8-day composites, as this is the maximum precision for wildfire date estimates that the input data allows. The indicators that were corrected for a systematic lag of one 8-day composite are denoted with the suffix “_1”. Results for the MODIS Burned Area products MCD45 and MCD64 area also given here, as “mcd45v51” and “mcd64v6”, respectively.....63

Table 2.4. Results from final extraction of fire occurrence dates, using the best-ranked indicator for each pixel, for all the burned area polygons of the national fire database above 100 ha (i.e., *big fires*). 66

Table 3.1. Summary of baseline environmental characteristics of the overall study area for regional-scale analyses (NW-IP), as well as the four selected burned patches selected for local-scale analyses (A–D). Elevation was extracted from *MERIT DEM* (Yamazaki *et al.* 2017); climate variables were extracted from the *CHELSA Bioclim* dataset (Karger *et al.* 2017); the percentages of land-cover

classes were extracted from *CORINE Land Cover* (CLC) 2000 (European Environment Agency 2020). 90

Table 3.2. MODIS-specific coefficients to calculate the tasseled cap transformation (TCT) features of *Brightness*, *Greenness*, and *Wetness*. These features result from a rigid rotation of principal component axes, which are aligned with the biophysical parameters of albedo, the amount of photosynthetically active vegetation, and soil moisture, respectively (Lobser and Cohen 2007). 92

Table 3.3. List of metrics extracted from each of the four satellite image time-series used in this study (i.e., Land Surface Temperature, and the Tasseled Cap Transformation features of *Brightness*, *Greenness*, and *Wetness*); as well as the number of predictive variables for models, extracted from each one. 93

Table 3.4. List of selected EFAs, with the corresponding effects categories, based on Cohen's *d* effect size statistic. The number of arrows in the *Effect category* columns symbolizes the magnitude of the effect size, with $|d| < 0.2$ *negligible*, $|d| < 0.5$ *small*, $|d| < 0.8$ *medium*, otherwise *large*. The direction and color of the arrows symbolize the sign of the effect size, with ascending arrows depicting positive (non-*negligible*) effect sizes while descending arrows depict negative (non-*negligible*) effect sizes (*negligible* effects are symbolized by a horizontal dash). 99

Table 4.1. MODIS-specific coefficients used to calculate the *Tasseled Cap Transformation* (TCT) features of *Brightness*, *Greenness*, and *Wetness*, which result from a rotation of principal component axes so that these are aligned with the biophysical parameters of albedo, amount of photosynthetically active vegetation, and soil/vegetation moisture, respectively (Lobser and Cohen 2007). 143

Table 4.2. Pairwise correlations between the indicators proposed in this study, for complete pairwise observations (maximum $n = 13{,}751$). Numbers in bold highlight values of Spearman rank correlation of $|\rho| > 0.50$. 148

Table 4.3. Pairwise agreement between the classifications of post-fire recovery and resilience, obtained for each of the four dimensions of ecosystem functioning considered (i.e., primary productivity, vegetation water content, albedo, and sensible heat), across all patches burned in 2005 in NW Iberian Peninsula. 149

Table 5.1. Some of the current and upcoming platform-sensor systems that could potentially be used in the future for post-fire monitoring. "MODIS" = Moderate Resolution Imaging Spectroradiometer; "ASTER" = Advanced Spaceborne Thermal

Emission and Reflection Radiometer; “VIIRS” = Visible Infrared Imaging Radiometer Suite; “S-NPP” = Suomi-National Polar-orbiting Partnership; “OLI” = Operational Land Imager; “TIRS” = Thermal InfraRed Sensor; “C-SAR” = C-band Synthetic-Aperture Radar; “MSI” = Multi-Spectral Instrument; “AHI” = Advanced Himawari Imager; “SLSTR” = Sea and Land Surface Temperature Radiometer; “PRISMA” = Precursore IperSpectrale della Missione Applicativa; “HSI” = Hyperspectral Imager; “EnMAP” = Environmental Mapping and Analysis; “FCI” = Flexible Combined Imager; and “MTG” = Meteosat Third Generation.....194

List of supplementary tables

Table S2.1. Fire statistics for the study area, extracted from the Portuguese national fire polygons database. "*w/date*" = fire polygons with information of date of occurrence. 75

Table S2.2. Dataset inter–comparisons for the date of occurrence of wildfire events, compared with the national fire database and MODIS fire products. 76

Table S3.1. Summary table of results for *Random Forest* models between EFA anomalies and *burned* vs. *unburned* areas, including *median variable importance score*, *rank*, *correlation*, and *effect size*, for each of the 12 EFAs selected for regional-scale analyses. 122

Table S4.1. Percentages of complete pairwise observations (maximum *n* = 13,751) for the indicators proposed in this study. 178

List of abbreviations

AF	Active fires
AHI	Advanced Himawari Imager
ASTER	Advanced Spaceborne Thermal Emission and Reflection Radiometer
AUC	Area under the curve
avg	Average
a.s.l.	Above sea level
b1–7	Band 1–7
BA	Burned areas
BAcc	Balanced accuracy
BFAST	Breaks For Additive Season and Trend
BRDF	Bidirectional reflectance distribution function
CBI	Composite Burn Index
CI	Confidence interval
CHELSA Bioclim	Climatologies at high resolution for the Earth's land surface areas – bioclimatic variables
CLC	CORINE land cover
CORINE	Co-ORdinated INformation on the Environment
cos	Cosine, a trigonometric operator
C-SAR	C-band Synthetic Aperture Radar
DB	Database
DEM	Digital elevation model
DOI	Digital object identifier
DOY	Day of the year
EBV	Essential Biodiversity Variable
ECV	Essential Climate Variable
EFFIS	European Forest Fire Information System
EFA	Ecosystem Functioning (or Functional) Attribute
EFT	Ecosystem Functioning (or Functional) Type
EnMAP	Environmental Mapping and Analysis

EOS	Earth Observation Satellites
EVI	Enhanced Vegetation Index
EVI2	Two-band Enhanced Vegetation Index
EU	European Union
FCI	Flexible Combined Imager
FOSS	Free and Open Source Software
GDAL	Geospatial Data Abstraction Layer
GEE	Google Earth Engine
GeoCBI	Geometrically structured Composite Burn Index
GEO BON	Group on Earth Observations Biodiversity Observation Network
GCOS	Global Climate Observation System
GeoTIFF	Georeferenced tag image file format
H1–H3	Research Hypothesis 1–3
ha	Hectare, a unit of area
HIS	Hyperspectral Imager
I1p	Inflection point
I1T	Time to Inflection indicator
ICNF	Instituto de Conservação da Natureza e Florestas
IQR	Interquartile range
K	Kelvin, a unit of temperature
km	Kilometer, a unit of length
L3	Level 3 satellite product
LGOCV	Leave-group-out cross-validation
LiDAR	Light detection and ranging
LOESS	Local (polynomial) regrESSion
LP DAAC	Land Processes Distributed Active Archive Center
LST	Land Surface Temperature
LSWI	Land Surface Water Index
m	Meter, a unit of length
MAD, mad	Median absolute deviation
MAE	Mean absolute error
max	Maximum value
MB	Mean bias

MCC	Multi-class Matthews correlation coefficient
MDAE	Median absolute error
MDB	Median bias
MDN, mdn	Median
MERIT DEM	Multi-Error-Removed Improved-Terrain DEM
MGDI	MODIS Global Disturbance Index
Mha	Million hectares (i.e., 10^{10} m^2), a unit of area
min	Minimum value
MODIS	Moderate Resolution Imaging Spectroradiometer
MSI	Multi-Spectral Instrument
MTG	Meteosat Third Generation
NASA	National Aeronautics and Space Administration
NBR	Normalized Burned Ratio
NDVI	Normalized Difference Vegetation Index
NDWI	Normalized Difference Water Index
NIR	Near infrared
No.	Number
NRT	Near-real time
NW	Northwest
NW-IP	Northwest Iberian Peninsula
OLI	Operational Land Imager
PFT	Plant Functional Type
Pg C	Petagrams (i.e., 10^{15} grams) of carbon, a unit of mass
PhD	Philosophy Doctor
PRISMA	Precursore IperSpectrale della Missione Applicativa
PROBA-V	Project for On-Board Autonomy – Vegetation
RaDAR	Radio detection and ranging
RBR	Relativized Burn Ratio
RΔNBR	Relative Normalized Burn Ratio
REp	Return-to-Equilibrium point
RET	Time to Return-to-Equilibrium indicator
RF	Random Forest
rng	Absolute range

rnp	Non-parametric relative range
ROC	Receiver operating curve
rrl	Relative range
RRp	Return-to-Reference point
RRT	Time to Return-to-Reference indicator
RS	Remote Sensing
S95	95%-percentile fire severity indicator
SAR	Synthetic Aperture Radar
SD, std	Standard deviation
SI	Spectral index
sin	Sine, a trigonometric operator
SITS	Satellite image time-series
SLSTR	Sea and Land Surface Temperature Radiometer
smn	Springness of the minimum value
smx	Springness of the maximum value
SPOT-VEGETATION	Satellite Pour l'Observation de la Terre – VEGETATION program
SR	Surface reflectance
STL	Seasonal-Trend time-series decomposition procedure based on LOESS smoother
SoE	Strength-of-Evidence
SWIR	Shortwave infrared
S-NPP	Suomi-National Polar-orbiting Partnership
TCT	Tasseled Cap Transformation
TCT{B,b}	Tasseled Cap features of Brightness
TCT{G,g}	Tasseled Cap features of Greenness
TCT{W,w}	Tasseled Cap features of Wetness
tmn	Time (of the year) of the minimum value
tmx	Time (of the year) of the maximum of the minimum value
TIRS	Thermal InfraRed Sensor
UAV	Unoccupied (or Unmanned) Aerial Vehicle
UAS	Unoccupied (or Unmanned) Aerial System
UN	United Nations Organization
UTM 29N	Universal Transverse Mercator zone 29-North

VI	Vegetation index
VIIRS	Visible Infrared Imaging Radiometer Suite
WGS84	World Geodetic System 1984
wmn	Winterness of the minimum value
wmx	Winterness of the maximum value
$W \cdot m^{-2}$	Watt per square meter, a unit of radiative flux
°C	Degrees Celsius, a unit of temperature
ΔNBR	Differenced Normalized Burn Ratio

CHAPTER 1. General introduction

1.1. The role of fire in terrestrial ecosystems

1.1.1. Fire on an intrinsically flammable planet

The nature of (wild)fire

Fire is an exothermic chemical reaction in which a fuel – usually a carbon-based compound such as wood – combines rapidly with an oxidizer – usually oxygen in air –, producing energy in the form of heat and light, as well as a range of other reaction products (Quintiere 2006). The ensemble of these three elements – Heat, Fuel, and Oxygen –, known as the *fire triangle* (**Figure 1.1**), is required for a fire to be sustained and propagated (Scott 2020). When all three elements of the fire triangle come together in a susceptible landscape, uncontrolled fires may occur. Those events have been called *wildfires*, *forest fires*, *wildland fires*, *bushfires*, *rural fires*, *unplanned fires*, or sometimes simply *fires* (Bowman *et al.* 2009, Krawchuk *et al.* 2009, Gill *et al.* 2013). Wildfire behavior is controlled by the conditions, influences, and modifying forces that constitute the fire environment (Scott 2020), which is summarized by the *fire environment triangle* (**Figure 1.1**) – Fuel (amount, moisture), Weather (temperature, wind, humidity), and Topography (slope).

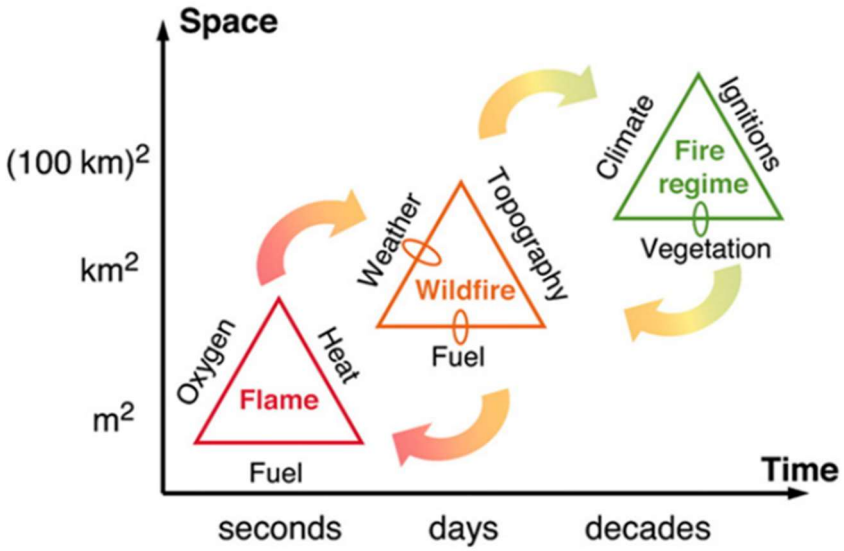

Figure 1.1. Dominant factors that influence fire at different scales: a flame, a single wildfire, and a fire regime. This is an extension of the traditional *fire triangle* concept, here including broad scales of space and time, the feedbacks that fire has on the controls themselves (small loops), as well as feedbacks between processes at different scales (arrows). [source: Moritz *et al.* 2005]

Wildfires as a natural process occurred naturally on Earth since the appearance of terrestrial vascular plants (**Figure 1.2**), as indicated by the presence of fossil charcoal in the geological record ca. 420 million years ago (Scott and Glasspool 2006, Bowman *et al.* 2009, van der Werf *et al.* 2017). Data from a wide variety of studies, based on historical meteorological records and national fire records, dendrochronology, or sedimentary charcoal (Westerling *et al.* 2006, Kitzberger *et al.* 2007), shows that climate is the primary driver of large regional fires, with the global fire size distribution changing along gradients of precipitation and aridity (Hantson *et al.* 2015). Past and current analyses of fire trends show that fire regimes respond to changes in climate and/or climate-induced vegetation changes, leading to increased fire activity, according to charcoal evidence over the past 21,000 years (Bowman *et al.* 2011). Earth is thus an intrinsically flammable planet (Bowman *et al.* 2009), with wildfires occurring due to its cover of carbon-rich vegetation, dry climates that vary seasonally, atmospheric oxygen, and global natural ignition sources such as lightning, earthquakes, meteors, and volcanic eruptions (Quintiere 2006).

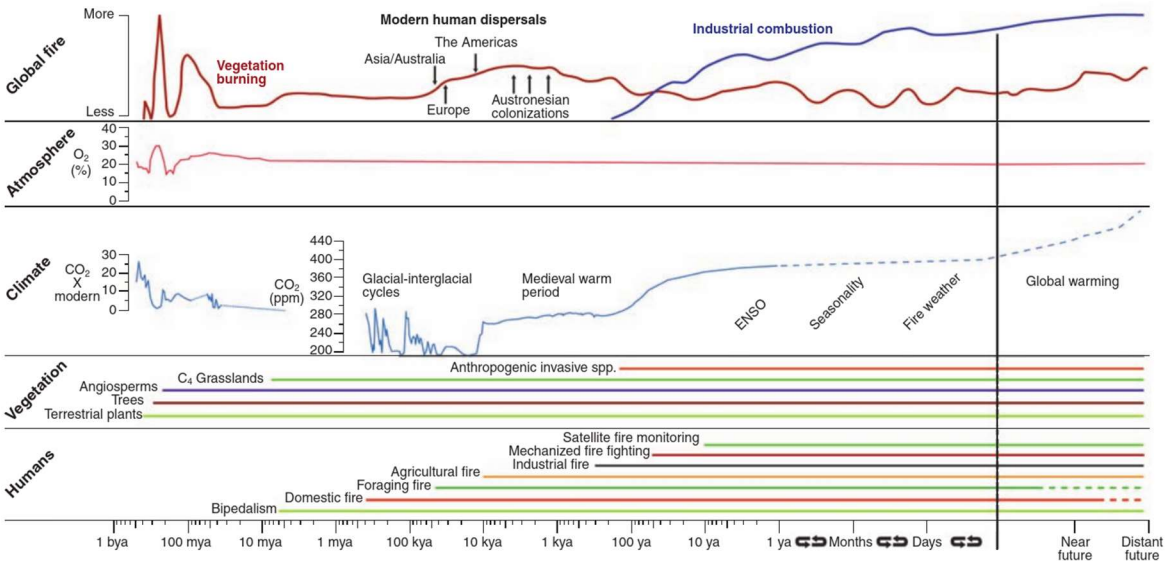

Figure 1.2. Qualitative schematic of global fire activity through time, based on the pre-Quaternary distribution of charcoal, Quaternary and Holocene charcoal records, and modern satellite observations, concerning the percentage of atmospheric O_2 content, parts per million (ppm) of CO_2, the appearance of certain vegetation types, and the presence of the genus Homo. Dotted lines indicate periods of uncertainty. [source: Bowman *et al.* 2009]

Fire as an evolutionary driver

It has long been recognized by fire ecologists that fire is a natural ecological factor influencing patterns and processes in most terrestrial ecosystems, including the carbon cycle, climate, and vegetation distribution and structure in many forests, woodland, shrubland, and grassland systems around the world (Bond and Keeley 2005, Bowman *et*

al. 2009, Pausas and Keeley 2009, He and Lamont 2018). Indeed, fire plays many ecological roles in ecosystems that cannot be duplicated by any other natural events (He *et al.* 2019), such that it can be as ecologically powerful when removed as when applied (Bowman *et al.* 2011). In this regard, fire has been compared to an herbivore – although consuming both dead and live materials –, for its role in selecting distinct plant traits and in the evolution of species and ecosystems (Bond and Keeley 2005).

Fires thus constitute a dynamic ecological force that holds evolutionary consequences (Bond and Keeley 2005, McLauchlan *et al.* 2020), leading to the co-evolution of biotas with wildfires, since they drive population turnover and diversification by promoting a wide range of adaptive responses to particular fire regimes (Pausas and Keeley 2009, He *et al.* 2019). In the case of plants, the two most common broad mechanisms for post-fire regeneration are resprouting – i.e., development of new sprouts from surviving tissues –, and seedling recruitment – i.e., regeneration by seed germination from local seed banks or seed dispersed after a fire from nearby populations (Clemente *et al.* 2005, Lloret *et al.* 2005, Pausas and Keeley 2014). The association of plant species having distinct reproductive and survival strategies with different fire regimes suggests that fire is a potent driver of biological processes, influencing biomass production, vegetation distribution, and thus the likelihood and behavior of fire (Bowman *et al.* 2009). Consequently, fire regimes often explain plant distribution and vegetation composition better than other constraints (e.g., climate, soil, pollinators, herbivores) at local scales (He *et al.* 2019). Fire can be viewed as an important evolutionary driver for animal diversity as well since many animals show specific phenotypic or behavioral adaptations to fire (Pausas and Parr 2018).

As a result of this high degree of adaptation to wildfires, many terrestrial ecosystems are fire-prone, since their composition, structure, and functioning are largely driven by fire regime, with fire acting as a major driver of their diversity and ecological processes, together with climate, resource availability and environmental heterogeneity (He *et al.* 2019). Fire has thus been a driving force of global biodiversity for millions of years, and still, today's variation in fire regimes continues to be a driver of biodiversity across the globe, with many plants, animals, and ecosystems depending on particular temporal and spatial patterns of fire (Kelly *et al.* 2020). Regions naturally affected by regular fires often harbor exceptionally high levels of species richness and endemism, and many are considered hotspots of global biodiversity (He *et al.* 2019).

1.1.2. The worldwide wildfire problem

Fire as a useful but unreliable tool

Fire is one of the first tools that humans used to re-shape their world (Bond and Keeley 2005), and one of mankind's most useful instruments since the early stages of civilization (**Figure 1.2**): a source of heat and light, an instrument for cooking and warming (Chuvieco 2009). Indeed, fire may be considered as a spark that ignited human evolution (Burton 2009), since it led to climate changes that favored the highly flammable savannas in which hominids originated (Bowman *et al.* 2009). Moreover, it has been suggested that mastery of fire almost two million years ago contributed to the rapid evolution of human species by permitting the cooking of food in the Lower Pleistocene (Ségalen *et al.* 2007, Bowman *et al.* 2011). However, the control of fire by humans extended the influence of fire beyond its ecological limits, offering human beings a powerful tool not only for their warming and cooking but also for protection, land clearing, and soil fertilization (Chuvieco 2009). The use of controlled fire only appeared after ca. 400,000 years ago, whereas domestic use of fire began ca. 50,000 to 100,000 years ago (Bar-Yosef 2002). More recently, fire has been widely used by humans over the last 10,000 years, to manage fuels and to convert forests into agricultural or pastoral landscapes (Bowman *et al.* 2009).

Today, fire is used globally by humans to minimize fuel hazards by modifying fuel structure, abundance, and continuity (Balch *et al.* 2017), but also to promote habitat quality, and to regenerate forests and pastures and other forms of land management (Archibald *et al.* 2009). Humans ignite few or many fires in different seasons under various weather conditions, while on the other hand also actively suppressing fires, or impeding fires through road networks, clearings, or sub-urban structures (Syphard *et al.* 2007). Humans enjoy a monopoly over the use of fire, with its possession being a defining trait of humanity. Dominating fire use has thus been a major important factor that made our world the way it is today, acting as a near-universal catalyst for most of our exchanges with the world around us, from technology to land use (Bowman *et al.* 2011). However, fire is also an unreliable tool that sometimes gets out of human control, despite our long-term experience of using fire to achieve economic and ecological benefits (Bowman *et al.* 2009).

The pyric transition

The strong climatic control over natural fire activity has been transformed during the last centuries (**Figure 1.3**), with humans becoming an increasingly important driver of fire occurrence (Chuvieco 2009, Bowman *et al.* 2011), leading to a *pyric transition* from natural to anthropogenic fire regimes (van der Werf *et al.* 2017). In a global context, most fires are now directly or indirectly caused by human activities (Chuvieco 2009). Humans are currently the dominant source of ignitions except in sparsely populated regions (Kasischke and Turetsky 2006), changing their number, distribution, and timing (i.e., seasonality), by

introducing ignitions where (and when) they were unlikely to occur but the landscape harbors fuels dry enough to ignite and carry fire (Balch *et al.* 2017). On the other hand, while human activity has increased fire ignitions in areas like deforestation zones, they have been decreasing in other areas, due not only to suppression efforts but also to conversion of fire-prone landscapes into agriculture or of fire-maintained open lands into closed-canopy forests (van der Werf *et al.* 2017).

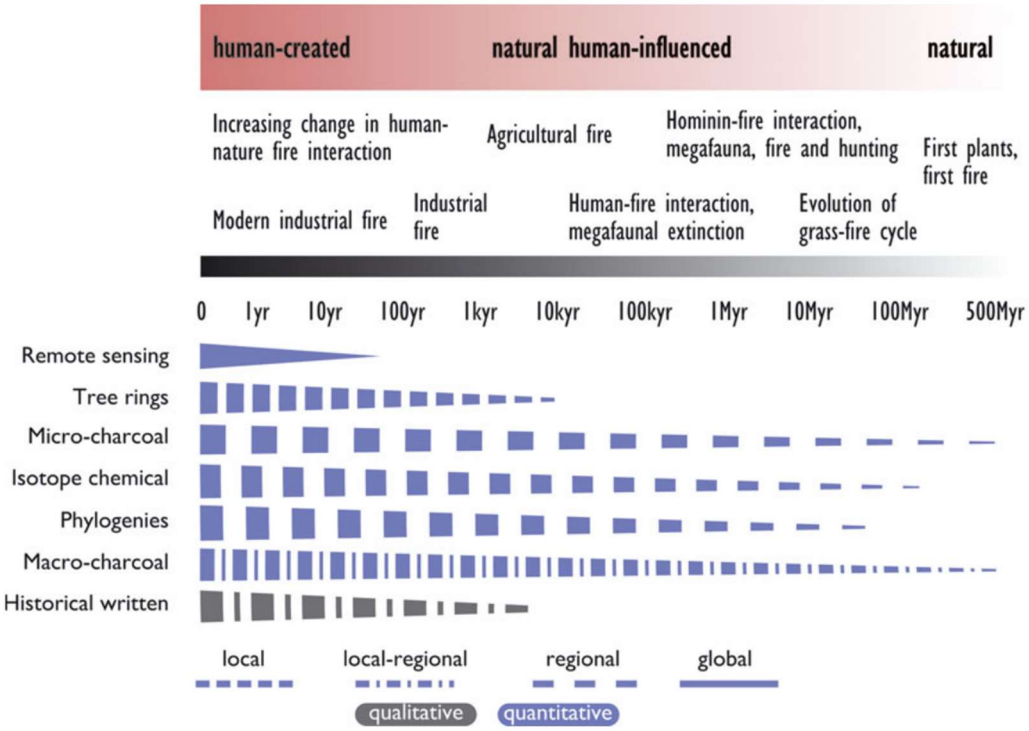

Figure 1.3. Summary of the available historical sources and palaeoecological proxies to reconstruct fire regimes, spanning the period from the advent of fire on Earth in deep time to the modern industrial period characterized by fossil fuel combustion. The spatial and temporal resolution of all these approaches varies and decays with increasing time depth, constraining our understanding of fire regimes, especially before the Industrial Revolution. [source: Bowman *et al.* 2011]

Interactions with other anthropogenic drivers such as climate change, land use, and invasive species are changing the nature of fire activity as well as its impacts (Kelly *et al.* 2020). New challenges in the interactions between fire and humans thus arise, with fire becoming not only a tool but also a hazard, affecting human lives, property, and ecosystems at temporal scales where impacts can be more detrimental (Chuvieco 2009). For instance, suburban sprawl into rural and natural landscapes juxtaposes people and their dwellings with flammable vegetation types (Theobald and Romme 2007).

In the future, the frequency and/or the intensity of wildfires are expected to increase in response to environmental change, potentially causing or accelerating changes in ecosystems (Smith *et al.* 2014). Furthermore, future projections suggest an impending shift

to a considerably stronger role of climate in driving global fire trends in the 21st century – a temperature-driven global fire regime –, outweighing direct human influence on fire (through both ignition and suppression), in contrast with the situation during the last two centuries, and potentially creating an unprecedentedly fire-prone environment (Pechony and Shindell 2010). The transition from local-scale fire use to the global industrialization that has triggered climate change requires that we turn our attention to the effects of altered fire regimes on the Earth system (Bowman *et al.* 2011).

1.1.3. The impacts and costs of wildfires

Ecological impacts

Wildfires are an important component of the Earth system (Bowman *et al.* 2009, Harrison *et al.* 2010) through their influence on biogeochemical cycles (Arneth *et al.* 2010), terrestrial ecology (Bond 2008), land surface (Bond-Lamberty *et al.* 2007), and atmospheric constituents (Langmann *et al.* 2009) and processes (Andreae and Merlet 2001). Throughout history, fire has been shaping biomes and landscapes, playing a key role in ecosystem composition and distribution (Bond *et al.* 2005, Chuvieco 2009, Pausas and Keeley 2009), and influencing climate through modulation of the carbon cycle and emissions of greenhouse gases and aerosols (Langmann *et al.* 2009, van der Werf *et al.* 2017).

Wildfires have a huge impact on the global carbon cycle (Schimel and Baker 2002), with estimations of worldwide fire emissions accounting for 3.5 Pg C each year – i.e., roughly 40% of the total fossil fuel carbon emissions (Van Der Werf *et al.* 2004, Running 2006). Moreover, the average annual burned area globally is estimated to be approximately 420 Mha, which is larger in area than the country of India (Giglio *et al.* 2018). There is a global fire issue, affecting almost all climates and vegetation types (Fischer *et al.* 2016). At a more local scale, fire can affect vegetation succession, soil erosion, and the hydrological cycle, potentially holding beneficial effects when it is aligned with the prevailing natural conditions, but acting harmfully when natural fire cycles are shortened or fire conditions are more severe (Chuvieco 2009).

Climate change has been correlated with observations that fire seasons are starting earlier and finishing later (Westerling 2016), with an associated trend towards more extreme wildfire events in terms of their geographic extent and duration, intensity, and severity (Tedim *et al.* 2013, 2018, Bowman *et al.* 2017). These large, uncontrolled fires – known as *megafires* – have been increasingly occurring, over the past two decades, on all vegetated continents, under extreme environmental conditions (Bowman *et al.* 2009, Tedim *et al.*

2013), culminating in substantial impacts on biodiversity (Moritz *et al.* 2014, Bowman *et al.* 2017). Furthermore, there is evidence for the declining ability of ecosystems to recover and persist in the face of wildfire disturbances (Scheffer *et al.* 2015) – i.e., ecosystem resilience – under climate change (Stevens-Rumann *et al.* 2018).

Impacts on human assets

Wildfires can also be regarded as a natural hazard that affects human communities and the ecosystems on which we depend (McCaffrey 2004). Wherever human population size is high and wildfires are catastrophic, unique near-term losses associated with large-scale economic disruptions are often generated, while long-term costs and losses are incurred in vegetation management, routine wildfire monitoring, and impacts on timber and other forest assets (Butry *et al.* 2001, Balch *et al.* 2017). Still, although wildfires are responsible for direct negative effects on human well-being – i.e., *ecosystem disservices* (Vaz *et al.* 2017, Sil *et al.* 2019) –, they can also be a driver of multiple *ecosystem services* (Pausas and Keeley 2019), such as those resulting from sustaining fire-dependent forested ecosystems (Butry *et al.* 2001), or enhancing fire protection in fire-prone landscapes (Regos *et al.* 2014, Sil *et al.* 2019).

Fires can have substantial negative effects on human health as a result of smoke pollution, ashes, and particulate matter produced by the combustion process (Reid *et al.* 2016), sometimes even resulting in the loss of human lives (Moritz *et al.* 2014, Bowman *et al.* 2017). Wildfires also create both short- and long-run economic impacts, such as costs of presuppression (e.g., recruitment and training of fire personnel, procurement, and maintenance of fire-fighting equipment and supplies, fuel treatment, fuel breaks, water sources) and prescribed burning, but also costs of suppression, fire-fighting capacity or management tactics, and disaster relief, as well as health care costs (e.g., from nefarious effects of smoke inhalation and damages), and property losses (Butry *et al.* 2001, Bowman *et al.* 2009). However, there is still uncertainty whether such events are mainly inevitable features of the Earth's fire ecology or a legacy of poor management and planning (Bowman *et al.* 2017).

Fire represents a rapidly growing societal challenge, due to increasingly destructive wildfires but also to fire exclusion in fire-dependent ecosystems (McLauchlan *et al.* 2020). There is also a growing awareness of the deleterious economic, social, and environmental impacts of wildfires (Lohman *et al.* 2007). In this regard, fire disturbance has been recognized as an Essential Climate Variable (ECV) by the Global Climate Observing System (GCOS) programme (GCOS 2010). Significantly, ecosystem disturbances (including fire) regime was also proposed by the Group on Earth Observations Biodiversity

Observation Network (GEO BON) as an Essential Biodiversity Variable (EBV) related to ecosystem functioning (Pereira *et al.* 2013). Wildfires, as well as their effects, are thus at the forefront of societal and environmental challenges (Catry *et al.* 2009). Nevertheless, knowledge is still lacking on the causes, effects, and feedbacks of wildfires, as well as on their impact on Earth system processes and their interactions with the environmental changes happening globally (Bowman *et al.* 2009).

1.2. Concepts and methods for wildfire disturbance assessment

1.2.1. The science of wildfires

Wildfire events

Wildfires have become a major topic of interest for several fields in the Environmental Sciences (Chuvieco 2012). As a result, scientific understanding of wildfires has grown exponentially during the last few decades (Jensen and McPherson 2008). Fire scientists have been assessing and evaluating fire risk and the ecological effects of wildfires by studying and predicting the phenomenon and its characteristics (Amatulli *et al.* 2007). Fire Ecology, in particular, is a scientific discipline that has emerged as a branch of the ecological sciences and is concerned with natural and human-mediated processes involving fire in an ecosystem – i.e., the direct and indirect effects, relations, and interactions between wildfires and the abiotic and biotic components of ecosystems (Bowman and Franklin 2005), as well as its broader-scale impacts on ecosystems and society (Bowman and Boggs 2006).

Fires burn with different properties, resulting in a wide variety of ecological effects (Bowman *et al.* 2009). The characterization of fire events is thus important to improve our understanding of the dynamics of individual wildfires, and the factors controlling fire occurrences, as well as how they affect (and are affected by) multiple environmental and socio-economic processes (Benali *et al.* 2016). Individual wildfires are discrete events characterized by their temporal and spatial dimensions (Bradstock 2008, He *et al.* 2019). These and other features (**Figure 1.4**) can be used in fire ecology to describe individual wildfires (Miller *et al.* 2012). In this regard, each particular fire event has a definite beginning and a definite end, with *fire duration* corresponding to the residence time, which can be expressed in minutes, hours, or months (Chuvieco 2009, Gill *et al.* 2013). On the other hand, the location of the *fire ignition* strongly influences fire properties such as rate and direction of spread, extent, intensity, and flame length and angle (Gill *et al.* 2013, Benali *et al.* 2016). Finally, *fire size* is the spatial extent, or area, of a burn patch (Chuvieco 2009).

Fire intensity and severity

Several other fire metrics are useful for different purposes (Keeley 2009). For instance, *fire intensity* describes the physical combustion process of energy release from organic matter, as heat, measured as time-averaged energy flux for the burning area, usually in $W \cdot m^{-2}$ (Chuvieco 2009, Keeley 2009). More loosely, it can also relate to other direct measures of fire behavior, such as flame length and rate of spread (Bond and Keeley

2005). Although fire intensity is a measure of immense importance to firefighters, ecologists are often more interested in *fire severity* (Bond and Keeley 2005), a broad concept that can be applied to a variety of fire effects (Tedim *et al.* 2013), including the social and the ecological impacts of fire (Chuvieco 2009). Indeed, fire intensity should not be confused with fire severity, which can be broadly defined as the degree of environmental change caused by fire (Keeley 2009). Finally, the term *burn severity*, while sometimes used interchangeably with fire severity, is a measure of the loss, injury, or mortality of organic matter aboveground and belowground, as well as of soil alteration by a wildfire (Keeley 2009, McLauchlan *et al.* 2020).

What is burned during a fire may be only a portion of what could be burned in a given area – i.e., *fuel* (Gill *et al.* 2013). In this regard, fire/burn severity may depend on the species survival traits (e.g., bark thickness, bud bank) and vegetation characteristics (e.g. density, continuity, flammability), while intensity is a physical component of the fire itself (He *et al.* 2019). Nonetheless, fire severity is correlated with fire intensity (Keeley 2009), and is also often closely associated with extremes in other fire properties – e.g., unusually frequent fires might also be regarded as having severe effects on the persistence of particular biota (He *et al.* 2019). Ecosystem responses include those processes that are differentially affected by fire intensity, measured either directly or indirectly with metrics of fire severity and/or recovery, and include erosion, vegetation regeneration, faunal recolonization, restoration of community structure, and a plethora of other response variables (Keeley 2009). Predicting how fire intensity or severity will affect these responses is critical to post-fire management (Keeley 2009).

Fire regimes

Studying and understanding ecological processes often requires a broad scope in time and space. Therefore, studying a single isolated wildfire does not enable managers or researchers to correctly understand the regional causes and/or consequences of wildfires. Instead, considering the *fire regime* is the usual process in wildfire research (Lloret *et al.* 2003, Lawson *et al.* 2010, Telesca and Pereira 2010), since wildfire disturbance is recognized as a recurrent ecological process (Bond and Keeley 2005, Moritz *et al.* 2005), which depends on the climate, vegetation (i.e., fuel), and ignitions (**Figure 1.1**). Fire regimes hence refer to the average properties of wildfires, or the usual range of fire characteristics, within a particular area and over a given period (Chuvieco 2009), which varies greatly among ecosystems, as do how human activities have altered them (Moritz *et al.* 2014).

Ecologists define the fire regime based on a range of properties including fuel type, temporal nature, spatial pattern, and consequences (Bond and Keeley 2005). For example,

fire seasonality refers to when fires occur during the year and how long the fire season lasts (if there is one) in months, whereas *fire frequency*, *fire interval*, or *fire recurrence* refers to how regularly fires occur in a particular region (Chuvieco 2009), and *fire return interval* is the time interval between fires at any one site (Bond and Keeley 2005). On the other hand, the (spatial) *density of fires* is the number of fires within a given area, whereas the average fire size – i.e., the average spatial extent of multiple burn patches – accounts for the overall impact of fire on the landscape pattern, whether fires are frequent and small or sporadic and large, creating different spatial mosaics (Chuvieco 2009).

The features of regional fire regimes can be summarized under the concept of *pyrodiversity*, which describes the variability in frequency, intensity, seasonality, and other properties of fire patterns across that region (Faivre *et al.* 2011). All these characteristics (**Figure 1.4**) will determine whether the impacts of fire on vegetation and soil are beneficial or detrimental (Chuvieco 2009). Understanding wildfire regimes, their causes, and dynamics are thus paramount to the sustainable management of ecosystems (McPherson and DeStefano 2003).

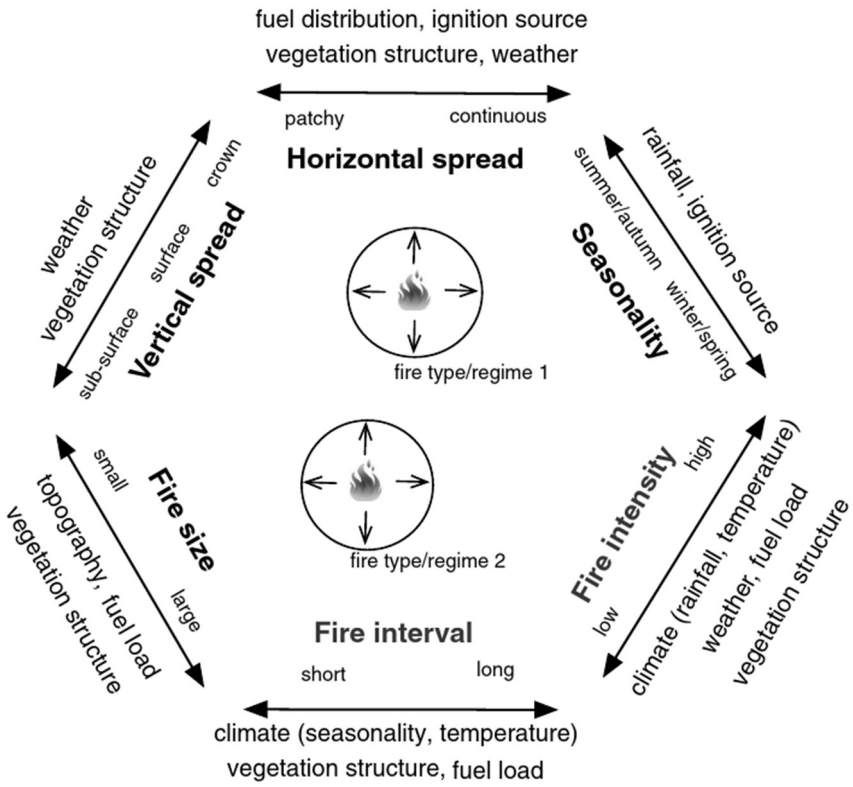

Figure 1.4. The six components of individual fire events and environmental factors controlling the properties of each component to defining the fire type. Ignition sources (lightning, anthropogenic) may affect the properties of each component rather than being a component itself. The fire regime arises from repeated patterns over time of the properties of the components for each fire. For a certain vegetation structure under a given climate, the fire regime is relatively predictable (as indicated by the circles) and selects for an adapted group of plants, microflora, and associated fauna. [source: He *et al.* 2019]

1.2.2. Wildfires and the functioning of ecosystems

The multi-dimensional concept of biodiversity

Wildfire disturbances potentially trigger impacts on the three primary aspects of biological diversity (i.e., *biodiversity*) – composition, structure, and functioning – in many terrestrial ecosystems, and those impacts can be evaluated at all levels of the biological organization – from genes to ecoregions (McLauchlan *et al.* 2020). Fire is thus a powerful ecological and evolutionary force that regulates several interconnected attributes of biodiversity – such as organismal traits, population sizes, species interactions, community composition, carbon, and nutrient cycling, and ecosystem functioning (Noss 1990, Alcaraz-Segura *et al.* 2013, Pettorelli *et al.* 2017) –, in a *nested hierarchy* (**Figure 1.5**). Compositional attributes refer to the identity and variety of entities in a collection (e.g., the genetic composition of a population, the list of species in a community or ecosystem, the spatial and temporal distribution of these communities across a landscape). Structural attributes deal with the physical organization or pattern of a system, and they include biotic and abiotic features that contribute to biodiversity by providing various habitats and patchiness at different levels of organization (e.g., habitat complexity as measured within communities, the pattern of patches and other elements at a landscape scale, the physiognomy of vegetation). Finally, functional attributes involve the ecological and evolutionary processes required to sustain biodiversity, including climatic, geologic, hydrologic, ecological, and evolutionary processes (e.g., gene flow, disturbances, and nutrient cycling).

Traditionally, biodiversity assessments have been mostly based on compositional attributes at the species level, such as species composition and abundance, and on structural attributes at the landscape level, such as patch size, heterogeneity, perimeter-area ratio, and connectivity/fragmentation (Noss 1990, Alcaraz-Segura *et al.* 2013). On the other hand, the effects of global environmental changes – such as wildfires – are particularly noticeable at the ecosystem level and regional scales (Vitousek *et al.* 1997, Alcaraz-Segura *et al.* 2009). Within ecosystems, the inertia associated with the responses of compositional (e.g., the composition of plant functional types) and structural attributes (e.g., vegetation physiognomy) to rapid changes in environmental conditions (Paruelo *et al.* 2001) leads to potential delays in the perception and quantification of such responses (Milchunas and Lauenroth 1995, Alcaraz *et al.* 2006, Mouillot *et al.* 2013). Thus, characterizing ecosystems based exclusively on compositional and structural attributes may not be sensitive enough to assess the impact of current environmental changes (Paruelo *et al.* 2001).

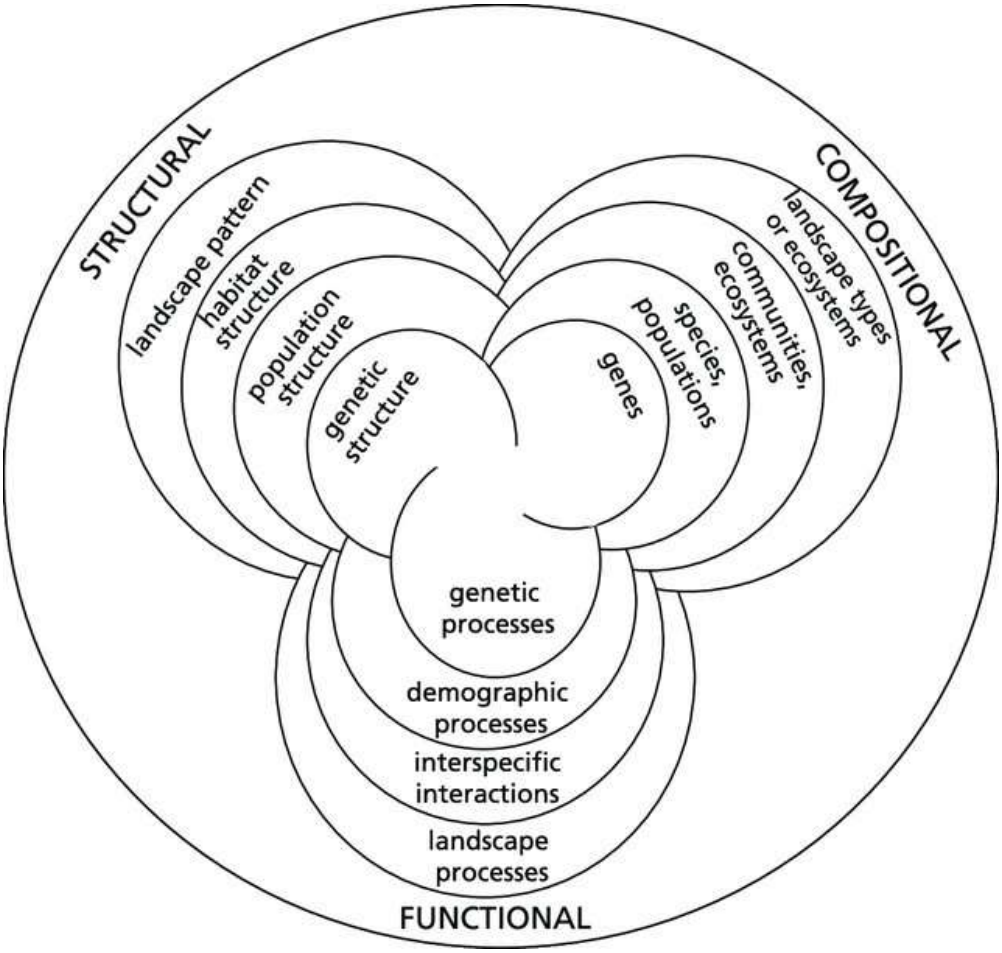

Figure 1.5. A diagrammatic representation of the hierarchy of biodiversity, composed of compositional, structural, and functional aspects of biodiversity, each encompassing multiple levels of organization. [adapted from Noss 1990]

The ecosystem functioning aspect of biodiversity

Both the terms *ecosystem function* and *ecosystem functioning* are sometimes used interchangeably to refer to the combined effects of all of the natural processes that sustain an ecological system (i.e., *ecosystem*) with the overall rate of functioning being governed by the interplay of abiotic (physical and chemical) and biotic factors (Jax 2005, Reiss *et al.* 2009, Bellwood *et al.* 2019). However, *ecosystem function* is more often used in the context of Functional Ecology to describe the roles – or functions – that organisms play in the community or ecosystem in which they occur (Jax 2005), whereas *ecosystem functioning* is more commonly used in the context of Ecosystem Ecology to address the biotic and abiotic aspects of the exchange of energy and matter in ecosystems (Noss 1990, Milchunas and Lauenroth 1995, Jax 2005, Alcaraz *et al.* 2006, Chapin *et al.* 2011, Mouillot *et al.* 2013). In the context of this thesis, the term *functional* will usually be used associated with the latter meaning.

In contrast to composition and structure, evaluation of functional attributes at the ecosystem level is still scarce (Alcaraz-Segura *et al.* 2013), which impairs environmental assessments (Pettorelli *et al.* 2017). Fortunately, the recognition of the importance of ecosystem functioning for environmental management and biodiversity conservation has significantly increased in the last two decades (Cabello *et al.* 2012, Alcaraz-Segura *et al.* 2013) since information on ecosystem functioning complements traditional descriptions based solely on environmental conditions or vegetation structure (Alcaraz-Segura *et al.* 2009, Villarreal *et al.* 2018). More specifically, ecosystem functioning exhibits a faster quantifiable response to environmental changes (Milchunas and Lauenroth 1995, Alcaraz *et al.* 2006, Mouillot *et al.* 2013), and facilitates the qualitative and quantitative assessment of ecosystem services (Costanza *et al.* 1997, Villarreal *et al.* 2018).

Ecosystem functioning and wildfire disturbances

As the human footprint extended, the Earth's vegetation has been increasingly shaped by fire, which is now a critical factor to understand ecosystem functioning worldwide (Chuvieco 2009). Fire plays a crucial role in vegetation composition, biodiversity, soil erosion, and the hydrological cycle (Chuvieco 2012). Furthermore, changes in fire disturbance regimes can produce significant impacts on biodiversity and ecosystem functioning (Cochrane 2003, Pettorelli *et al.* 2016). Namely, wildfires have an impact on the global carbon cycle (Schimel and Baker 2002), contributing to accelerating the natural cycle of primary production and respiration (Bowman *et al.* 2009). Fire also influences climate by changing surface albedo due to the release of aerosols into the atmosphere (Randerson *et al.* 2006, Ramanathan and Carmichael 2008). Fire thus links the atmosphere, the biosphere, and the hydrosphere via the release of gases (notably water vapor), matter (such as particles and ashes), and heat (Bowman *et al.* 2009).

Ecosystem functioning attributes are hence calling for more attention from fire ecologists (Bond and Keeley 2005). Also, fire integrates complex feedbacks among biological, social, and geophysical processes, requiring coordination across several fields and scales of study (McLauchlan *et al.* 2020). Considering the functional characteristics of ecosystems allows adding a dynamic component to wildfire analyses, which is particularly useful when dealing with global change issues such as predicting future fire behavior under different climatic and environmental scenarios (Bajocco *et al.* 2010). Ecosystem functioning can also be monitored at regional scales through attention to disturbance-recovery processes and rates of biogeochemical, hydrologic, and energy flows (Noss 1990), offering an integrative view of ecosystem response to environmental drivers and changes (Nagendra *et al.* 2013, Vaz *et al.* 2015, Villarreal *et al.* 2018). In addition, functional

attributes of ecosystems can be easily and frequently monitored over large areas through remote sensing (Paruelo *et al.* 2001), which is particularly useful for monitoring vegetation dynamics and ecosystem responses to environmental changes (Alcaraz-Segura *et al.* 2009).

1.2.3. Remote sensing of wildfires and ecosystem functioning

Remotely sensed Earth observations

The term *remote sensing* has been used since the early 1960s, initially referring to the acquisition of information about an object, area, or phenomenon through devices that are not in physical contact with it (Lillesand *et al.* 2015, Chuvieco 2020). Since then, it has taken on a more discipline-oriented meaning, within the scope of *Earth observation* (Jones and Vaughan 2010), which, in this context, can be defined as the process of gathering information about planet Earth's biological, physical or chemical systems via remote sensing technologies (Kwok 2018, Murray *et al.* 2018, Chuvieco 2020). In this sense, the overarching goal of remote sensing techniques is to provide valuable information about Earth's terrestrial landscapes, oceans, ice sheets, and atmosphere (Purkis and Klemas 2011).

In broader terms, remote sensing encompasses a multitude of activities, including the operation of platform-sensor systems, image data acquisition and storage, and the subsequent data processing, analysis, validation, and interpretation, as well as the dissemination of the processed data and image products (Chuvieco 2020). These can either complement or be complemented by ground measurements, offering the opportunity to deliver consistent information in time and space with a synoptic view, i.e., showing *big-picture* views of large areas of the surface (Vanden Borre *et al.* 2011). Indeed, validation based on independent reference information acquired from statistically planned surveys is a critical phase of any new remote sensing-based product (Chuvieco *et al.* 2020).

In the context of remote sensing, the device that is not in contact with the subject under investigation is usually a sensor installed into a static or moving platform, such as an aircraft or a satellite, positioned at a specific altitude or orbit (Kerle and Bakker 2004, Lillesand *et al.* 2015). These remote sensors are typically divided into two groups – the active and the passive sensors (Turner 2003, Jensen 2007, Lavender and Lavender 2016). Whereas active sensors (e.g., radio detection and ranging, RaDAR; light detection and ranging, LiDAR) – emit energy to the surface and subsequently recapture the reflected energy – usually electromagnetic radiation (Chuvieco 2020) –, passive sensors (e.g., aerial

cameras, multispectral and thermal scanners, hyperspectral imagers) only capture reflected or emitted energy. Examples of remote sensing data thus include aerial photography, satellite imagery, radar altimetry, and laser bathymetry (Purkis and Klemas 2011).

Remote sensing and the electromagnetic spectrum

Electromagnetic radiation is defined as all energy that moves with the velocity of light in a harmonic wave pattern (Purkis and Klemas 2011), consisting of waves that occur at equal intervals in time (i.e., *frequency*), and with a certain distance between a given point at the same position on two consecutive waves (i.e., *wavelength*). Remote sensors have been refined over the past several decades to cover the ultraviolet, visible, reflected infrared, thermal infrared, and microwave regions of the electromagnetic spectrum (**Figure 1.6**), corresponding to wavelengths ranging from nanometers to meters (Jones and Vaughan 2010). Each sensor captures different types of information because of the ways a particular wavelength interacts with surface materials or the intervening atmosphere (Lavender and Lavender 2016, Chuvieco 2020).

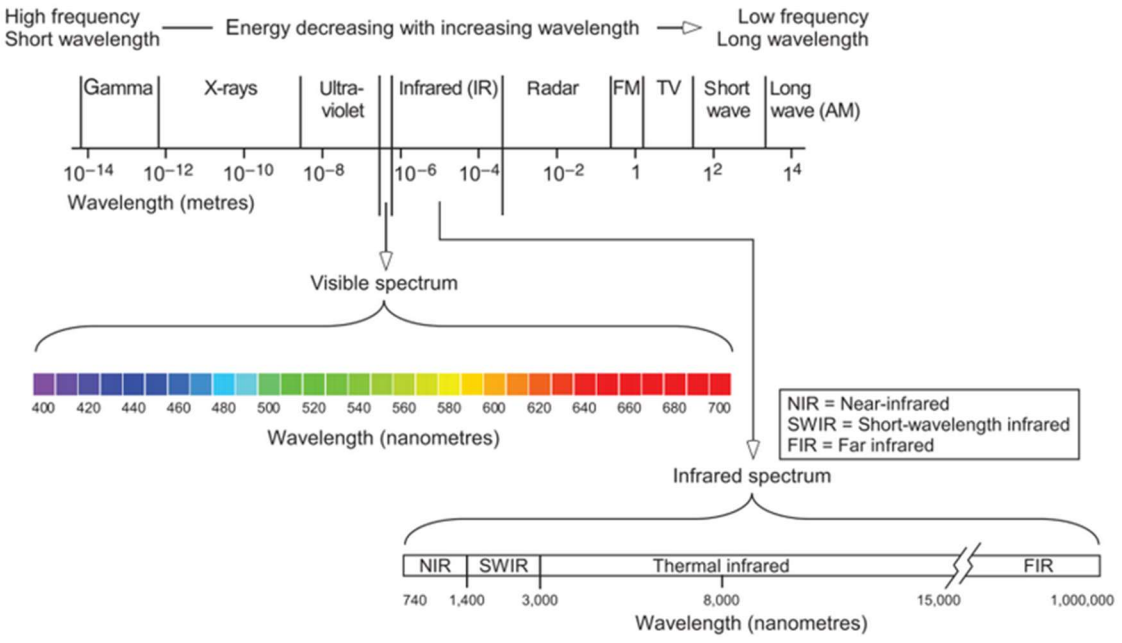

Figure 1.6. The electromagnetic spectrum, which is divided into regions based on wavelengths, ranging from the very short wavelengths of the gamma-ray region to the long wavelengths of the radio region. [source: Purkis and Klemas 2011]

Electromagnetic energy in specific wavelengths can be either absorbed or scattered by the different constituents of the Earth's atmosphere – i.e., water vapor, aerosols, and gases such as oxygen (O_2), ozone (O_3), carbon dioxide (CO_2), and methane (CH_4) –, before reaching the surface, thusly disturbing the signal reaching remote sensors (Kerle and

Bakker 2004). This influences which parts of the spectrum are available for remote sensing interpretations, and generates the need to use filters or atmospheric correction techniques to diminish such effects (Purkis and Klemas 2011). Among the *windows* of electromagnetic energy that is transmitted through the Earth's atmosphere (**Figure 1.7**), the visible (400–750nm) and parts of the infrared (near-infrared: 750–1300nm; shortwave-infrared: 1300–2500nm; thermal infrared: 8000–13,000nm) regions (corresponding to optical and thermal remote sensing) are of particular importance for land observations.

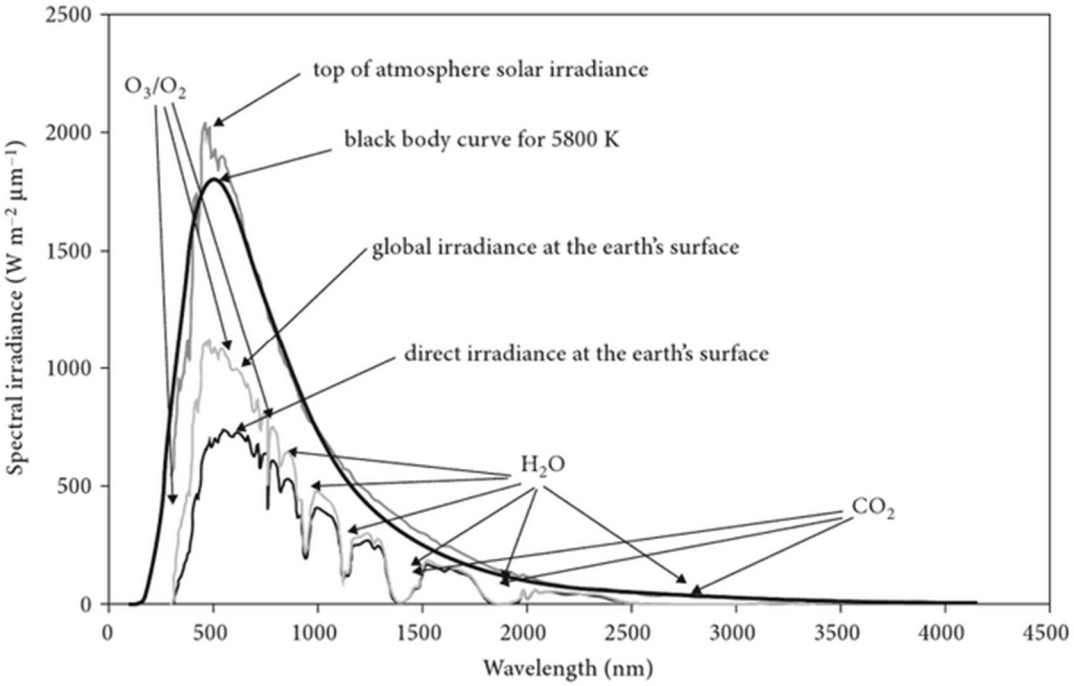

Figure 1.7. Illustration of the solar spectrum expressed in terms of energy per unit wavelength at the top of the Earth's atmosphere as compared with the black body curve for an emitter at 5800 K, together with the corresponding total and direct radiation received on a horizontal surface for typical clear-sky conditions. Also shown are the main absorption bands due to O_3, O_2, water vapor, and carbon dioxide. [source: Jones and Vaughan 2010]

Differences in either *radiance* (i.e., the electromagnetic energy that reaches the sensor) or *reflectance* (i.e., the ratio between the electromagnetic energy coming from the sun and the one going back to the sensor) in these regions of the electromagnetic spectrum allows for the distinction between objects and features on the ground (Purkis and Klemas 2011). For instance, vegetation indices such as the widely used Normalized Difference Vegetation Index (NDVI) take advantage of the contrast between the high absorption of electromagnetic radiation in the red part of the visible region, but a high reflection in the near-infrared region, by plant pigments such as chlorophyll, which is commonly associated with plant biomass, vigor, primary productivity, and leaf area index (Jobbágy *et al.* 2002,

Pettorelli *et al.* 2005, 2014, Clerici *et al.* 2012). On the other hand, the contrast between thermal bands and vegetation indices is important to detect disturbance patterns (Duro *et al.* 2007, Mildrexler *et al.* 2009) or to retrieve land surface energy fluxes and soil surface moisture (Petropoulos *et al.* 2009).

Characteristics and advantages of remotely sensed images

A large number of remote observation satellites are in orbit around the Earth, carrying a wide variety of sensors with different characteristics, depending on the purpose (Vanden Borre *et al.* 2011). Accordingly, satellite image data can be characterized by different properties (Kerle and Bakker 2004, Jensen 2007, Lavender and Lavender 2016) – which depend on sensor design as well as orbital features (e.g., altitude, inclination angle, revisiting period). These properties include (Kerle and Bakker 2004, Purkis and Klemas 2011, Lillesand *et al.* 2015): (i) spatial coverage (i.e., the total area covered by one image); (ii) spatial resolution (i.e., the area of each pixel measured, related to the size of the smallest object that can be recognized in the image); (iii) spectral resolution (i.e., the number of bands, or spectral wavelengths, in the electromagnetic spectrum that the sensor is sensitive to); (iv) radiometric resolution (i.e., the smallest difference in, or the number of, levels of energy that the sensor can distinguish); and (v) temporal resolution (i.e., the time it takes for a sensor to return and collect data from the same place).

Space-based observations using remote sensors possess capabilities that offer several advantages (Chuvieco 2020, Chuvieco *et al.* 2020), such as: (i) global coverage of information; (ii) a synoptic (i.e., *big-picture*) view; (iii) multiscale observations, using different spatial resolutions; (iv) observations over different spectral regions, including the non-visible regions of the electromagnetic spectrum; (v) information is derived without destructive sampling since it is inherently non-invasive; (vi) repeated observation, by systematic observation of the Earth surface, therefore providing ideal conditions for multitemporal analysis; (vii) immediate transmission; and (viii) digital format. All these properties and advantages explain the wide use of remotely sensed data, since the early 1970s, for analyzing conditions and monitoring changes over large geographic extents, making it useful for a wide range of applications (Szpakowski and Jensen 2019, Chuvieco *et al.* 2020). Indeed, satellite images have been extensively explored by scientists and resource managers worldwide to study multidisciplinary environmental science problems, highlighting the importance of remote sensing in measuring characteristics or detecting changes in the environment that occur as a result of human or natural drivers, and in improving the assessment of disturbance events and regimes (de Santana *et al.* 2021).

Remote sensing applications to wildfire science

Fires can be characterized using different sources of information, such as data collected in the field (including spectral data), fire-occurrence records, and both air-borne and space-borne remotely sensed data (Benali *et al.* 2016). Recent improvements in the quality (e.g., temporal and spatial resolutions), as well as in the availability of global fire data derived from satellite images have unlocked our understanding of recent fire activity at the global scale (Bowman *et al.* 2009, Chuvieco 2009, McLauchlan *et al.* 2020), contributing to advance wildfire science and management (Chuvieco *et al.* 2020), and complementing other data sources by allowing to overcome some of their scale-dependent limitations (Benali *et al.* 2016).

In the field of fire ecology, applications of remote sensing technologies and techniques promoted the development of studies with different scopes (de Santana *et al.* 2021), providing biophysical measurements that have been used to assist in several fire-related applications (Szpakowski and Jensen 2019), complemented with varying levels of field observations for ground verification (McLauchlan *et al.* 2020). These applications can be grouped according to the main phase of the fire event (**Figure 1.8**) in which they are focused (Chuvieco *et al.* 2020) – either before (i.e., *pre-fire*), during, or after (i.e., *post-fire*) – linking to fire prevention, fire suppression, and the assessment and monitoring of fire effects, respectively (Szpakowski and Jensen 2019).

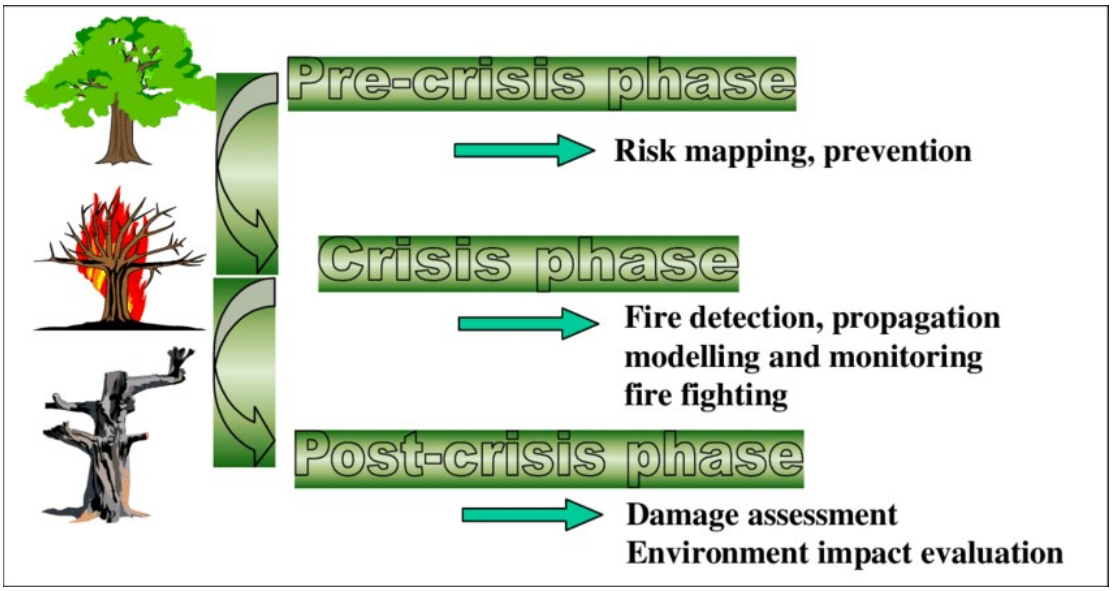

Figure 1.8. Illustration of the main phases of wildfire management, with the term “crisis” referring to the wildfire event, from ignition to extinction. [source: Faour *et al.* 2004]

Applications focusing on the pre-fire period include fire risk assessment and mapping (Adab *et al.* 2013, Yu *et al.* 2017), fuel type mapping (Saatchi *et al.* 2007, Arroyo *et al.* 2008, Gale *et al.* 2021), and fuel moisture content estimates (Petropoulos *et al.* 2009). As for applications corresponding to the period during the fire occurrence, these can include active fire detection (Schroeder *et al.* 2014, 2016, Xu and Zhong 2017); fire behavior modeling (Pimont *et al.* 2011, Parsons *et al.* 2017), and ignition source identification (Benali *et al.* 2016, Fusco *et al.* 2016, Sherstjuk *et al.* 2018). Finally, applications of remote sensing focusing on the post-fire period include burned area estimates (Randerson *et al.* 2012, Fornacca *et al.* 2018, Giglio *et al.* 2018), fire/burn severity assessment (Epting *et al.* 2005, Harris *et al.* 2011, Fernández-Manso *et al.* 2016), post-fire recovery monitoring (Gouveia *et al.* 2010, Bastos *et al.* 2011, Veraverbeke *et al.* 2012, João *et al.* 2018, Pérez-Cabello *et al.* 2021), resilience evaluation (Rogan and Yool 2001, Adámek *et al.* 2016), and predicting emissions resulting from the fire (van der Werf *et al.* 2017, Wei *et al.* 2018).

The ecosystem functioning approach to wildfire assessment

Besides fire applications, remote sensing has played an increasingly important role in detecting, mapping, analyzing, and monitoring, and predicting changes in the environment, over large geographic extents (Rose *et al.* 2015), improving our ecological understanding of several phenomena (McLauchlan *et al.* 2020). Indeed, remote sensing data and techniques are used in a wide variety of ecological applications, including predicting the distribution of species (He *et al.* 2015) and biological invasions (Rocchini *et al.* 2015, Vaz *et al.* 2019), monitoring species' habitats from space (Vanden Borre *et al.* 2011, Vaz *et al.* 2015), as well as applications to forest ecology and management (Lechner *et al.* 2020), and water resources and flood risk management (Wang and Xie 2018).

As mentioned before, the inertia of structural attributes may delay the perception of ecosystem responses to environmental changes, whereas the exchanges of energy and matter of an ecosystem (i.e., ecosystem functioning) are modified faster (Milchunas and Lauenroth 1995, Alcaraz *et al.* 2006). In this regard, remote sensing can be used to describe the spatial heterogeneity of ecosystem functioning at regional and global scales, through the definition of *Ecosystem Functioning Attributes* (EFAs), which can also be used to statistically define *Ecosystem Functional Types* (EFTs) – a concept related to *Plant Functional Types* (PFTs). While PFTs group similarly functioning species, independently of phylogeny, based on their functional features (i.e. relative growth rates, nitrogen fixation), EFTs group similarly functioning ecosystems, independently of structure, based on different aspects of matter/energy flows (Paruelo *et al.* 2001, Alcaraz *et al.* 2006). Remotely sensed EFAs and EFTs have been increasingly used in a wide range of ecological applications due

to their strong relation to biophysical properties and processes of ecosystems (Alcaraz-Segura *et al.* 2008), such as describing major ecological patterns (Alcaraz *et al.* 2006, Duro *et al.* 2007, Coops *et al.* 2008), predicting and projecting species distributions (Gonçalves *et al.* 2016, Arenas-Castro *et al.* 2018, Regos *et al.* 2020), predicting species abundance (Arenas-Castro *et al.* 2019), and supporting the definition of conservation priorities (Cazorla *et al.* 2020).

Remote sensing technology has also facilitated new approaches to advancing the study of fire ecology (Szpakowski and Jensen 2019). Remote sensing and fire ecology are today complementary sciences that contribute to studies on biodiversity, conservation, and environmental monitoring (de Santana *et al.* 2021). Still, the potential of approaches based on ecosystem functioning to improve our understanding of the effects of wildfire disturbances on ecosystems is largely under-explored, namely regarding the translation of spectral indices into meaningful, informative ecosystem variables.

1.3. Research goals and thesis structure

1.3.1. Research goals and hypotheses

Motivation

As exposed in the previous sections, changing wildfire regimes potentially pose a major threat to a wide range of social, economic, and environmental assets (Bowman *et al.* 2009). Wildfires constitute a major driver of ecological change, modifying the composition, structure, and functioning of ecosystems, and can contribute to eroding their resilience (Johnstone *et al.* 2010, Scheffer *et al.* 2015), increasing the risk of sudden collapse or regime-shifts (Folke *et al.* 2004). There is thus an increasing need for methods to assess and monitor the ecological consequences of wildfire disturbances. To this end, approaches based on ecosystem functioning have advantages over structural or compositional ones (Alcaraz-Segura *et al.* 2008), since fire can cause rapid and profound modifications on multiple key aspects of the flows of matter and energy (Petropoulos *et al.* 2009). However, most resilience assessments do not account for ecosystem functioning after disturbance events (Frazier *et al.* 2013), and multi-dimensional assessments of the environmental impacts of wildfires on ecosystem functioning are still lacking. There is therefore a growing need for more comprehensive sets of indicators to assess and monitor the impacts of wildfire disturbances and post-fire processes on ecosystems.

Remote sensing data and techniques have been increasingly employed to derive indicators to assess and characterize different aspects of the post-fire period (Lentile *et al.* 2006) – such as burned area mapping, fire severity evaluation, post-fire recovery monitoring, and resilience assessment (João *et al.* 2018). Nevertheless, to fully understand the effects of wildfire disturbances on multiple dimensions of ecosystems, a better translation of spectral indices into informative ecosystem variables is needed. Therefore, there is a need to devise consistent frameworks, linking ecological theory and remotely sensed data, that can improve the assessment and mapping of the spatiotemporal heterogeneous effects of wildfires on ecosystem functioning, as well as the responses and resilience of ecosystems to those disturbances. Such frameworks would represent a major asset not only for risk assessment and governance but also for post-fire management and restoration (Keeley 2009, Tedim *et al.* 2013, Smith *et al.* 2014, Parks *et al.* 2019).

Overarching research goals

Taking this rationale into account, the broad overarching goal of this thesis is to **improve the assessment and monitoring of wildfire disturbances**, by proposing, developing, and showcasing an integrative satellite-driven framework to evaluate the effects of wildfire disturbances on multiple key dimensions of the matter and energy fluxes on ecosystems and ecosystem responses to those disturbances. This conceptual and experimental framework aims to apply to a wide variety of geographical and environmental contexts and target areas, under the remote sensing paradigm shift in terrestrial ecosystems monitoring (Kwok 2018).

Overall, this thesis seeks to introduce the ecosystem functioning dimensions into fire ecology, contributing to the advancement of scientific knowledge in that field, as well as to ecosystem functioning, and ecological resilience. Furthermore, it also aims to contribute to important strategic objectives underlying the development and implementation of regional monitoring programs supported by land observation systems, namely:

(i) clarifying and mainstreaming the links between ecological processes, fire disturbance, and remotely-sensed observations; and

(ii) improving the comprehensiveness and cost-efficiency of monitoring systems, by showcasing the opportunities enabled by using cost-free data derived from remote sensing, processed and analyzed with highly reproducible, code-based workflows developed in free and open-source software environments.

Research hypotheses

To tackle these overarching research goals, three research hypotheses (H1–H3) were assessed, based on the rationale that indicators related to multiple aspects of matter and energy fluxes, derived from satellite image time-series, provide detailed insights of different aspects of ecosystem functioning that are useful for characterizing baseline (i.e., pre-fire reference) conditions and for assessing the ecological effects of fire events:

- **Research Hypothesis 1** (H1): *"The location, extension, and date of occurrence of wildfire disturbance events can be identified using indicators of multiple dimensions of ecosystem functioning, related to matter and energy exchanges, to enhance existing burned area maps and fill important gaps in fire databases"*;

- **Research Hypothesis 2** (H2): *"The short-, medium-, and long-term effects of wildfires on ecosystem functioning, and ecosystem responses to those disturbances can be better estimated with the synergistic use of multiple indicators, enabling in-depth multi-dimensional and synoptic assessments of wildfire disturbance severity and post-fire recovery"*;
- **Research Hypothesis 3** (H3): *"Indicators extracted from post-fire trajectories of remotely-sensed variables of ecosystem functioning allow for the identification and characterization of potential regime shifts after wildfires and, consequently, the assessment of (changes in) ecological resilience to those disturbances"*.

Successfully testing these hypotheses would provide strong support to the added value of a framework combining resilience theory and remote sensing of ecosystem functioning for an integrative assessment of fire patterns and impacts.

1.3.2. Thesis structure

This thesis is structured in five chapters describing the research context, goals, workflow, main results, and conclusions.

Chapter 1 describes the broad theoretical and methodological context under which the research was developed. In the first section, the broader scientific and societal problem of wildfires is presented, describing wildfires as both a natural and anthropogenic phenomenon, and discussing the potential impacts of wildfire events and changes in fire regimes. A second section is focused on presenting basic concepts and methodologies within the three core scientific fields employed in the thesis: fire ecology, ecosystem functioning, and remote sensing. Finally, a third and last section presents the motivation for this thesis, the research goals, and finally the thesis structure.

Chapters 2–4 present the research papers that compose the core of the thesis and materialize the goals of the research plan, each chapter with its specific objectives, centered on addressing the three research hypotheses outlined above (H1–H3).

In **Chapter 2**, aimed to address research hypothesis H1, a generic framework is described to compare, rank, and combine multiple remotely-sensed indicators of wildfire disturbances to improve the detection of wildfire disturbance events in space and time. In particular, this study aimed to assess the ability and performance of different remotely-sensed variables to discriminate burned areas, as well as for detection and mapping of

wildfire occurrences within a given year, including the estimation of the date of occurrence, to complement missing information on available fire databases.

Addressing research hypothesis H2, **Chapter 3** describes a second study in which the main objective was to propose, describe, and showcase a framework to support enhanced assessments of the ecological effects of wildfire disturbances, at short (i.e., the year of the fire) to medium term (i.e., up to the second year after the fire). The workflow was based on detecting inter-annual anomalies (i.e., deviations from the normal inter-annual variability) of a large set of remotely-sensed descriptors of the intra-annual dynamics – i.e., Ecosystem Functioning Attributes (EFAs) – of four essential dimensions of the flows of matter and energy in ecosystems: (i) primary productivity; (ii) vegetation water content; (iii) albedo; and (iv) sensible heat.

Chapter 4 presents a study on post-fire trajectories, addressing research hypotheses H2 and H3. In this study, the main objective was to propose, describe, and showcase a framework for enhanced characterization and classification of the resilience of ecosystems following wildfire disturbances, including the identification of potential regime shifts. The approach considers indicators covering aspects related to resistance (based on estimates of fire severity) and recovery at short, medium-, and long-term, extracted from time-series of satellite images for the same four key aspects of ecosystem functioning (primary productivity, vegetation water content, albedo, and sensible heat).

Finally, **Chapter 5** provides an integrative discussion of the main contributions from the three research papers (Chapters 2–4), as well as some general and overarching conclusions from the research developed for this thesis, together with an outlook on future directions. This final chapter emphasizes the added value, limitations, and required future developments of the proposed (and showcased) framework integrating multiple dimensions, components, and temporal scales of wildfire effects on ecosystems, grounded on ecological theory and supported by remote sensing data and methods.

References

Adab, H., Kanniah, K.D., and Solaimani, K., 2013. Modeling forest fire risk in the northeast of Iran using remote sensing and GIS techniques. *Natural Hazards*, 65 (3), 1723–1743. DOI: 10.1007/s11069-012-0450-8.

Adámek, M., Hadincová, V., and Wild, J., 2016. Long-term effect of wildfires on temperate Pinus sylvestris forests: Vegetation dynamics and ecosystem resilience. *Forest Ecology and Management*, 380, 285–295. DOI: 10.1016/j.foreco.2016.08.051.

Alcaraz-Segura, D., Cabello, J., and Paruelo, J., 2009. Baseline characterization of major Iberian vegetation types based on the NDVI dynamics. *Plant Ecology*, 202 (1), 13–29. DOI: 10.1007/s11258-008-9555-2.

Alcaraz-Segura, D., Cabello, J., Paruelo, J.M., and Delibes, M., 2008. Trends in the surface vegetation dynamics of the national parks of Spain as observed by satellite sensors. *Applied Vegetation Science*, 11 (4), 431–440. DOI: 10.3170/2008-7-18522.

Alcaraz-Segura, D., Paruelo, J.M., Epstein, H.E., and Cabello, J., 2013. Environmental and Human Controls of Ecosystem Functional Diversity in Temperate South America. *Remote Sensing*, 5 (1), 127–154. DOI: 10.3390/rs5010127.

Alcaraz, D., Paruelo, J.M., and Cabello, J., 2006. Identification of current ecosystem functional types in the Iberian Peninsula. *Global Ecology and Biogeography*, 15 (2), 200–212. DOI: 10.1111/j.1466-822X.2006.00215.x.

Amatulli, G., Peréz-Cabello, F., and de la Riva, J., 2007. Mapping lightning/human-caused wildfires occurrence under ignition point location uncertainty. *Ecological Modelling*, 200 (3–4), 321–333. DOI: 10.1016/j.ecolmodel.2006.08.001.

Andreae, M.O. and Merlet, P., 2001. Emission of trace gases and aerosols from biomass burning. *Global Biogeochemical Cycles*, 15 (4), 955–966. DOI: 10.1029/2000GB001382.

Archibald, S., Roy, D.P., van Wilgen, B.W., and Scholes, R.J., 2009. What limits fire? An examination of drivers of burnt area in Southern Africa. *Global Change Biology*, 15 (3), 613–630. DOI: 10.1111/j.1365-2486.2008.01754.x.

Arenas-Castro, S., Gonçalves, J., Alves, P., Alcaraz-Segura, D., and Honrado, J.P., 2018. Assessing the multi-scale predictive ability of ecosystem functional attributes for species distribution modelling. *PLOS ONE*, 13 (6), e0199292. DOI: 10.1371/journal.pone.0199292.

Arenas-Castro, S., Regos, A., Gonçalves, J.F., Alcaraz-Segura, D., and Honrado, J., 2019. Remotely Sensed Variables of Ecosystem Functioning Support Robust Predictions of Abundance Patterns for Rare Species. *Remote Sensing*, 11 (18), 2086. DOI: 10.3390/rs11182086.

Arneth, A., Harrison, S.P., Zaehle, S., Tsigaridis, K., Menon, S., Bartlein, P.J., Feichter, J., Korhola, A., Kulmala, M., O'Donnell, D., Schurgers, G., Sorvari, S., and Vesala, T., 2010. Terrestrial biogeochemical feedbacks in the climate system. *Nature Geoscience*, 3 (8), 525–532. DOI: 10.1038/ngeo905.

Arroyo, L.A., Pascual, C., and Manzanera, J.A., 2008. Fire models and methods to map fuel types: The role of remote sensing. *Forest Ecology and Management*, 256 (6), 1239–1252. DOI: 10.1016/j.foreco.2008.06.048.

Bajocco, S., Pezzatti, G.B., Mazzoleni, S., and Ricotta, C., 2010. Wildfire seasonality and land use: When do wildfires prefer to burn? *Environmental Monitoring and Assessment*, 164 (1–4), 445–452. DOI: 10.1007/s10661-009-0905-x.

Balch, J.K., Bradley, B.A., Abatzoglou, J.T., Nagy, R.C., Fusco, E.J., and Mahood, A.L., 2017. Human-started wildfires expand the fire niche across the United States. *Proceedings of the National Academy of Sciences*, 114 (11), 2946–2951. DOI: 10.1073/pnas.1617394114.

Bar-Yosef, O., 2002. The Upper Paleolithic Revolution. *Annual Review of Anthropology*, 31 (1), 363–393. DOI: 10.1146/annurev.anthro.31.040402.085416.

Bastos, A., Gouveia, C.M., DaCamara, C.C., and Trigo, R.M., 2011. Modelling post-fire vegetation recovery in Portugal. *Biogeosciences*, 8 (12), 3593–3607. DOI: 10.5194/bg-8-3593-2011.

Bellwood, D.R., Streit, R.P., Brandl, S.J., and Tebbett, S.B., 2019. The meaning of the term 'function' in ecology: A coral reef perspective. *Functional Ecology*, 33 (6), 948–961. DOI: 10.1111/1365-2435.13265.

Benali, A., Russo, A., Sá, A., Pinto, R., Price, O., Koutsias, N., and Pereira, J., 2016. Determining Fire Dates and Locating Ignition Points With Satellite Data. *Remote Sensing*, 8 (4), 326. DOI: 10.3390/rs8040326.

Bond-Lamberty, B., Peckham, S.D., Ahl, D.E., and Gower, S.T., 2007. Fire as the dominant driver of central Canadian boreal forest carbon balance. *Nature*, 450 (7166), 89–92. DOI: 10.1038/nature06272.

Bond, W. and Keeley, J., 2005. Fire as a global 'herbivore': the ecology and evolution of flammable ecosystems. *Trends in Ecology & Evolution*, 20 (7), 387–394. DOI: 10.1016/j.tree.2005.04.025.

Bond, W.J., 2008. What Limits Trees in C 4 Grasslands and Savannas? *Annual Review of Ecology, Evolution, and Systematics*, 39 (1), 641–659. DOI: 10.1146/annurev.ecolsys.39.110707.173411.

Bond, W.J., Woodward, F.I., and Midgley, G.F., 2005. The global distribution of ecosystems in a world without fire. *New Phytologist*, 165 (2), 525–538. DOI: 10.1111/j.1469-8137.2004.01252.x.

Vanden Borre, J., Paelinckx, D., Mücher, C.A., Kooistra, L., Haest, B., De Blust, G., and Schmidt, A.M., 2011. Integrating remote sensing in Natura 2000 habitat monitoring: Prospects on the way forward. *Journal for Nature Conservation*, 19 (2), 116–125. DOI: 10.1016/j.jnc.2010.07.003.

Bowman, D.M.J.S., Balch, J., Artaxo, P., Bond, W.J., Cochrane, M.A., D'Antonio, C.M., DeFries, R., Johnston, F.H., Keeley, J.E., Krawchuk, M.A., Kull, C.A., Mack, M., Moritz, M.A., Pyne, S., Roos, C.I., Scott, A.C., Sodhi, N.S., and Swetnam, T.W., 2011. The human dimension of fire regimes on Earth. *Journal of Biogeography*, 38 (12), 2223–2236. DOI: 10.1111/j.1365-2699.2011.02595.x.

Bowman, D.M.J.S., Balch, J.K., Artaxo, P., Bond, W.J., Carlson, J.M., Cochrane, M.A., D'Antonio, C.M., DeFries, R.S., Doyle, J.C., Harrison, S.P., Johnston, F.H., Keeley, J.E., Krawchuk, M.A., Kull, C.A., Marston, J.B., Moritz, M.A., Prentice, I.C., Roos, C.I., Scott, A.C., Swetnam, T.W., van der Werf, G.R., and Pyne, S.J., 2009. Fire in the Earth System. *Science*, 324 (5926), 481–484. DOI: 10.1126/science.1163886.

Bowman, D.M.J.S. and Boggs, G.S., 2006. Fire ecology. *Progress in Physical Geography: Earth and Environment*, 30 (2), 245–257. DOI: 10.1191/0309133306pp482pr.

Bowman, D.M.J.S. and Franklin, D.C., 2005. Fire ecology. *Progress in Physical Geography: Earth and Environment*, 29 (2), 248–255. DOI: 10.1191/0309133305pp446pr.

Bowman, D.M.J.S., Williamson, G.J., Abatzoglou, J.T., Kolden, C.A., Cochrane, M.A., and Smith, A.M.S.S., 2017. Human exposure and sensitivity to globally extreme wildfire events. *Nature Ecology & Evolution*, 1 (3), 0058. DOI: 10.1038/s41559-016-0058.

Bradstock, R.A., 2008. Effects of large fires on biodiversity in south-eastern Australia: Disaster or template for diversity? *International Journal of Wildland Fire*, 17 (6), 809–822. DOI: 10.1071/WF07153.

Burton, F.D., 2009. *Fire: The Spark That Ignited Human Evolution*. Illustrate. Albuquerque: University of New Mexico Press.

Butry, D.T., Mercer, E.D., Prestemon, J.P., Pye, J.M., and Holmes, T.P., 2001. What Is the Price of Catastrophic Wildfire? *Journal of Forestry*, 99 (11), 9–17. DOI: 10.1093/JOF/99.11.9.

Cabello, J., Fernández, N., Alcaraz-Segura, D., Oyonarte, C., Piñeiro, G., Altesor, A., Delibes, M., and Paruelo, J.M., 2012. The ecosystem functioning dimension in conservation: insights from remote sensing. *Biodiversity and Conservation*, 21 (13), 3287–3305. DOI: 10.1007/s10531-012-0370-7.

Catry, F.X.F., Rego, F.C.F.F.C., Bação, F.L., Moreira, 2009. Modeling and mapping wildfire ignition risk in Portugal. *International Journal of Wildland Fire*, 18 (8), 921. DOI: 10.1071/WF07123.

Cazorla, B.P., Cabello, J., Peñas, J., Garcillán, P.P., Reyes, A., and Alcaraz-Segura, D., 2020. Incorporating Ecosystem Functional Diversity into Geographic Conservation Priorities Using Remotely Sensed Ecosystem Functional Types. *Ecosystems*, 24 (3), 1–17. DOI: 10.1007/s10021-020-00533-4.

Chapin, F.S., Matson, P.A., and Vitousek, P.M., 2011. *Principles of Terrestrial Ecosystem Ecology*. New York, NY: Springer New York. DOI: 10.1007/978-1-4419-9504-9.

Chuvieco, E., 2009. *Earth observation of wildland fires in mediterranean ecosystems*. Springer Berlin Heidelberg. DOI: 10.1007/978-3-642-01754-4.

Chuvieco, E., 2012. *Remote Sensing of Large Wildfires: in the European Mediterranean Basin*. Springer Science & Business Media.

Chuvieco, E., 2020. *Fundamentals of Remote Sensing: An Environmental Approach*. 3rd ed. CRC Press.

Chuvieco, E., Aguado, I., Salas, J., García, M., Yebra, M., and Oliva, P., 2020. Satellite Remote Sensing Contributions to Wildland Fire Science and Management. *Current Forestry Reports*, 6 (2), 81–96. DOI: 10.1007/s40725-020-00116-5.

Clemente, A.S., Rego, F.C., and Correia, O.A., 2005. Growth, water relations and photosynthesis of seedlings and resprouts after fire. *Acta Oecologica*, 27 (3), 233–243. DOI: 10.1016/j.actao.2005.01.005.

Clerici, N., Weissteiner, C.J., and Gerard, F., 2012. Exploring the use of MODIS NDVI-based phenology indicators for classifying forest general habitat categories. *Remote Sensing*, 4 (6), 1781–1803. DOI: 10.3390/rs4061781.

Cochrane, M.A., 2003. Fire science for rainforests. *Nature*, 421 (6926), 913–919. DOI: 10.1038/nature01437.

Coops, N.C., Wulder, M.A., Duro, D.C., Han, T., and Berry, S., 2008. The development of a Canadian dynamic habitat index using multi-temporal satellite estimates of canopy light absorbance. *Ecological Indicators*, 8 (5), 754–766. DOI: 10.1016/j.ecolind.2008.01.007.

Costanza, R., d'Arge, R., de Groot, R., Farber, S., Grasso, M., Hannon, B., Limburg, K., Naeem, S., O'Neill, R. V., Paruelo, J.M., Raskin, R.G., Sutton, P., and van den Belt, M., 1997. The value of the world's ecosystem services and natural capital. *Nature*, 387 (6630), 253–260. DOI: 10.1038/387253a0.

Duro, D.C., Coops, N.C., Wulder, M.A., and Han, T., 2007. Development of a large area biodiversity monitoring system driven by remote sensing. *Progress in Physical Geography*, 31 (3), 235–260. DOI: 10.1177/0309133307079054.

Epting, J., Verbyla, D., and Sorbel, B., 2005. Evaluation of remotely sensed indices for assessing burn severity in interior Alaska using Landsat TM and ETM+. *Remote Sensing of Environment*, 96 (3–4), 328–339. DOI: 10.1016/j.rse.2005.03.002.

Faivre, N., Roche, P., Boer, M.M., McCaw, L., and Grierson, P.F., 2011. Characterization of landscape pyrodiversity in Mediterranean environments: Contrasts and similarities between south-western Australia and south-eastern France. *Landscape Ecology*, 26 (4), 557–571. DOI: 10.1007/s10980-011-9582-6.

Faour, G., Kheir, R.B., Karam, C., Ayoub, M., and Abdallah, C., 2004. *Forest fire fighting in Lebanon using remote sensing and GIS*. DOI: 10.13140/RG.2.2.28371.78884.

Fernández-Manso, A., Fernández-Manso, O., and Quintano, C., 2016. SENTINEL-2A red-edge spectral indices suitability for discriminating burn severity. *International Journal of Applied Earth Observation and Geoinformation*, 50, 170–175. DOI: 10.1016/j.jag.2016.03.005.

Fischer, A.P., Spies, T.A., Steelman, T.A., Moseley, C., Johnson, B.R., Bailey, J.D., Ager, A.A., Bourgeron, P., Charnley, S., Collins, B.M., Kline, J.D., Leahy, J.E., Littell, J.S., Millington, J. DA, Nielsen-Pincus, M., Olsen, C.S., Paveglio, T.B., Roos, C.I., Steen-Adams, M.M., Stevens, F.R., Vukomanovic, J., White, E.M., and Bowman, D.M., 2016. Wildfire risk as a socioecological pathology. *Frontiers in Ecology and the Environment*, 14 (5), 276–284. DOI: 10.1002/fee.1283.

Folke, C., Carpenter, S., Walker, B., Scheffer, M., Elmqvist, T., Gunderson, L., and Holling, C.S., 2004. Regime Shifts, Resilience, and Biodiversity in Ecosystem Management.

Annual Review of Ecology, Evolution, and Systematics, 35 (1), 557–581. DOI: 10.1146/annurev.ecolsys.35.021103.105711.

Fornacca, D., Ren, G., and Xiao, W., 2018. Evaluating the Best Spectral Indices for the Detection of Burn Scars at Several Post-Fire Dates in a Mountainous Region of Northwest Yunnan, China. *Remote Sensing*, 10 (8), 1196. DOI: 10.3390/rs10081196.

Frazier, A.E., Renschler, C.S., and Miles, S.B., 2013. Evaluating post-disaster ecosystem resilience using MODIS GPP data. *International Journal of Applied Earth Observation and Geoinformation*, 21, 43–52. DOI: 10.1016/j.jag.2012.07.019.

Fusco, E.J., Abatzoglou, J.T., Balch, J.K., Finn, J.T., and Bradley, B.A., 2016. Quantifying the human influence on fire ignition across the western USA. *Ecological Applications*, 26 (8), 2388–2399. DOI: 10.1002/eap.1395.

Gale, M.G., Cary, G.J., Van Dijk, A.I.J.M., and Yebra, M., 2021. Forest fire fuel through the lens of remote sensing: Review of approaches, challenges and future directions in the remote sensing of biotic determinants of fire behaviour. *Remote Sensing of Environment*. DOI: 10.1016/j.rse.2020.112282.

GCOS, 2010. *Implementation Plan for the Global Observing System for Climate in support of the UNFCCC (2010 Udate)*. Geneva: World Meteorological Organization (WMO).

Giglio, L., Boschetti, L., Roy, D.P., Humber, M.L., and Justice, C.O., 2018. The Collection 6 MODIS burned area mapping algorithm and product. *Remote Sensing of Environment*, 217, 72–85. DOI: 10.1016/j.rse.2018.08.005.

Gill, A.M., Stephens, S.L., and Cary, G.J., 2013. The worldwide ‘wildfire’ problem. *Ecological Applications*, 23 (2), 438–454. DOI: 10.1890/10-2213.1.

Gonçalves, J., Alves, P., Pôças, I., Marcos, B., Sousa-Silva, R., Lomba, Â., and Honrado, J.P., 2016. Exploring the spatiotemporal dynamics of habitat suitability to improve conservation management of a vulnerable plant species. *Biodiversity and Conservation*, 25 (14). DOI: 10.1007/s10531-016-1206-7.

Gouveia, C., DaCamara, C.C., and Trigo, R.M., 2010. Post-fire vegetation recovery in Portugal based on spot/vegetation data. *Natural Hazards and Earth System Science*, 10 (4), 673–684. DOI: 10.5194/nhess-10-673-2010.

Hantson, S., Pueyo, S., and Chuvieco, E., 2015. Global fire size distribution is driven by human impact and climate. *Global Ecology and Biogeography*, 24 (1), 77–86. DOI: 10.1111/geb.12246.

Harris, S., Veraverbeke, S., and Hook, S., 2011. Evaluating Spectral Indices for Assessing Fire Severity in Chaparral Ecosystems (Southern California) Using MODIS/ASTER (MASTER) Airborne Simulator Data. *Remote Sensing*, 3 (12), 2403–2419. DOI: 10.3390/rs3112403.

Harrison, S.P., Marlon, J.R., and Bartlein, P.J., 2010. Fire in the Earth System. *In*: *Changing Climates, Earth Systems and Society*. Springer Netherlands, 21–48. DOI: 10.1007/978-90-481-8716-4_3.

He, K.S., Bradley, B.A., Cord, A.F., Rocchini, D., Tuanmu, M.-N.N., Schmidtlein, S., Turner, W., Wegmann, M., and Pettorelli, N., 2015. Will remote sensing shape the next generation of species distribution models? *Remote Sensing in Ecology and Conservation*, 1 (1), 4–18. DOI: 10.1002/rse2.7.

He, T. and Lamont, B.B., 2018. Baptism by fire: the pivotal role of ancient conflagrations in evolution of the Earth's flora. *National Science Review*, 5 (2), 237–254. DOI: 10.1093/nsr/nwx041.

He, T., Lamont, B.B., and Pausas, J.G., 2019. Fire as a key driver of Earth's biodiversity. *Biological Reviews*, 94 (6), 1983–2010. DOI: 10.1111/brv.12544.

Jax, K., 2005. Function and "functioning" in ecology: what does it mean? *Oikos*, 111 (3), 641–648. DOI: 10.1111/j.1600-0706.2005.13851.x.

Jensen, J.R., 2007. *Remote Sensing of the Environment: An Earth Resource Perspective*. 2nd ed. Prentice Hall.

Jensen, S.E. and McPherson, G.R., 2008. *Living with Fire: Fire Ecology and Policy for the Twenty-first Century*. University of California Press.

João, T., João, G., Bruno, M., and João, H., 2018. Indicator-based assessment of post-fire recovery dynamics using satellite NDVI time-series. *Ecological Indicators*, 89, 199–212. DOI: 10.1016/j.ecolind.2018.02.008.

Jobbágy, E.G., Sala, O.E., Paruelo, J.M., Jobbágy, E.G., Sala, O.E., and Paruelo, J.M., 2002. Patterns and controls of primary production in the patagonian steppe: A remote sensing approach : Regional ecological analysis. *Ecology*, 83 (2), 307–319.

Johnstone, J.F., Chapin, F.S., Hollingsworth, T.N., Mack, M.C., Romanovsky, V., and Turetsky, M., 2010. Fire, climate change, and forest resilience in interior alaska1. *Canadian Journal of Forest Research*, 40 (7), 1302–1312. DOI: 10.1139/X10-061.

Jones, H.G. and Vaughan, R.A., 2010. *Remote Sensing of Vegetation: Principles, Techniques, and Applications*. OUP Oxford.

Kasischke, E.S. and Turetsky, M.R., 2006. Recent changes in the fire regime across the North American boreal region - Spatial and temporal patterns of burning across Canada and Alaska. *Geophysical Research Letters*, 33 (9). DOI: 10.1029/2006GL025677.

Keeley, J.E., 2009. Fire intensity, fire severity and burn severity: a brief review and suggested usage. *International Journal of Wildland Fire*, 18 (1), 116. DOI: 10.1071/WF07049.

Kelly, L.T., Giljohann, K.M., Duane, A., Aquilué, N., Archibald, S., Batllori, E., Bennett, A.F., Buckland, S.T., Canelles, Q., Clarke, M.F., Fortin, M.-J., Hermoso, V., Herrando, S., Keane, R.E., Lake, F.K., McCarthy, M.A., Morán-Ordóñez, A., Parr, C.L., Pausas, J.G., Penman, T.D., Regos, A., Rumpff, L., Santos, J.L., Smith, A.L., Syphard, A.D., Tingley, M.W., and Brotons, L., 2020. Fire and biodiversity in the Anthropocene. *Science*, 370 (6519), eabb0355. DOI: 10.1126/science.abb0355.

Kerle, N. and Bakker, W.H., 2004. *Principles of Remote Sensing: An Introductory Textbook*. 3rd ed. International Institute for Geo-Information Science and Earth observation.

Kitzberger, T., Brown, P.M., Heyerdahl, E.K., Swetnam, T.W., and Veblen, T.T., 2007. Contingent Pacific-Atlantic Ocean influence on multicentury wildfire synchrony over western North America. *Proceedings of the National Academy of Sciences of the United States of America*, 104 (2), 543–548. DOI: 10.1073/pnas.0606078104.

Krawchuk, M.A., Moritz, M.A., Parisien, M.-A., Van Dorn, J., and Hayhoe, K., 2009. Global Pyrogeography: the Current and Future Distribution of Wildfire. *PLoS ONE*, 4 (4), e5102. DOI: 10.1371/journal.pone.0005102.

Kwok, R., 2018. Ecology's remote-sensing revolution. *Nature*, 556 (7699), 137–138. DOI: 10.1038/d41586-018-03924-9.

Langmann, B., Duncan, B., Textor, C., Trentmann, J., and van der Werf, G.R., 2009. Vegetation fire emissions and their impact on air pollution and climate. *Atmospheric Environment*, 43 (1), 107–116. DOI: 10.1016/j.atmosenv.2008.09.047.

Lavender, S. and Lavender, A., 2016. *Practical Handbook of Remote Sensing*. CRC Press.

Lawson, D.M., Regan, H.M., Zedler, P.H., and Franklin, J., 2010. Cumulative effects of land use, altered fire regime and climate change on persistence of Ceanothus verrucosus, a rare, fire-dependent plant species. *Global Change Biology*, 16 (9), 2518–2529. DOI: 10.1111/j.1365-2486.2009.02143.x.

Lechner, A.M., Foody, G.M., and Boyd, D.S., 2020. Applications in Remote Sensing to Forest Ecology and Management. *One Earth*, 2 (5), 405–412. DOI: 10.1016/j.oneear.2020.05.001.

Lentile, L.B., Holden, Z.A., Smith, A.M.S.S., Falkowski, M.J., Hudak, A.T., Morgan, P., Lewis, S.A., Gessler, P.E., Benson, N.C., Lentile, L.B., Holden, Z.A., Smith, A.M.S.S., Falkowski, M.J., Hudak, A.T., Morgan, P., Lewis, S.A., Gessler, P.E., and Benson, N.C., 2006. Remote sensing techniques to assess active fire characteristics and post-fire effects. *International Journal of Wildland Fire*, 15 (3), 319. DOI: 10.1071/WF05097.

Lillesand, T., Kiefer, R.W., and Chipman, J., 2015. *Remote Sensing and Image Interpretation*. 7th ed. John Wiley & Sons.

Lloret, F., Estevan, H., Vayreda, J., and Terradas, J., 2005. Fire regenerative syndromes of forest woody species across fire and climatic gradients. *Oecologia*, 146 (3), 461–468. DOI: 10.1007/s00442-005-0206-1.

Lloret, F., Pausas, J.G., and Vilà, M., 2003. Responses of Mediterranean Plant Species to different fire frequencies in Garraf Natural Park (Catalonia, Spain): Field observations and modelling predictions. *Plant Ecology*, 167 (2), 223–235. DOI: 10.1023/A:1023911031155.

Lohman, D.J., Bickford, D., and Sodhi, N.S., 2007. The Burning Issue. *Science*, 316 (5823), 376. DOI: 10.1126/science.1140278.

McCaffrey, S., 2004. Thinking of Wildfire as a Natural Hazard. *Society & Natural Resources*, 17 (6), 509–516. DOI: 10.1080/08941920490452445.

McLauchlan, K.K., Higuera, P.E., Miesel, J., Rogers, B.M., Schweitzer, J., Shuman, J.K., Tepley, A.J., Varner, J.M., Veblen, T.T., Adalsteinsson, S.A., Balch, J.K., Baker, P., Batllori, E., Bigio, E., Brando, P., Cattau, M., Chipman, M.L., Coen, J., Crandall, R., Daniels, L., Enright, N., Gross, W.S., Harvey, B.J., Hatten, J.A., Hermann, S., Hewitt, R.E., Kobziar, L.N., Landesmann, J.B., Loranty, M.M., Maezumi, S.Y., Mearns, L., Moritz, M., Myers, J.A., Pausas, J.G., Pellegrini, A.F.A., Platt, W.J., Roozeboom, J., Safford, H., Santos, F., Scheller, R.M., Sherriff, R.L., Smith, K.G., Smith, M.D., and Watts, A.C., 2020. Fire as a fundamental ecological process: Research advances and frontiers. *Journal of Ecology*, 108 (5), 2047–2069. DOI: 10.1111/1365-2745.13403.

McPherson, G.R. and DeStefano, S., 2003. *Applied Ecology and Natural Resource Management*. Cambridge University Press.

Milchunas, D.G. and Lauenroth, W.K., 1995. Inertia in plant community structure: state changes after cessation of nutrient enrichment stress. *Ecological Applications*, 5 (2), 1195–2005. DOI: 10.2307/1942035.

Mildrexler, D.J., Zhao, M., and Running, S.W., 2009. Testing a MODIS Global Disturbance Index across North America. *Remote Sensing of Environment*, 113 (10), 2103–2117. DOI: 10.1016/j.rse.2009.05.016.

Miller, J.D., Skinner, C.N., Safford, H.D., Knapp, E.E., and Ramirez, C.M., 2012. Trends and causes of severity, size, and number of fires in northwestern California, USA. *Ecological Applications*, 22 (1), 184–203. DOI: 10.1890/10-2108.1.

Moritz, M.A., Batllori, E., Bradstock, R.A., Gill, A.M., Handmer, J., Hessburg, P.F., Leonard, J., McCaffrey, S., Odion, D.C., Schoennagel, T., and Syphard, A.D., 2014. Learning to coexist with wildfire. *Nature*, 515 (7525), 58–66. DOI: 10.1038/nature13946.

Moritz, M.A., Morais, M.E., Summerell, L.A., Carlson, J.M., and Doyle, J., 2005. Wildfires, complexity, and highly optimized tolerance. *Proceedings of the National Academy of Sciences of the United States of America*, 102 (50), 17912–17917. DOI: 10.1073/pnas.0508985102.

Mouillot, D., Graham, N.A.J., Villéger, S., Mason, N.W.H., and Bellwood, D.R., 2013. A functional approach reveals community responses to disturbances. *Trends in Ecology & Evolution*, 28 (3), 167–177. DOI: 10.1016/j.tree.2012.10.004.

Murray, N.J., Keith, D.A., Bland, L.M., Ferrari, R., Lyons, M.B., Lucas, R., Pettorelli, N., and Nicholson, E., 2018. The role of satellite remote sensing in structured ecosystem risk assessments. *Science of The Total Environment*, 619–620, 249–257. DOI: 10.1016/j.scitotenv.2017.11.034.

Nagendra, H., Lucas, R., Honrado, J.P., Jongman, R.H.G., Tarantino, C., Adamo, M., and Mairota, P., 2013. Remote sensing for conservation monitoring: Assessing protected areas, habitat extent, habitat condition, species diversity, and threats. *Ecological Indicators*, 33, 45–59. DOI: 10.1016/j.ecolind.2012.09.014.

Noss, R.F., 1990. Indicators for Monitoring Biodiversity: A Hierarchical Approach. *Conservation Biology*, 4 (4), 355–364. DOI: 10.1111/j.1523-1739.1990.tb00309.x.

Parks, S.A., Holsinger, L.M., Koontz, M.J., Collins, L., Whitman, E., Parisien, M.-A., Loehman, R.A., Barnes, J.L., Bourdon, J.-F., Boucher, J., Boucher, Y., Caprio, A.C., Collingwood, A., Hall, R.J., Park, J., Saperstein, L.B., Smetanka, C., Smith, R.J., Soverel, N., 2019. Giving Ecological Meaning to Satellite-Derived Fire Severity

Metrics across North American Forests. *Remote Sensing*, 11 (14), 1735. DOI: 10.3390/rs11141735.

Parsons, R., Linn, R., Pimont, F., Hoffman, C., Sauer, J., Winterkamp, J., Sieg, C., and Jolly, W., 2017. Numerical Investigation of Aggregated Fuel Spatial Pattern Impacts on Fire Behavior. *Land*, 6 (2), 43. DOI: 10.3390/land6020043.

Paruelo, J.M., Jobbágy, E.G., and Sala, O.E., 2001. Current Distribution of Ecosystem Functional Types in Temperate South America. *Ecosystems*, 4 (7), 683–698. DOI: 10.1007/s10021-001-0037-9.

Pausas, J.G. and Keeley, J.E., 2009. A burning story: The role of fire in the history of life. *BioScience*, 59 (7), 593–601. DOI: 10.1525/bio.2009.59.7.10.

Pausas, J.G. and Keeley, J.E., 2014. *Evolutionary ecology of resprouting and seeding in fire-prone ecosystems*. New Phytologist. Blackwell Publishing Ltd. DOI: 10.1111/nph.12921.

Pausas, J.G. and Keeley, J.E., 2019. Wildfires as an ecosystem service. *Frontiers in Ecology and the Environment*, 17 (5). DOI: 10.1002/fee.2044.

Pausas, J.G. and Parr, C.L., 2018. Towards an understanding of the evolutionary role of fire in animals. *Evolutionary Ecology*, 32 (2–3), 113–125. DOI: 10.1007/s10682-018-9927-6.

Pechony, O. and Shindell, D.T., 2010. Driving forces of global wildfires over the past millennium and the forthcoming century. *Proceedings of the National Academy of Sciences of the United States of America*, 107 (45), 19167–19170. DOI: 10.1073/pnas.1003669107.

Pereira, H.M., Ferrier, S., Walters, M., Geller, G.N., Jongman, R.H.G., Scholes, R.J., Bruford, M.W., Brummitt, N., Butchart, S.H.M., Cardoso, A.C., Coops, N.C., Dulloo, E., Faith, D.P., Freyhof, J., Gregory, R.D., Heip, C., Hoft, R., Hurtt, G., Jetz, W., Karp, D.S., McGeoch, M.A., Obura, D., Onoda, Y., Pettorelli, N., Reyers, B., Sayre, R., Scharlemann, J.P.W., Stuart, S.N., Turak, E., Walpole, M., and Wegmann, M., 2013. Essential Biodiversity Variables. *Science*, 339 (6117), 277–278. DOI: 10.1126/science.1229931.

Pérez-Cabello, F., Montorio, R., and Alves, D.B., 2021. Remote Sensing Techniques to assess Post-Fire Vegetation Recovery. *Current Opinion in Environmental Science & Health*, 21, 100251. DOI: 10.1016/j.coesh.2021.100251.

Petropoulos, G., Carlson, T.N., Wooster, M.J., and Islam, S., 2009. A review of Ts/VI remote sensing based methods for the retrieval of land surface energy fluxes and soil surface

moisture. *Progress in Physical Geography*, 33 (2), 224–250. DOI: 10.1177/0309133309338997.

Pettorelli, N., Laurance, W.F., O'Brien, T.G., Wegmann, M., Nagendra, H., and Turner, W., 2014. Satellite remote sensing for applied ecologists: opportunities and challenges. *Journal of Applied Ecology*, 51 (4), 839–848. DOI: 10.1111/1365-2664.12261.

Pettorelli, N., Schulte to Bühne, H., Tulloch, A., Dubois, G., Macinnis-Ng, C., Queirós, A.M., Keith, D.A., Wegmann, M., Schrodt, F., Stellmes, M., Sonnenschein, R., Geller, G.N., Roy, S., Somers, B., Murray, N., Bland, L., Geijzendorffer, I., Kerr, J.T., Broszeit, S., Leitão, P.J., Duncan, C., El Serafy, G., He, K.S., Blanchard, J.L., Lucas, R., Mairota, P., Webb, T.J., and Nicholson, E., 2017. Satellite remote sensing of ecosystem functions: opportunities, challenges and way forward. *Remote Sensing in Ecology and Conservation*, 4 (2), 71–93. DOI: 10.1002/rse2.59.

Pettorelli, N., Vik, J.O., Mysterud, A., Gaillard, J.-M., Tucker, C.J., and Stenseth, N.C., 2005. Using the satellite-derived NDVI to assess ecological responses to environmental change. *Trends in Ecology & Evolution*, 20 (9), 503–510. DOI: 10.1016/j.tree.2005.05.011.

Pettorelli, N., Wegmann, M., Skidmore, A., Mücher, S., Dawson, T.P., Fernandez, M., Lucas, R., Schaepman, M.E., Wang, T., O'Connor, B., Jongman, R.H.G., Kempeneers, P., Sonnenschein, R., Leidner, A.K., Böhm, M., He, K.S., Nagendra, H., Dubois, G., Fatoyinbo, T., Hansen, M.C., Paganini, M., de Klerk, H.M., Asner, G.P., Kerr, J.T., Estes, A.B., Schmeller, D.S., Heiden, U., Rocchini, D., Pereira, H.M., Turak, E., Fernandez, N., Lausch, A., Cho, M.A., Alcaraz-Segura, D., McGeoch, M.A., Turner, W., Mueller, A., St-Louis, V., Penner, J., Vihervaara, P., Belward, A., Reyers, B., and Geller, G.N., 2016. Framing the concept of satellite remote sensing essential biodiversity variables: challenges and future directions. *Remote Sensing in Ecology and Conservation*, 2 (3), 122–131. DOI: 10.1002/rse2.15.

Pimont, F., Dupuy, J.L., Linn, R.R., and Dupont, S., 2011. Impacts of tree canopy structure on wind flows and fire propagation simulated with FIRETEC. *Annals of Forest Science*, 68 (3), 523–530. DOI: 10.1007/s13595-011-0061-7.

Purkis, S.J. and Klemas, V. V., 2011. *Remote Sensing and Global Environmental Change*. John Wiley & Sons.

Quintiere, J.G., 2006. *Fundamentals of Fire Phenomena*. Fundamentals of Fire Phenomena. Chichester, UK: John Wiley & Sons, Ltd. DOI: 10.1002/0470091150.

Ramanathan, V. and Carmichael, G., 2008. Global and regional climate changes due to black carbon. *Nature Geoscience*, 1 (4), 221–227. DOI: 10.1038/ngeo156.

Randerson, J.T., Chen, Y., Van Der Werf, G.R., Rogers, B.M., and Morton, D.C., 2012. Global burned area and biomass burning emissions from small fires. *Journal of Geophysical Research G: Biogeosciences*, 117 (4), 4012. DOI: 10.1029/2012JG002128.

Randerson, J.T., Liu, H., Flanner, M.G., Chambers, S.D., Jin, Y., Hess, P.G., Pfister, G., Mack, M.C., Treseder, K.K., Welp, L.R., Chapin, F.S., Harden, J.W., Goulden, M.L., Lyons, E., Neff, J.C., Schuur, E.A.G., and Zender, C.S., 2006. The Impact of Boreal Forest Fire on Climate Warming. *Science*, 314 (5802), 1130–1132. DOI: 10.1126/science.1132075.

Regos, A., Aquilué, N., Retana, J., De Cáceres, M., and Brotons, L., 2014. Using Unplanned Fires to Help Suppressing Future Large Fires in Mediterranean Forests. *PLOS ONE*, 9 (4), e94906. DOI: 10.1371/journal.pone.0094906.

Regos, A., Gómez-Rodríguez, P., Arenas-Castro, S., Tapia, L., Vidal, M., and Domínguez, J., 2020. Model-Assisted Bird Monitoring Based on Remotely Sensed Ecosystem Functioning and Atlas Data. *Remote Sensing*, 12 (16), 2549. DOI: 10.3390/rs12162549.

Reid, C.E., Brauer, M., Johnston, F.H., Jerrett, M., Balmes, J.R., and Elliott, C.T., 2016. Critical Review of Health Impacts of Wildfire Smoke Exposure. *Environmental Health Perspectives*, 124 (9), 1334–1343. DOI: 10.1289/ehp.1409277.

Reiss, J., Bridle, J.R., Montoya, J.M., and Woodward, G., 2009. Emerging horizons in biodiversity and ecosystem functioning research. *Trends in Ecology & Evolution*, 24 (9), 505–514. DOI: 10.1016/j.tree.2009.03.018.

Rocchini, D., Andreo, V., Förster, M., Garzon-Lopez, C.X., Gutierrez, A.P., Gillespie, T.W., Hauffe, H.C., He, K.S., Kleinschmit, B., Mairota, P., Marcantonio, M., Metz, M., Nagendra, H., Pareeth, S., Ponti, L., Ricotta, C., Rizzoli, A., Schaab, G., Zebisch, M., Zorer, R., Neteler, M., Förster, 2015. Potential of remote sensing to predict species invasions: A modelling perspective. *Progress in Physical Geography*, 39 (3), 0309133315574659-. DOI: 10.1177/0309133315574659.

Rogan, J. and Yool, S.R., 2001. Mapping fire-induced vegetation depletion in the Peloncillo Mountains, Arizona and New Mexico. *International Journal of Remote Sensing*, 22 (16), 3101–3121. DOI: 10.1080/01431160152558279.

Rose, R.A., Byler, D., Eastman, J.R., Fleishman, E., Geller, G., Goetz, S., Guild, L., Hamilton, H., Hansen, M., Headley, R., Hewson, J., Horning, N., Kaplin, B.A., Laporte, N., Leidner, A., Leimgruber, P., Morisette, J., Musinsky, J., Pintea, L., Prados, A., Radeloff, V.C., Rowen, M., Saatchi, S., Schill, S., Tabor, K., Turner, W., Vodacek, A., Vogelmann, J., Wegmann, M., Wilkie, D., and Wilson, C., 2015. Ten ways remote sensing can contribute to conservation. *Conservation Biology*, 29 (2), 350–359. DOI: 10.1111/cobi.12397.

Running, S.W., 2006. CLIMATE CHANGE: Is Global Warming Causing More, Larger Wildfires? *Science*, 313 (5789), 927–928. DOI: 10.1126/science.1130370.

Saatchi, S., Halligan, K., Despain, D.G., and Crabtree, R.L., 2007. Estimation of forest fuel load from radar remote sensing. *IEEE Transactions on Geoscience and Remote Sensing*, 45 (6), 1726–1740. DOI: 10.1109/TGRS.2006.887002.

de Santana, M.M.M., Mariano-Neto, E., de Vasconcelos, R.N., Dodonov, P., and Medeiros, J.M.M., 2021. Mapping the research history, collaborations and trends of remote sensing in fire ecology. *Scientometrics*, 1–30. DOI: 10.1007/s11192-020-03805-x.

Scheffer, M., Carpenter, S.R., Dakos, V., and van Nes, E.H., 2015. Generic Indicators of Ecological Resilience: Inferring the Chance of a Critical Transition. *Annual Review of Ecology, Evolution, and Systematics*, 46 (1), 145–167. DOI: 10.1146/annurev-ecolsys-112414-054242.

Schimel, D. and Baker, D., 2002. The wildfire factor. *Nature*, 420 (6911), 29–30. DOI: 10.1038/420029a.

Schroeder, T.A., Healey, S.P., Moisen, G.G., Frescino, T.S., Cohen, W.B., Huang, C., Kennedy, R.E., and Yang, Z., 2014. Improving estimates of forest disturbance by combining observations from Landsat time series with U.S. Forest Service Forest Inventory and Analysis data. *Remote Sensing of Environment*, 154, 61–73. DOI: 10.1016/j.rse.2014.08.005.

Schroeder, W., Oliva, P., Giglio, L., Quayle, B., Lorenz, E., and Morelli, F., 2016. Active fire detection using Landsat-8/OLI data. *Remote Sensing of Environment*, 185, 210–220. DOI: 10.1016/j.rse.2015.08.032.

Scott, A.C., 2020. *Fire: a Very Short Introduction*. Oxford University Press.

Scott, A.C. and Glasspool, I.J., 2006. The diversification of Paleozoic fire systems and fluctuations in atmospheric oxygen concentration. *Proceedings of the National Academy of Sciences of the United States of America*, 103 (29), 10861–10865. DOI: 10.1073/pnas.0604090103.

Ségalen, L., Lee-Thorp, J.A., and Cerling, T., 2007. Timing of C4 grass expansion across sub-Saharan Africa. *Journal of Human Evolution*, 53 (5), 549–559. DOI: 10.1016/j.jhevol.2006.12.010.

Sherstjuk, V., Zharikova, M., and Sokol, I., 2018. Forest Fire Monitoring System Based on UAV Team, Remote Sensing, and Image Processing. *In*: *Proceedings of the 2018 IEEE 2nd International Conference on Data Stream Mining and Processing, DSMP 2018*. Institute of Electrical and Electronics Engineers Inc., 590–594. DOI: 10.1109/DSMP.2018.8478590.

Sil, Â., Azevedo, J.C., Fernandes, P.M., Regos, A., Vaz, A.S., and Honrado, J.P., 2019. (Wild)fire is not an ecosystem service. *Frontiers in Ecology and the Environment*, 17 (8), 429–430. DOI: 10.1002/fee.2106.

Smith, A.M.S.S., Kolden, C.A., Tinkham, W.T., Talhelm, A.F., Marshall, J.D., Hudak, A.T., Boschetti, L., Falkowski, M.J., Greenberg, J.A., Anderson, J.W., Kliskey, A., Alessa, L., Keefe, R.F., and Gosz, J.R., 2014. Remote sensing the vulnerability of vegetation in natural terrestrial ecosystems. *Remote Sensing of Environment*, 154, 322–337. DOI: 10.1016/j.rse.2014.03.038.

Stevens-Rumann, C.S., Kemp, K.B., Higuera, P.E., Harvey, B.J., Rother, M.T., Donato, D.C., Morgan, P., and Veblen, T.T., 2018. Evidence for declining forest resilience to wildfires under climate change. *Ecology Letters*, 21 (2), 243–252. DOI: 10.1111/ele.12889.

Syphard, A.D., Radeloff, V.C., Keeley, J.E., Hawbaker, T.J., Clayton, M.K., Stewart, S.I., and Hammer, R.B., 2007. Human influence on California fire regimes. *Ecological Applications*, 17 (5), 1388–1402. DOI: 10.1890/06-1128.1.

Szpakowski, D.M. and Jensen, J.L.R., 2019. A Review of the Applications of Remote Sensing in Fire Ecology. *Remote Sensing*, 11 (22), 2638. DOI: 10.3390/rs11222638.

Tedim, F., Leone, V., Amraoui, M., Bouillon, C., Coughlan, M., Delogu, G., Fernandes, P., Ferreira, C., McCaffrey, S., McGee, T., Parente, J., Paton, D., Pereira, M., Ribeiro, L., Viegas, D., and Xanthopoulos, G., 2018. Defining Extreme Wildfire Events: Difficulties, Challenges, and Impacts. *Fire*, 1 (1), 9. DOI: 10.3390/fire1010009.

Tedim, F., Remelgado, R., Borges, C., Carvalho, S., and Martins, J., 2013. Exploring the occurrence of mega-fires in Portugal. *Forest Ecology and Management*, 294, 86–96. DOI: 10.1016/j.foreco.2012.07.031.

Telesca, L. and Pereira, M.G., 2010. Time-clustering investigation of fire temporal fluctuations in Portugal. *Natural Hazards and Earth System Science*, 10 (4), 661–666. DOI: 10.5194/nhess-10-661-2010.

Theobald, D.M. and Romme, W.H., 2007. Expansion of the US wildland-urban interface. *Landscape and Urban Planning*, 83 (4), 340–354. DOI: 10.1016/j.landurbplan.2007.06.002.

Turner, W., 2003. Remote sensing for biodiversity science and conservation. *Trends in Ecology & Evolution*, 18 (6), 306–314. DOI: 10.1016/S0169-5347(03)00070-3.

Vaz, A.S., Alcaraz-Segura, D., Vicente, J.R., and Honrado, J.P., 2019. The Many Roles of Remote Sensing in Invasion Science. *Frontiers in Ecology and Evolution*, 7, 370. DOI: 10.3389/fevo.2019.00370.

Vaz, A.S., Kueffer, C., Kull, C.A., Richardson, D.M., Vicente, J.R., Kühn, I., Schröter, M., Hauck, J., Bonn, A., and Honrado, J.P., 2017. Integrating ecosystem services and disservices: insights from plant invasions. *Ecosystem Services*. DOI: 10.1016/j.ecoser.2016.11.017.

Vaz, A.S., Marcos, B., Gonçalves, J., Monteiro, A., Alves, P., Civantos, E., Lucas, R., Mairota, P., Garcia-Robles, J., Alonso, J., Blonda, P., Lomba, A., and Honrado, J.P., 2015. Can we predict habitat quality from space? A multi-indicator assessment based on an automated knowledge-driven system. *International Journal of Applied Earth Observation and Geoinformation*, 37, 106–113. DOI: 10.1016/j.jag.2014.10.014.

Veraverbeke, S., Gitas, I., Katagis, T., Polychronaki, A., Somers, B., and Goossens, R., 2012. Assessing post-fire vegetation recovery using red–near infrared vegetation indices: Accounting for background and vegetation variability. *ISPRS Journal of Photogrammetry and Remote Sensing*, 68 (1), 28–39. DOI: 10.1016/j.isprsjprs.2011.12.007.

Villarreal, S., Guevara, M., Alcaraz-Segura, D., Brunsell, N.A., Hayes, D., Loescher, H.W., and Vargas, R., 2018. Ecosystem functional diversity and the representativeness of environmental networks across the conterminous United States. *Agricultural and Forest Meteorology*, 262, 423–433. DOI: 10.1016/j.agrformet.2018.07.016.

Vitousek, P.M., Mooney, H.A., Lubchenco, J., and Melillo, J.M., 1997. Human domination of Earth's ecosystems. *Science*, 277 (5325), 494–499. DOI: 10.1126/science.277.5325.494.

Wang, X. and Xie, H., 2018. A review on applications of remote sensing and geographic information systems (GIS) in water resources and flood risk management. *Water (Switzerland)*. DOI: 10.3390/w10050608.

Wei, X., Hayes, D.J., Fraver, S., and Chen, G., 2018. Global Pyrogenic Carbon Production During Recent Decades Has Created the Potential for a Large, Long-Term Sink of

Atmospheric CO2. *Journal of Geophysical Research: Biogeosciences*, 123 (12), 3682–3696. DOI: 10.1029/2018JG004490.

Van Der Werf, G.R., Randerson, J.T., Collatz, G.J., Giglio, L., Kasibhatla, P.S., Arellano, A.F., Olsen, S.C., and Kasischke, E.S., 2004. Continental-Scale Partitioning of Fire Emissions during the 1997 to 2001 El Niño/La Niña Period. *Science*, 303 (5654), 73–76. DOI: 10.1126/science.1090753.

van der Werf, G.R., Randerson, J.T., Giglio, L., van Leeuwen, T.T., Chen, Y., Rogers, B.M., Mu, M., van Marle, M.J.E.E., Morton, D.C., Collatz, G.J., Yokelson, R.J., and Kasibhatla, P.S., 2017. Global fire emissions estimates during 1997–2016. *Earth System Science Data*, 9 (2), 697–720. DOI: 10.5194/essd-9-697-2017.

Westerling, A.L., Hidalgo, H.G., Cayan, D.R., and Swetnam, T.W., 2006. Warming and earlier spring increase Western U.S. forest wildfire activity. *Science*, 313 (5789), 940–943. DOI: 10.1126/science.1128834.

Westerling, A.L.R., 2016. Increasing western US forest wildfire activity: Sensitivity to changes in the timing of spring. *Philosophical Transactions of the Royal Society B: Biological Sciences*, 371 (1696). DOI: 10.1098/rstb.2015.0178.

Xu, G. and Zhong, X., 2017. Real-time wildfire detection and tracking in Australia using geostationary satellite: Himawari-8. *Remote Sensing Letters*, 8 (11), 1052–1061. DOI: 10.1080/2150704X.2017.1350303.

Yu, B., Chen, F., Li, B., Wang, L., and Wu, M., 2017. Fire risk prediction using remote sensed products: A case of Cambodia. *Photogrammetric Engineering and Remote Sensing*, 83 (1), 19–25. DOI: 10.14358/PERS.83.1.19.

CHAPTER 2. Improving the detection of wildfire disturbances

Disclaimer

This Chapter is based on a manuscript that is an original contribution of this thesis published in the International Journal of Applied Earth Observation and Geoinformation, in 2019, under the title *"Improving the detection of wildfire disturbances in space and time based on indicators extracted from MODIS data: a case study in northern Portugal"*, with the DOI: 10.1016/j.jag.2018.12.003. The full list of authors is: Bruno Marcos[1,2], João Gonçalves[1,2], Domingo Alcaraz-Segura[3,4,5], Mário Cunha[2,6], and João P. Honrado[1,2]. Bruno Marcos led the work with contributions from all co-authors.

For the research in this manuscript, Bruno Marcos and João Gonçalves were financially supported by the Portuguese Foundation for Science and Technology (FCT), through Ph.D. Grants SFRH/BD/99469/2014 and SFRH/BD/90112/2012, respectively, funded by the Ministry of Education and Science, and the European Social Fund, within the 2014–2020 EU Strategic Framework. Domingo Alcaraz-Segura received funding from the JC2015-00316 grant and CGL2014-61610-EXP.

[1] Research Centre in Biodiversity and Genetic Resources, Research Network in Biodiversity and Evolutionary Biology (CIBIO-InBIO), Campus Agrário de Vairão, Universidade do Porto, Rua Padre Armando Quintas,4485-661 Vairão, Portugal.

[2] Faculty of Sciences, University of Porto, Rua Campo Alegre s/n, 4169-007 Porto, Portugal.

[3] Department of Botany, Faculty of Sciences, University of Granada, Av. Fuentenueva, 18071 Granada, Spain.

[4] iEcolab. Interuniversity Institute for Earth System Research (IISTA), University of Granada, Av. del Mediterráneo, 18006 Granada, Spain.

[5] Andalusian Center for the Assessment and Monitoring of Global Change (CAESCG), Universidad de Almería, Crta. San Urbano, 04120 Almería, Spain.

[6] Institute for Systems and Computer Engineering, Technology and Science (INESC TEC), Campus da Faculdade de Engenharia da Universidade do Porto, Rua Dr. Roberto Frias, 4200-465 Porto, Portugal.

Abstract

Wildfires constitute an important threat to human lives and livelihoods worldwide, as well as a major ecological disturbance. However, available wildfire databases often provide incomplete or inaccurate information, namely regarding the timing and extension of fire events. In this study, we described a generic framework to compare, rank, and combine multiple remotely-sensed indicators of wildfire disturbances, to not only select the best indicators for each specific case, as well as to provide multi-indicator consensus approaches that can be used to detect wildfire disturbances in space and time. To this end, we compared the performance of different remotely-sensed variables to discriminate burned areas, by applying a simple change-point analysis procedure on time-series of MODIS imagery for the northern half of Portugal, without external information (e.g., active fire maps). Overall, our results highlight the importance of adopting a multi-indicator consensus approach for mapping and detecting wildfire disturbances at a regional scale, that allows to profit from spectral indices capturing different aspects of the Earth's surface, and derived from distinct regions of the electromagnetic spectrum. Finally, we argue that the framework here described can be used: (i) in a wide variety of geographical and environmental contexts; (ii) to support the identification of the best possible remotely-sensed functional indicators of wildfire disturbance; and (iii) for improving and complementing incomplete wildfire databases.

Keywords

Wildfire disturbance, Burned area mapping, Burn date estimation, Spectral indices, TCT, LST.

2.1. Introduction

Worldwide, wildfires pose a major threat to a wide range of environmental, social, and economic assets. In the Mediterranean biome, wildfire activity has increased in the previous decades (San-Miguel-Ayanz *et al.* 2013). Today, they constitute one of the major ecological disturbances as they can disrupt populations, communities, and ecosystems, in terms of structure, composition, and function (Pickett and White 1985). Indeed, fire (or disturbance regime) has been proposed not only as an Essential Climate Variable (ECV) but also as an Essential Biodiversity Variable (EBV) related to ecosystem function to assess biodiversity status (Pereira *et al.* 2013). There is thus a need to detect and characterize wildfire events to better understand how fire extent, frequency, and timing affect multiple environmental and socioeconomic processes (Benali *et al.* 2016).

However, currently available fire databases may be hindered by errors, including coarse spatial resolutions, limited temporal extent, missing data, and unknown accuracy (e.g., ICNF 2017). Furthermore, the costs of acquiring spatially comprehensive and consistent in-field data regarding wildfires (e.g., burn perimeters, ignition sources, deflagration time) can be high, as it is a time consuming and difficult process, and also because the allocated resources to it by land management authorities can highly fluctuate across time and space (Benali *et al.* 2016, Giglio *et al.* 2016). There is thus a need to employ consistent frameworks to characterize wildfire disturbances that can help overcome those problems, by correcting or complementing the information provided by available fire databases.

In this context, an important contribution has been provided by Remote Sensing (RS) based on Earth Observation Satellites (EOS), which has particular utility for rapidly measuring, monitoring, and developing low-cost indicators for fire-related applications, with an increasing number of products being made available in recent years (Mouillot *et al.* 2014). As one of the sensors that currently provides frequent data with spectral bands appropriate for wildfire applications, the Moderate Resolution Imaging Spectroradiometer (MODIS) aboard the Terra and Aqua satellite platforms has been broadly used for fire applications. Although this sensor provides information at moderate to coarse spatial resolutions for wildfire disturbance mapping, it can be a valuable tool for monitoring, mainly at regional scales, due to its high data acquisition rate, wide availability of the datasets, and a data archive spanning almost two decades (Justice *et al.* 2002, Giglio *et al.* 2018).

RS-based approaches to map and detect wildfire disturbances can be categorized in one of two types (Joyce *et al.* 2009), namely: (i) active fires (e.g., MODIS Thermal Anomalies and Fires products MCD45 and MCD64, VIIRS NRT 375 Active Fire products);

or (ii) burned areas (e.g., MODIS Burned Area products MOD14/MYD14/MCD14, Fire_cci Global Burned Area products). Detection of fire itself – *active fires* (AF) – consists in identifying thermal anomalies, usually at moderate to coarse spatial resolutions, but with high temporal frequency (e.g., daily), to detect phenomena that can be sometimes very concentrated in time, and do not account for the immediate effects of the fire on ecosystems directly (Lentile *et al.* 2006, Chu and Guo 2013). In turn, detection of the short-term effects of fire events on the land surface – *burned areas* (BA) – consists of mapping areas with burnt vegetation, by comparing pre- and post-fire reflectance information, and also against surrounding areas. As this uses optical and/or non-thermal infra-red data, it can be obtained at finer spatial scales, but often at lower temporal frequencies (Lentile *et al.* 2006, Chu and Guo 2013), although this has been improving throughout the years. Finally, as this second type of approaches provides more direct observations of the effects of fire on the land surface (e.g., change in vegetation), rather than the physical phenomenon itself, they are more suitable for environmental applications that focus on biotic components (e.g., loss of biomass and/or habitats, water, and nutrient availability), rather than abiotic components (e.g., gas emissions, pollution), and thus more fit to study post-fire responses of ecosystems to wildfire disturbances (Lentile *et al.* 2006).

In this context, several different variables extracted from time-series of satellite images (SITS), have been used for detecting wildfire disturbances, and their immediate effects on terrestrial ecosystems. Perhaps the most well-known of those are band ratios and normalized indices – sometimes referred to as vegetation indices (VI) or spectral indices (SI) –, such as the *Normalized Difference Vegetation Index* (NDVI), the *Enhanced Vegetation Index* (EVI), or the *Normalized Burn Ratio* (NBR; e.g., Veraverbeke *et al.* 2011, Moreno Ruiz *et al.* 2012). In a different approach, the variation in the LST / SI can be used for a wide range of applications related to disturbance events (e.g., Petropoulos *et al.* 2009). For instance, the MODIS Global Disturbance Index (MGDI; Mildrexler *et al.* 2009) uses the contrast between LST and EVI to map disturbances such as wildfires, with the underlying principle that LST decreases with an increase in vegetation density, given the greater latent heat transfer from increased evapotranspiration.

The Tasseled Cap Transformation (TCT; Lobser and Cohen 2007) has also been previously used for the development of indicators of wildfire disturbances (e.g., Hilker *et al.* 2009). The three TCT main features – *Brightness*, *Greenness*, and *Wetness* – are SI but contain information on a wider portion of the electromagnetic spectrum, as more bands are used in their computation. These have been compared with several biophysical parameters, including albedo, amount of photosynthetically active vegetation, and soil moisture, respectively (Mildrexler *et al.* 2009). Using these variables, Healey *et al.* (2005) and Thayn

and Buss (2015) proposed a simple and weighted version, respectively, of a wildfire disturbance indicator, based on the principle that the *Brightness* feature increases after a fire, while the *Greenness* and the *Wetness* features decrease. On the other hand, as noted by Thayn and Buss (2015), in the period immediately after the fire event, the Brightness values decrease, since the burned areas are covered in charcoal and ash and thus are darker than the unburned areas. In a more recent study (Fornacca *et al.* 2018), TCT components were also shown to be useful for burn scar mapping, and for evaluating burn severity and post-fire recovery, from short- to long-term.

It is known that results can vary depending on spectral index and methods (Hislop *et al.* 2018). Therefore, to optimize the accuracy of burned area detection algorithms, the best spectral indices (SI) should be selected accordingly (Fornacca *et al.* 2018). However, there is still uncertainty around which are the most essential variables for detecting and assessing wildfire disturbance, and their advantages and limitations (Hislop *et al.* 2018). In this study, we describe a generic framework to compare, rank, and combine multiple remotely-sensed indicators of wildfire disturbances, to not only select the best indicators for each specific case, as well as to provide multi-indicator consensus approaches that can be used to detect wildfire disturbances in space and time. To this end, we compared the performance of different remotely-sensed variables to discriminate burned areas, by applying a simple change-point analysis procedure on time-series of MODIS imagery for the northern half of Portugal, without external information (e.g., active fire maps). In particular, we assessed which variables: (i) performed better in detecting and mapping wildfire occurrences at an annual temporal resolution; (ii) estimated better the date of occurrence (i.e., the start of the wildfire); and (iii) could better complement missing information on available national fire databases, such as the one demonstrated for our study area. We finally discuss which variables may hold the greatest potential to contribute to assess and monitor wildfire disturbance, to be used as essential variables, or to improve algorithms of wildfire disturbance detection and mapping.

2.2. Material and Methods

2.2.1. Study area and data description

Study area

To illustrate our proposed framework, we used a study area that corresponds to the northern half of mainland Portugal, located in the northwest Iberian Peninsula (**Figure 2.1**). This region is among those with the highest incidence of wildfires across Europe (Barros and Pereira 2014), both in terms of the number of occurrences, and burned area (San-Miguel-Ayanz *et al.* 2017). It includes a strong climatic gradient (from humid Atlantic to dry Mediterranean), and a large diversity of bedrock formations, soil types, land cover, and land use types (Vicente *et al.* 2013, Carvalho-Santos *et al.* 2014). Moreover, socioeconomic drivers (e.g., land abandonment) and environmental conditions (e.g., steep slopes, terrain ruggedness, pyrophytic vegetation) contribute to a highly fire-prone region (Oliveira *et al.* 2012).

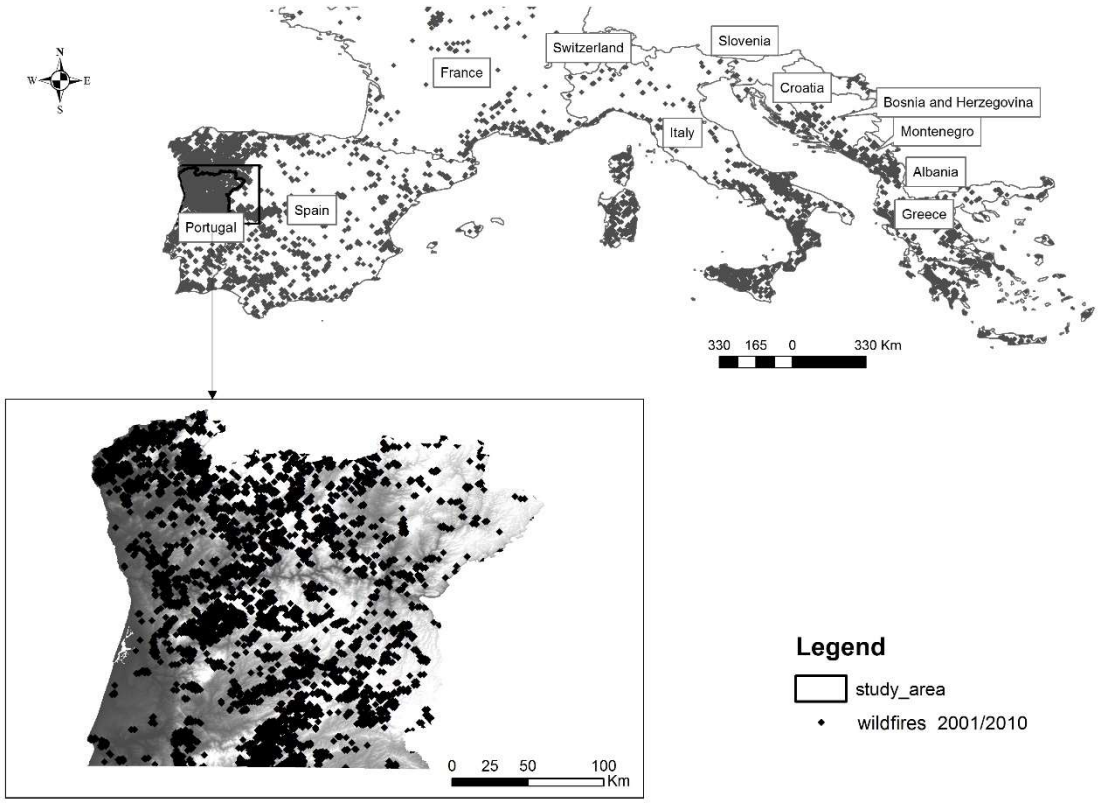

Figure 2.1. The study area (bottom), in the context of southern Europe (top), with a representation of fire occurrences in the decade of 2001–2010 (dots), which was extracted from the *European Forest Fire Information System* (EFFIS).

Spectral variables

Two MODIS products were downloaded and preprocessed using the *MODIStsp* R package (Busetto and Ranghetti 2016), for all available dates between 2001 and 2016: (i) the Surface Reflectance (SR) product MOD09A1 (8-Day, L3, Global, 500), Collection 6 (Vermote 2015); and (ii) the Land Surface Temperature (LST) and Emissivity product MOD11A2 (8-Day, L3, Global, 1-km), Collection 6 (Wan *et al.* 2015). Both products were re-projected to WGS84 / UTM zone 29N coordinate system, converted to GeoTIFF format, and re-sampled to 500 m using the nearest neighbor method so that all raster data were at the same resolution.

To reduce noise that hinders time-series data we employed a filter based on the *Hampel* outlier identifier (Hampel 1971, 1974) (*window* = 7 dates). This filter is considered robust, and efficient in identifying outliers, as well as extremely effective in removing time-series outliers (Pearson 2002).

Then, the day LST from the LST product was extracted and calibrated according to the guidelines described in the product's official documentation, and several spectral indices (SI) were computed by combining spectral bands from the SR product (**Table 2.1**), using *GDAL* (GDAL contributors 2017), and the *rasterio* Python package (Gillies *et al.* 2013). The final selection of variables was based on a literature review focused on potential indicators of wildfire disturbance and includes SI that are commonly used in fire studies, such as vegetation indices, *wetness* indices, fire-specific indices (e.g., Mildrexler *et al.* 2007, Harris *et al.* 2011, Veraverbeke *et al.* 2012, Schepers *et al.* 2014, Abade *et al.* 2015), and individual, or combinations of, tasseled cap features (e.g., Patterson and Yool 1998, Rogan and Yool 2001, Thayn 2013, Hermosilla *et al.* 2015, Santos *et al.* 2017, Axel 2018). Finally, the Whittaker-Henderson smoother (Whittaker 1922, Henderson 1924) (with *lambda* = 2) was applied to these variables, to further reduce the remaining noise present in the data.

Reference fire datasets

The results from the wildfire disturbance detection were compared against three reference datasets, for the period between 2001 and 2016: the MODIS burned areas products (i) MCD45A1 (Collection 5.1; Roy *et al.* 2008), and (ii) MCD64A1 (Collection 6; Giglio *et al.* 2018), and (iii) the Portuguese national database of burned area polygons (ICNF 2017).

Table 2.1. List of spectral indices used in this study to derive wildfire disturbance indicators. The b1, b2, b3, b4, b5, b6, and b7 correspond to MODIS bands 1–7, with bandwidth ranges at 620–670 nm, 841–876 nm, 459–479 nm, 545–565 nm, 1230–1250 nm, 1628–1652 nm, and 2105–2155 nm, respectively.

Index	Designation	Formula
NDVI	Normalized Difference Vegetation Index	(b2 – b1) / (b2 + b1)
EVI2	Two-band Enhanced Vegetation Index	2.5 × (b2 – b1) / (b2 + (2.4 × b1) + 1)
NDWI	Normalized Difference Water Index	(b4 – b6) / (b4 + b6)
LSWI	Land Surface Water Index	(b2 – b6) / (b2 + b6)
NBR	Normalized Burn Ratio	(b2 – b7) / (b2 + b7)
TCTb	Tasseled Cap Brightness	(0.4395 × b1) + (0.5945 × b2) + (0.2460 × b3) + (0.3918 × b4) + (0.3506 × b5) + (0.2136 × b6) + (0.2678 × b7)
TCTg	Tasseled Cap Greenness	(–0.4064 × b1) + (0.5129 × b2) – (0.2744 × b3) – (0.2893 × b4) + (0.4882 × b5) – (0.0036 × b6) – (0.4169 × b7)
TCTw	Tasseled Cap Wetness	(0.1147 × b1) + (0.2489 × b2) + (0.2408 × b3) + (0.3132 × b4) – (0.3122 × b5) – (0.6416 × b6) – (0.5087 × b7)
TCTbg	Tasseled Cap Brightness+Greenness	(TCTb + TCTg) / 2
TCTgw	Tasseled Cap Greenness+Wetness	(TCTg + TCTw) / 2
TCTbw	Tasseled Cap Brightness+Wetness	(TCTb + TCTw) / 2
TCTbgw	Tasseled Cap Brightness+Greenness+Wetness	(TCTb + TCTg + TCTw) / 3

The MCD45A1 algorithm uses a bidirectional reflectance distribution function (BRDF) model-based change detection approach to handle angular variations in the data and analyzes the daily surface reflectance dynamics to locate rapid changes (Roy *et al.* 2008). It then uses that information to detect the approximate date of burning and maps only the spatial extent of recent fires.

The MCD64A1 algorithm uses a burn-sensitive VI, derived from shortwave infrared SR bands 5 and 7 with a measure of temporal texture, to create dynamic thresholds that are applied to the composite data. Compared to previous products (e.g., MCD45A1), MCD64A1 features a general improvement (reduced omission error) in burned area detection, including significantly better detection of small burns, as well as a modest reduction in burn-date temporal uncertainty (Giglio *et al.* 2018).

The Portuguese national database of burned area polygons, provided by the Portuguese national agency for nature conservation and forests (ICNF), contains annual fire perimeters from 1975 to 2017, with unknown accuracy, and heterogeneous characteristics – e.g., some perimeters were obtained from ground collected data, while others were derived from satellite imagery with different resolutions, such as Landsat and

Sentinel; and only a small proportion of fires (i.e., ca. 11% of *big fires*) have information on the date of occurrence (see *Supplementary material—Table S2.1*). The ICNF dataset was rasterized and re-projected to WGS84 / UTM zone 29N, using GDAL/OGR v2.2.2 (GDAL contributors 2017), to match MODIS products.

The three reference datasets were converted to the same resolution as the spectral variables derived from MODIS. Then, fires with burned areas smaller than 100 ha (equivalent to 4 pixels) were excluded from the comparisons, to account for limitations of detectability inherent to the spatial scale of the MODIS products (van der Werf *et al.* 2017). This has also been the threshold used by Portuguese authorities to define *big fires* until 2013 (Ferreira-Leite *et al.* 2013) (later redefined to 500 ha).

2.2.2. Methodology

Detection of wildfire disturbances

Each selected spectral variable was used both on its own, and contrasted with LST, in a simple ratio (i.e., LST / index), and then normalized using *Z-scores* normalization, pixel-wise, as $Z = (x - \mu) / \sigma$, where x is the original value, μ is the time-series average, and σ is the time-series standard deviation, giving a total of 24 indicators. To minimize the effects of both long-term and seasonal variation on each indicator time-series, as well as to highlight abrupt changes such as those associated with wildfire disturbance events, we decomposed the normalized time-series using a Seasonal-Trend decomposition procedure based on the LOESS smoother (STL; Cleveland *et al.* 1990). This was done with the *s.window* and *t.window* parameters both equal to 47, as it corresponds to the next odd number from the frequency of the time-series – i.e., 46 images per year –, and the *robust* parameter set as *TRUE*. The LOESS procedure decomposes time-series into *trend*, *seasonal*, and *remainder* components. The resulting *remainder* component was used as a disturbance indicator, as it corresponds to the *detrended* and *deseasonalized* time-series, and thus contains the non-periodical variations, as well as any remaining noise (which was greatly reduced in previous steps).

Tukey's fences (Tukey 1977) were used for detecting wildfire disturbances, by identifying which peaks could be considered outliers, i.e., peaks farther away than k times (in this case $k = 3$, for *far away* outliers) the interquartile range from the nearest quartile were considered as positive detections, as those represent the values that most likely correspond to severe outliers within each pixel-wise time-series (Tukey 1977). This approach also allows for obtaining estimates of the period of occurrence of the wildfire

disturbance event, i.e., in which 8-day composite it was detected. These computations were undertaken using the R statistical programming environment (R Core Team 2018).

Evaluation of indicators' performance

To evaluate the performance of each indicator to detect and map wildfire disturbances, at the annual temporal resolution, the following single-class performance measures were extracted from the confusion matrices (Fawcett 2006): *Sensitivity* (i.e., true positive rate) or *Producer's Accuracy* (i.e., the complement of omission error), *Specificity* (i.e., true negative rate), *User's Accuracy* (i.e., the complement of commission error), *Overall Accuracy*, and *Cohen's Kappa*. Both the values and their respective confidence intervals for *Kappas* were estimated using bootstrap with 10,000 repetitions, to test the statistical significance of the differences between the indicators' burned areas maps. For simplification purposes, the detections resulting from the wildfire disturbance indicators, and the two reference datasets obtained from MODIS products were compared against the national reference database.

The results of the temporal estimations from the 24 indicators were compared against the reference datasets, for the fires for which occurrence dates were available, within the 2012–2016 period. This allowed for the evaluation of the indicators in terms of both temporal precision (i.e., dispersion in the temporal estimations) – through *standard deviation* (SD) and *median absolute deviation* (MAD), and *interquartile range* (IQR) –, and temporal accuracy (i.e., degree of success in estimating dates of occurrence) – using *mean absolute error* (MAE), *median absolute error* (MDAE), *mean bias* (MB) and *median bias* (MDB). Based on this, ten of the indicators were excluded. However, four of those were reconsidered, as they exhibited high precision, only with a systematic error of only one composite. Those four indicators were then corrected for systematic lag (i.e., a temporal shift of one composite was applied), and added to the list of indicators, elevating the final count of indicators considered to 28.

Finally, based on the performance metrics, the wildfire disturbance indicators were ranked, which was used to find the *best* occurrence date estimate for each pixel, i.e., the date estimate given by the highest-ranked indicator for which there was a positive detection. This, along with the median of the date estimates from the indicators that were not excluded by this process, provided two estimates of the date of occurrence, for each pixel. Then, these estimates, as well as the dates given by the two reference datasets from MODIS burned area products, were extracted and aggregated to match the geometry of the *big fires* polygons (i.e., above 100 ha) of the national reference dataset, including all burned area polygons both with and without prior information of the date of occurrence, for the period of

2001–2016. This was done to provide estimates of the dates of occurrence of the wildfire disturbance events, to complement the information previously available in the national reference dataset, from only a portion (ca. 11%) of the *big fire* polygons for years between 2012 and 2016, to all *big fire* polygons of the dataset, from 2001 to 2016 (see *Supplementary Material—Table S2.2*).

2.3. Results and Discussion

2.3.1. Burned area mapping performance

Mapping accuracies of annual burned areas, when compared to the national fire reference dataset, were generally high across all indicators (*Overall Accuracy* ≥ 0.75; *Kappa* ≥ 0.50), with non-overlapping confidence intervals for *Kappa* estimates in most cases (**Table 2.2**; **Figure 2.2**). Only the ones based on *wetness* indices (except LSWI) attained lower performance (**Table 2.2**). The highest values for *Specificity* and *User's Accuracy* were achieved for the indicators based on TCTb and the LST/TCTb ratio, respectively, while for the remaining performance metrics, the highest values all resulted from the indicator derived from the LST/TCTbgw ratio (**Figure 2.2**).

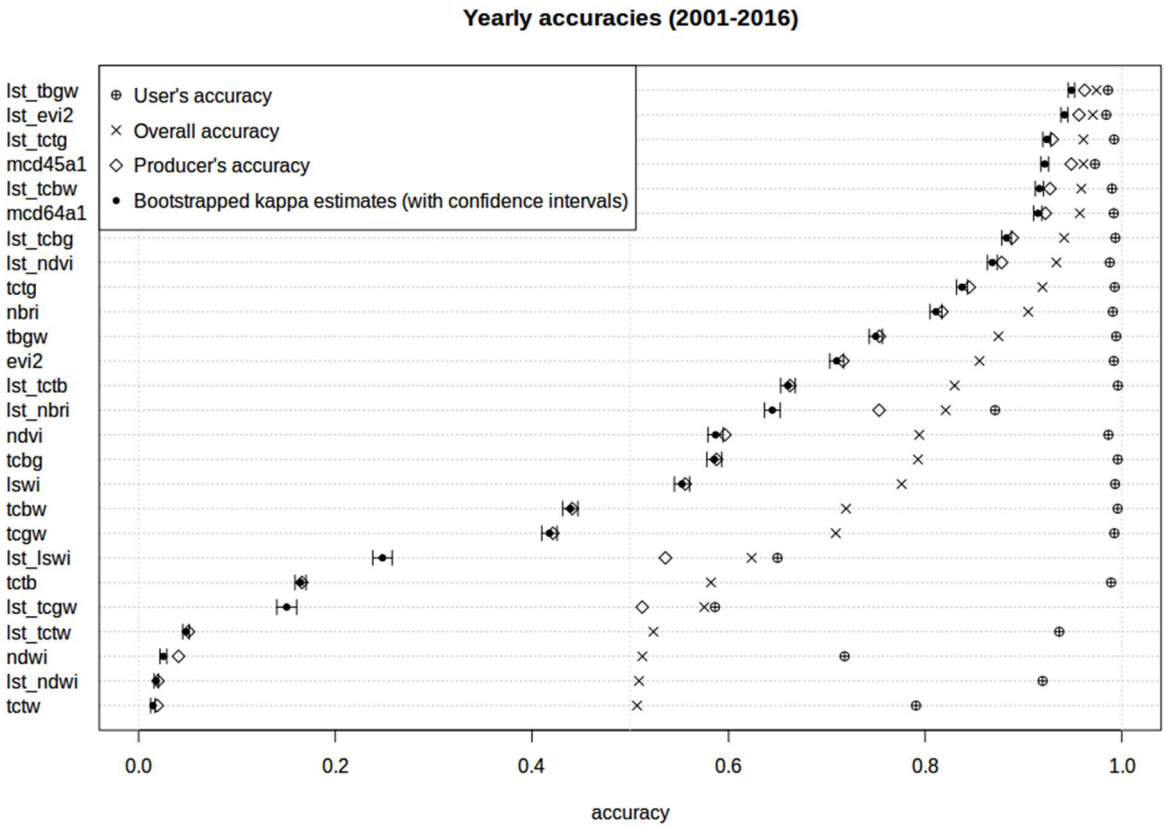

Figure 2.2. Dot chart representing the yearly burned area mapping accuracy measures for 2001–2016, for each one of the indicators used, as well as the MODIS burned area products MCD45 and MCD64 (as "mcd45_v51" and "mcd64_v6", respectively), compared to the national fire database. Bootstrapped estimates for *Kappa* are shown with their respective confidence intervals.

Table 2.2. Performance of burned area mapping, on an annual basis (2001–2016), for the selected indicators, compared to the Portuguese national fire polygons database. MODIS burned area products MCD45 and MCD64 were also compared, and their performance results are also presented (as "mcd45_v1" and "mcd64_v6", respectively). Note that indicators here are presented with lower case, to denote the difference between each indicator and the index, indices, or product on which it was based (indicator names with underscore were based on ratios, as described in the text). Both estimates for Kappas and their respective confidence intervals (CI) were obtained by bootstrapping with 10,000 repetitions.

Indicator	Formula	Sensitivity	Specificity	Producer's accuracy	User's accuracy	Overall accuracy	Kappa	Kappa CI
mcd45_v51	-	0.929	0.992	0.929	0.991	0.960	0.921	0.918–0.926
mcd64_v6	-	0.922	0.992	0.922	0.992	0.957	0.915	0.910–0.919
lst_tbgw	LST / TCTbgw	0.962	0.988	0.962	0.987	0.975	0.950	0.946–0.952
lst_evi2	LST / EVI2	0.956	0.985	0.956	0.985	0.971	0.941	0.938–0.945
lst_tctg	LST / TCTg	0.949	0.975	0.949	0.974	0.962	0.923	0.920–0.928
lst_tcbw	LST / TCTbw	0.927	0.991	0.927	0.990	0.959	0.918	0.912–0.920
lst_tcbg	LST / TCTbg	0.889	0.994	0.889	0.994	0.941	0.883	0.878–0.888
lst_ndvi	LST / NDVI	0.878	0.989	0.878	0.988	0.934	0.867	0.863–0.873
tctg	TCTg	0.845	0.993	0.845	0.992	0.919	0.837	0.832–0.843
nbri	NBR	0.817	0.992	0.817	0.991	0.905	0.809	0.805–0.817
tbgw	TCTbgw	0.753	0.996	0.753	0.994	0.874	0.749	0.743–0.756
evi2	EVI2	0.716	0.993	0.716	0.991	0.855	0.710	0.703–0.717
lst_tctb	LST / TCTb	0.662	0.997	0.662	0.996	0.830	0.660	0.653–0.668
lst_nbri	LST / NBR	0.753	0.889	0.753	0.872	0.821	0.643	0.637–0.652
ndvi	NDVI	0.596	0.991	0.596	0.985	0.794	0.587	0.579–0.595
tcbg	TCTbg	0.588	0.996	0.588	0.993	0.792	0.584	0.578–0.593
lswi	LSWI	0.556	0.996	0.556	0.993	0.776	0.552	0.545–0.560
tcbw	TCTbw	0.441	0.998	0.441	0.994	0.719	0.438	0.432–0.447
tcgw	TCTgw	0.421	0.710	0.421	0.992	0.709	0.418	0.410–0.426
lst_lswi	LST / LSWI	0.536	0.710	0.536	0.649	0.623	0.246	0.238–0.258
tctb	TCTb	0.166	0.998	0.166	0.990	0.582	0.164	0.159–0.170
lst_tcgw	LST / TCTgw	0.512	0.641	0.512	0.588	0.577	0.154	0.140–0.161
lst_tctw	LST / TCTw	0.051	0.997	0.051	0.937	0.524	0.047	0.045–0.051
ndwi	NDWI	0.041	0.985	0.041	0.724	0.513	0.025	0.022–0.029
lst_ndwi	LST / NDWI	0.020	0.998	0.020	0.910	0.509	0.018	0.016–0.020
tctw	TCTw	0.019	0.995	0.019	0.794	0.507	0.014	0.012–0.017

Overall, mapping accuracies, at the annual temporal resolution, resulted in better performances when using indicators based on LST / SI ratios, in comparison with the indicators using the same indices but without the contrast with LST. This is in line with results from previous studies (e.g., Mildrexler *et al.* 2007, 2009) where the coupling of LST and SI, particularly in LST / SI ratios, substantially improved the detection of changes, as

the two variables in the ratio respond to different biophysical processes, thereby complementing the information content of one another.

When compared with indicators based on more widely-used SI (e.g., NDVI, EVI2, NBR), indicators based on tasseled cap features, and tasseled cap features combinations, resulted in improved accuracies, confirming the importance of considering their use for mapping burned areas (Healey *et al.* 2005, Arnett *et al.* 2014, Santos *et al.* 2017). This could be because tasseled cap features use a wider portion of the electromagnetic spectrum (including visible, near-infrared, and shortwave infrared) than other SI, which may provide more complete pictures of wildfire disturbance processes (Fornacca *et al.* 2018).

2.3.2. Temporal estimates of wildfire disturbances

The performance of estimates of wildfire occurrence dates, using 8-day composites from the period 2012–2016, yielded diverse results across different indicators when compared to the dates available in the national fire dataset (**Figure 2.3**). Of a total of 28 indicators considered, 16 of those achieved very good results in terms of both temporal precision and temporal accuracy, with values of median absolute deviations (MAD), median absolute errors (MDAE), and median biases (MDB) around zero, while interquartile ranges (IQR) were between 0 and 1 composites of 8 days. Values of mean bias (MB), standard deviation (SD) and mean absolute deviance (MAE) were used to differentiate and rank the indicators, with values for the two MODIS reference datasets generally worse than the top 16 indicators (**Table 2.3**). The remaining 12 indicators were excluded from the final estimates extracted for the national fire database, since they had overall lower scores for temporal precision and accuracy, ranking below the two MODIS reference datasets (used for comparison).

The indicators “tcbg”, “tbgw”, “tctg” and “evi2” were ranked, in that order, in the first four places, being the indicators with the lowest values for SD and MAE, and low values of MB (i.e., below 4.25, 1, and 0.50, respectively). Here, “mcd45_v51” and “mcd64_v6” correspond to the MODIS burned area products MCD45 and MCD64, respectively. On the other hand, the majority of the indicators based on an LST / SI ratio were among the ones excluded.

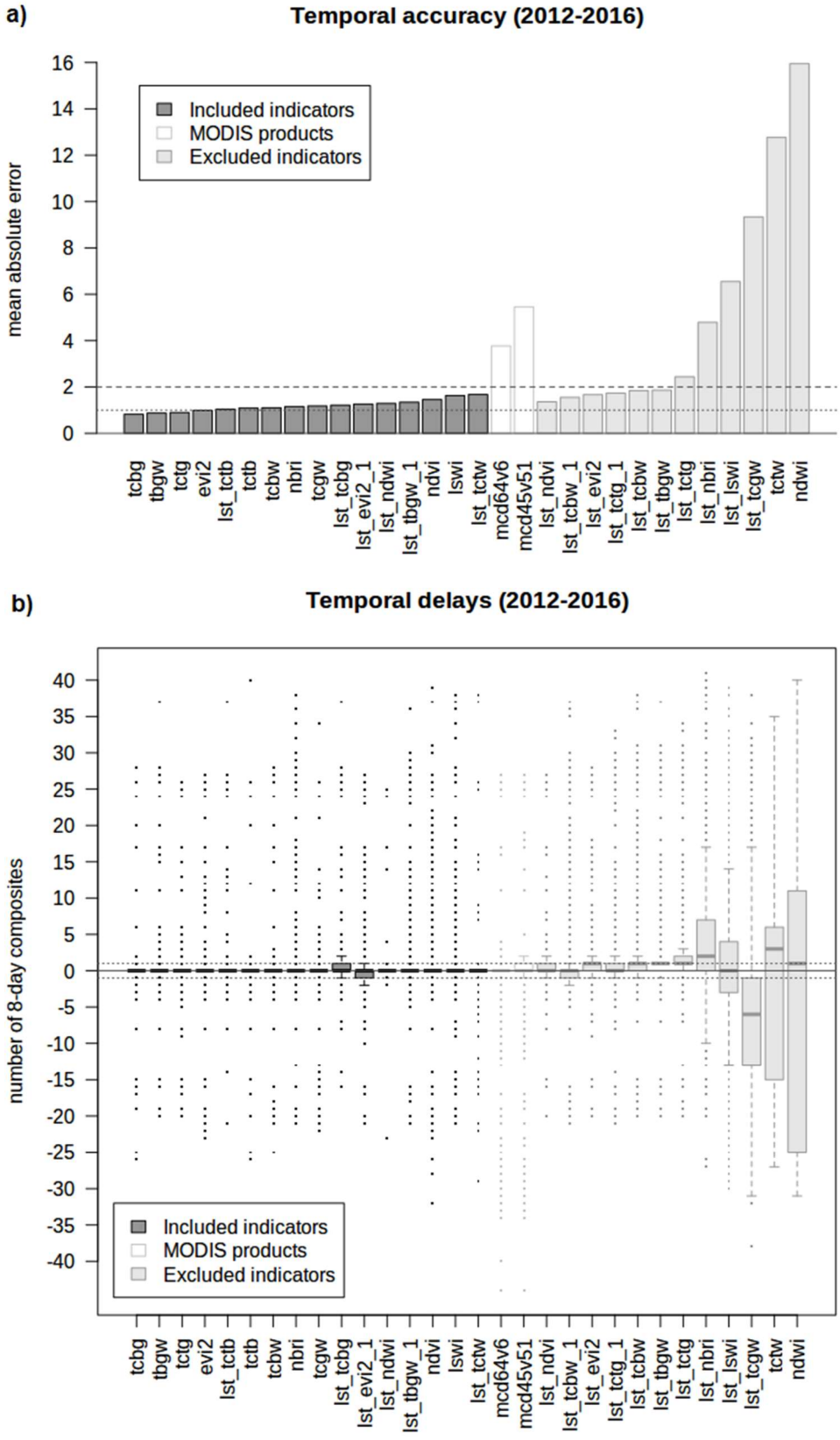

Figure 2.3. Temporal accuracies (a) and delays (i.e., errors) (b) of the estimates of wildfire occurrence date, compared to the Portuguese national fire database. The horizontal lines mark especially remarkable values for the mean absolute errors: 1 (dots), and 2 (dashes). Besides the estimates for the indicators, the comparison of the dates given by the MODIS Burned Area products MCD45 and MCD64, in comparison with the national database, is shown as "mcd45v51" and "mcd64v6", respectively. Additional information such as sample sizes is presented in **Table 2.3**.

Table 2.3. Performance statistics of temporal delays, compared to the national reference dataset. The values are expressed in the number of 8-day composites, as this is the maximum precision for wildfire date estimates that the input data allows. The indicators that were corrected for a systematic lag of one 8-day composite are denoted with the suffix "_1". Results for the MODIS Burned Area products MCD45 and MCD64 area also given here, as "mcd45v51" and "mcd64v6", respectively.

Rank	Indicator	n	MAD	MDAE	IQR	SD	MAE	MDB	MB
1	tcbg	2851	0	0	0	3.89	0.82	0	+0.39
2	tbgw	3462	0	0	0	3.99	0.87	0	+0.43
3	tctg	3976	0	0	0	4.02	0.90	0	+0.40
4	evi2	3599	0	0	0	4.24	0.99	0	+0.46
5	lst_tctb	3325	0	0	0	4.25	1.04	0	+0.70
6	tctb	909	0	0	0	4.68	1.09	0	+0.21
7	tcbw	2121	0	0	0	4.56	1.10	0	+0.44
8	nbri	3798	0	0	0	4.56	1.15	0	+0.63
9	tcgw	2430	0	0	0	4.58	1.18	0	+0.49
10	lst_tcbg	4218	0	0	1	4.15	1.21	0	+0.91
11	lst_evi2_1	4537	0	0	1	4.16	1.26	0	+0.32
12	lst_ndwi	241	0	0	0	4.87	1.29	0	+0.71
13	lst_tbgw_1	4533	0	0	0	4.32	1.34	0	+0.60
14	ndvi	3268	0	0	0	5.23	1.46	0	+0.80
15	lswi	2530	0	0	0	5.46	1.63	0	+0.95
16	lst_tctw	336	0	0	0	5.39	1.67	0	-0.20
17	mcd64v6	4659	0	0	0	9.72	3.77	0	-2.37
18	mcd45v51	4637	0	0	1	11.49	5.46	0	-3.76
19	lst_ndvi	4091	1.48	1	1	4.10	1.36	0	+1.05
20	lst_tcbw_1	4353	1.48	1	1	4.79	1.55	0	+0.55
21	lst_evi2	4537	0	1	1	4.16	1.67	+1	+1.32
22	lst_tctg_1	4484	1.48	1	1	4.35	1.73	0	+1.20
23	lst_tcbw	4353	1.48	1	1	4.79	1.84	+1	+1.55
24	lst_tbgw	4533	0	1	0	4.32	1.86	+1	+1.60
25	lst_tctg	4484	1.48	1	1	4.35	2.44	+1	+2.20
26	lst_nbri	3824	2.97	2	7	6.46	4.79	+2	+4.37
27	lst_lswi	2876	4.45	3	7	9.86	6.55	0	+0.04
28	lst_tcgw	2844	8.90	8	12	10.47	9.34	-6	-6.04
29	tctw	155	19.27	14	21	14.79	12.77	+3	-2.41
30	ndwi	658	23.72	16	36	18.76	15.95	+1	-2.99

In perspective, when estimating dates of occurrence, indicators that included at least one TCT component – but not LST – showed better overall results of temporal precision and accuracy. This contrasts with the results from the annual mapping performance, suggesting that including both TCT features and LST may help improve burned area mapping, however, the inclusion of LST may result in less accurate and less precise burn date estimation. Also, it must be noted that the indicators that included all three TCT components, with or without LST, (i.e., "tbgw" and "lst_tbgw") ranked in one of the top two positions for both wildfire disturbance mapping and detection, while, to the best of our knowledge, these indicators have not been previously used for those specific purposes.

Together, these results reinforce that no single indicator is the best for all purposes simultaneously, pointing to a trade-off situation, in which the *best* (i.e., top-ranked) indicators for burned area mapping, and the best ones for estimating the respective time of occurrence, may not be necessarily the same. This suggests that, for those purposes, adopting a multi-indicator approach may be advantageous to obtain the best possible results, in that different indicators may complement the potential that each has while compensating each other's drawbacks, to detect and map wildfire disturbances.

2.3.3. Complementing fire databases gaps

For the final estimations of the date of occurrence of wildfire disturbance events, inter-comparison of density distributions of the dates given by all the five datasets compared (**Figure 2.4**) showed an overall high degree of similarity between the different datasets (see *Supplementary material—Table S2.2*). This suggests a high congruence between the date estimates given by the different datasets, and thus a reasonable confidence level in the date estimates obtained for the remaining polygons of the national fire database, assuming the similarities between datasets would hold.

The top-ranked indicator (i.e., "tcbg") provided estimates for 41.4% of the complete set of *big fires* polygons of burned areas from the national fire database, while the indicators ranked in second and third (i.e., "tbgw" and "tctg") contributed with further 16.1% and 12.4%, respectively (**Figure 2.5**). Although the indicators ranked next provided estimates for relatively low percentages of fire polygons, three other indicators contributed to estimate dates for additional percentages of *big fires* polygons above 5% (**Table 2.4**).

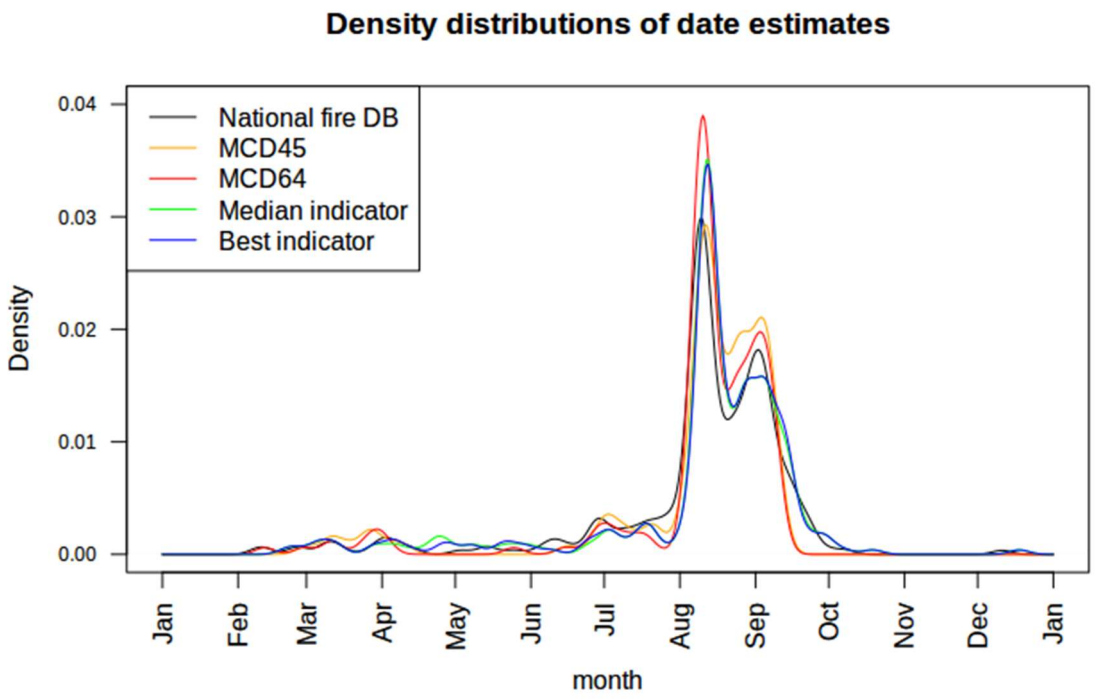

Figure 2.4. Density distributions of dates from all the five datasets compared (i.e., reference – National fire DB, MCD45 and MCD64, and date estimates from the *Median* and *Best* indicators). For comparability purposes, only the dates available for the same polygons as the ones with date information on the national fire database were plotted.

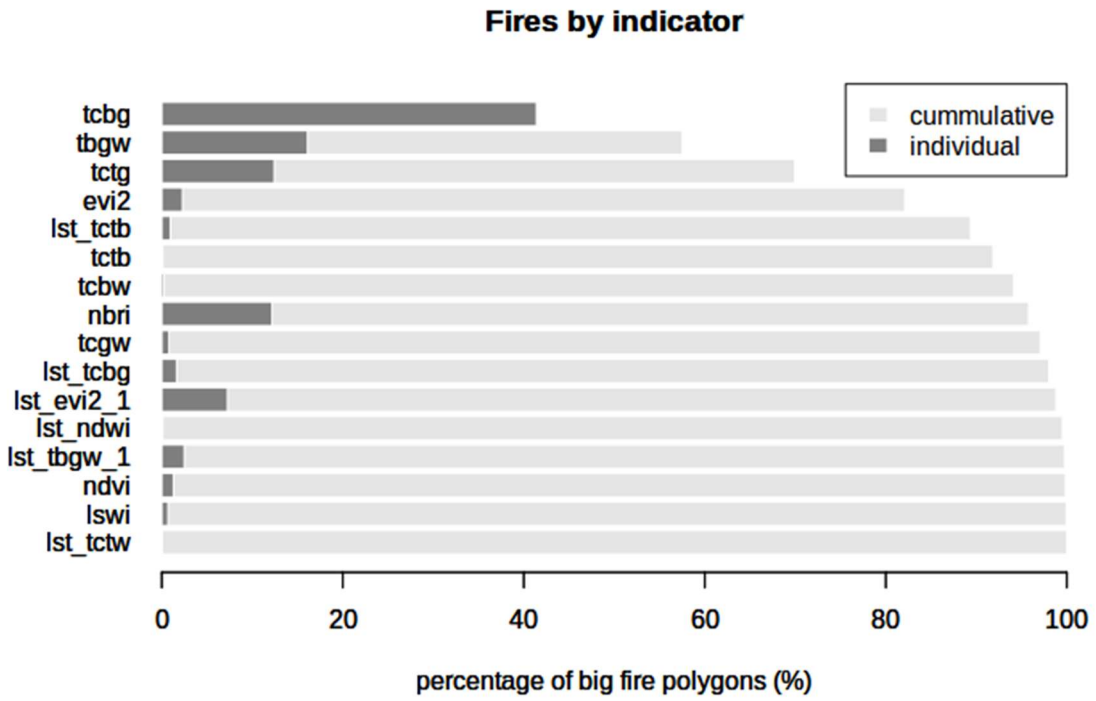

Figure 2.5. Percentage of burned area polygons of the Portuguese national fire database (with an area above 100 ha) for which each indicator was considered the *best* (i.e., the top-ranked) indicator. For more information, including sample sizes, see **Table 2.4**.

Table 2.4. Results from final extraction of fire occurrence dates, using the best-ranked indicator for each pixel, for all the burned area polygons of the national fire database above 100 ha (i.e., *big fires*).

Rank	Indicator	No. pixels	% pixels	No. polygons	% polygons	Accumulated % polygons
1	tcbg	2851	59.8%	833	41.4%	41.4%
2	tbgw	3462	72.6%	324	16.1%	57.5%
3	tctg	3976	83.4%	250	12.4%	69.9%
4	evi2	3599	75.5%	245	2.3%	72.2%
5	lst_tctb	3325	69.7%	146	0.9%	73.2%
6	tctb	909	19.1%	50	0.1%	73.3%
7	tcbw	2121	44.5%	46	0.2%	73.5%
8	nbri	3798	79.6%	33	12.2%	85.7%
9	tcgw	2430	51.0%	26	0.8%	86.5%
10	lst_tcbg	4218	88.4%	19	1.6%	88.1%
11	lst_evi2_1	4537	95.1%	16	7.3%	95.4%
12	lst_ndwi	241	5.1%	14	0.1%	95.5%
13	lst_tbgw_1	4533	95.1%	6	2.5%	98.0%
14	ndvi	3268	68.5%	2	1.3%	99.3%
15	lswi	2530	53.1%	2	0.7%	100.0%
16	lst_tctw	336	7.0%	1	0.0%	100.0%
17	mcd64_v6	4659	97.7%	-	-	
18	mcd45_51	4637	97.2%	-	-	

In comparison, when each of the same indicators was used independently, rather than in a rank-based sequence, the ones that were able to provide estimates for the highest percentages of fire polygons, were “lst_evi2” and “lst_tbgw” (after systematic error correction), with 95.1% each, while the top three indicators achieved percentages between 59.8% (for “tctb”) and 83.4% (for “tctg”).

Our results further highlight the potential of TCT components to be used to estimate the date of occurrence of wildfire disturbances, and – together with the results from burned area mapping – for their application in fire studies using remotely-sensed data. This, as pointed out in other studies (e.g., Fornacca *et al.* 2018), indicates that, since these SI use the information of all seven spectral bands in the optical-NIR-SWIR regions, they may possess enhanced capabilities to capture more aspects of ecosystem functioning change due to fires, especially when combined. In turn, this suggests that TCT components constitute a more complete, comprehensive, and compact package of base information to

study wildfire disturbance processes than the more commonly used SI, making them a particularly interesting option for fire-related monitoring (e.g., ECV, EBV).

All in all, to systematically select the best spectral indices to derive indicators of wildfire disturbances, extracted from satellite images time-series, and for complementing the information already available in fire databases, the framework here presented is generic enough to apply to other study areas. This is because the signal patterns that allow for the detection of such disturbances within satellite images time-series, as well as the spectral responses of vegetation to wildfire disturbance, tend to be similar across different biomes, vegetation types, and climatic regimes (e.g., Hope *et al.* 2012, Leon *et al.* 2012, Lanorte *et al.* 2014).

2.4. Conclusions

Despite the vast amount of remote-sensing studies that assess wildfires, there is still a need for protocols to systematically select the best indicators at the local or regional scale to develop algorithms that detect, map, and assess such disturbances, and to complement the information on existing databases. For tackling this, in this study, we analyzed and compared several indices, derived from time-series of MODIS imagery, for the assessment and monitoring of wildfire disturbances. Moreover, this work contributed to improving the selection of the best indicators, derived from remotely sensed indices, with the potential to improve existing information in national fire databases, for ecological and environmental applications, at a regional scale. This was accomplished by proposing a multi-indicator consensus approach which allowed to profit from spectral indices capturing different aspects of the Earth's surface, and derived from distinct regions of the electromagnetic spectrum. Finally, although satellite data with coarse spatial resolution was used here, the same principles (and a similar framework) could be used employing satellite time-series data from recent or upcoming platforms with higher spatial resolution and high temporal frequency (e.g., Sentinel-2 or PRISMA sensors).

References

Abade, N., Júnior, O., Guimarães, R., and de Oliveira, S., 2015. Comparative Analysis of MODIS Time-Series Classification Using Support Vector Machines and Methods Based upon Distance and Similarity Measures in the Brazilian Cerrado-Caatinga Boundary. *Remote Sensing*, 7 (9), 12160–12191. DOI: 10.3390/rs70912160.

Arnett, J.T.T.R., Coops, N.C., Gergel, S.E., Falls, R.W., and Baker, R.H., 2014. Detecting Stand-Replacing Disturbance using RapidEye Imagery: a Tasseled Cap Transformation and Modified Disturbance Index. *Canadian Journal of Remote Sensing*, 40 (1), 1–14. DOI: 10.1080/07038992.2014.899878.

Axel, A., 2018. Burned Area Mapping of an Escaped Fire into Tropical Dry Forest in Western Madagascar Using Multi-Season Landsat OLI Data. *Remote Sensing*, 10 (3), 371. DOI: 10.3390/rs10030371.

Barros, A.M.G. and Pereira, J.M.C., 2014. Wildfire selectivity for land cover type: does size matter? *PloS one*, 9 (1), e84760. DOI: 10.1371/journal.pone.0084760.

Benali, A., Russo, A., Sá, A., Pinto, R., Price, O., Koutsias, N., and Pereira, J., 2016. Determining Fire Dates and Locating Ignition Points With Satellite Data. *Remote Sensing*, 8 (4), 326. DOI: 10.3390/rs8040326.

Busetto, L. and Ranghetti, L., 2016. MODIStsp: An R package for automatic preprocessing of MODIS Land Products time series. *Computers and Geosciences*, 97, 40–48. DOI: 10.1016/j.cageo.2016.08.020.

Carvalho-Santos, C., Honrado, J.P., and Hein, L., 2014. Hydrological services and the role of forests: Conceptualization and indicator-based analysis with an illustration at a regional scale. *Ecological Complexity*, 20, 69–80. DOI: 10.1016/j.ecocom.2014.09.001.

Chu, T. and Guo, X., 2013. Remote Sensing Techniques in Monitoring Post-Fire Effects and Patterns of Forest Recovery in Boreal Forest Regions: A Review. *Remote Sensing*, 6 (1), 470–520. DOI: 10.3390/rs6010470.

Cleveland, R.B., Cleveland, W.S., McRae, J.E., and Terpenning, I., 1990. STL: A seasonal-trend decomposition procedure based on loess. *Journal of Official Statistics*, 6 (1), 3–73. DOI: citeulike-article-id:1435502.

Fawcett, T., 2006. An introduction to ROC analysis. *Pattern Recognition Letters*, 27 (8), 861–874. DOI: 10.1016/j.patrec.2005.10.010.

Ferreira-Leite, F., Lourenço, L., and Bento-Gonçalves, A., 2013. Large forest fires in mainland Portugal, brief characterization. *Méditerranée*, (121), 53–65. DOI: 10.4000/mediterranee.6863.

Fornacca, D., Ren, G., and Xiao, W., 2018. Evaluating the Best Spectral Indices for the Detection of Burn Scars at Several Post-Fire Dates in a Mountainous Region of Northwest Yunnan, China. *Remote Sensing*, 10 (8), 1196. DOI: 10.3390/rs10081196.

GDAL contributors, 2017. GDAL – Geospatial Data Abstraction Library v2.2.2.

Giglio, L., Boschetti, L., Roy, D.P., Humber, M.L., and Justice, C.O., 2018. The Collection 6 MODIS burned area mapping algorithm and product. *Remote Sensing of Environment*, 217, 72–85. DOI: 10.1016/j.rse.2018.08.005.

Giglio, L., Schroeder, W., and Justice, C.O., 2016. The collection 6 MODIS active fire detection algorithm and fire products. *Remote Sensing of Environment*, 178, 31–41. DOI: 10.1016/j.rse.2016.02.054.

Gillies, S., Ward, B., and Petersen, A.S., 2013. Rasterio: geospatial raster I/O for Python programmers version 0.36.0.

Hampel, F.R., 1971. A General Qualitative Definition of Robustness. *The Annals of Mathematical Statistics*, 42 (6), 1887–1896.

Hampel, F.R., 1974. The Influence Curve and its Role in Robust Estimation. *Journal of the American Statistical Association*, 69 (346), 383–393. DOI: 10.1080/01621459.1974.10482962.

Harris, S., Veraverbeke, S., and Hook, S., 2011. Evaluating Spectral Indices for Assessing Fire Severity in Chaparral Ecosystems (Southern California) Using MODIS/ASTER (MASTER) Airborne Simulator Data. *Remote Sensing*, 3 (12), 2403–2419. DOI: 10.3390/rs3112403.

Healey, S., Cohen, W., Zhiqiang, Y., and Krankina, O., 2005. Comparison of Tasseled Cap-based Landsat data structures for use in forest disturbance detection. *Remote Sensing of Environment*, 97 (3), 301–310. DOI: 10.1016/j.rse.2005.05.009.

Henderson, R., 1924. A new method of graduation. *Transactions of the Actuarial Society of America*, 25, 29–40.

Hermosilla, T., Wulder, M.A., White, J.C., Coops, N.C., and Hobart, G.W., 2015. An integrated Landsat time series protocol for change detection and generation of annual gap-free surface reflectance composites. *Remote Sensing of Environment*, 158, 220–234. DOI: 10.1016/j.rse.2014.11.005.

Hilker, T., Wulder, M.A., Coops, N.C., Linke, J., McDermid, G., Masek, J.G., Gao, F., and White, J.C., 2009. A new data fusion model for high spatial- and temporal-resolution mapping of forest disturbance based on Landsat and MODIS. *Remote Sensing of Environment*, 113 (8), 1613–1627. DOI: 10.1016/j.rse.2009.03.007.

Hislop, S., Jones, S., Soto-Berelov, M., Skidmore, A., Haywood, A., and Nguyen, T., 2018. Using Landsat Spectral Indices in Time-Series to Assess Wildfire Disturbance and Recovery. *Remote Sensing*, 10 (3), 460. DOI: 10.3390/rs10030460.

Hope, A., Albers, N., and Bart, R., 2012. Characterizing post-fire recovery of fynbos vegetation in the Western Cape Region of South Africa using MODIS data. *International Journal of Remote Sensing*, 33 (4), 979–999. DOI: 10.1080/01431161.2010.543184.

ICNF, 2017. Forest fires – Geographical information [online]. Available from: http://www.icnf.pt/portal/florestas/dfci/inc/info-geo [Accessed 10 Jan 2017].

Joyce, K.E., Belliss, S.E., Samsonov, S. V., McNeill, S.J., and Glassey, P.J., 2009. A review of the status of satellite remote sensing and image processing techniques for mapping natural hazards and disasters. *Progress in Physical Geography*, 33 (2), 183–207. DOI: 10.1177/0309133309339563.

Justice, C., Giglio, L., Korontzi, S., Owens, J., Morisette, J., Roy, D., Descloitres, J., Alleaume, S., Petitcolin, F., and Kaufman, Y., 2002. The MODIS fire products. *Remote Sensing of Environment*, 83 (1–2), 244–262. DOI: 10.1016/S0034-4257(02)00076-7.

Lanorte, A., Lasaponara, R., Lovallo, M., and Telesca, L., 2014. Fisher–Shannon information plane analysis of SPOT/VEGETATION Normalized Difference Vegetation Index (NDVI) time series to characterize vegetation recovery after fire disturbance. *International Journal of Applied Earth Observation and Geoinformation*, 26, 441–446. DOI: 10.1016/J.JAG.2013.05.008.

Lentile, L.B., Holden, Z.A., Smith, A.M.S.S., Falkowski, M.J., Hudak, A.T., Morgan, P., Lewis, S.A., Gessler, P.E., Benson, N.C., Lentile, L.B., Holden, Z.A., Smith, A.M.S.S., Falkowski, M.J., Hudak, A.T., Morgan, P., Lewis, S.A., Gessler, P.E., and Benson, N.C., 2006. Remote sensing techniques to assess active fire characteristics and post-fire effects. *International Journal of Wildland Fire*, 15 (3), 319. DOI: 10.1071/WF05097.

Leon, J.R.R., van Leeuwen, W.J.D., Casady, G.M., Leon, J.R.R., van Leeuwen, W.J.D., and Casady, G.M., 2012. Using MODIS-NDVI for the Modeling of Post-Wildfire Vegetation

Response as a Function of Environmental Conditions and Pre-Fire Restoration Treatments. *Remote Sensing*, 4 (3), 598–621. DOI: 10.3390/rs4030598.

Lobser, S.E. and Cohen, W.B., 2007. MODIS tasselled cap: land cover characteristics expressed through transformed MODIS data. *International Journal of Remote Sensing*, 28 (22), 5079–5101. DOI: 10.1080/01431160701253303.

Mildrexler, D.J., Zhao, M., and Running, S.W., 2009. Testing a MODIS Global Disturbance Index across North America. *Remote Sensing of Environment*, 113 (10), 2103–2117. DOI: 10.1016/j.rse.2009.05.016.

Mildrexler, D.J., Zhao, M.S., Heinsch, F.A., and Running, S.W., 2007. A new satellite-based methodology for continental-scale disturbance detection. *Ecological Applications*, 17 (1), 235–250. DOI: 10.1890/1051-0761(2007)017[0235:ANSMFC]2.0.CO;2.

Moreno Ruiz, J.A., Riaño, D., Arbelo, M., French, N.H.F., Ustin, S.L., and Whiting, M.L., 2012. Burned area mapping time series in Canada (1984–1999) from NOAA-AVHRR LTDR: A comparison with other remote sensing products and fire perimeters. *Remote Sensing of Environment*, 117, 407–414. DOI: 10.1016/J.RSE.2011.10.017.

Mouillot, F., Schultz, M.G., Yue, C., Cadule, P., Tansey, K., Ciais, P., and Chuvieco, E., 2014. Ten years of global burned area products from spaceborne remote sensing—A review: Analysis of user needs and recommendations for future developments. *International Journal of Applied Earth Observation and Geoinformation*, 26 (1), 64–79. DOI: 10.1016/j.jag.2013.05.014.

Oliveira, S.L.J., Pereira, J.M.C., Carreiras, J.M.B, 2012. Fire frequency analysis in Portugal (1975 - 2005), using Landsat-based burnt area maps. *International Journal of Wildland Fire*, 21 (1), 48. DOI: 10.1071/WF10131.

Patterson, M.W. and Yool, S.R., 1998. Mapping Fire-Induced Vegetation Mortality Using Landsat Thematic Mapper Data: A Comparison of Linear Transformation Techniques. *Remote Sensing of Environment*, 65 (2), 132–142. DOI: 10.1016/S0034-4257(98)00018-2.

Pearson, R.K., 2002. Outliers in process modeling and identification. *IEEE Transactions on Control Systems Technology*, 10 (1), 55–63. DOI: 10.1109/87.974338.

Pereira, H.M., Ferrier, S., Walters, M., Geller, G.N., Jongman, R.H.G., Scholes, R.J., Bruford, M.W., Brummitt, N., Butchart, S.H.M., Cardoso, A.C., Coops, N.C., Dulloo, E., Faith, D.P., Freyhof, J., Gregory, R.D., Heip, C., Hoft, R., Hurtt, G., Jetz, W., Karp, D.S., McGeoch, M.A., Obura, D., Onoda, Y., Pettorelli, N., Reyers, B., Sayre, R., Scharlemann, J.P.W., Stuart, S.N., Turak, E., Walpole, M., and Wegmann, M., 2013.

Essential Biodiversity Variables. *Science*, 339 (6117), 277–278. DOI: 10.1126/science.1229931.

Petropoulos, G., Carlson, T.N., Wooster, M.J., and Islam, S., 2009. A review of Ts/VI remote sensing based methods for the retrieval of land surface energy fluxes and soil surface moisture. *Progress in Physical Geography*, 33 (2), 224–250. DOI: 10.1177/0309133309338997.

Pickett, S.T. and White, P.S., 1985. *The ecology of natural disturbance and patch dynamics*. San Diego, CA, USA: Academic Press.

R Core Team, 2018. R: A Language and Environment for Statistical Computing version 3.4.

Rogan, J. and Yool, S.R., 2001. Mapping fire-induced vegetation depletion in the Peloncillo Mountains, Arizona and New Mexico. *International Journal of Remote Sensing*, 22 (16), 3101–3121. DOI: 10.1080/01431160152558279.

Roy, D.P., Boschetti, L., Justice, C.O., and Ju, J., 2008. The collection 5 MODIS burned area product — Global evaluation by comparison with the MODIS active fire product. *Remote Sensing of Environment*, 112 (9), 3690–3707. DOI: 10.1016/J.RSE.2008.05.013.

San-Miguel-Ayanz, J., Durrant, T., Boca, R., Libertà, G., Branco, A., de Rigo, D., Ferrari, D., Maianti, P., Vivancos, T.A., Schulte, E., and Loffler, P., 2017. *Forest Fires in Europe, Middle East and North Africa 2016*. Luxembourg. DOI: 10.2760/66820.

San-Miguel-Ayanz, J., Moreno, J.M., and Camia, A., 2013. Analysis of large fires in European Mediterranean landscapes: Lessons learned and perspectives. *Forest Ecology and Management*, 294, 11–22. DOI: 10.1016/j.foreco.2012.10.050.

Santos, F., Dubovyk, O., and Menz, G., 2017. Monitoring Forest Dynamics in the Andean Amazon: The Applicability of Breakpoint Detection Methods Using Landsat Time-Series and Genetic Algorithms. *Remote Sensing*, 9 (1), 68. DOI: 10.3390/rs9010068.

Schepers, L., Haest, B., Veraverbeke, S., Spanhove, T., Vanden Borre, J., and Goossens, R., 2014. Burned Area Detection and Burn Severity Assessment of a Heathland Fire in Belgium Using Airborne Imaging Spectroscopy (APEX). *Remote Sensing*, 6 (3), 1803–1826. DOI: 10.3390/rs6031803.

Thayn, J.B., 2013. Using a remotely sensed optimized Disturbance Index to detect insect defoliation in the Apostle Islands, Wisconsin, USA. *Remote Sensing of Environment*, 136, 210–217. DOI: 10.1016/j.rse.2013.05.008.

Thayn, J.B. and Buss, K.L., 2015. Monitoring fire recovery in a tallgrass prairie using a weighted disturbance index. *GIScience & Remote Sensing*, 52 (5), 527–542. DOI: 10.1080/15481603.2015.1064254.

Tukey, J.W., 1977. *Exploratory Data Analysis*. Reading, MA, USA: Addison-Wesley.

Veraverbeke, S., Hook, S., and Hulley, G., 2012. An alternative spectral index for rapid fire severity assessments. *Remote Sensing of Environment*, 123, 72–80. DOI: 10.1016/J.RSE.2012.02.025.

Veraverbeke, S., Lhermitte, S., Verstraeten, W.W., and Goossens, R., 2011. Evaluation of pre/post-fire differenced spectral indices for assessing burn severity in a Mediterranean environment with Landsat Thematic Mapper. *International Journal of Remote Sensing*, 32 (12), 3521–3537. DOI: 10.1080/01431161003752430.

Vermote, E., 2015. MOD09A1 MODIS/Terra Surface Reflectance 8-Day L3 Global 500m SIN Grid V006. *NASA EOSDIS Land Processes DAAC.*

Vicente, J.R., Fernandes, R.F., Randin, C.F., Broennimann, O., Gonçalves, J., Marcos, B., Pôças, I., Alves, P., Guisan, A., and Honrado, J.P., 2013. Will climate change drive alien invasive plants into areas of high protection value? An improved model-based regional assessment to prioritise the management of invasions. *Journal of Environmental Management*, 131, 185–195. DOI: 10.1016/j.jenvman.2013.09.032.

Wan, Z., Hook, S., and Hulley, G., 2015. MOD11A2 MODIS/Terra Land Surface Temperature/Emissivity 8-Day L3 Global 1km SIN Grid V006. *NASA EOSDIS Land Processes DAAC*.

van der Werf, G.R., Randerson, J.T., Giglio, L., van Leeuwen, T.T., Chen, Y., Rogers, B.M., Mu, M., van Marle, M.J.E.E., Morton, D.C., Collatz, G.J., Yokelson, R.J., and Kasibhatla, P.S., 2017. Global fire emissions estimates during 1997–2016. *Earth System Science Data*, 9 (2), 697–720. DOI: 10.5194/essd-9-697-2017.

Whittaker, E.T., 1922. On a new method of graduation. *Proceedings of the Edinburgh Mathematical Society*, 41, 63–75.

Supplementary material

Table S2.1. Fire statistics for the study area, extracted from the Portuguese national fire polygons database. "*w/date*" = fire polygons with information of date of occurrence.

Year		Count			Area		
		All fires (no.)	*Big fires (no.)*	*Big fires (%)*	*All fires (ha)*	*Big fires (ha)*	*Big fires (%)*
2001	*all*	1861	180	9.67%	97,543.80	60,028.37	61.54%
	w/ date	0	–	–	–	–	–
2002	*all*	1851	255	13.78%	133,118.18	95,317.07	71.60%
	w/ date	0	–	–	–	–	–
2003	*all*	1186	238	20.07%	439,620.93	418,284.84	95.15%
	w/ date	0	–	–	–	–	–
2004	*all*	722	141	19.53%	114,902.17	99,101.06	86.25%
	w/ date	0	–	–	–	–	–
2005	*all*	1459	393	26.94%	34,6134.05	315,721.84	91.21%
	w/ date	0	–	–	–	–	–
2006	*all*	715	126	17.62%	72,626.83	57,326.22	78.93%
	w/ date	0	–	–	–	–	–
2007	*all*	737	91	12.35%	38,298.28	23,702.18	61.89%
	w/ date	0	–	–	–	–	–
2008	*all*	733	17	2.32%	12,079.70	4,720.67	39.08%
	w/ date	100	0	–	516.37	0	–
2009	*all*	1436	196	13.65%	92,682.72	68,537.15	73.95%
	w/ date	167	8	4.79%	4,261.78	1,534.01	35.99%
2010	*all*	2540	197	7.76%	131,234.03	102,879.46	78.39%
	w/ date	0	–	–	–	–	–
2011	*all*	3723	148	3.98%	80,185.05	47,469.41	59.20%
	w/ date	0	–	–	–	–	–
2012	*all*	2979	148	4.97%	113,510.39	82,622.76	72.79%
	w/ date	1095	32	2.92%	25,132.28	19,192.65	76.37%
2013	*all*	3400	228	6.71%	149,348.66	120,316.35	80.56%
	w/ date	1187	76	6.40%	47,208.26	37,736.25	79.94%
2014	*all*	1141	28	2.45%	18,317.63	12,056.13	65.82%
	w/ date	941	10	1.06%	6,384.59	3,079.86	48.24%
2015	*all*	1617	112	6.93%	56,208.40	44,440.48	79.06%
	w/ date	1455	48	3.30%	34,760.66	25,414.97	73.11%
2016	*all*	2831	198	6.99%	161,338.93	144,109.96	89.32%
	w/ date	2518	114	4.53%	106,657.70	93,747.18	87.89%

Table S2.2. Dataset inter–comparisons for the date of occurrence of wildfire events, compared with the national fire database and MODIS fire products.

		National fire DB	**MCD45**	**MCD64**	***Median* indicator**	***Best* indicator**
National fire DB	*MB*	—	–2.8	–1.6	–2.6	–2.4
	MAE	—	9.3	9.9	9.5	9.3
	MDAE	—	2	3	0	0
	Pearson corr.	—	0.73	0.76	0.78	0.76
MCD45	*MB*	–2.8	—	1.2	–0.1	–0.3
	MAE	9.3	—	1.5	2.9	2.8
	MDAE	2	—	1	2	2
	Pearson corr.	0.73	—	0.87	0.90	0.90
MCD64	*MB*	–1.6	1.2	—	1.0	0.8
	MAE	9.9	1.5	—	2.8	2.6
	MDAE	3	1	—	2.25	2.5
	Pearson corr.	0.76	0.87	—	0.93	0.93
***Median* indicator**	*MB*	–2.6	–0.1	1.0	—	0.2
	MAE	9.5	2.9	2.8	—	0.5
	MDAE	0	2	2.25	—	0
	Pearson corr.	0.78	0.90	0.93	—	1.00
***Best* indicator**	*MB*	–2.4	–0.3	0.8	0.2	—
	MAE	9.3	2.8	2.6	0.5	—
	MDAE	0	2	2.5	0	—
	Pearson corr.	0.76	0.90	0.93	1.00	—

Compared with the national fire polygons database, all datasets (i.e. the *Best* and *Median* indicator date estimates (*Table S2.1*), as well as the dates provided by the two MODIS burned area products) achieved good results, with correlations between 0.73, for MCD45, and 0.78, for the median of multiple indicators (*Median*).

However, higher correlation values were obtained between all other indicators, ranging from 0.87 between MCD45 and MCD64 to 1.00 between the median of multiple indicators and the *Best* indicator. As for median absolute error (MDAE), results ranged from 0 (between *Median* and *Best*, and between each one of those two and the national fire polygons database) to 3 (between MCD64 and the national fire polygons database).

Mean biases varied between –2.8 (for the pair MCD45/national fire polygons database), and 1.2 (for the pair MCD45/MCD64), with –0.1 (for the pair *Median*/MCD45) being the closest value to zero.

CHAPTER 3. Expanding the assessment of wildfire disturbance severity

Disclaimer

This Chapter is based on a manuscript that is an original contribution of this thesis published in Remote Sensing journal (Special Issue "Advances in Remote Sensing of Post-fire Environmental Damage and Recovery Dynamics"), in 2021, under the title *"A framework for multi-dimensional assessment of wildfire disturbance severity from remotely-sensed Ecosystem Functioning Attributes"*, with the DOI: 10.3390/rs13040780. The full list of authors is: Bruno Marcos[1,2], João Gonçalves[1,3], Domingo Alcaraz-Segura[4,5,6], Mário Cunha[2,7] and João P. Honrado[1,2]. Bruno Marcos led the work with contributions from all co-authors.

The research in this manuscript was supported by Portuguese national funds through FCT – Foundation for Science and Technology, I.P., under the GreenRehab project (PCIF/RPG/0077/2017). This work was partially supported by the collaboration between Domingo Alcaraz-Segura and João Honrado under the projects RESISTE (P18-RT-1927) funded by Consejería de Economía, Conocimiento, Empresas y Universidad from the Junta de Andalucía, and DETECTOR (A-RNM-256-UGR18), with the contribution of the European Union Funds for Regional Development. Bruno Marcos was supported by FCT the Ministry of Education and Science, and the European Social Fund, within the 2014–2020 EU Strategic Framework, through FCT (Ph.D. scholarship SFRH/BD/99469/2014). João Gonçalves was funded by the Individual Scientific Employment Stimulus Program (2017), through FCT (contract nr. CEECIND/02331/2017). The authors acknowledge the use of MODIS imagery obtained from NASA's Land Processes Distributed Active Archive Center (LP DAAC), available at no charge. The authors would like to thank the anonymous reviewers for providing comments and suggestions that helped to improve the quality of the original manuscript.

[1] Research Centre in Biodiversity and Genetic Resources, Research Network in Biodiversity and Evolutionary Biology (CIBIO-InBIO), Campus Agrário de Vairão, Universidade do Porto, Rua Padre Armando Quintas,4485-661 Vairão, Portugal.

[2] Faculty of Sciences, University of Porto, Rua Campo Alegre s/n, 4169-007 Porto, Portugal.

[3] proMetheus –Research Unit in Materials, Energy and Environment for Sustainability, Instituto Politécnico de Viana do Castelo (IPVC), Avenida do Atlântico, no. 644, 4900-348 Viana do Castelo, Portugal.

[4] Department of Botany, Faculty of Sciences, University of Granada, Av. Fuentenueva, 18071 Granada, Spain.

[5] iEcolab. Interuniversity Institute for Earth System Research (IISTA), University of Granada, Av. del Mediterráneo, 18006 Granada, Spain.

[6] Andalusian Center for the Assessment and Monitoring of Global Change (CAESCG), Universidad de Almería, Crta. San Urbano, 04120 Almería, Spain.

[7] Institute for Systems and Computer Engineering, Technology and Science (INESC TEC), Campus da Faculdade de Engenharia da Universidade do Porto, Rua Dr. Roberto Frias, 4200-465 Porto, Portugal.

Abstract

Wildfire disturbances can cause modifications in different dimensions of ecosystem functioning, i.e., the flows of matter and energy. There is an increasing need for methods to assess such changes, as functional approaches offer advantages over those focused solely on structural or compositional attributes. In this regard, remote sensing can support indicators for estimating a wide variety of effects of fire on ecosystem functioning, beyond burn severity assessment. These indicators can be described using intra-annual metrics of quantity, seasonality, and timing, called Ecosystem Functioning Attributes (EFAs). Here, we propose a satellite-based framework to evaluate the impacts, at short to medium term (i.e., from the year of fire to the second year after), of wildfires on four dimensions of ecosystem functioning: (i) primary productivity, (ii) vegetation water content, (iii) albedo, and (iv) sensible heat. We illustrated our approach by comparing inter-annual anomalies in satellite-based EFAs in the northwest of the Iberian Peninsula, from 2000 to 2018. Random Forest models were used to assess the ability of EFAs to discriminate burned vs. unburned areas and to rank the predictive importance of EFAs. Together with effect sizes, this ranking was used to select a parsimonious set of indicators for analyzing the main effects of wildfire disturbances on ecosystem functioning, for both the whole study area (i.e., regional scale), as well as for four selected burned patches with different environmental conditions (i.e., local scale). With both high accuracies (area under the receiver operating characteristic curve (AUC) > 0.98) and effect sizes (Cohen's $|d| > 0.8$), we found important effects on all four dimensions, especially on primary productivity and sensible heat, with the best performance for quantity metrics. Different spatiotemporal patterns of wildfire severity across the selected burned patches for different dimensions further highlighted the importance of considering the multi-dimensional effects of wildfire disturbances on key aspects of ecosystem functioning at different timeframes, which allowed us to diagnose both abrupt and lagged effects. Finally, we discuss the applicability as well as the potential advantages of the proposed approach for more comprehensive assessments of fire severity.

Keywords

Ecological disturbance, Ecosystem functioning, EFAs, Fire severity, Satellite image time-series, Wildfires.

3.1. Introduction

Wildfire disturbances are considered an integral part of the natural dynamics of ecosystems in several biomes (San-Miguel-Ayanz *et al.* 2013, Adámek *et al.* 2016). Notwithstanding, wildfire events can modify the composition, structure, and functioning of ecosystems, and consequently the provision of ecosystem services to humankind (João *et al.* 2018). Among those alterations, changes in ecosystem functioning are of particular interest, as fire can cause rapid modifications in the matter and energy budgets of ecosystems (Petropoulos *et al.* 2009). This is because attributes of ecosystem functioning have a shorter response time to disturbances than structural or compositional attributes of landscapes, and are more directly connected to ecosystem services (Alcaraz-Segura *et al.* 2008).

Wildfires can have profound impacts on many key aspects of the flows of matter and energy. These include dimensions of ecosystem functioning related to the biogeochemical cycles of carbon (e.g., primary productivity, biomass), and water (e.g., vegetation water content, soil moisture), as well as to energy balances (e.g., albedo, latent heat, sensible heat). Namely, fires play an important role in the terrestrial biosphere carbon cycle (Wei *et al.* 2018), as they can cause substantial losses in carbon storage (Dunnette *et al.* 2014), including both aboveground biomass (Sparks *et al.* 2018), as well as soil organic matter (Pellegrini *et al.* 2018). Moreover, fire-mediated changes in nutrient concentrations can ultimately limit productivity (Leys *et al.* 2016), as well as induce phenological changes (Wang and Zhang 2017). Wildfires can also affect both water supply (Carvalho-Santos *et al.* 2019) and quality (Smith *et al.* 2011, Santos *et al.* 2015), as well as induce vegetation mortality due to prolonged loss of foliar moisture (Senf and Seidl 2020). Additionally, wildfires can have negative impacts on evapotranspiration (Vlassova *et al.* 2014, Poon and Kinoshita 2018), which in turn also influences radiation exchanges, as evapotranspiration is related to latent heat flux (Sun *et al.* 2019). Changes in wildfire frequency and/or severity may also have strong impacts on Earth's surface radiative budget (Liu *et al.* 2019, Rother and De Sales 2021). Burn severity influences the magnitude of changes in land surface albedo (French *et al.* 2016, Quintano *et al.* 2019), which can undergo a darkening and/or a brightening that can persist in time (Gatebe *et al.* 2014, Saha *et al.* 2017). Such alterations cause an increase in land surface temperature immediately following fires (Liu *et al.* 2018), which influences both burned area and the duration of fires (Maffei *et al.* 2018) since vegetation is a regulator of land surface energy fluxes (Veraverbeke *et al.* 2012). Although the effects of wildfires span across multiple dimensions of ecosystem functioning, most studies evaluating those effects seldom address those multiple dimensions at a time, thus

failing to fully depict spatiotemporal changes caused by these disturbances and limiting the assessment of environmental impacts.

As wildfire events have been increasing in previous decades, both in terms of frequency and intensity (Bowman *et al.* 2009, Koutsias *et al.* 2016), exacerbated by global climate change and by shifts in land use and forest management (Tedim *et al.* 2013), there is an increasing need for methods to assess and monitor the ecological consequences of such disturbances (van Leeuwen *et al.* 2010). Over the last decades, Remote Sensing (RS) has revolutionized the way environmental changes are monitored, with new satellite sensors (e.g., Sentinel-2 MSI, Landsat-8 OLI/TIRS) providing valuable data at increasingly higher temporal, spatial and spectral resolutions. Other satellites provide long-term archives of images useful to support temporal studies (e.g., Terra/Aqua MODIS, Landsat 5/7 missions). This growing variety and quality of remotely-sensed data enable a wide range of fire-related applications, from the detection of fire occurrences (Verbesselt, Hyndman, Zeileis, *et al.* 2010) to an evaluation of fire severity (Veraverbeke *et al.* 2011a) and monitoring of post-fire recovery (Alcaraz-Segura *et al.* 2010, van Leeuwen *et al.* 2010, Bastos *et al.* 2011) and resilience (Frazier *et al.* 2013). The ability to assess and map the heterogeneous (both spatially and temporally) effects of wildfires on ecosystems with remotely sensed data is a major asset not only for risk assessment and governance but also for post-fire management and restoration (Keeley 2009, Tedim *et al.* 2013, Smith *et al.* 2014, Parks *et al.* 2019). In this regard, spectral indices and metrics derived from satellite multi-spectral images have been used to assess different aspects of fire severity, usually through the comparison of pre-fire versus post-fire values. For instance, spectral indices sensitive to photosynthetically active radiation and/or water content, such as the Normalized Difference Vegetation Index (NDVI) and the Normalized Burn Ratio (NBR), have been used, in combination with data collected in-field (e.g., through the Composite Burn Index; CBI), to assess *burn severity* (e.g., Veraverbeke *et al.* 2011b, Cardil *et al.* 2019, Parks *et al.* 2019), which is a post-fire measure of organic matter loss and soil alteration (Keeley 2009, Tedim *et al.* 2013, Bowman *et al.* 2015). Furthermore, both satellite-derived land surface temperature (LST; (Quintano *et al.* 2015)) and albedo (Quintano *et al.* 2019) have been used for the same end. Nevertheless, to fully characterize and understand the effects of wildfire disturbances on multiple dimensions of ecosystems, a better translation of spectral indices into informative ecosystem variables is needed. More diverse sets of indicators are thus required to extend *burn severity* assessments to a wider variety of fire effects, i.e., towards more comprehensive approaches in *fire severity* assessment.

In recent decades, Ecosystem Functioning Attributes (EFAs) derived from SITS have been increasingly used in a wide range of ecological applications, due to their strong relation

to biophysical properties and processes of ecosystems (Alcaraz-Segura *et al.* 2008). These include wildfire-related applications, such as improving the detection of wildfire disturbances in space and time (Marcos *et al.* 2019), but also a wide range of other ecological applications, such as describing major ecological patterns (Alcaraz *et al.* 2006, Duro *et al.* 2007, Coops *et al.* 2008), predicting and projecting species distributions (Gonçalves *et al.* 2016, Arenas-Castro *et al.* 2018, Regos *et al.* 2020), and supporting the definition of conservation priorities (Cazorla, Cabello, Peñas, *et al.* 2020). More specifically, EFAs extracted from SITS can provide information on inter-annual quantity (e.g., mean, minimum, maximum), seasonality (i.e., seasonal range, or variability), and timing (e.g., dates of specific moments) components, over multiple dimensions of ecosystem functioning. These include frequently used satellite-derived descriptors of the intra-annual dynamics of carbon gains, such as primary productivity, vegetation seasonality, and phenology (e.g., Paruelo *et al.* 2005, Alcaraz *et al.* 2006, Cazorla, Cabello, Reyes, *et al.* 2020). However, analogous measures can also be extracted from RS-derived proxy descriptors related to other dimensions of ecosystem functioning, such as water content, albedo, and sensible heat (e.g., Arenas-Castro *et al.* 2019, Regos *et al.* 2020). By combining these four complementary dimensions of ecosystem functioning across each component (i.e., quantity, seasonality, and timing), remotely-sensed EFAs can enable in-depth and integrative characterizations of fire severity (João *et al.* 2018, Marcos *et al.* 2019).

The main objective of this study is to propose, describe, and showcase a framework to support enhanced assessments of fire severity, encompassing multiple dimensions of ecosystem functioning. Our approach is based on the effects of wildfire disturbances, at *short-* (i.e., the year of fire) to *medium-term* (i.e., up to the second year after the fire), on descriptors of the intra-annual dynamics (i.e., EFAs) of four essential dimensions of the flows of matter and energy in ecosystems: (i) primary productivity; (ii) vegetation water content; (iii) albedo; and (iv) sensible heat. To illustrate our approach, we assessed the potential of inter-annual anomalies (i.e., deviations from the normal inter-annual variability) of a large set of EFAs extracted from MODIS data, for the period between 2000 and 2018 in the NW Iberian Peninsula, as estimators of the effects of wildfire disturbances. To this end, we compared, ranked, and analyzed the main patterns of those inter-annual anomalies, at the regional scale. We then showcased the translation of inter-annual anomalies of selected EFAs into indicators of wildfire disturbance severity, for four selected burned patches within the study area, and compared and analyzed their main spatial and temporal patterns, at the local scale. Finally, we discussed the potential and added value of the proposed approach to improve RS-based assessment, mapping, and monitoring of wildfire disturbance severity on multiple dimensions of ecosystem functioning.

3.2. Materials and Methods

3.2.1. Generic framework

General workflow

The proposed approach to evaluate the effects of wildfire disturbances on ecosystem functioning consists of using indicators derived from Ecosystem Functioning Attributes (EFAs), for each of the four key dimensions of ecosystem functioning (i.e., primary productivity, vegetation water content, albedo, and sensible heat). **Figure 3.1** presents the general workflow of the proposed approach, which is composed of five steps, described in the following sub-sections.

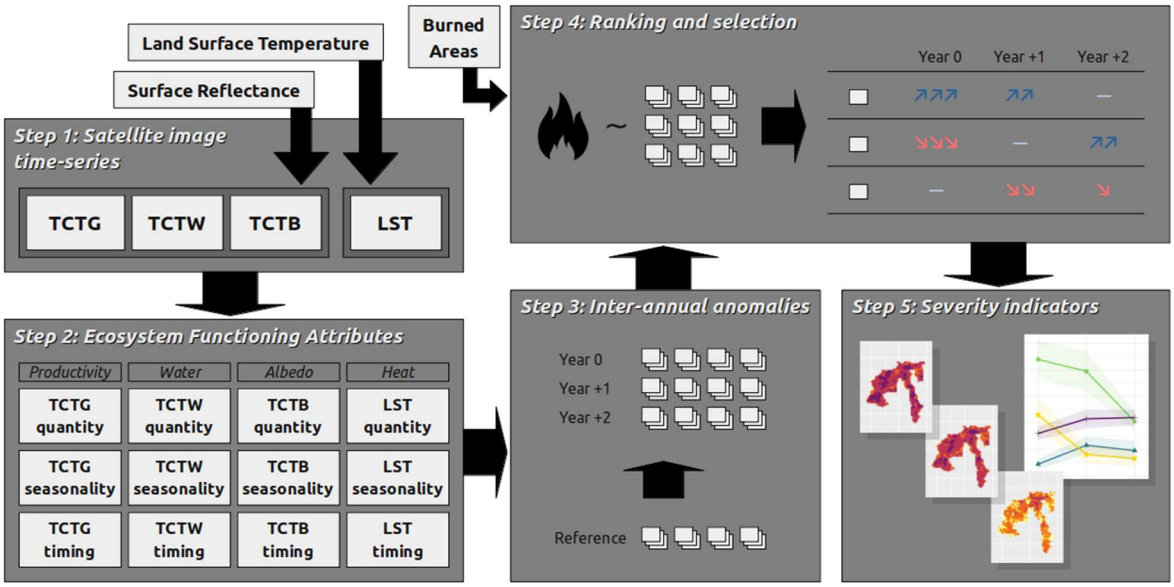

Figure 3.1. General workflow of the proposed approach to assess wildfire disturbance severity using indicators based on Ecosystem Functioning Attributes (EFAs) derived from satellite image time-series (SITS). TCTB: Tasseled Cap Transformation Brightness feature; TCTG: Tasseled Cap Transformation Greenness feature; TCTW: Tasseled Cap Transformation Wetness feature; and LST: Land Surface Temperature.

Step 1 – Satellite time-series

First, satellite image time-series (SITS) for each of the four dimensions of ecosystem functioning have to be collected from available satellite products, and preprocessed, (**Figure 3.1** – "Step 1"). From a large number of spectral band combinations and vegetation indices available that have been successfully used for fire applications (e.g., Healey *et al.* 2005, Mildrexler *et al.* 2009, Verbesselt, Hyndman, Newnham, *et al.* 2010, Quintano *et al.* 2015, Marcos *et al.* 2019), we propose, for that end, the use of Land Surface Temperature

(LST) for the *heat* dimension, as well as the Tasseled Cap Transformation (TCT) features of *Brightness* (TCTB), *Greenness* (TCTG), and *Wetness* (TCTW) for the *albedo*, *primary productivity*, and *vegetation water content* dimensions, respectively. The LST is a measure of the thermal energy emitted by different surfaces, calibrated from thermal emissivity measured by the satellite instrument (Duan *et al.* 2019). On the other hand, TCT features are well-known, sensor-specific, linear combinations of bands in the visible, near-infrared, and short-wave infrared regions of the electromagnetic spectrum (Lobser and Cohen 2007). These three TCT features of *Brightness*, *Greenness*, and *Wetness* result from a rotation of principal component axes, derived from a global sample, to be aligned with the biophysical parameters of albedo, amount of photosynthetically active vegetation, and soil moisture, respectively (Mildrexler *et al.* 2009).

Step 2 – Extraction of EFAs

Next, metrics describing aspects of the intra-annual dynamics of ecosystem functioning (i.e., EFAs) have to be extracted from SITS, for each target year (**Figure 3.1** – "Step 2"). These types of metrics are commonly used to describe intra-annual aspects of ecosystem functioning related to quantity, seasonality, and timing (e.g., Alcaraz *et al.* 2006, Alcaraz-Segura *et al.* 2008, Arenas-Castro *et al.* 2018). Examples of *quantity* metrics are the annual mean or median, the maximum or minimum values, or an integrated cumulative sum during a particular part of the year (e.g., the growing season). For *seasonality*, metrics such as the intra-annual standard deviation or range can be used. Examples of *timing* metrics are the dates of the annual maximum, minimum, or other important moments (e.g., the start/end of the growing season).

Step 3 – Computation of EFA anomalies

To obtain inter-annual EFA anomalies, it is necessary to first compute reference values for each pixel (**Figure 3.1** – "Step 3a"). To this end, EFAs are extracted for a multi-annual reference profile, which is obtained by averaging all years, after excluding values for years with any record of wildfire occurrences (this procedure is similar to the one used in (Gouveia *et al.* 2010, Bastos *et al.* 2011), except for the exclusion of values in years with fire occurrences). Then, the anomalies are calculated by subtracting the reference values to those of each year, for each EFA (**Figure 3.1** – "Step 3b"). More precisely, in the case of linear (i.e., non-circular) metrics, the anomalies are calculated using the following expression:

$$A_m = X_m - R_m \quad 3.1$$

where A_m represents the annual anomalies of EFA *m*; X_m represents the annual values of EFA *m*, and R_m represents the values of the reference-year for EFA *m*. In the case of circular metrics – e.g., a day-of-the-year (DOY) –, anomalies are calculated through the smallest differences between angles, in the following manner:

$$A_m = \left(\frac{365}{2\pi} \times \theta\right) + 35 \quad 3.2$$

where A_m represent the annual anomalies of EFA *m*, and θ is defined as follows:

$$\theta = \begin{cases} arctan\left(\frac{y}{x}\right), & if\ x > 0 \\ arctan\left(\frac{y}{x}\right) + \pi, & if\ x < 0\ and\ y \geq 0 \\ arctan\left(\frac{y}{x}\right) - \pi, & if\ x < 0\ and\ y < 0 \\ \frac{\pi}{2}, & if\ x = 0\ and\ y > 0 \\ -\frac{\pi}{2}, & if\ x = 0\ and\ y < 0 \\ undefined, & if\ x = 0\ and\ y = 0 \end{cases} \quad 3.3$$

with:

$$x = cos(X_m - R_m) \quad 3.4$$

and:

$$y = sin(X_m - R_m) \quad 3.5$$

where X_m and R_m represent the same as in *Equation 3.1*.

Step 4 – EFA ranking and selection procedures

Since multiple aspects of the intra-annual dynamics of ecosystem functioning can be obtained through the computation of EFAs, a selection process is necessary to reduce the initial set of metrics to an essential (i.e., relevant and less correlated) parsimonious set. In this selection process, classification models are used to rank all the EFAs considered in terms of their potential to measure the remotely-sensed effects (as proxies of severity) of wildfire disturbances on the different EFAs (**Figure 3.1** – "Step 4a"). To this end, the burned area maps considered the response variable, while the anomalies of all EFAs are

considered the predictive variables. The resulting ranking of EFA anomalies are used to compare all EFAs across (i) base SITS, each corresponding to a different dimension of ecosystem functioning (i.e., primary productivity, vegetation water content, albedo, and sensible heat); and (ii) the specific metric (e.g., mean vs. median), and (iii) component of the inter-annual dynamics of ecosystem functioning (i.e., quantity, seasonality, and timing) used, each corresponding to an EFA. Furthermore, potential temporally lagged effects can also be evaluated, by including values of EFA anomalies of different years concerning the year of the wildfire disturbance event (e.g., the anomalies for the year of the fire event, plus the first year after, the second year after, etc.).

The resulting ranking can be coupled with additional selection criteria, such as pairwise correlations, to minimize potential redundancy between EFAs, so that a compact set of twelve EFAs (i.e., one for each dimension and each component of the inter-annual dynamics of ecosystem functioning) are selected (**Figure 3.1** – "Step 4b"). Then, both magnitude and direction of the pairwise relationship between the response variable (e.g., burned areas) and each of the selected EFAs is assessed (e.g., using Cohen's d effect size statistics; Cohen 1992). This allows for the inter-comparison of selected EFAs across all the dimensions and components of ecosystem functioning, as well as other factors considered (e.g., the year of the early post-fire period). Based on these procedures, a final selection of EFAs is carried out to support the analysis of the main patterns of wildfire disturbance severity on the dimensions of ecosystem functioning considered.

Step 5 – Translation into indicators of wildfire disturbance severity

To support a multi-dimensional assessment of the effects of wildfire disturbances on ecosystem functioning, the final set of selected EFAs are then converted into indicators of wildfire disturbance severity (**Figure 3.1** – "Step 5"). For obtaining these indicators, the absolute values of the corresponding EFA anomalies are used, as these constitute measures of the magnitude of deviations from reference, thus allowing easier comparison across different dimensions. The resulting compact set of indicators is then used to support more detailed analyses.

3.2.2. Test case

Study area

To illustrate our proposed approach, we chose the northwest of the Iberian Peninsula (NW-IP) as the overall study area (**Figure 3.2**), since this is a hotspot in terms of wildfire

occurrences, within the European context, being a highly fire-prone landscape (João *et al.* 2018). This area extends to the north and the west to the Atlantic Ocean, while its southern boundary was delimited by the edge of MODIS tile h17v04. Its eastern boundary, on the other hand, was defined to include the northern half of mainland Portugal, as well as the Spanish autonomous community of Galicia.

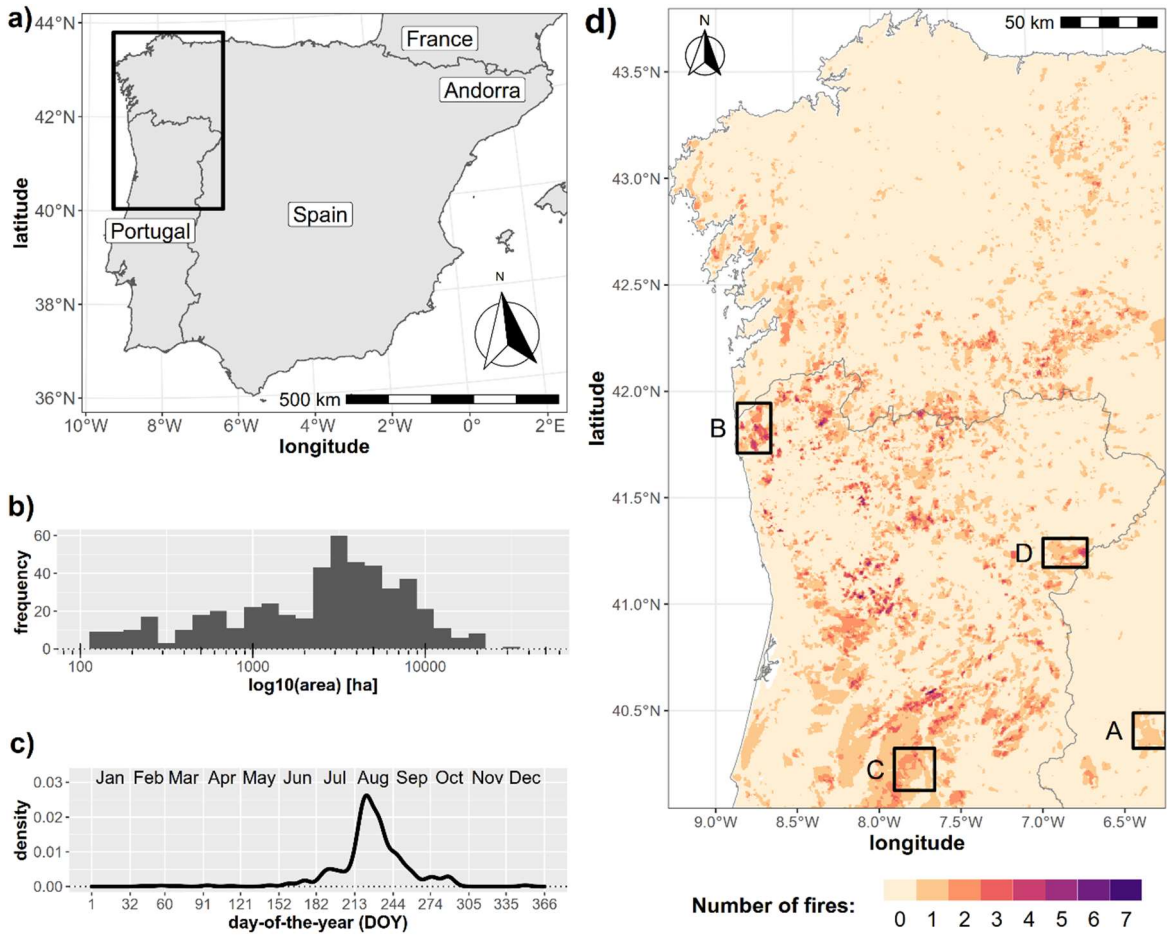

Figure 3.2. The study area for the illustrative test case, with: (a) location of the overall study area, for regional-scale analyses, within the Iberian Peninsula; (b) size distribution of all fires; (c) distribution of the area burned, by day-of-the-year (DOY); and (d) location of the four individual burned patches selected for local-scale analyses (labels A–D), overlapped with the number of fires occurred. For these figures, all wildfires with an area > 100 ha which occurred between 2000 and 2018 (according to the MODIS MCD64A1 Burned Areas product) were considered.

The NW-IP features strong environmental gradients and includes a major biogeographic transition, from Atlantic climate with Temperate deciduous broadleaf and mixed forests in the north and northwest, to a Mediterranean climate with evergreen sclerophyllous vegetation towards the southeast. Land cover and uses are well diversified and highly heterogeneous (see **Table 3.1**), including cropland areas, urban areas, plantation forests (mostly maritime-pine, eucalyptus, and mixed stands), and shrublands in different successional stages, along with historical use of fire for agrosilvopastoral

purposes. Wildfire occurrences are more frequent during the months between July and October – but especially in August –, with burned areas over 10,000 ha being increasingly common. Wildfire events have been increasing in the last decades because of changes in land use, which mainly resulted from extensive abandonment of farming and husbandry, increasing the fuel load and its continuity in the landscape (Tedim *et al.* 2013, Caon *et al.* 2014). The frequency of extreme fire events, also known as mega-fires (i.e., complex catastrophic events in terms of size, intensity, resistance to control, severity, etc.; Tedim *et al.* 2013), has also been increasing, despite the huge investments in fire suppression (Koutsias *et al.* 2016), making this one of the regions with both the highest annual values of burnt area in Europe and the highest density of ignitions among southern European countries (Catry *et al.* 2009).

Table 3.1. Summary of baseline environmental characteristics of the overall study area for regional-scale analyses (NW-IP), as well as the four selected burned patches selected for local-scale analyses (A–D). Elevation was extracted from *MERIT DEM* (Yamazaki *et al.* 2017); climate variables were extracted from the *CHELSA Bioclim* dataset (Karger *et al.* 2017); the percentages of land-cover classes were extracted from *CORINE Land Cover* (CLC) 2000 (European Environment Agency 2020).

	NW-IP	**A**	**B**	**C**	**D**
Year of fire	–	2003	2005	2005	2013
Average burned area [ha]	3617	14 625	17 600	19 325	14 850
Distance to coast [km]	–	212	9	91	153
Average elevation [m a.s.l.]	580	801	261	712	505
Average temperature [°C]	12.7	13.0	14.1	12.5	14.1
Minimum temperature [°C]	3.1	1.2	7.5	1.0	2.8
Maximum temperature [°C]	2.5	28.9	21.8	26.7	29.1
Average total precipitation [$mm \cdot yr^{-1}$]	1139	1075	1747	1229	620
% of Urban	1.8	0.0	1.1	0.1	0.2
% of Agricultural	29.0	9.3	8.0	5.8	26.0
% of Broad-leaf forests	7.1	0.8	1.6	0.2	4.9
% of Coniferous forests	5.9	34.5	17.7	32.8	10.8
% of Mixed forests	8.7	4.5	9.1	3.4	1.5
% of Natural grasslands	5.6	0.2	4.0	0.0	17.4
% of Shrublands	20.2	50.1	32.7	57.1	38.2
% of Bare rocks or sparsely vegetated	2.0	0.6	25.7	0.6	1.0

To showcase our proposed framework, the full study area in NW-IP, including both burned and unburned areas of NW-IP, between 2000 and 2018, was used for regional-scale analyses. Then, for local-scale analyses, four individual burned patches (see boxes labeled A–D in **Figure 3.2**) were selected, from different geographical locations within the study area, featuring diverse baseline environmental characteristics (e.g., altitude, distance to coast, climate, the proportions of major vegetation types), and with the focal wildfire event

having occurred at different years within the considered period (A: 2003; B and C: 2005; and D: 2013). **Table 3.1** presents a summary of the characteristics of both the full study area, used for regional-scale analyses (i.e., NW-IP), as well as of the four individual burned patches used for local-scale analyses.

Satellite data preprocessing

In our test case, we used SITS extracted from MODIS products. Most tasks were undertaken within the R statistical programming environment (R Core Team 2019), using mainly the *raster* package (Hijmans 2016), with additional R packages complemented by other software, for more particular tasks, as specified whenever relevant.

We started by downloading and preprocessing all available images encompassing NW-IP (i.e., MODIS tile h17v04), between 2000 and 2018, from the following MODIS products, using the *MODIStsp* R package (Busetto and Ranghetti 2016):

- MODIS/Terra+Aqua Burned Area Monthly L3 Global 500m (MCD64A1), Collection 6 (Giglio *et al.* 2018);
- MODIS/Terra Land Surface Temperature/Emissivity 8-Day L3 Global 1km (MOD11A2), Collection 6 (Wan *et al.* 2015); and
- MODIS/Terra Surface Reflectance 8-Day L3 Global 500m (MOD09A1), Collection 6 (Vermote 2015).

Preprocessing consisted of converting to the GeoTIFF file format, re-projecting to a common reference system (WGS84/UTM29N), and resampling to 500m pixel size using the nearest neighbor interpolation algorithm. Additionally, a filter based on the *Hampel* outlier identifier (Hampel 1971, 1974) with a window size of 5, was applied to the resulting SITS, to reduce residual noise that hinders time-series data.

Next, LST, TCTB, TCTG, and TCTW were extracted from the MOD11A2 and MOD01A1 products, respectively, using *GDAL* (GDAL contributors 2020) and the *rasterio* python package (Gillies *et al.* 2013). For LST, only the day temperatures were used, which were then rescaled to degrees Celsius. The three TCT features of *Brightness*, *Greenness*, and *Wetness* were obtained by combining the 7 bands available in the MOD09A1 product, using the coefficients presented in **Table 3.2** (Lobser and Cohen 2007).

Burned areas extracted from the MCD64A1 product were filtered by size, eliminating all burned patches smaller than 100 ha, following a set of criteria detailed in previous work (see Marcos *et al.* 2019). To further reduce the remaining noise in the data, a Whittaker-Henderson smoother (Whittaker 1922, Eilers 2003) was applied to the four extracted SITS,

with a *lambda* parameter equal to 2 (a rather low value, to conserve the characteristics of the time-series, while still reducing extreme noise).

Table 3.2. MODIS-specific coefficients to calculate the tasseled cap transformation (TCT) features of *Brightness*, *Greenness*, and *Wetness*. These features result from a rigid rotation of principal component axes, which are aligned with the biophysical parameters of albedo, the amount of photosynthetically active vegetation, and soil moisture, respectively (Lobser and Cohen 2007).

Band			Coefficients		
No.	*Name*	*Range [nm]*	*Brightness*	*Greenness*	*Wetness*
1	Red	620 – 670	0.4395	–0.4064	0.1147
2	NIR 1	841 – 876	0.5945	0.5129	0.2489
3	Blue	459 – 479	0.2460	–0.2744	0.2408
4	Green	545 – 565	0.3918	–0.2893	0.3132
5	NIR 2	1230 – 1250	0.3506	0.4882	–0.3122
6	SWIR 1	1628 – 1652	0.2136	–0.0036	–0.6416
7	SWIR 2	2105 – 2155	0.2678	–0.4169	–0.5087

NIR: near-infrared; SWIR: short-wavelength infrared.

EFA anomalies computation

A total number of 60 EFAs were extracted, using 15 different intra-annual metrics (**Table 3.3**), from each of the four SITS – LST, TCTB, TCTG, and TCTW –, for each year between 2000 and 2018, for NW-IP. Among these, well-known measures were computed for *quantity* – mean, median, maximum, and minimum annual values – and *seasonality* – standard deviation, median absolute deviation, and absolute range. In addition to those, also the relative range, and a non-parametric relative range were computed, using the following expressions:

$$rrl = log_{10}\left(\left|\frac{rng}{avg}\right|\right) \quad 3.6$$

and:

$$npr = log_{10}\left(\left|\frac{rng}{mdn}\right|\right) \quad 3.7$$

where *rrl* is the relative range metric, while *rng* is the absolute range, *avg* is the mean, *npr* is the non-parametric relative range, and *mdn* is the median.

Table 3.3. List of metrics extracted from each of the four satellite image time-series used in this study (i.e., Land Surface Temperature, and the Tasseled Cap Transformation features of *Brightness*, *Greenness*, and *Wetness*); as well as the number of predictive variables for models, extracted from each one.

Component	Metric	Abbreviation	No. of variables for models
Quantity	Mean (or average)	avg	12
	Median	mdn	12
	Maximum	max	12
	Minimum	min	12
Seasonality	Standard deviation	std	12
	Median absolute deviation	mad	12
	Absolute range	rng	12
	Relative range	rrl	12
	Non-parametric relative range	rnp	12
Timing	Time (of the year) of maximum	tmx	12
	Winterness of maximum	wmx	12
	Springness of maximum	smx	12
	Time (of the year) of minimum	tmn	12
	Winterness of minimum	wmn	12
	Springness of minimum	smn	12
Total			180

As for *timing*, the time (of the year) of the maximum and minimum values were used. However, as variables of time of the year are circular by definition, we also tested two linearized versions for each, called *winterness* and *springness*, using the following expressions:

$$winterness = cos\left(\frac{2\pi}{365} \times (x - 35)\right) \quad 3.8$$

and:

$$springness = sin\left(\frac{2\pi}{365} \times (x - 35)\right) \quad 3.9$$

where *x* is the day-of-the-year (DOY) of either the maximum or minimum values (*tmx* or *tmn*, respectively). Note that these last two expressions (i.e., *Equations 3.8* and *3.9*) include the conversion from DOY to radians, assuming that a full year has 365 days; as well as a

rotational realignment of -35 days so that the maximum and minimum values of *winterness* and *springness* (i.e., 1 and -1, respectively) correspond to the mid-point of each season (in the case of NW-IP, as it is located in the northern hemisphere, the mid-point of winter is in early February). These metrics can be interpreted as corresponding to the temporal proximity, within the year, to either the start of winter or spring, respectively.

Finally, anomalies were then obtained for all EFAs, for each of the four SITS, by calculating either linear differences (see *Equation 3.1*), for all metrics except *tmx* and *tmn* or the smallest differences between angles, for those two circular metrics (see *Equations 3.2–3.5*).

Ranking and selection of EFAs

A ranking of EFA anomalies was obtained for NW-IP, through a classification modeling procedure, in which the response variable was the binary burned class (i.e., burned vs. unburned) extracted from the MODIS burned area product. As predictive variables for these models, we used the inter-annual anomalies in each one of the 60 EFAs (i.e., each of the 15 intra-annual metrics described in **Table 3.3**, for each of the four SITS), for each one of three years since the fire occurrence: the year of fire, as well as the first and second years after (i.e., years 0, +1 and +2). This was to allow for the evaluation of potential temporally lagged effects (for which only the years from 2003 to 2016 were used). In total, the number of predictive variables used in these models was 180. To this end, the *Random Forest* (RF) *ensemble learning* algorithm was used, since this technique scales well on large and/or high dimensional data (Couronné *et al.* 2018), thus allowing for the full set of variables to be tested without the need for a selection before modeling.

As the number of pixels identified as *burned* represented only ca. 1.3% of the total overall study area (i.e., NW-IP), data balancing through down-sampling of the majority class (i.e., *unburned*) was applied. For that end, 100 random sample sets were defined, consisting of all the pixels identified as *burned*, as well as an equal number of randomly selected *unburned* pixels for each year, in a total of 122,658 observations (i.e., n = 61,329, per class). Then, an RF classification model was calibrated for each one of the 100 sample sets, using the *caret* R package (Kuhn *et al.* 2016), with the hyperparameters set to the default values (including a fixed value for *mtry* equal to the default squared root of the number of predictive variables), and under a *leave-group-out-cross-validation* (LGOCV) scheme with 50%–50% train/test split in each one of 10 repetitions.

Model performance was then evaluated using measures specific to two-class problems – *Sensitivity* (or true positive rate), *Specificity* (or true negative rate), and the *Area*

Under the Receiver Operating Characteristic Curve (AUC) – which were then averaged across the 100 resulting models. Finally, *Variable Importance Scores* – a common approach to extract interpretable information on the contribution of different variables from RF models (Couronné *et al.* 2018) –, based on the *Mean Decrease in Accuracy*, were extracted, and also aggregated to the median values across the 100 sample sets, to support the EFA ranking.

Based on the ranking of variable importance scores obtained from the RF models, one EFA was selected for each dimension and each component, giving a total of 12, to support the analysis of the main patterns of wildfire disturbance severity on multiple dimensions of ecosystem functioning in NW-IP.

Analysis of indicators of wildfire disturbance severity

To support the analysis of both the directionality (i.e., increasing or decreasing) and magnitude of the pairwise relationships between the regional-scale burned areas and each of the selected EFAs, *Cohen's d* effect size statistics (Cohen 1992) and *Spearman pairwise rank correlations* were calculated for the 100 sample sets. From this, as well as from the distributions of the selected EFA anomalies, the main overall patterns of the effects of wildfire disturbances on ecosystem functioning were analyzed for NW-IP and compared across the four dimensions and three components of ecosystem functioning, as well as across years of the early post-fire period.

It should be noted that effect sizes were applied here to avoid the use of statistical hypothesis testing based on significance (i.e., *p*-values), which have important known limitations, such as not measuring the effect size or the importance of a result (Wasserstein and Lazar 2016), or the strong influence of sample size which is hugely influential in determining significance levels (Hubbard and Lindsay 2008) (i.e., when sample sizes are large enough, any effect, can produce a small p-value if the sample size or measurement precision is high enough (Wasserstein and Lazar 2016); with large sample sizes often happening at a pixel-level analysis of SITS).

We then computed four indicators of the effects of wildfire disturbances on ecosystem functioning (i.e., one for each dimension), for four selected burned areas (see **Figure 3.2**), at a local scale, to illustrate the proposed approach for RS-based assessment, mapping, and monitoring of wildfire disturbance severity on multiple dimensions of ecosystem functioning. The selection of EFAs for these final indicators took into consideration the results from both the random forest model-based ranking and the pairwise correlations between EFAs. The translation of the selected EFAs into indicators was done by taking the

absolute values of the anomalies of the selected EFAs, for the four burned areas. Finally, spatial patterns between all indicators, across years, were further analyzed, local-scale, through local spearman correlations, with a neighborhood window size of 5 pixels.

3.3. Results

3.3.1. EFA ranking

In terms of performance of the Random Forest (RF) models for our test case, the results obtained for leave-group-out cross-validation can be considered very good across all sample sets, with around 0.9815±0.0004 for AUC, 0.9080±0.0015 for Sensitivity, and 0.9647±0.0010 for Specificity.

As for variable importance scores, EFAs extracted from TCTG had overall higher values than the other dimensions (**Figure 3.3**; see also *Supplementary material—Figure S3.1* for the full plot of variable importance scores for all non-aggregated variables). Considering each of the three different EFA components, the ones measuring aspects of *quantity* – particularly the mean and either one of the extreme values (minimum or the maximum, depending on the specific case), – obtained overall higher variable importance scores than *seasonality* or *timing* EFAs, with the notable exception of seasonality EFAs, extracted from TCTG at year 0. Conversely, the same exception was observed within all seasonality EFAs, where otherwise LST was the dimension from which EFA anomalies obtained higher variable importance scores overall, especially for standard deviation. As for timing EFAs, the scores obtained were generally lower than for the two other groups, except for the ones extracted from either TCTG or LST, at year 0, particularly the *springness* of the time-of-the-year of the minimum TCTG value, and the *winterness* of the time-of-the-year of the maximum LST value, following closely the corresponding quantity EFAs.

Across the four different dimensions of ecosystem functioning, those extracted for the year of fire (i.e., year 0) generally obtained better scores than those of the two subsequent years. However, for quantity EFAs extracted from TCTW, the first year after the fire (i.e., year +1) obtained better scores. Furthermore, quantity EFAs extracted from TCTB also achieved higher scores for the second year after the fire (i.e., year +2), although not as high as for year 0. Finally, in terms of individual EFAs, the top-ranked ones were extracted from TCTG, with the minimum value (TCTG-min) and the standard deviation of TCTG (TCTG-std) at year 0 holding the highest scores among all EFAs tested.

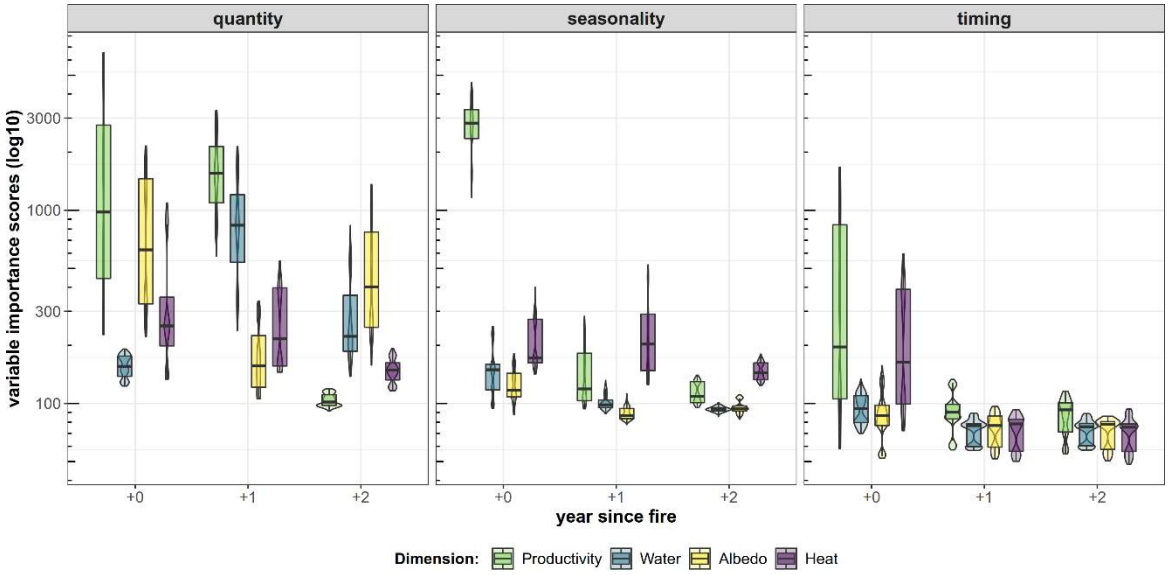

Figure 3.3. Distributions of variable importance scores obtained from Random Forest models, to assess the effects of wildfire disturbances on four dimensions of ecosystem functioning: Primary productivity ("Productivity"), vegetation water content ("Water"), "Albedo", and Sensible heat ("Heat"), in the same year as the respective fire ("year 0"), and the two years after ("year +1" and "year +2"), for each of the three components considered: *quantity* (left); *seasonality* (center); and *timing* (right). (Note that the scale of the y-axis is logarithmic.)

3.3.2. Analysis of effects

Considering the RF-based importance ranking, 12 EFAs (**Table 3.4**) were selected, one for each dimension (i.e., primary productivity, vegetation water content, albedo, and sensible heat) and each component of intra-annual dynamics (i.e., quantity, seasonality, and timing). As for *timing* EFAs, it should be noted that the selected metrics do not correspond to the highest-ranked ones for each case. In this instance, parsimony and interpretability criteria were also considered, since linearized versions of timing EFAs (i.e., *winterness* and *springness*) often require the use of both at the same time to better understand in which month/season the minima/maxima occur (see *Supplementary material—Figure S3.2* for partial dependence plots of the predictive variables of the models, extracted from the 12 selected EFAs).

Table 3.4 summarizes the results for the effect sizes (both magnitudes and directions) between the response variable and each of the selected EFA anomalies (see *Supplementary material—Table S3.1* for additional information on the effect size results). These showed overall strong negative effects (i.e., lower values associated with wildfire disturbances) for TCTG-min and TCTW-avg (especially at years 0 and +1, and +1 and +2, respectively), while positive (i.e., raised values associated with wildfire disturbances) for LST-max (especially at years 0 and +1). For TCTB-avg, however, the effects changed from strongly negative at year 0, to strongly positive at year +2. As for *seasonality* EFAs, the

effects were overall positive, with the strongest magnitude associated with TCTG-std and LST-std. Finally, *timing* EFAs had overall weaker effects, except for TCTG-tmn (with large negative effects), and LST-tmx (with large positive effects), both only at year 0.

Table 3.4. List of selected EFAs, with the corresponding effects categories, based on Cohen's *d* effect size statistic. The number of arrows in the *Effect category* columns symbolizes the magnitude of the effect size, with | *d* | < 0.2 *negligible*, | *d* | < 0.5 *small*, | *d* | < 0.8 *medium*, otherwise *large*. The direction and color of the arrows symbolize the sign of the effect size, with ascending arrows depicting positive (non-*negligible*) effect sizes while descending arrows depict negative (non-*negligible*) effect sizes (*negligible* effects are symbolized by a horizontal dash).

Dimension	Component	Attributes (EFA)	Effect category		
			year 0	*year +1*	*year +2*
Primary productivity	Quantity	TCTG-min	↘↘↘	↘↘↘	—
	Seasonality	TCTG-std	↗↗↗	↗↗	—
	Timing	TCTG-tmn	↘↘↘	—	—
Vegetation water content	Quantity	TCTW-avg		↘↘↘	↘↘↘
	Seasonality	TCTW-std	—	↗↗	—
	Timing	TCTW-tmn	—	—	—
Albedo	Quantity	TCTB-avg	↘↘↘	↗	↗↗↗
	Seasonality	TCTB-std	—	↗	—
	Timing	TCTB-tmx	—	—	—
Sensible heat	Quantity	LST-max	↗↗↗	↗↗↗	↗
	Seasonality	LST-std	↗↗	↗↗↗	↗
	Timing	LST-tmx	↗↗↗	—	—

3.3.3. Main patterns in EFA anomalies

The distributions of the deviations from the normal variation (i.e., anomalies) for each of the twelve selected EFAs, grouped by year-after-fire (i.e., years 0, +1, and +2), and by burned vs. unburned pixels, are shown in **Figure 3.4** (see also *Supplementary material—Figure S3.3* for the distributions of the reference values of all pixels in the NW-IP).

Overall, there are notable differences in the distributions obtained for burned vs. unburned pixels, with the most notable contrast having been observed for TCTG-tmn at year 0, with median anomalies corresponding to occurrences of 80–88 days earlier than reference. Within the same dimension, differences were also notable for TCTG-min (especially at years 0 and +1), and also for TCTG-std (especially at year 0), with values of burned pixels considerably below/above (respectively) those of unburned pixels. Considerable differences between burned vs. unburned were also obtained for TCTW-avg,

but only at years +1 and +2, while for TCTB-avg they were observable at years 0 and +2, with opposite directions (i.e., negative vs. positive). As for heat-related EFAs, differences in the distributions of anomalies, between burned and unburned pixels, were notable for LST-max and LST-std across all years after the fire, but especially at years 0 and +1. Finally, LST-tmx showed a contrast between burned and unburned pixels, with median anomalies corresponding to delays of 8–16 days.

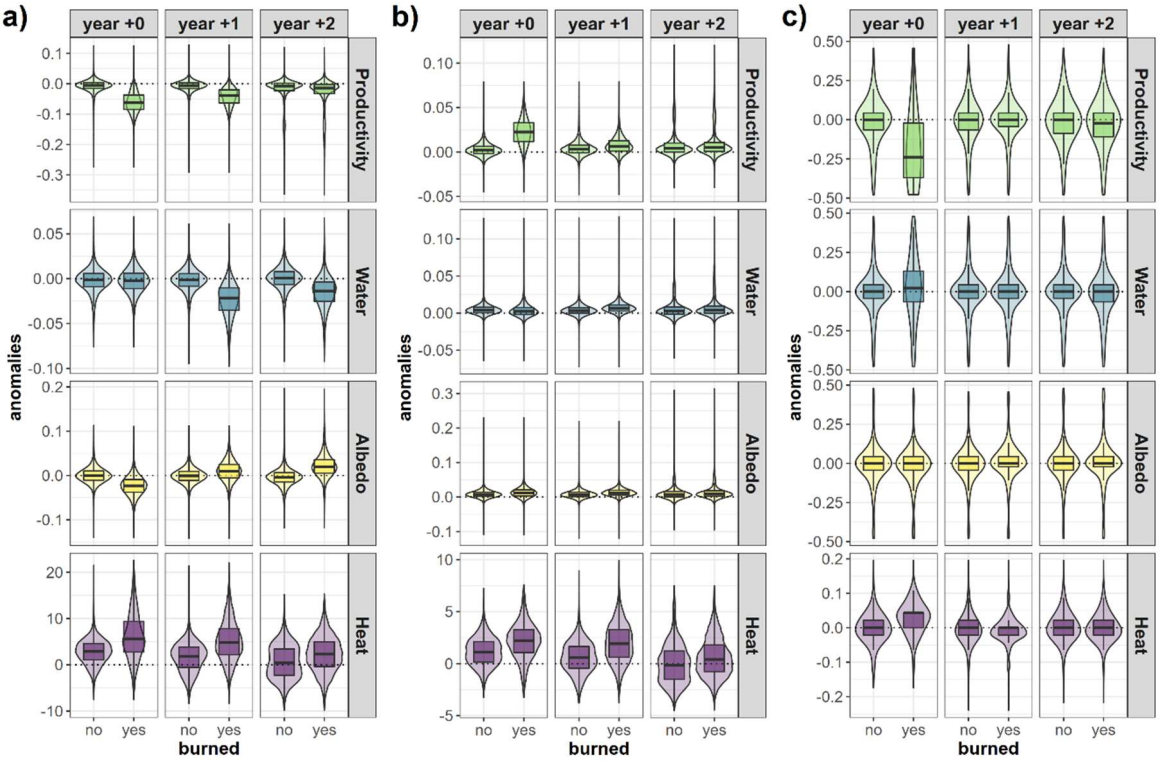

Figure 3.4. Distributions of the anomalies of the 12 selected EFAs, in the same year as the respective fire (*year 0*), and the two years after (*year +1* and *year +2*), for each of the three components considered: (a) *quantity*; (b) *seasonality*; and (c) *timing*. The specific intra-annual metrics selected for each of the four dimensions of ecosystem functioning considered were the following: Primary productivity ("Productivity") – *Tasseled Cap Transformation* (TCT) *Greenness* feature minimum value (TCTG-min), standard deviation (TCTG-std), and time-of-the-year of the minimum value (TCTG-tmn); Vegetation water content ("Water") – TCT *Wetness* feature average value (TCTW-avg), standard deviation (TCTW-std), and time-of-the-year of the minimum value (TCTW-tmn); "Albedo" – TCT *Brightness* feature average value (TCTB-avg), standard deviation (TCTB-std), and time-of-the-year of the maximum value (TCTB-tmx); and Sensible heat ("Heat") – *Land Surface Temperature* (LST) maximum value (LST-max), standard deviation (LST-std), and time-of-the-year of the maximum value (LST-tmx).

3.3.4. Multi-dimensional assessment of wildfire disturbance severity

For the RS-based assessment of wildfire disturbance severity on the four dimensions of ecosystem functioning considered, at the local level, one indicator for each dimension was used, based on the previously selected anomalies in quantity EFAs (i.e., TCTG-min, TCTW-avg, TCTB-avg, and LST-max). This selection took into consideration the results from both the model-based ranking (i.e., quantity EFAs ranked overall better than those of

seasonality or timing) and pairwise correlations (up to ±0.83; see *Supplementary material—Figure S3.4* for a correlations heatmap).

Figure 3.5 shows the median (±0.5 median absolute deviations) profiles of each of the four selected indicators, across the three years-after-fire, for each of the four burned areas-of-interest (see *Supplementary material—Figure S3.5* for additional information on the spatial and temporal patterns of the indicators of wildfire disturbance severity in the four burned areas A–D). This figure illustrates different post-fire trajectories, with varying relations between the four dimensions of ecosystem functioning, across individual burned areas. Specifically, different areas had different ratios between *Productivity* and *Heat* (e.g., A vs. D). Also, *Water* seemed to be less affected on area D than on the other areas, while *Albedo* in area D exhibited a different post-fire trajectory, relatively to the other areas, with the value for year +1 being slightly higher than for year 0.

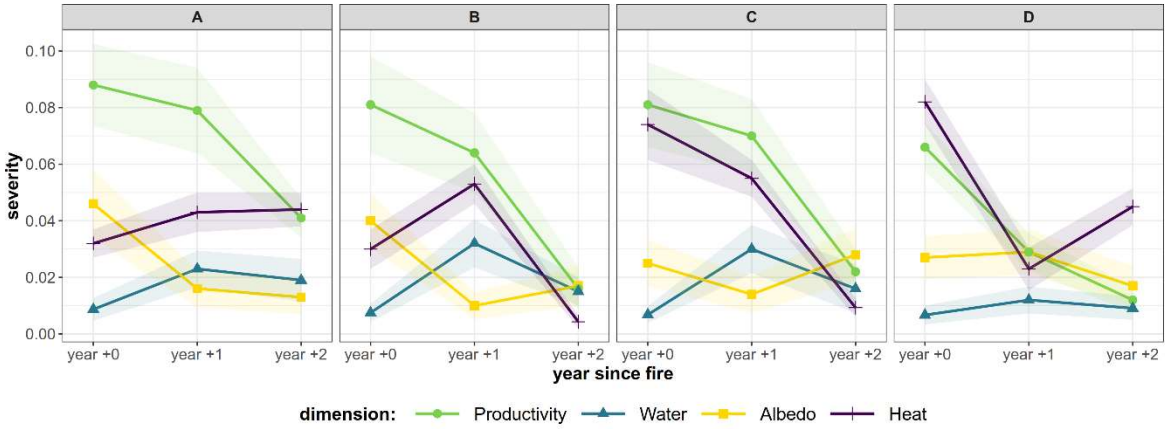

Figure 3.5. Profiles of wildfire disturbance severity on the four dimensions of ecosystem functioning: primary productivity ("Productivity"), vegetation water content ("Water"), "Albedo", and sensible heat ("Heat"), at short-to-medium term (i.e., between years 0 and +2 after the fire event), for four individual burned areas (letters A–D; see **Figure 3.2** for their location within the study area). Dots connected by thick lines represent median values across all pixels of each individual burned area, while shaded areas of the corresponding color represent ±0.5 × median absolute deviation. Values for the *Heat* dimension are scaled by a factor of 0.005, for visual comparability purposes.

Finally, **Figure 3.6** shows the variation in the spatial and temporal patterns of each of the four selected indicators of primary productivity, vegetation water content, albedo, and sensible heat, for each of the four individual burned areas of interest (A–D). Overall, some wildfire disturbance severity *hotspots* are observable, while not necessarily coinciding across dimensions (see also *Supplementary material—Figure S3.5*). Moreover, different burned areas exhibited different patterns across time, between dimensions of ecosystem functioning, with temporal trends being divergent in some cases, while convergent in others (e.g., *Water* and *Albedo* dimensions in areas-of-interest C vs. D), or with different relative preponderances (e.g., *Productivity* vs. *Heat* in areas of interest A vs. D), further illustrating the patterns observed in **Figure 3.5**.

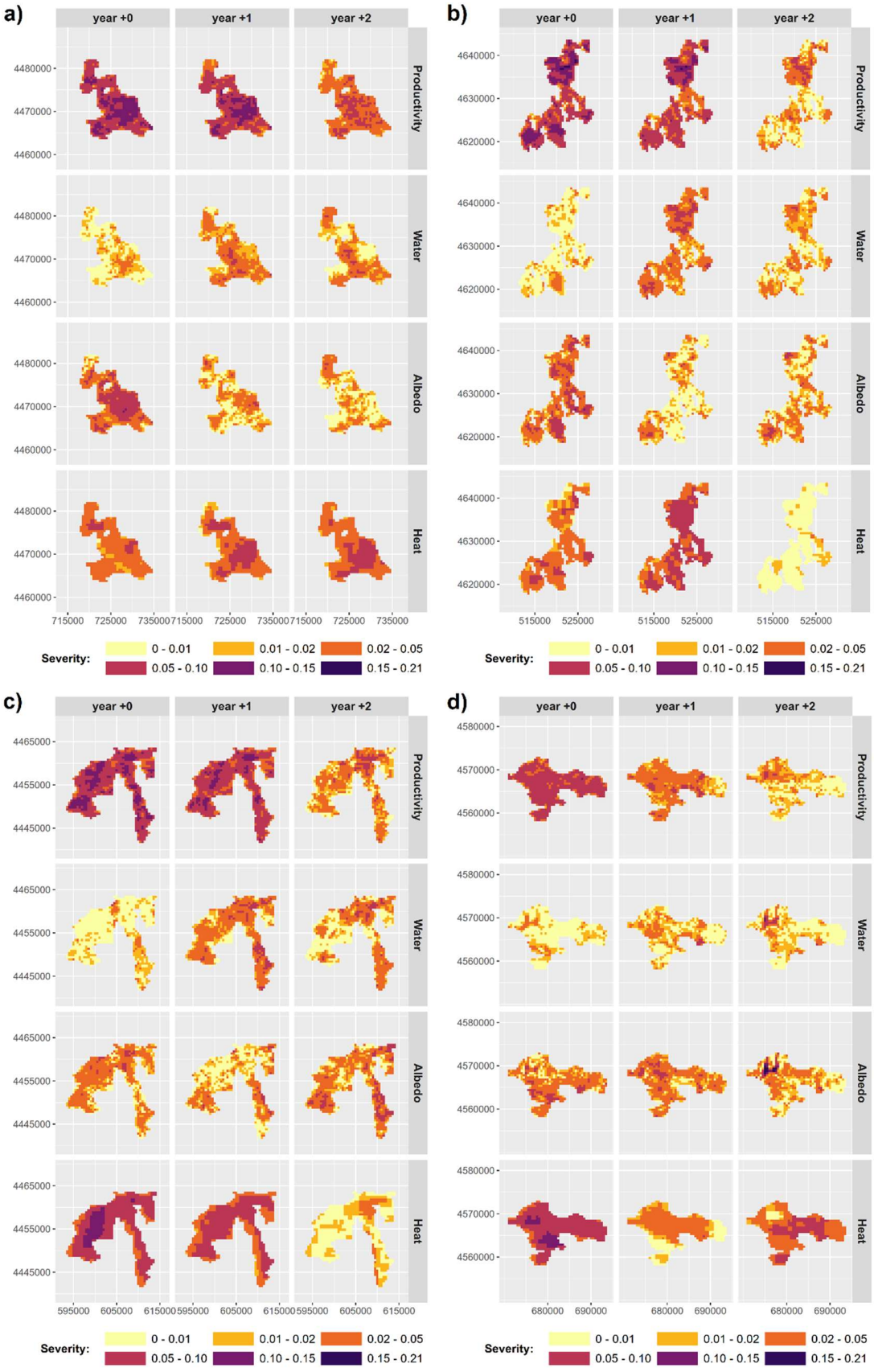

Figure 3.6. Maps of wildfire severity on primary productivity ("Productivity"), vegetation water content ("Water"), "Albedo", and sensible heat ("Heat"), at short-to-medium term (i.e., between years 0 and +2 after the fire event), for four individual burned areas (letters A–D), based on indicators derived from inter-annual anomalies in quantity EFAs extracted from satellite image time-series.

3.4. Discussion

3.4.1. Fire severity patterns in the NW Iberian Peninsula

Effects of wildfires across dimensions and components

In our test case, we found that the associations between burned areas and inter-annual EFA anomalies were particularly strong for *primary productivity* and *sensible heat*, although *albedo* and *vegetation water content* also revealed important effects caused by wildfire disturbances. This is in line with previously published research, as the sudden removal of green vegetation due to fire usually translates into abrupt breaks that are commonly observable in time-series of spectral vegetation indices (e.g., TCTG). This removal can result in substantial carbon losses, both in terms of aboveground biomass (Sparks *et al.* 2018), as well as soil organic matter (Mack *et al.* 2011, Pellegrini *et al.* 2018). Moreover, fire-mediated changes in nutrient concentrations can ultimately limit productivity over long periods (Leys *et al.* 2016). Because vegetation is a regulator of land surface energy fluxes (Veraverbeke *et al.* 2012), the removal of vegetation causes an increase in observed LST induced by a reduction in evapotranspiration (Liu *et al.* 2018), thus increasing the sensible to latent heat ratio (Vlassova *et al.* 2014). Furthermore, observed effects in albedo are also consistent with studies reporting either a darkening or a brightening (or both) effects after a fire (e.g., Ramanathan and Carmichael 2008, Quintano *et al.* 2019), due to the vegetation removal, as well as the presence (or not) of black carbon in soot, which absorbs visible solar radiation (Ramanathan and Carmichael 2008). Finally, effects on *vegetation water content* could be related to loss of moisture in canopy foliage due to damage caused by fire, eventually leading to vegetation mortality (Senf and Seidl 2020). Indeed, our results show that using information from multiple dimensions of ecosystem functioning can yield improved results, over the use of fewer – or only one – indices, for enhanced detection, mapping, and evaluation of ecological effects of disturbances such as wildfires.

Across the three different components of ecosystem functioning considered, anomalies in *quantity* EFAs (e.g., mean, minimum, maximum) had overall stronger associations with wildfire disturbances than *seasonality* (e.g., standard deviation) or *timing* (e.g., time of minimum or maximum) ones. For severity assessment purposes, quantity and seasonality EFAs seemed to be somewhat redundant, as there can be, in some cases, high pairwise correlations between EFA anomalies of those two types. Conversely, for other types of disturbances, such as land clearing for agriculture and ranging, the impact on

seasonality (i.e., seasonal variability) can be much stronger than on quantities (see Volante *et al.* 2012). While some studies show that wildfire disturbances can have profound impacts on aspects of the timing of key dimensions of ecosystem functioning (e.g., by inducing phenological changes; Wang and Zhang 2017), our approach may not be best suited to assess such modifications. This is because the intra-annual descriptors used (i.e., EFAs) seemed to more likely capture the location of extreme values (i.e., minimum/maximum) within the year corresponding to direct effects of the wildfire disturbance, rather than translating changes (e.g., delays or lags) in the annual cycles of the underlying ecological processes.

As for the specific statistical measures used to extract EFAs, stronger effects can result from the use of parametric measures, over that of their non-parametric equivalents. This may be because parametric measures are generally more sensitive (and susceptible) to extreme or abnormal values than non-parametric ones, which may or may not be desirable, depending on the specific application purpose. On the other hand, non-parametric measures may be more adequate for extracting long-term inter-annual trends than parametric ones (e.g., Alcaraz-Segura *et al.* 2008).

The results obtained point to a strong added value of the proposed approach to discriminate the effects of wildfire disturbances on different aspects of ecosystem functioning.

Temporal effects of wildfires

Short-term effects of wildfire disturbances on ecosystem functioning seemed to attain better overall performance than medium-term effects since inter-annual anomalies in intra-annual EFAs for the year of the fire occurrence obtained much better scores, overall, than for the first and second years following the fire. This is partially in line with other studies, as the majority of studies analyzing RS-based effects of fires focus on either short-term (i.e., abrupt) wildfire disturbance severity (e.g., Verbesselt, Hyndman, Newnham, *et al.* 2010, Verbesselt, Hyndman, Zeileis, *et al.* 2010), or on longer-term effects more related to post-fire recovery (e.g., Bastos *et al.* 2011, João *et al.* 2018), while the medium-term effects (i.e., from one or two years to five years after the fire) are often overlooked.

EFAs derived from TCTW (i.e., *vegetation water content*) seemed to be more affected by wildfire disturbances in the first year after the fire, than the year in which the fire occurred, suggesting a temporal lag associated with this dimension, relative to both the fire event and other dimensions. This observation (which to our knowledge, has not been previously reported) could be linked to changes in hydrological dynamics, such as increased soil water

repellency, precipitation run-off, and increased quantities of impervious materials such as ashes and soot (Ramanathan and Carmichael 2008), which can clog soil pores (Bodí *et al.* 2014). Alternatively, this effect could be due to post-fire changes in foliar moisture leading to mortality occurring over an extended period after a fire (Senf and Seidl 2020), since TCTW is quite sensitive to the moisture content of vegetation (Lobser and Cohen 2007).

As to the observed effects of wildfire disturbances on *albedo* (i.e., TCTB), this dimension of ecosystem functioning seemed to exhibit a shift in directionality, from negative in year 0, to positive in years +1 and +2, denoting a change in the relationships with the wildfire disturbance at short- vs. medium-term. This is also in line with the findings reported in other studies (Quintano *et al.* 2019, Saha *et al.* 2019), which observed both a decrease of albedo (i.e., a darkening effect) immediately after the fire, and usually for a brief period, as well as a small increase (i.e., brightening) one year after the fire, which can be persistent. On the other hand, this darkening, which can be due to changes in the relative abundance of surfaces with distinct reflective properties (Lentile *et al.* 2006) (e.g., ash, char, soot, bare soil), can, in some cases, persist for multiple years after fire (Gatebe *et al.* 2014).

Finally, the effects of wildfire disturbances on both *primary productivity* and *sensible heat* (though TCTG and LST, respectively) seemed to be reflected across the three time periods analyzed. However, they were especially noticeable for the year of the fire occurrence. This also goes in the same direction as other studies addressing the impacts of fire on ecosystems, which report usually short-term effects, for satellite-derived proxies of primary productivity (e.g., Veraverbeke *et al.* 2011b, García-Llamas *et al.* 2019), after a fire. An increase in observed LST immediately following fires is also frequently reported in the literature (Liu *et al.* 2018). This can sometimes still be observed one year following the fire (Liu *et al.* 2019), after which LST anomalies tend to become smaller, and seasonality starts governing the LST time-series (Veraverbeke *et al.* 2012).

Together, these results highlight the importance of taking into consideration both *short-* and *medium-term* effects of wildfire disturbances on multiple dimensions of ecosystem functioning.

General patterns

Overall, EFA anomalies were able to discriminate efficiently *burned* and *unburned* areas, with very high values obtained for both effect sizes and performance measures of the Random Forest (RF) models, between EFA anomalies (predictive variables) and burned areas (response variable). This allowed supporting the selection of EFAs from which a

compact set of indicators was employed to assess the main patterns of wildfire disturbance severity in our test area.

Diverse spatiotemporal patterns of wildfire disturbance severity on the four dimensions of ecosystem functioning – primary productivity, vegetation water content, albedo, and sensible heat – could be observed both between-, as well as within-, individual burned areas, across years (i.e., from the year of fire to two years after). These results showcase the added value of (i) analyzing the effects of wildfire disturbances for multiple dimensions of ecosystem functioning, as opposed to addressing only overall burn severity in commonly used approaches (e.g., based on the *Differenced Normalized Burn Ratio*, ΔNBR); and (ii) taking into consideration both the short- and medium-term, thus enabling to obtain insights on potentially lagged effects of fires on ecosystem functioning, as different dimensions can exhibit different severities, and with different timings.

3.4.2. General considerations about the proposed framework

Satellite image time-series

While in the presented test case we used data extracted from MODIS products exclusively, other sources of satellite image time-series (SITS) are available, and can equally be applied using the proposed approach. Such data sources include platforms with diverse characteristics in terms of spatial, temporal, and spectral resolutions, and the length of the historical archive, such as SPOT-VEGETATION, PROBA-V, Landsat 5/7/8, or Sentinel-2/3 (e.g., Mallinis *et al.* 2018).

As to the base SITS to be extracted from those sources, we recommend, in the proposed approach, the use of LST and the TCT features of *Brightness*, *Greenness*, and *Wetness*, as RS-based proxies of albedo, primary productivity, and vegetation water content, respectively. This option allows to derive information on the four above-mentioned dimensions of ecosystem functioning, from the smallest number of sources (the three TCT features are derived from the same source), compactly and coherently, and is often available for the major satellite data sources (e.g., Shi and Xu 2019). However, in the case of primary productivity and vegetation water content, if data is not available to derive all four RS-based variables, alternative spectral indices could be used instead, such as the *Normalized Difference Vegetation Index* (NDVI), or the *Enhanced Vegetation Index* (EVI), for *Productivity*; or the *Normalized Difference Water Index* (NDWI), or *Land Surface Water Index* (LSWI), for *Water*.

Additional data sources

Well-designed field-based measurements could be used, if available, to validate the information provided by SITS, further enhancing the proposed approach, although it is not a mandatory requirement. To that end, data can be collected in the field, following robust sampling designs, such as spectral/radiometric readings, aerial surveys using cameras and sensors mounted on *Unmanned Aerial Vehicles* (UAVs), or data collected under already existing and commonly used protocols (or adapted versions from these), such as the *Composite Burn Index* (CBI; e.g., Marcos *et al.* 2018), or the improved *Geometrically structured Composite Burn Inde*x (GeoCBI; e.g., De Santis and Chuvieco 2009), to complement the information derived from SITS. Such data can, however, be difficult and/or costly to obtain, even more so if multiple observations are required to produce a coherent time-series. These types of field-level measurements are usually compared to commonly used indicators of burn severity (e.g., Cardil *et al.* 2019), such as the *Differenced Normalized Burn Ratio* (ΔNBR) – or any of its enhanced forms, such as the *Relative Normalized Burn Ratio* (RΔNBR), and the *Relativized Burn Ratio* (RBR).

Unlike the more commonly used RS-derived methods to estimate burn severity, the approach proposed in this study can provide information on the effects of wildfire disturbances on multiple dimensions of ecosystem functioning – namely: primary productivity, vegetation water content, albedo, and sensible heat –, simultaneously, towards a comprehensive evaluation of fire severity.

Applicability and future directions

Multi-dimensional approaches to wildfire disturbances using EFA-like metrics are, to our knowledge, scarce (e.g., Landi *et al.* 2021). Very few studies have adopted a multi-dimensional approach using EFAs, regardless of the specific application (e.g., Fernández *et al.* 2010, Arenas-Castro *et al.* 2018, Regos *et al.* 2020). More studies should be conducted in the future, with diverse contexts in terms of baseline environmental conditions and fire disturbance regimes, to further test and improve the proposed approach. It is important to highlight that, although the results obtained for the test case presented in this study may be somewhat specific to the study area and the analyzed period, the general approach could be applied, with relative ease, to other contexts and timeframes, to conduct informed selections of the most efficient and informative EFA-based indicators for wildfire disturbance severity assessment.

The proposed approach makes use of annual descriptors of the dynamics of multiple dimensions of ecosystem functioning – so-called *Ecosystem Functioning Attributes* (EFAs)

–, extracted from SITS, to derive indicators of wildfire disturbance severity. However, another possible approach could be to derive indicators directly from the time-series, without the need to compute EFAs first. This would open the possibilities for other kinds of indicators, with finer temporal (i.e., < 1 year) resolutions, on a (semi-)continuous basis, to be derived from SITS (e.g., João *et al.* 2018). On the other hand, although additional types of indicators could be obtained in this way, others would not – e.g., metrics of timing based on annual cycles, such as the dates of the maximum or minimum, would only make sense on an annual basis. Besides, the annual nature of EFAs – and the derived indicators –, facilitates both their computation, as well as their interpretation, as it offers a better translation of spectral indices into informative ecosystem variables. This can be advantageous for some application purposes, such as for reporting from official authorities. Notwithstanding approaches adopting either an annual or continuous basis could complement each other to characterize the effects of wildfire disturbances on ecosystem functioning.

Finally, in this study, we focused on the short-to-medium-term impacts of wildfire disturbances. However, long(er)-term effects of wildfire disturbance severity have been observed (e.g., Cocking *et al.* 2014). Indeed, long-term impacts of wildfire disturbances on ecosystem functioning could also be monitored using the approach proposed in this study, provided that long enough SITS are available. However, this was not tested in this study, as that would considerably increase both computational requirements, as well as methodological complexity.

3.5. Conclusions

Here we described a framework to assess the effects of wildfire disturbances on four key dimensions of ecosystem functioning – primary productivity, vegetation water content, albedo, and sensible heat. This approach is based on indicators derived from several descriptors of the intra-annual dynamics of ecosystem functioning – called Ecosystem Functioning Attributes (EFAs) –, extracted from remotely-sensed satellite image time-series (SITS). We found that all four dimensions of ecosystem functioning suffered important effects of wildfire disturbances – especially primary productivity, and sensible heat. We also found that quantity EFAs held the highest potential for indicating wildfire severity. Finally, we found important differences in short- and medium-term effects between the four different dimensions of ecosystem functioning, suggesting temporally lagged effects in vegetation water content, as well as directionality shifts in albedo. Together, these results highlight the added value of the proposed framework to enhance RS-based assessment, mapping, diagnostics, and monitoring of wildfire disturbances. Using this approach, a more comprehensive evaluation of fire severity can be attained, which is not captured by indicators derived from only one spectral index, measuring only overall burn severity. As such, this multi-dimensional framework can contribute to a deeper and more detailed understanding of the impact of fires in ecosystems, with the potential to support assessments of severity, recovery, and resilience, and their interactions with biodiversity and ecosystem services.

References

Adámek, M., Hadincová, V., and Wild, J., 2016. Long-term effect of wildfires on temperate Pinus sylvestris forests: Vegetation dynamics and ecosystem resilience. *Forest Ecology and Management*, 380, 285–295. DOI: 10.1016/j.foreco.2016.08.051.

Alcaraz-Segura, D., Cabello, J., Paruelo, J.M., and Delibes, M., 2008. Trends in the surface vegetation dynamics of the national parks of Spain as observed by satellite sensors. *Applied Vegetation Science*, 11 (4), 431–440. DOI: 10.3170/2008-7-18522.

Alcaraz-Segura, D., Chuvieco, E., Epstein, H.E., Kasischke, E.S., and Trishchenko, A., 2010. Debating the greening vs. browning of the North American boreal forest: differences between satellite datasets. *Global Change Biology*, 16 (2), 760–770. DOI: 10.1111/j.1365-2486.2009.01956.x.

Alcaraz, D., Paruelo, J.M., and Cabello, J., 2006. Identification of current ecosystem functional types in the Iberian Peninsula. *Global Ecology and Biogeography*, 15 (2), 200–212. DOI: 10.1111/j.1466-822X.2006.00215.x.

Arenas-Castro, S., Gonçalves, J., Alves, P., Alcaraz-Segura, D., and Honrado, J.P., 2018. Assessing the multi-scale predictive ability of ecosystem functional attributes for species distribution modelling. *PLOS ONE*, 13 (6), e0199292. DOI: 10.1371/journal.pone.0199292.

Arenas-Castro, S., Regos, A., Gonçalves, J.F., Alcaraz-Segura, D., and Honrado, J., 2019. Remotely Sensed Variables of Ecosystem Functioning Support Robust Predictions of Abundance Patterns for Rare Species. *Remote Sensing*, 11 (18), 2086. DOI: 10.3390/rs11182086.

Bastos, A., Gouveia, C.M., DaCamara, C.C., and Trigo, R.M., 2011. Modelling post-fire vegetation recovery in Portugal. *Biogeosciences*, 8 (12), 3593–3607. DOI: 10.5194/bg-8-3593-2011.

Bodí, M.B., Martin, D.A., Balfour, V.N., Santín, C., Doerr, S.H., Pereira, P., Cerdà, A., and Mataix-Solera, J., 2014. Wildland fire ash: Production, composition and eco-hydro-geomorphic effects. *Earth-Science Reviews*, 130, 103–127. DOI: 10.1016/j.earscirev.2013.12.007.

Bowman, D.M.J.S., Balch, J.K., Artaxo, P., Bond, W.J., Carlson, J.M., Cochrane, M.A., D'Antonio, C.M., DeFries, R.S., Doyle, J.C., Harrison, S.P., Johnston, F.H., Keeley, J.E., Krawchuk, M.A., Kull, C.A., Marston, J.B., Moritz, M.A., Prentice, I.C., Roos, C.I., Scott, A.C., Swetnam, T.W., van der Werf, G.R., and Pyne, S.J., 2009. Fire in the Earth System. *Science*, 324 (5926), 481–484. DOI: 10.1126/science.1163886.

Bowman, D.M.J.S., Perry, G.L.W., and Marston, J.B., 2015. Feedbacks and landscape-level vegetation dynamics. *Trends in Ecology & Evolution*, 30 (5), 255–260. DOI: 10.1016/j.tree.2015.03.005.

Busetto, L. and Ranghetti, L., 2016. MODIStsp: An R package for automatic preprocessing of MODIS Land Products time series. *Computers and Geosciences*, 97, 40–48. DOI: 10.1016/j.cageo.2016.08.020.

Caon, L., Vallejo, V.R., Ritsema, C.J., and Geissen, V., 2014. Effects of wildfire on soil nutrients in Mediterranean ecosystems. *Earth-Science Reviews*, 139, 47–58. DOI: 10.1016/j.earscirev.2014.09.001.

Cardil, A., Mola-Yudego, B., Blázquez-Casado, Á., and González-Olabarria, J.R., 2019. Fire and burn severity assessment: Calibration of Relative Differenced Normalized Burn Ratio (RdNBR) with field data. *Journal of Environmental Management*, 235, 342–349.

Carvalho-Santos, C., Marcos, B., Nunes, J., Regos, A., Palazzi, E., Terzago, S., Monteiro, A., and Honrado, J., 2019. Hydrological Impacts of Large Fires and Future Climate: Modeling Approach Supported by Satellite Data. *Remote Sensing*, 11 (23), 2832. DOI: 10.3390/rs11232832.

Catry, F.X.F., Rego, F.C.F.F.C., Bação, F.L., Moreira, 2009. Modeling and mapping wildfire ignition risk in Portugal. *International Journal of Wildland Fire*, 18 (8), 921. DOI: 10.1071/WF07123.

Cazorla, B., Cabello, J., Reyes, A., Guirado, E., Peñas, J., Pérez-Luque, A.J., and Alcaraz-Segura, D., 2020. A remote sensing-based dataset to characterize the ecosystem functioning and functional diversity of a Biosphere Reserve: Sierra Nevada (SE Spain). *Earth Syst. Sci. Data Discuss.*, 2020, 1–20. DOI: 10.5194/essd-2019-198.

Cazorla, B.P., Cabello, J., Peñas, J., Garcillán, P.P., Reyes, A., and Alcaraz-Segura, D., 2020. Incorporating Ecosystem Functional Diversity into Geographic Conservation Priorities Using Remotely Sensed Ecosystem Functional Types. *Ecosystems*, 24 (3), 1–17. DOI: 10.1007/s10021-020-00533-4.

Cocking, M.I., Varner, J.M., and Knapp, E.E., 2014. Long-term effects of fire severity on oak–conifer dynamics in the southern Cascades. *Ecological Applications*, 24 (1), 94–107. DOI: 10.1890/13-0473.1.

Cohen, J., 1992. A power primer. *Psychological Bulletin*, 112 (1), 155–159. DOI: 10.1037/0033-2909.112.1.155.

Coops, N.C., Wulder, M.A., Duro, D.C., Han, T., and Berry, S., 2008. The development of a Canadian dynamic habitat index using multi-temporal satellite estimates of canopy

light absorbance. *Ecological Indicators*, 8 (5), 754–766. DOI: 10.1016/j.ecolind.2008.01.007.

Couronné, R., Probst, P., and Boulesteix, A.L., 2018. Random forest versus logistic regression: A large-scale benchmark experiment. *BMC Bioinformatics*, 19 (1), 270. DOI: 10.1186/s12859-018-2264-5.

Duan, S.-B., Li, Z.-L., Li, H., Göttsche, F.-M., Wu, H., Zhao, W., Leng, P., Zhang, X., and Coll, C., 2019. Validation of Collection 6 MODIS land surface temperature product using in situ measurements. *Remote Sensing of Environment*, 225, 16–29. DOI: 10.1016/j.rse.2019.02.020.

Dunnette, P. V., Higuera, P.E., McLauchlan, K.K., Derr, K.M., Briles, C.E., and Keefe, M.H., 2014. Biogeochemical impacts of wildfires over four millennia in a Rocky Mountain subalpine watershed. *New Phytologist*, 203 (3), 900–912. DOI: 10.1111/nph.12828.

Duro, D.C., Coops, N.C., Wulder, M.A., and Han, T., 2007. Development of a large area biodiversity monitoring system driven by remote sensing. *Progress in Physical Geography*, 31 (3), 235–260. DOI: 10.1177/0309133307079054.

Eilers, P.H.C., 2003. A Perfect Smoother. *Analytical Chemistry*, 75 (14), 3631–3636. DOI: 10.1021/ac034173t.

European Environment Agency, 2020. CLC 2000 — Copernicus Land Monitoring Service [online]. Available from: https://land.copernicus.eu/pan-european/corine-land-cover/clc-2000 [Accessed 11 Feb 2021].

Fernández, N., Paruelo, J.M., and Delibes, M., 2010. Ecosystem functioning of protected and altered Mediterranean environments: A remote sensing classification in Doñana, Spain. *Remote Sensing of Environment*, 114 (1), 211–220. DOI: 10.1016/J.RSE.2009.09.001.

Frazier, A.E., Renschler, C.S., and Miles, S.B., 2013. Evaluating post-disaster ecosystem resilience using MODIS GPP data. *International Journal of Applied Earth Observation and Geoinformation*, 21, 43–52. DOI: 10.1016/j.jag.2012.07.019.

French, N.H.F., Whitley, M.A., and Jenkins, L.K., 2016. Fire disturbance effects on land surface albedo in Alaskan tundra. *Journal of Geophysical Research: Biogeosciences*, 121 (3), 841–854. DOI: 10.1002/2015JG003177.

García-Llamas, P., Suárez-Seoane, S., Taboada, A., Fernández-Manso, A., Quintano, C., Fernández-García, V., Fernández-Guisuraga, J.M., Marcos, E., and Calvo, L., 2019. Environmental drivers of fire severity in extreme fire events that affect Mediterranean

pine forest ecosystems. *Forest Ecology and Management*, 433, 24–32. DOI: 10.1016/j.foreco.2018.10.051.

Gatebe, C.K.K., Ichoku, C.M.M., Poudyal, R., Román, M.O.O., and Wilcox, E., 2014. Surface albedo darkening from wildfires in northern sub-Saharan Africa. *Environmental Research Letters*, 9 (6), 065003. DOI: 10.1088/1748-9326/9/6/065003.

GDAL contributors, 2020. GDAL – Geospatial Data Abstraction Library v3.0.4.

Giglio, L., Boschetti, L., Roy, D.P., Humber, M.L., and Justice, C.O., 2018. The Collection 6 MODIS burned area mapping algorithm and product. *Remote Sensing of Environment*, 217, 72–85. DOI: 10.1016/j.rse.2018.08.005.

Gillies, S., Ward, B., and Petersen, A.S., 2013. Rasterio: geospatial raster I/O for Python programmers version 0.36.0.

Gonçalves, J., Alves, P., Pôças, I., Marcos, B., Sousa-Silva, R., Lomba, Â., and Honrado, J.P., 2016. Exploring the spatiotemporal dynamics of habitat suitability to improve conservation management of a vulnerable plant species. *Biodiversity and Conservation*, 25 (14). DOI: 10.1007/s10531-016-1206-7.

Gouveia, C., DaCamara, C.C., and Trigo, R.M., 2010. Post-fire vegetation recovery in Portugal based on spot/vegetation data. *Natural Hazards and Earth System Science*, 10 (4), 673–684. DOI: 10.5194/nhess-10-673-2010.

Hampel, F.R., 1971. A General Qualitative Definition of Robustness. *The Annals of Mathematical Statistics*, 42 (6), 1887–1896.

Hampel, F.R., 1974. The Influence Curve and its Role in Robust Estimation. *Journal of the American Statistical Association*, 69 (346), 383–393. DOI: 10.1080/01621459.1974.10482962.

Healey, S., Cohen, W., Zhiqiang, Y., and Krankina, O., 2005. Comparison of Tasseled Cap-based Landsat data structures for use in forest disturbance detection. *Remote Sensing of Environment*, 97 (3), 301–310. DOI: 10.1016/j.rse.2005.05.009.

Hijmans, R.J., 2016. raster: Geographic Data Analysis and Modeling. R package version 2.5-8.

Hubbard, R. and Lindsay, R.M., 2008. Why *P* Values Are Not a Useful Measure of Evidence in Statistical Significance Testing. *Theory & Psychology*, 18 (1), 69–88. DOI: 10.1177/0959354307086923.

João, T., João, G., Bruno, M., and João, H., 2018. Indicator-based assessment of post-fire recovery dynamics using satellite NDVI time-series. *Ecological Indicators*, 89, 199–212. DOI: 10.1016/j.ecolind.2018.02.008.

Karger, D.N., Conrad, O., Böhner, J., Kawohl, T., Kreft, H., Soria-Auza, R.W., Zimmermann, N.E., Linder, H.P., and Kessler, M., 2017. Climatologies at high resolution for the earth's land surface areas. *Scientific Data*, 4 (1), 170122. DOI: 10.1038/sdata.2017.122.

Keeley, J.E., 2009. Fire intensity, fire severity and burn severity: a brief review and suggested usage. *International Journal of Wildland Fire*, 18 (1), 116. DOI: 10.1071/WF07049.

Koutsias, N., Allgöwer, B., Kalabokidis, K., Mallinis, G., Balatsos, P., and Goldammer, J.G., 2016. Fire occurrence zoning from local to global scale in the European Mediterranean basin: Implications for multi-scale fire management and policy. *IForest*, 9 (APR2016), 195–204. DOI: 10.3832/ifor1513-008.

Kuhn, M., Weston, S., Keefer, C., Engelhardt, A., Cooper, T., Mayer, Z., Kenkel, B., Team, R.C., Benesty, M., Lescarbeau, R., Ziem, A., Scrucca, L., Tang, Y., and Candan, C., 2016. caret: Classification and Regression Training. R package version 6.0-70.

Landi, M.A., Di Bella, C.M., Bravo, S.J., and Bellis, L.M., 2021. Structural resistance and functional resilience of the Chaco forest to wildland fires: an approach with MODIS time series. *Austral Ecology*, 46 (2), 277–289. DOI: 10.1111/aec.12977.

van Leeuwen, W.J.D., Casady, G.M., Neary, D.G., Bautista, S., Alloza, J.A., Carmel, Y., Wittenberg, L., Malkinson, D., and Orr, B.J., 2010. Monitoring post-wildfire vegetation response with remotely sensed time-series data in Spain, USA and Israel. *International Journal of Wildland Fire*, 19 (1), 75. DOI: 10.1071/WF08078.

Lentile, L.B., Holden, Z.A., Smith, A.M.S.S., Falkowski, M.J., Hudak, A.T., Morgan, P., Lewis, S.A., Gessler, P.E., Benson, N.C., Lentile, L.B., Holden, Z.A., Smith, A.M.S.S., Falkowski, M.J., Hudak, A.T., Morgan, P., Lewis, S.A., Gessler, P.E., and Benson, N.C., 2006. Remote sensing techniques to assess active fire characteristics and post-fire effects. *International Journal of Wildland Fire*, 15 (3), 319. DOI: 10.1071/WF05097.

Leys, B., Higuera, P.E., McLauchlan, K.K., and Dunnette, P. V., 2016. Wildfires and geochemical change in a subalpine forest over the past six millennia. *Environmental Research Letters*, 11 (12), 125003. DOI: 10.1088/1748-9326/11/12/125003.

Liu, H., Zhan, Q., Yang, C., and Wang, J., 2018. Characterizing the Spatiotemporal Pattern of Land Surface Temperature through Time Series Clustering: Based on the Latent Pattern and Morphology. *Remote Sensing*, 10 (4), 654. DOI: 10.3390/rs10040654.

Liu, Z., Ballantyne, A.P., and Cooper, L.A., 2019. Biophysical feedback of global forest fires on surface temperature. *Nature Communications*, 10 (1), 1–9. DOI: 10.1038/s41467-018-08237-z.

Lobser, S.E. and Cohen, W.B., 2007. MODIS tasselled cap: land cover characteristics expressed through transformed MODIS data. *International Journal of Remote Sensing*, 28 (22), 5079–5101. DOI: 10.1080/01431160701253303.

Mack, M.C., Bret-Harte, M.S., Hollingsworth, T.N., Jandt, R.R., Schuur, E.A.G., Shaver, G.R., and Verbyla, D.L., 2011. Carbon loss from an unprecedented Arctic tundra wildfire. *Nature*, 475 (7357), 489–492. DOI: 10.1038/nature10283.

Maffei, C., Alfieri, S.M., Menenti, M., 2018. Relating Spatiotemporal Patterns of Forest Fires Burned Area and Duration to Diurnal Land Surface Temperature Anomalies. *Remote Sensing*, 10 (11), 1777. DOI: 10.3390/rs10111777.

Mallinis, G., Mitsopoulos, I., and Chrysafi, I., 2018. Evaluating and comparing sentinel 2A and landsat-8 operational land imager (OLI) spectral indices for estimating fire severity in a mediterranean pine ecosystem of Greece. *GIScience and Remote Sensing*, 55 (1), 1–18. DOI: 10.1080/15481603.2017.1354803.

Marcos, B., Gonçalves, J., Alcaraz-Segura, D., Cunha, M., and Honrado, J.P., 2019. Improving the detection of wildfire disturbances in space and time based on indicators extracted from MODIS data: a case study in northern Portugal. *International Journal of Applied Earth Observation and Geoinformation*, 78, 77–85. DOI: 10.1016/j.jag.2018.12.003.

Marcos, E., Fernández-García, V., Fernández-Manso, A., Quintano, C., Valbuena, L., Tárrega, R., Luis-Calabuig, E., and Calvo, L., 2018. Evaluation of Composite Burn Index and Land Surface Temperature for Assessing Soil Burn Severity in Mediterranean Fire-Prone Pine Ecosystems. *Forests*, 9 (8), 494. DOI: 10.3390/f9080494.

Mildrexler, D.J., Zhao, M., and Running, S.W., 2009. Testing a MODIS Global Disturbance Index across North America. *Remote Sensing of Environment*, 113 (10), 2103–2117. DOI: 10.1016/j.rse.2009.05.016.

Parks, S.A., Holsinger, L.M., Koontz, M.J., Collins, L., Whitman, E., Parisien, M.-A., Loehman, R.A., Barnes, J.L., Bourdon, J.-F., Boucher, J., Boucher, Y., Caprio, A.C.,

Collingwood, A., Hall, R.J., Park, J., Saperstein, L.B., Smetanka, C., Smith, R.J., Soverel, N., 2019. Giving Ecological Meaning to Satellite-Derived Fire Severity Metrics across North American Forests. *Remote Sensing*, 11 (14), 1735. DOI: 10.3390/rs11141735.

Paruelo, J.M., Piñeiro, G., Escribano, P., Oyonarte, C., Alcaraz-Segura, D., and Cabello, J., 2005. Temporal and spatial patterns of ecosystem functioning in protected arid areas in southeastern Spain. *Applied Vegetation Science*, 8 (1), 93–102. DOI: 10.1111/j.1654-109X.2005.tb00633.x.

Pellegrini, A.F.A., Ahlström, A., Hobbie, S.E., Reich, P.B., Nieradzik, L.P., Staver, A.C., Scharenbroch, B.C., Jumpponen, A., Anderegg, W.R.L., Randerson, J.T., and Jackson, R.B., 2018. Fire frequency drives decadal changes in soil carbon and nitrogen and ecosystem productivity. *Nature*, 553 (7687), 194–198. DOI: 10.1038/nature24668.

Petropoulos, G., Carlson, T.N., Wooster, M.J., and Islam, S., 2009. A review of Ts/VI remote sensing based methods for the retrieval of land surface energy fluxes and soil surface moisture. *Progress in Physical Geography*, 33 (2), 224–250. DOI: 10.1177/0309133309338997.

Poon, P.K. and Kinoshita, A.M., 2018. Spatial and temporal evapotranspiration trends after wildfire in semi-arid landscapes. *Journal of Hydrology*, 559, 71–83. DOI: 10.1016/j.jhydrol.2018.02.023.

Quintano, C., Fernández-Manso, A., Calvo, L., Marcos, E., and Valbuena, L., 2015. Land surface temperature as potential indicator of burn severity in forest Mediterranean ecosystems. *International Journal of Applied Earth Observation and Geoinformation*, 36, 1–12. DOI: 10.1016/j.jag.2014.10.015.

Quintano, C., Fernandez-Manso, A., Marcos, E., and Calvo, L., 2019. Burn Severity and Post-Fire Land Surface Albedo Relationship in Mediterranean Forest Ecosystems. *Remote Sensing*, 11 (19), 2309. DOI: 10.3390/rs11192309.

R Core Team, 2019. R: A Language and Environment for Statistical Computing version 3.5.1.

Ramanathan, V. and Carmichael, G., 2008. Global and regional climate changes due to black carbon. *Nature Geoscience*, 1 (4), 221–227. DOI: 10.1038/ngeo156.

Regos, A., Gómez-Rodríguez, P., Arenas-Castro, S., Tapia, L., Vidal, M., and Domínguez, J., 2020. Model-Assisted Bird Monitoring Based on Remotely Sensed Ecosystem

Functioning and Atlas Data. *Remote Sensing*, 12 (16), 2549. DOI: 10.3390/rs12162549.

Rother, D. and De Sales, F., 2021. Impact of Wildfire on the Surface Energy Balance in Six California Case Studies. *Boundary-Layer Meteorology*, 178 (1), 143–166. DOI: 10.1007/s10546-020-00562-5.

Saha, M. V., D'Odorico, P., and Scanlon, T.M., 2017. Albedo changes after fire as an explanation of fire-induced rainfall suppression. *Geophysical Research Letters*, 44 (8), 3916–3923. DOI: 10.1002/2017GL073623.

Saha, M. V., D'Odorico, P., and Scanlon, T.M., 2019. Kalahari Wildfires Drive Continental Post-Fire Brightening in Sub-Saharan Africa. *Remote Sensing*, 11 (9), 1090. DOI: 10.3390/rs11091090.

San-Miguel-Ayanz, J., Moreno, J.M., and Camia, A., 2013. Analysis of large fires in European Mediterranean landscapes: Lessons learned and perspectives. *Forest Ecology and Management*, 294, 11–22. DOI: 10.1016/j.foreco.2012.10.050.

De Santis, A. and Chuvieco, E., 2009. GeoCBI: A modified version of the Composite Burn Index for the initial assessment of the short-term burn severity from remotely sensed data. *Remote Sensing of Environment*, 113 (3), 554–562. DOI: 10.1016/j.rse.2008.10.011.

Santos, R.M.B., Sanches Fernandes, L.F., Pereira, M.G., Cortes, R.M.V., and Pacheco, F.A.L., 2015. Water resources planning for a river basin with recurrent wildfires. *Science of the Total Environment*, 526, 1–13. DOI: 10.1016/j.scitotenv.2015.04.058.

Senf, C. and Seidl, R., 2020. Mapping the forest disturbance regimes of Europe. *Nature Sustainability*, 4 (1). DOI: 10.1038/s41893-020-00609-y.

Shi, T. and Xu, H., 2019. Derivation of Tasseled Cap Transformation Coefficients for Sentinel-2 MSI At-Sensor Reflectance Data. *IEEE Journal of Selected Topics in Applied Earth Observations and Remote Sensing*, 12 (10), 4038–4048. DOI: 10.1109/JSTARS.2019.2938388.

Smith, A.M.S.S., Kolden, C.A., Tinkham, W.T., Talhelm, A.F., Marshall, J.D., Hudak, A.T., Boschetti, L., Falkowski, M.J., Greenberg, J.A., Anderson, J.W., Kliskey, A., Alessa, L., Keefe, R.F., and Gosz, J.R., 2014. Remote sensing the vulnerability of vegetation in natural terrestrial ecosystems. *Remote Sensing of Environment*, 154, 322–337. DOI: 10.1016/j.rse.2014.03.038.

Smith, H.G., Sheridan, G.J., Lane, P.N.J., Nyman, P., and Haydon, S., 2011. Wildfire effects on water quality in forest catchments: A review with implications for water supply. *Journal of Hydrology*, 396 (1–2), 170–192. DOI: 10.1016/j.jhydrol.2010.10.043.

Sparks, A.M., Kolden, C.A., Smith, A.M.S., Boschetti, L., Johnson, D.M., and Cochrane, M.A., 2018. Fire intensity impacts on post-fire temperate coniferous forest net primary productivity. *Biogeosciences*, 15 (4), 1173–1183. DOI: 10.5194/bg-15-1173-2018.

Sun, X., Zou, C.B., Wilcox, B., and Stebler, E., 2019. Effect of Vegetation on the Energy Balance and Evapotranspiration in Tallgrass Prairie: A Paired Study Using the Eddy-Covariance Method. *Boundary-Layer Meteorology*, 170 (1), 127–160. DOI: 10.1007/s10546-018-0388-9.

Tedim, F., Remelgado, R., Borges, C., Carvalho, S., and Martins, J., 2013. Exploring the occurrence of mega-fires in Portugal. *Forest Ecology and Management*, 294, 86–96. DOI: 10.1016/j.foreco.2012.07.031.

Veraverbeke, S., Lhermitte, S., Verstraeten, W.W., and Goossens, R., 2011a. A time-integrated MODIS burn severity assessment using the multi-temporal differenced normalized burn ratio (dNBRMT). *International Journal of Applied Earth Observation and Geoinformation*, 13 (1), 52–58. DOI: 10.1016/j.jag.2010.06.006.

Veraverbeke, S., Lhermitte, S., Verstraeten, W.W., and Goossens, R., 2011b. Evaluation of pre/post-fire differenced spectral indices for assessing burn severity in a Mediterranean environment with Landsat Thematic Mapper. *International Journal of Remote Sensing*, 32 (12), 3521–3537. DOI: 10.1080/01431161003752430.

Veraverbeke, S., Verstraeten, W.W., Lhermitte, S., Van De Kerchove, R., and Goossens, R., 2012. Assessment of post-fire changes in land surface temperature and surface albedo, and their relation with fire - burn severity using multitemporal MODIS imagery. *International Journal of Wildland Fire*, 21 (3), 243. DOI: 10.1071/WF10075.

Verbesselt, J., Hyndman, R., Newnham, G., and Culvenor, D., 2010. Detecting trend and seasonal changes in satellite image time series. *Remote Sensing of Environment*, 114 (1), 106–115. DOI: 10.1016/j.rse.2009.08.014.

Verbesselt, J., Hyndman, R., Zeileis, A., and Culvenor, D., 2010. Phenological change detection while accounting for abrupt and gradual trends in satellite image time series. *Remote Sensing of Environment*, 114 (12), 2970–2980. DOI: 10.1016/j.rse.2010.08.003.

Vermote, E., 2015. MOD09A1 MODIS/Terra Surface Reflectance 8-Day L3 Global 500m SIN Grid V006. *NASA EOSDIS Land Processes DAAC.*

Vlassova, L., Pérez-Cabello, F., Mimbrero, M., Lloverría, R., and García-Martín, A., 2014. Analysis of the Relationship between Land Surface Temperature and Wildfire Severity in a Series of Landsat Images. *Remote Sensing*, 6 (7), 6136–6162. DOI: 10.3390/rs6076136.

Volante, J.N., Alcaraz-Segura, D., Mosciaro, M.J., Viglizzo, E.F., and Paruelo, J.M., 2012. Ecosystem functional changes associated with land clearing in NW Argentina. *Agriculture, Ecosystems & Environment*, 154, 12–22. DOI: 10.1016/j.agee.2011.08.012.

Wan, Z., Hook, S., and Hulley, G., 2015. MOD11A2 MODIS/Terra Land Surface Temperature/Emissivity 8-Day L3 Global 1km SIN Grid V006. *NASA EOSDIS Land Processes DAAC*.

Wang, J. and Zhang, X., 2017. Impacts of wildfires on interannual trends in land surface phenology: An investigation of the Hayman Fire. *Environmental Research Letters*, 12 (5), 054008. DOI: 10.1088/1748-9326/aa6ad9.

Wasserstein, R.L. and Lazar, N.A., 2016. The ASA Statement on p-Values: Context, Process, and Purpose. *The American Statistician*, 70 (2), 129–133. DOI: 10.1080/00031305.2016.1154108.

Wei, X., Hayes, D.J., Fraver, S., and Chen, G., 2018. Global Pyrogenic Carbon Production During Recent Decades Has Created the Potential for a Large, Long-Term Sink of Atmospheric CO2. *Journal of Geophysical Research: Biogeosciences*, 123 (12), 3682–3696. DOI: 10.1029/2018JG004490.

Whittaker, E.T., 1922. On a new method of graduation. *Proceedings of the Edinburgh Mathematical Society*, 41, 63–75.

Yamazaki, D., Ikeshima, D., Tawatari, R., Yamaguchi, T., O'Loughlin, F., Neal, J.C., Sampson, C.C., Kanae, S., and Bates, P.D., 2017. A high-accuracy map of global terrain elevations. *Geophysical Research Letters*, 44 (11), 5844–5853. DOI: 10.1002/2017GL072874.

Supplementary material

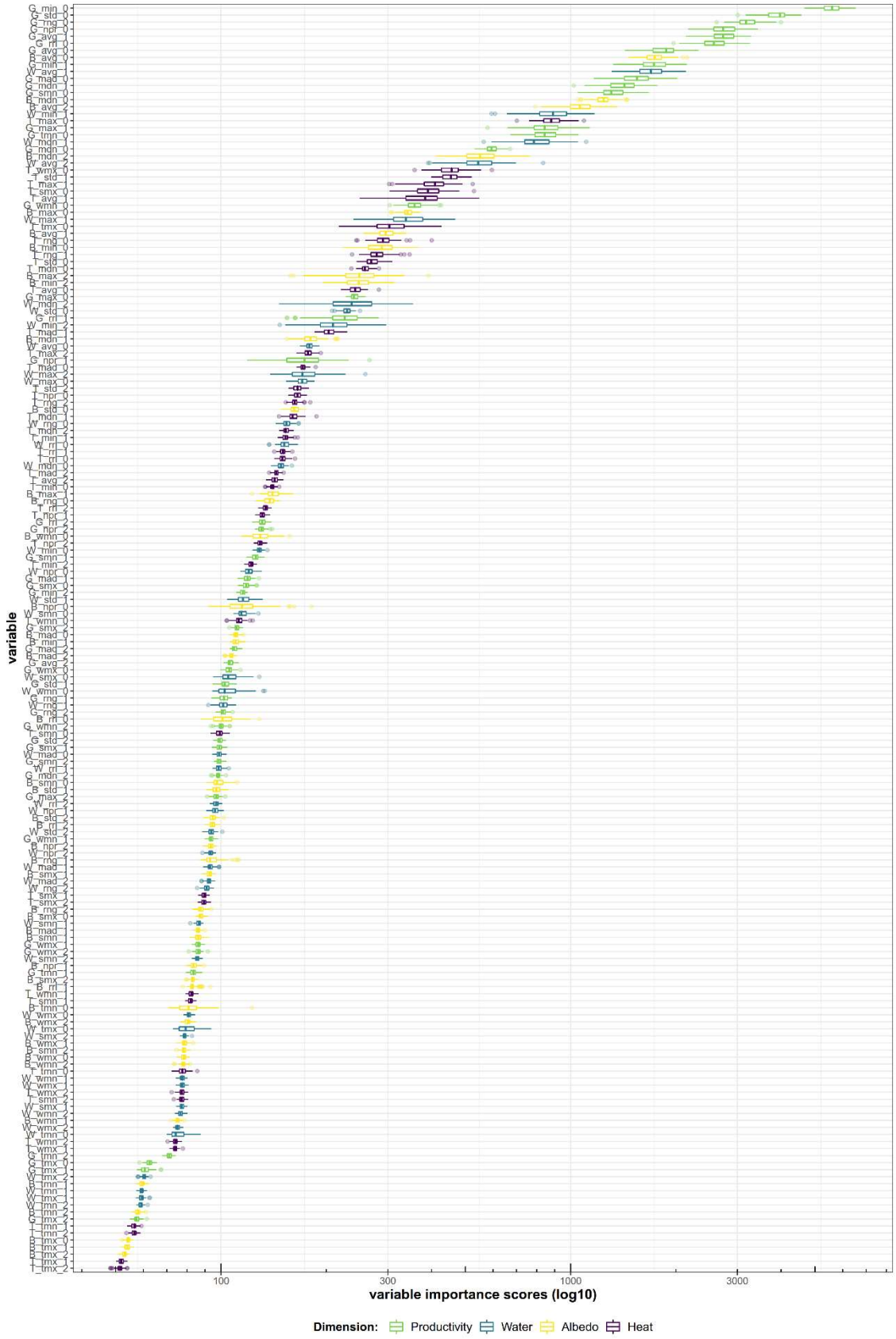

Figure S3.1. Distributions of the variable importance scores of all individual predictive variables, extracted from *Random Forest* models for all 100 random samples.

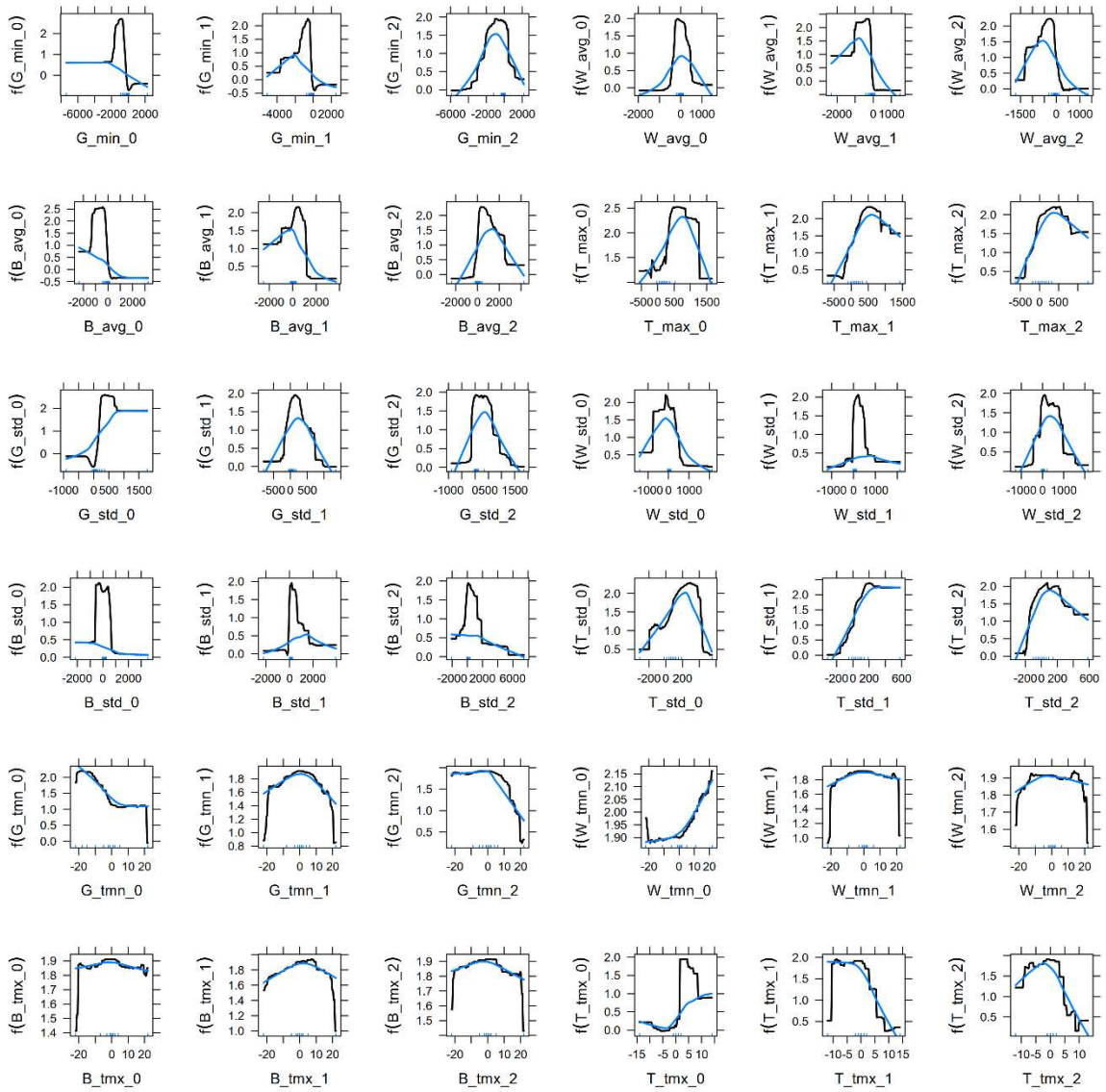

Figure S3.2. Partial dependence plots of the 36 predictive variables of the *Random Forest* models, extracted from the 12 EFAs selected for regional-scale analyses.

Table S3.1. Summary table of results for *Random Forest* models between EFA anomalies and *burned* vs. *unburned* areas, including *median variable importance score*, *rank*, *correlation*, and *effect size*, for each of the 12 EFAs selected for regional-scale analyses.

Dimension	Metric	Component	Year	Median score	Rank	Correlation (Spearman *ρ*)	Effect size (Cohen's *d*)	Effect category
Primary productivity (TCTG)	*min*	quantity	+0	5593.6	1	-0.69	-1.56	↘↘↘
			+1	1731.4	9	-0.58	-1.04	↘↘↘
			+2	115.6	85	-0.12	-0.08	—
	std	variability	+0	3968.4	2	+0.65	+1.49	↗↗↗
			+1	102.6	97	+0.20	+0.34	↗↗
			+2	99.1	105	+0.04	+0.01	—
	tmn	timing	+0	842.3	19	-0.43	-0.86	↘↘↘
			+1	83.4	138	+0.05	+0.09	—
			+2	71.2	164	-0.05	-0.14	—
Vegetation water content (TCTW)	*avg*	quantity	+0	179.1	49	-0.03	-0.05	—
			+1	1697.7	10	-0.58	-1.26	↘↘↘
			+2	544.5	23	-0.47	-0.92	↘↘↘
	std	variability	+0	229.5	44	-0.12	-0.15	—
			+1	115.6	84	+0.26	+0.32	↗↗
			+2	93.6	118	+0.08	+0.14	—
	tmn	timing	+0	74.2	161	+0.10	+0.15	—
			+1	59.3	169	-0.01	+0.00	—
			+2	59.1	171	-0.03	-0.05	—
Albedo (TCTB)	*avg*	quantity	+0	1739.5	8	-0.53	-1.08	↘↘↘
			+1	295.8	33	+0.25	+0.41	↗
			+2	1062.6	15	+0.52	+0.93	↗↗↗
	std	variability	+0	161.9	58	+0.16	+0.14	—
			+1	97.0	112	+0.25	+0.28	↗
			+2	94.7	116	+0.08	+0.09	—
	tmx	timing	+0	54.3	176	-0.02	-0.01	—
			+1	53.9	177	+0.11	+0.15	—
			+2	53.1	178	+0.05	+0.05	—
Heat (LST)	*max*	quantity	+0	880.2	17	+0.37	+0.83	↗↗↗
			+1	408.9	26	+0.41	+0.91	↗↗↗
			+2	177.2	50	+0.21	+0.44	↗
	std	variability	+0	269.2	37	+0.32	+0.65	↗↗
			+1	454.1	25	+0.37	+0.81	↗↗↗
			+2	165.6	55	+0.17	+0.34	↗
	tmx	timing	+0	303.3	32	+0.37	+0.68	↗↗↗
			+1	51.8	179	-0.06	-0.16	—
			+2	51.5	180	-0.03	-0.04	—

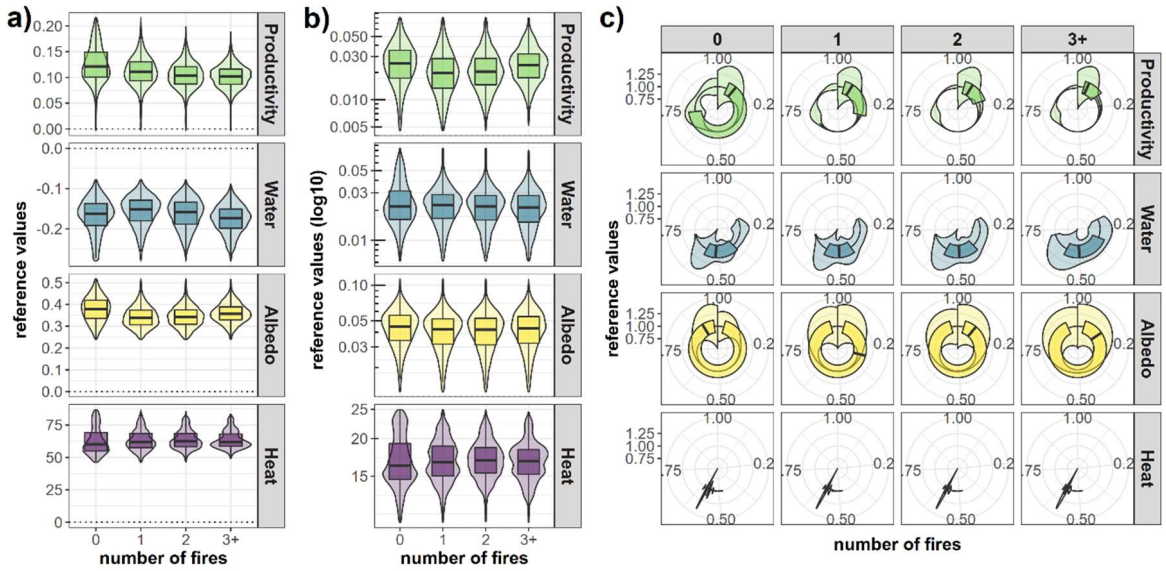

Figure S3.3. Distributions of the reference values (i.e. inter-annual median of values from unburned years) of the selected EFAs of *quantity* (a), *seasonality* (b), and *timing* (c), for pixels with zero (n_0 = 279,962), one (n_1 = 49,384), two (n_2 = 12,714), and three or more (n_{3+} = 3581) fires identified by the MODIS burned areas product, for the period of 2000–2018, in the study area.

Additional notes: The plots in *Figure S3.3* show the normal variation (i.e. excluding the values of the respective year of fire) of each of the twelve selected EFAs, with pixels grouped by different numbers of fires identified by the MODIS burned areas product in the rest of the years of the time-series, between 2000 and 2018, in the *northwest Iberian Peninsula*. Overall, the selected EFAs did not vary too much with the number of fires. The distributions of the EFAs of *quantity* (i.e. TCTG-min, TCTW-avg, TCTB-avg, and LST-max) and *seasonality* (i.e. TCTG-std, TCTW-std, TCTB-std, and LST-std) were mostly unimodal while being wider for the latter than the former. As for EFAs of *timing*, the distributions of LST-tmx were very narrow, and concentrated around late July, across different numbers of fires. On the other hand, distributions of TCTG-tmn, TCTW-tmn, and TCTB-tmx were wider, with primary peaks between late December to early January, mid-January, or mid-August, respectively.

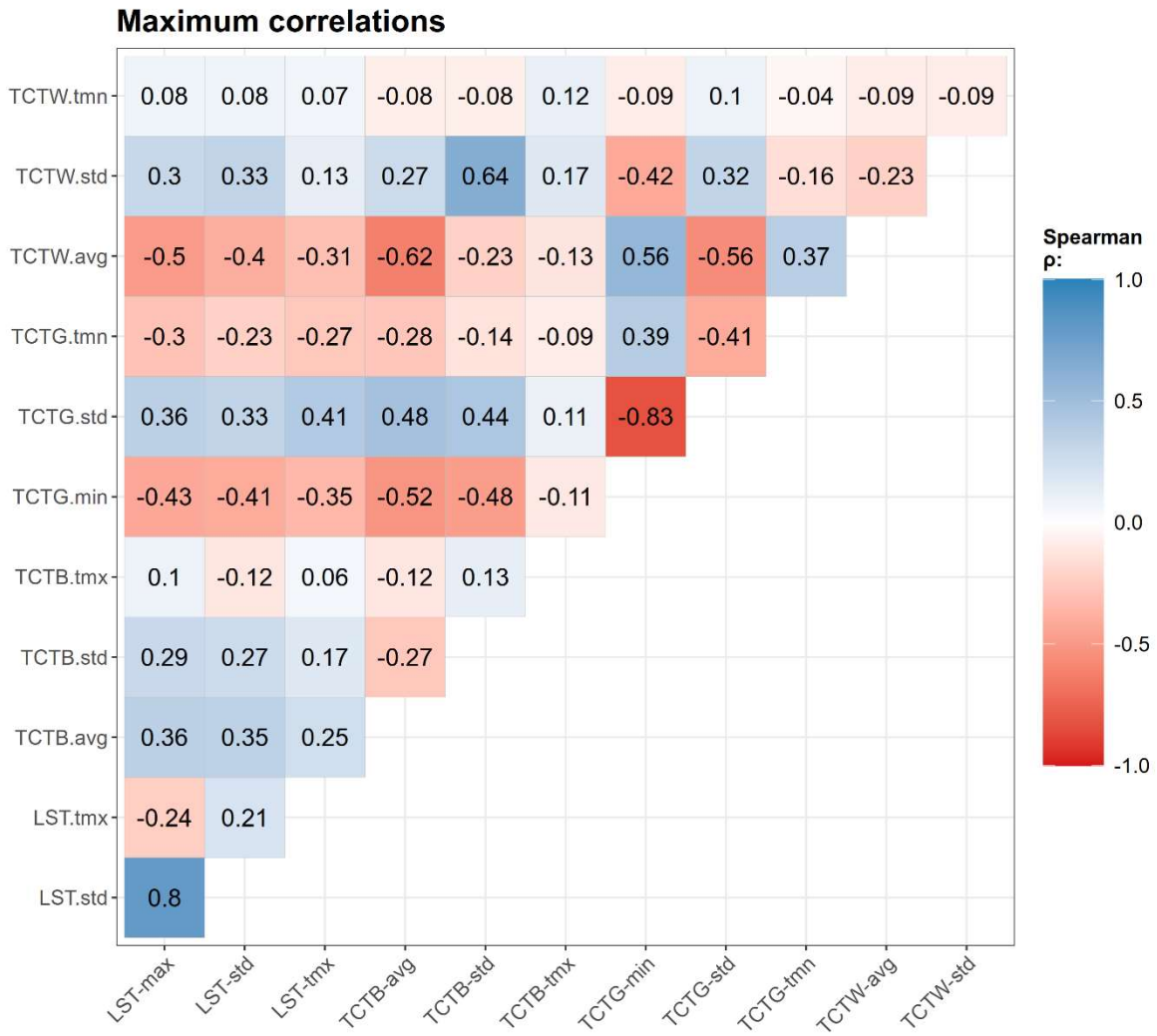

Figure S3.4. Heatmap summarizing the maximum *Spearman* rank pairwise correlations between the 12 selected metrics.

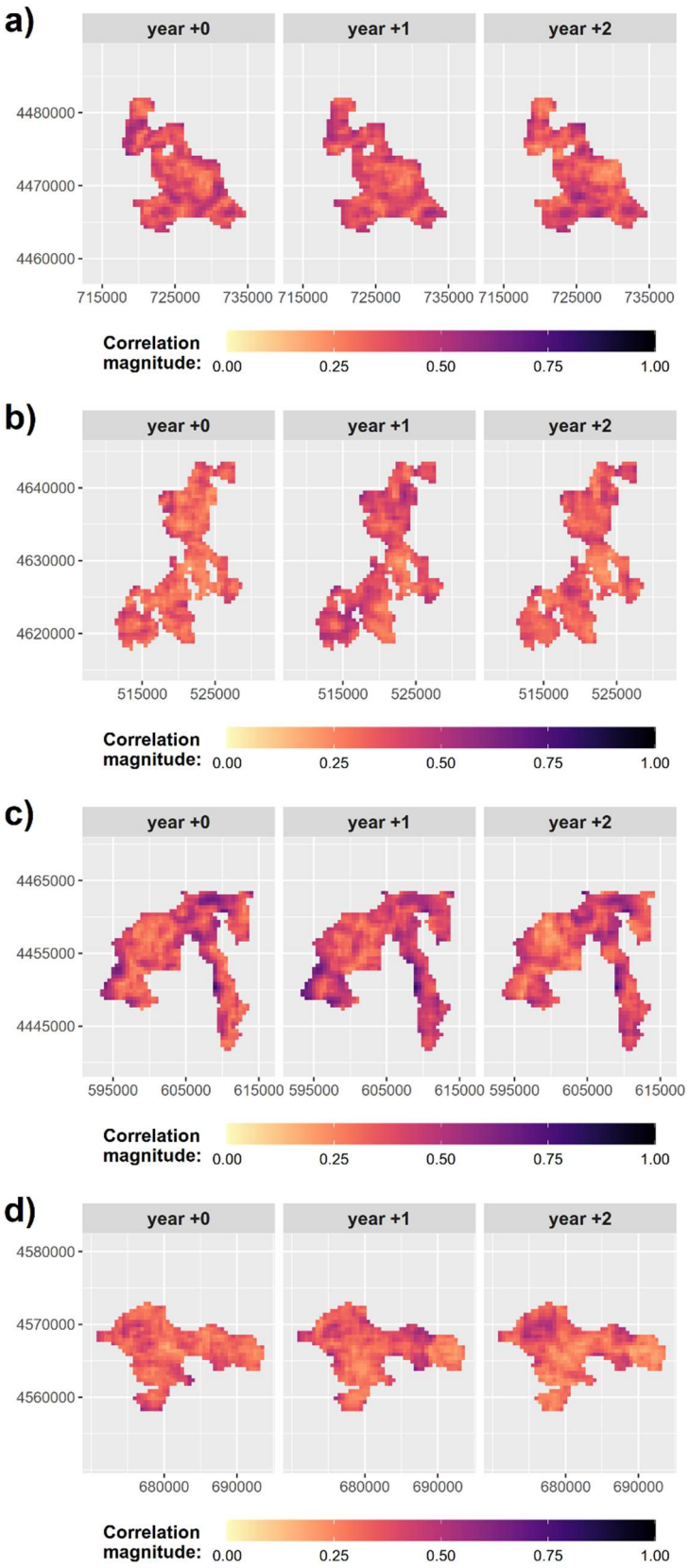

Figure S3.5. Maps of local *Spearman* rank correlations across the selected wildfire severity indicators, at short-to-medium term (i.e. between years 0 and +2 after the fire event), for four individual burned areas (letters A–D; see Figure 2 for their location within the study area).

CHAPTER 4. Characterizing post-fire recovery and resilience

Disclaimer

This Chapter is based on a manuscript that is an original contribution of this thesis currently in preparation to be submitted for in a peer-review scientific journal to be decided soon, under the working title *"Satellite-based indicators for characterizing post-fire resilience on multiple dimensions of ecosystem functioning"*. The full list of authors is: Bruno Marcos[1,2], João Gonçalves[1,3], Domingo Alcaraz-Segura[4,5,6], Mário Cunha[2,7] and João P. Honrado[1,2]. Bruno Marcos led the work with contributions from all co-authors.

The research in this manuscript was partially supported by the collaboration between Domingo Alcaraz-Segura and João Honrado under the projects RESISTE (P18-RT-1927) funded by Consejería de Economía, Conocimiento, Empresas y Universidad from the Junta de Andalucía, and DETECTOR (A-RNM-256-UGR18), with the contribution of the European Union Funds for Regional Development. Bruno Marcos was supported by FCT the Ministry of Education and Science, and the European Social Fund, within the 2014–2020 EU Strategic Framework, through FCT (Ph.D. scholarship SFRH/BD/99469/2014). João Gonçalves was funded by the Individual Scientific Employment Stimulus Program (2017), through FCT (contract nr. CEECIND/02331/2017). The authors acknowledge the use of MODIS imagery obtained from NASA's Land Processes Distributed Active Archive Center (LP DAAC), available at no charge.

[1] Research Centre in Biodiversity and Genetic Resources, Research Network in Biodiversity and Evolutionary Biology (CIBIO-InBIO), Campus Agrário de Vairão, Universidade do Porto, Rua Padre Armando Quintas,4485-661 Vairão, Portugal.

[2] Faculty of Sciences, University of Porto, Rua Campo Alegre s/n, 4169-007 Porto, Portugal.

[3] proMetheus –Research Unit in Materials, Energy and Environment for Sustainability, Instituto Politécnico de Viana do Castelo (IPVC), Avenida do Atlântico, no. 644, 4900-348 Viana do Castelo, Portugal.

[4] Department of Botany, Faculty of Sciences, University of Granada, Av. Fuentenueva, 18071 Granada, Spain.

[5] iEcolab. Interuniversity Institute for Earth System Research (IISTA), University of Granada, Av. del Mediterráneo, 18006 Granada, Spain.

[6] Andalusian Center for the Assessment and Monitoring of Global Change (CAESCG), Universidad de Almería, Crta. San Urbano, 04120 Almería, Spain.

[7] Institute for Systems and Computer Engineering, Technology and Science (INESC TEC), Campus da Faculdade de Engenharia da Universidade do Porto, Rua Dr. Roberto Frias, 4200-465 Porto, Portugal.

Abstract

Wildfire disturbances can profoundly impact many aspects of ecosystem functioning, contributing to eroding ecosystem resilience and potentially leading to regime shifts. This study describes a framework for characterization and classification of the resilience of ecosystems following wildfire disturbances, based on four key aspects of ecosystem functioning: (i) primary productivity; (ii) vegetation water content; (iii) albedo; and (iv) sensible heat. To that end, both resistance and recovery indicators were extracted from post-fire trajectories of satellite image time-series. Using our approach, potential regime shifts can also be identified, since recovery times either to pre-fire conditions or to alternative stable states can be estimated. We showcased our proposed framework for 2005 fires in NW Iberian Peninsula, using MODIS data for 2000–2018, and analyzed the main patterns of post-fire trajectories and potential regime shifts. Primary productivity generally decreased immediately after the fire, with steep post-fire trajectories, usually starting to recover within the first six months and reaching the pre-fire reference interval in the first two years after the fire, eventually stabilizing within the analyzed period. Vegetation water content also decreased after the fire, although with slower and more gradual post-fire recovery than primary productivity. In some cases, albedo decreased after the fire, only to increase above pre-fire reference levels one or two years after the fire, sometimes with persisting effects for many years afterward. Finally, sensible heat increased for a short duration after the fire, however starting to dissipate after one year, since the effects of wildfire disturbances on sensible heat are more transient than for the other dimensions of ecosystem functioning. Overall, our results suggest that the indicators proposed successfully depict key features of the post-fire processes in ecosystem functioning, at different timeframes, both at the regional scale, for spatially explicit prioritization, and to subsequent local-scale assessments. The high degree of complementarity between indicators, and especially between the different dimensions of ecosystem functioning, highlight the added value of a multi-dimensional approach for analyzing ecosystem resilience to wildfire disturbances. We argue that such frameworks can provide enhanced characterization and classification of the resilience of ecosystems to those disturbances, ultimately upholding promising implications for post-fire ecosystem management.

Keywords

Ecological disturbance; Ecological resilience; Post-fire recovery; Post-fire trajectories; Remote sensing; Wildfires.

4.1. Introduction

Wildfire disturbance events have been increasing, both in terms of frequency and intensity, in previous decades (Bowman *et al.* 2009), exacerbated by shifts in land use and forest management, as well as global climate change (Tedim *et al.* 2013). Such disturbances can profoundly impact many aspects of the composition, structure, and functioning of ecosystems, despite being considered an integral part of the natural dynamics of ecosystems in several biomes (San-Miguel-Ayanz *et al.* 2013, Adámek *et al.* 2016). Furthermore, wildfires can contribute to eroding the *resilience* of ecosystems (Folke *et al.* 2004, Johnstone *et al.* 2010), i.e., their ability to persist in the face of disturbances (Scheffer *et al.* 2015), decreasing their self-repairing capacity (Folke *et al.* 2004). International environmental policies and targets such as the Aichi Biodiversity Targets and the Sustainable Development Goals include conserving resilient ecosystems as a key priority (Willis *et al.* 2018). Thorough assessments of the ecological consequences of wildfire disturbances, as well as of the responses and resilience of ecosystems to those disturbances, are thus needed to bridge gaps between science, policy, and management (Gouveia *et al.* 2010, van Leeuwen *et al.* 2010, Baho *et al.* 2017).

In this regard, several measures based on concepts related to ecosystem stability have been used to characterize both the effects of and responses to, wildfire disturbances in ecosystems. Traditionally, both *resistance* and *resilience* were considered independent components of ecological *stability* (the third being *persistence*; Harrison, 1979). The concept of *resistance* expresses the ability of ecosystems to withstand environmental disturbances (De Keersmaecker *et al.* 2015) and is related to the instantaneous impact of exogenous disturbance on ecosystem state (Hodgson *et al.* 2015). Resistance to wildfire disturbances can be measured by the magnitude of change in ecosystems following those disturbances (Meng *et al.* 2021), which is related to the magnitude of *fire severity* (De Keersmaecker *et al.* 2015).

Within the classical concept of ecosystem stability, *resilience* was often quantified by measuring the speed at which an ecosystem returns to the original equilibrium, after disturbance (Meng *et al.* 2021). This measure concentrates on stability near that equilibrium, which is connected to the concept of *engineering resilience*. This notion of resilience assumes that only one stable state exists, focusing on maintaining the efficiency of function (Holling 1973, 1996). However, as the use of resilience in the context of wildfires has increased in management and research documents (Selles and Rissman 2020), and our understanding of resilience has been continuously advancing, this notion has gradually been replaced by the broader concept of *ecological resilience* (Fan *et al.* 2021). This updated view of resilience explicitly recognizes the existence of *multiple alternative stable*

states (Scheffer and Carpenter, 2003), since ecosystem disturbances can trigger sudden ecosystem collapse or *regime shifts* (Boettiger *et al.* 2013) when critical thresholds (called *tipping points*) are exceeded (Scheffer *et al.*, 2012, 2009). Ecosystems may thus endure critical transitions leading to their reconfiguration from one dynamic equilibrium state (i.e., the *basin of attraction* near which they tend to fluctuate; Scheffer *et al.*, 2009) to an alternative contrasting stable state (e.g., Dwomoh and Wimberly, 2017; Hirota *et al.*, 2011), mediated through *adaptive capacity* (Andersen *et al.* 2009). Ecological resilience can hence be regarded as the property that mediates transition among multiple stable states (Gunderson 2000). Furthermore, whereas engineering resilience focuses on maintaining functioning *efficiency*, ecological resilience instead focuses on maintaining functioning *existence* (Holling 1973, 1996). In a hierarchical perspective of resilience, *engineering resilience* is associated with higher persistence than *ecological resilience* (Delettre 2021). Nonetheless, engineering resilience and ecological resilience can both be regarded as two complementary perspectives of stability (Ingrisch and Bahn 2018), corresponding to two different types of resilience (Delettre 2021).

The terms resistance and resilience have both been used interchangeably as the amount of disturbance that a system can take before changing state (Meng *et al.* 2021). However, more recently, the two concepts are no longer regarded as two independent components of ecosystem stability, with resilience now encompassing aspects of both resistance and recovery (Fan *et al.* 2021). Whereas *resistance* is related to the impact of exogenous disturbances on ecosystems, *recovery* captures the endogenous processes that pull the disturbed system back towards equilibrium (Hodgson *et al.* 2015). Recovery can be measured by the duration of the period from a disturbed to a stable state (i.e., *return time*, as in the classical definition of resilience; Hodgson *et al.*, 2015), even if this stable state does not correspond to pre-fire conditions. As critical transitions and regime shifts imply changes in ecosystem functions and services with subsequent impacts on human societies (Folke *et al.* 2004), the ability to assess ecosystem state and resilience is critical for effective ecosystem management and resource exploitation (Holling 1973, Meng *et al.* 2021).

Within the alterations induced by wildfires, changes in ecosystem functioning are of particular interest, since functional attributes have a shorter response time to disturbances than structural or compositional ones, and are more directly connected to ecosystem services (Alcaraz-Segura *et al.* 2008). This is because fire can cause rapid modifications in multiple dimensions of matter and energy flows in ecosystems (Petropoulos *et al.* 2009, Marcos *et al.* 2021). For instance, wildfires play an important role in the terrestrial biosphere carbon cycle (Wei *et al.* 2018), such as in biomass (Pellegrini *et al.* 2018, Sparks *et al.* 2018), and primary productivity (Leys *et al.* 2016). Furthermore, water supply and quality

(Smith *et al.* 2011, Santos *et al.* 2015, Carvalho-Santos *et al.* 2019), as well as vegetation water content (Senf and Seidl 2020), can also be directly or indirectly affected by wildfire disturbances. Moreover, different aspects of energy balances, such as albedo (e.g., French *et al.*, 2016; Gatebe *et al.*, 2014; Quintano *et al.*, 2019; Saha *et al.*, 2017), latent heat (e.g., Sun *et al.*, 2019), and sensible heat (e.g., Liu *et al.*, 2018; Maffei *et al.*, 2018; Veraverbeke *et al.*, 2012) can also suffer profound alterations induced by wildfires. However, few studies have addressed wildfire effects on multiple dimensions of ecosystem functioning (however, see Marcos *et al.*, 2021). Therefore, since both wildfire disturbances and resilience are *multi-dimensional* (Donohue *et al.* 2013, 2016), and *post-fire trajectories* of each dimension of ecosystem functioning are different (Ryu *et al.* 2018), more comprehensive indicators are still needed to understand post-fire processes better.

Due to lower costs and improved technology for providing up-to-date information on the status of ecosystem resources, *remote sensing* (RS) techniques have been increasingly employed to derive indicators to assess and characterize different aspects of the post-fire period (Lentile *et al.* 2006). Specifically, RS data has been used to map burned areas (Mouillot *et al.* 2014, Giglio *et al.* 2018, Chuvieco *et al.* 2019, Roy *et al.* 2019), as well as to assess and map burn and fire severity (Veraverbeke *et al.* 2011a, Marcos *et al.* 2021). Characterization of post-fire recovery has taken advantage of multi-temporal spectral data recorded from different space and airborne sensors, such as Landsat missions (Hope *et al.* 2007, van Leeuwen *et al.* 2010, Veraverbeke, Gitas, *et al.* 2012, Viana-Soto *et al.* 2020), SPOT-Vegetation (Gouveia *et al.* 2010, Bastos *et al.* 2011), Terra/Aqua – Moderate Resolution Imaging Spectroradiometer (MODIS) sensors (Hope *et al.* 2012, Caccamo *et al.* 2015, João *et al.* 2018), and multi-spectral cameras onboard *Unoccupied Aircraft Systems* (UAS; Samiappan *et al.*, 2019). Furthermore, the utility of RS to evaluate resilience to wildfire disturbances has received increased attention, although mostly focusing on the *engineering resilience* paradigm (e.g., Bisson *et al.*, 2008; Cui *et al.*, 2013; Di Mauro *et al.*, 2014; Díaz-Delgado *et al.*, 2002; Dwomoh and Wimberly, 2017; Fernandez-Manso *et al.*, 2016; Harris *et al.*, 2014; Prodon and Diaz-Delgado, 2021; Spasojevic *et al.*, 2016; Staal *et al.*, 2018). Indicators derived from satellite image time-series (SITS) can provide information on multiple dimensions of ecosystem functioning, thus enabling in-depth and integrative characterizations of post-fire recovery and resilience (João *et al.* 2018, Marcos *et al.* 2019). Notwithstanding, most resilience assessments based on RS data do not account for ecosystem functioning after disturbance events (Frazier *et al.* 2013). The ability to assess and map the spatiotemporal heterogeneous effects of wildfire disturbances on ecosystem functioning and the responses and resilience of ecosystems to those disturbances makes RS data a major asset not only for risk assessment and governance but also for post-fire

management and restoration (Keeley 2009, Tedim *et al.* 2013, Smith *et al.* 2014, Parks *et al.* 2019).

In this study, we propose, describe, and showcase a framework for enhanced characterization and classification of the resilience of ecosystems following wildfire disturbances, based on four key aspects of ecosystem functioning: (i) primary productivity; (ii) vegetation water content; (iii) albedo; and (iv) sensible heat. Our approach is based on indicators covering aspects related to both resistance (i.e., fire severity) and recovery at short, medium-, and long-term, extracted from SITS. We illustrated our approach by analyzing and comparing the main patterns of four indicators of both short-term, as well as medium-to-long-term responses of each of the four dimensions of ecosystem functioning to wildfire disturbances, extracted from time-series of MODIS data covering the 2000–2018 period, for fires occurring in the focal year of 2005, in the NW Iberian Peninsula. We then used the two indicators of medium-to-long-term recovery to classify each post-fire trajectory into one of five major types of post-fire recovery and resilience and to identify potential regime shifts in each of the four dimensions of ecosystem functioning. Finally, these classifications were combined into a synthetic indicator to evaluate the strength-of-evidence for regime shifts, across dimensions. Finally, we discussed the potential and added value of the proposed approach to improve RS-based characterization and classification of resilience to wildfire disturbances over multiple dimensions of ecosystem functioning.

4.2. Materials and Methods

4.2.1. Generic framework

General workflow

The proposed framework for characterization and classification of resilience to wildfire disturbances consists of using different indicators to describe essential aspects of post-fire processes for four key aspects of matter and energy flows in ecosystems: (i) primary productivity (ii) vegetation water content, (iii) albedo, and (iv) sensible heat. To this end, metrics extracted from the post-fire trajectories obtained from satellite image time-series (SITS) are used for each of those four dimensions of ecosystem functioning. The general workflow of our proposed approach is composed of four main steps (Figure 4.1), which will be described in the following sub-sections.

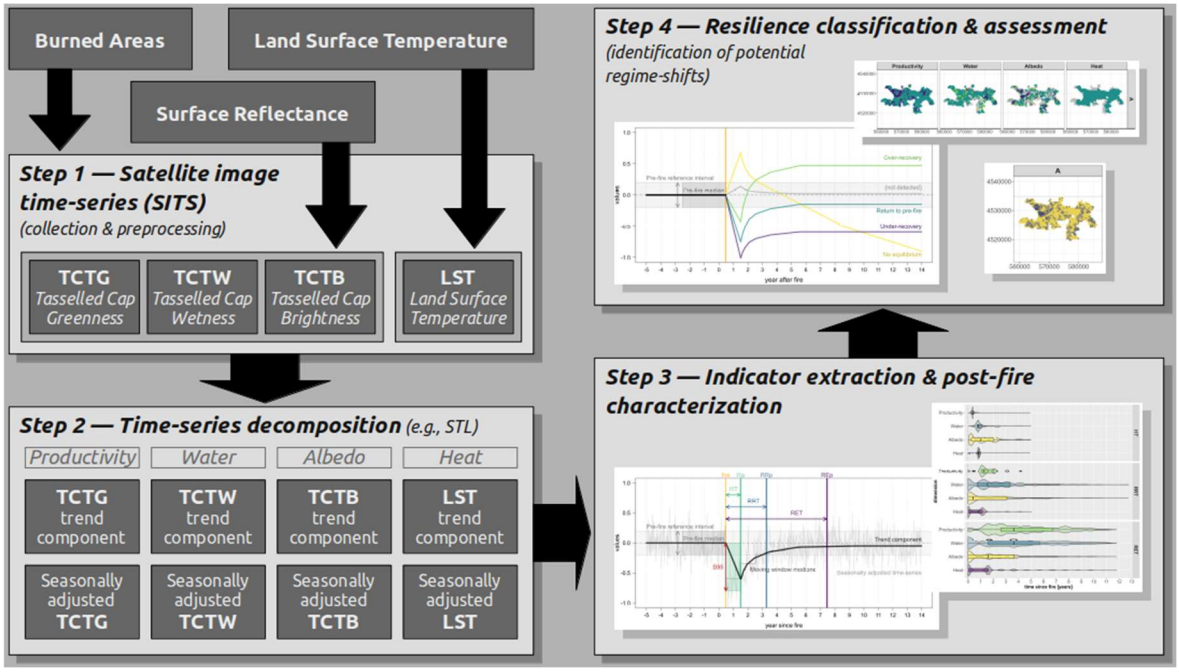

Figure 4.1. General workflow of the proposed framework for characterizing and classifying post-fire trajectories of satellite image time-series related with the four key dimensions of ecosystem functioning of *primary productivity*, *vegetation water content*, *albedo*, and *sensible heat*, according to different attributes of their resilience (resistance and recovery) to wildfire disturbances.

Step 1 – Collect and preprocess satellite image time-series

Firstly, SITS have to be collected, for each of the four dimensions of ecosystem functioning, from available satellite products, and then preprocessed (**Figure 4.1** – "Step 1"). To this end, the *Tasseled Cap Transformation* (TCT) features of *Greenness* (TCTG),

Wetness (TCTW), and *Brightness* (TCTB), as well as *land surface temperature* (LST), have successfully been used in fire-related applications (e.g., Bowman *et al.*, 2015; Coops *et al.*, 2008; Marcos *et al.*, 2021, 2019; Quintano *et al.*, 2015; San-Miguel-Ayanz *et al.*, 2013). These TCT features are computed as sensor-specific linear combinations of bands in the visible, near-infrared, and short-wave infrared regions of the electromagnetic spectrum (Lobser and Cohen 2007). To compute these TCT features, principal component axes derived from a global sample are rotated to maximize the association of each axis with biophysical parameters (Mildrexler *et al.*, 2009), such as the amount of photosynthetically active vegetation (*Greenness*), vegetation water content, and soil moisture (*Wetness*), and albedo (*Brightness*). These variables, in turn, can be used as proxies for the ecosystem functioning key attributes of *primary productivity*, *vegetation water content,* and *albedo*, respectively (Marcos *et al.*, 2021). The LST is a calibrated measure of the thermal emissivity of the land surface (Duan *et al.* 2019), and therefore can be used as a proxy of *sensible heat*.

Step 2 – Decompose time-series

To extract meaningful post-fire recovery metrics from SITS, time-series decomposition methods must first be employed to separate seasonality effects in the data from long-term changes due to wildfire disturbances. To that end, algorithms such as the *Seasonal and Trend decomposition using Loess* (STL) can be used. STL is a versatile and robust method for additive time-series decomposition, which consists of a sequence of applications of the loess smoother that results in the extraction of a *seasonal*, *trend*, and *remainder* components (Cleveland *et al.* 1990), as:

$$y_t = S_t + T_t + R_t \qquad 4.1$$

where y_t is the original data, S_t is the *seasonal* component, T_t is the *trend* component, and R_t is the *remainder* component, all at period *t*.

The *seasonal* component extracted from STL decomposition comprises fluctuations in the data with a fixed and known frequency. In our approach, the *seasonally adjusted time-series* – i.e., the original time-series with the seasonal component removed – is used to establish pre-fire reference conditions, against which post-fire values are compared to evaluate if, when, and how they have recovered since it is considered to be useful for estimating central tendencies and non-seasonal variability (Hyndman and Athanasopoulos 2018).

On the other hand, the *trend* component includes both the long-term variation in the data and cyclic effects (i.e., fluctuations in the data that are not of a fixed frequency). In contrast, the *remainder* component can include noise and other non-seasonal, non-cyclic fluctuations (Hyndman and Athanasopoulos 2018), such as abrupt shifts related to distinct disturbances. In our approach, the *trend* component is used to calculate median values for each moving window in the post-fire period, instead of the *seasonally adjusted time-series*, since it is considered to be more useful to look for *turning points* in a series, and interpret changes in direction (Hyndman and Athanasopoulos 2018). These *moving window medians*, with a fixed width *w*, represent the long-term incremental variation in post-fire trajectories and aim to support the extraction of indicators of post-fire recovery and resilience, as well as the classification of post-fire trajectories.

Among the STL decomposition procedure parameters, *t.window* and *s.window* play a crucial role, as these two parameters control how rapidly the *trend* and *seasonal* components can change. The *t.window* and *s.window* parameters correspond to the span (in lags) of the *loess* window for *trend* and *seasonal* extraction, respectively, and should both be odd numbers, as described in Cleveland *et al.* (1990).

Step 3 – Characterize post-fire resistance and recovery using indicators extracted from post-fire trajectories

Several indicators can be extracted from the decomposed time-series of post-fire trajectories, to support the assessment and characterization of key features related to both resistance and recovery aspects of post-fire resilience. The generic approach to extract such indicators, illustrated in **Figure 4.2**, is described in the following paragraphs.

To extract indicators of post-fire short-term effects, for each of the four dimensions of ecosystem functioning, the first inflection point in the trend component after the wildfire occurrence (i.e., the I1p point) has to be determined. If this point exists, it represents the first major change of directionality after the wildfire occurrence, which can be used as an estimator of the date of the start of recovery. Furthermore, the amount of time between this date and the date of fire occurrence – called *Time to Inflection* (I1T) – can be regarded as a measure of the duration of the disturbance effects. Conversely, this can also be used to estimate the time needed to start post-fire recovery, thus relating to both the resistance to wildfire disturbances and short-term recovery speed. Moreover, the S95 indicator is defined as the difference between the pre-fire median and the 95% percentile of the seasonally adjusted time-series values within the first moving window immediately after a fire. As an estimate of the near-maximum short-term impact of the wildfire disturbance on the corresponding dimension of ecosystem functioning, this indicator is related to wildfire

disturbance severity, and the resistance of ecosystems to those disturbances (De Keersmaecker *et al.* 2015, Meng *et al.* 2021).

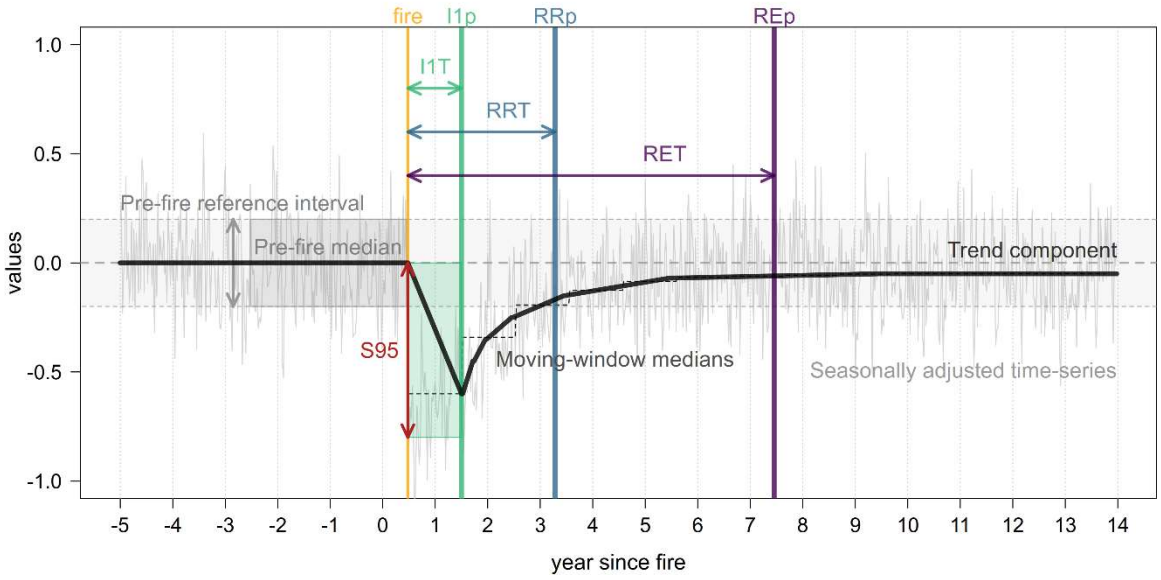

Figure 4.2. Illustration of the indicators of post-fire resilience extracted from satellite-derived trajectories, used in this study. "S95" corresponds to the difference between the pre-fire median and the 95% percentile of the seasonally-adjusted values in the first moving window after the date of the wildfire event. "I1p", "RRp", and "REp" represent the post-fire points of: *inflection* in the trend component of the time-series, *return-to-reference*, and *return-to-equilibrium*, respectively. "I1T", "RRT", and "RET" represent the amount of time between the date of the fire occurrence and the dates of the I1p, RRp, and REp, respectively.

Indicators that portray aspects more related to the medium-to-long-term responses of ecosystem functioning to wildfire disturbances can also be extracted from the same post-fire trajectories. To this end, the *Return-to-Reference* (RRp) point, and the *Return-to-Equilibrium* (REp) point (if each one exists) must first be determined. The RRp point is determined by identifying the first value of the trend component, after the inflection point within the pre-fire reference interval, while its corresponding moving window median is also within that interval, to minimize false detections caused by short-term oscillations. The duration of the time segment between the date of fire occurrence and the date of the RRp point – called *Time to Return-to-Reference* (RRT) – gives an estimation of the amount of time needed to achieve the pre-fire conditions once again (if applicable). This can be regarded as an indicator of medium-to-long-term recovery speed which is in line with the concept of *engineering resilience* (Holling 1996). On the other hand, the REp point is determined by finding the first of at least two consecutive moving window medians, after the inflection point, that exhibit relative change rates below a predefined threshold. The duration of the time segment between the date of fire occurrence and the date of the REp point – *Time to Return-to-Equilibrium* (RET) – approximates the amount of time needed to achieve

a stable state after a fire. As this stable state can be different (or not) from pre-fire conditions, this indicator can be regarded as an indicator of long-term recovery speed that is more in line with the concept of *ecological resilience* (Holling 1996).

Step 4 – Classify resilience to wildfire disturbances and identify potential regime shifts

According to their main temporal patterns, post-fire trajectories of any one of the four dimensions of ecosystem functioning can be grouped. In this sense, we propose a simple combination of the RRp and the REp points for each of the four dimensions of ecosystem functioning for classifying post-fire trajectories into major types and identify potential regime shifts. Since these two points contain information about the type of outcome of post-fire trajectories, this combination results in a classification scheme that categorizes long-term post-fire resilience into one of five classes (**Figure 4.3**).

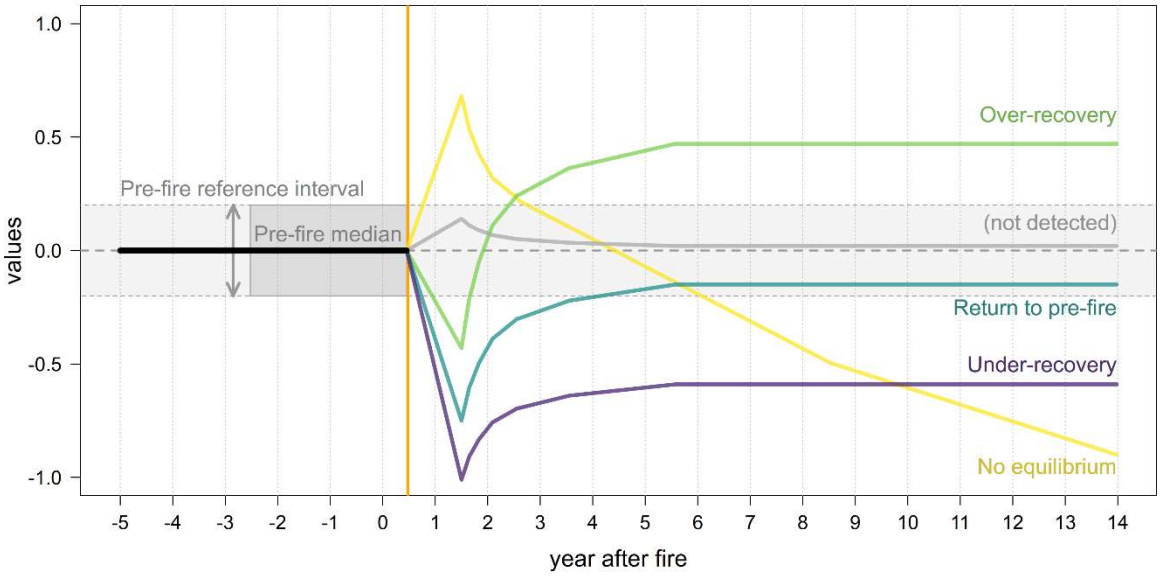

Figure 4.3. Illustration of the classification of post-fire recovery and resilience based on the *Time to Return-to-Reference* (RRT) and *Time to Return-to-Equilibrium* (RET) indicators, which measure the duration of the periods between the date of the wildfire event and the date in which the post-fire trajectory crosses the pre-fire reference interval (i.e., the *Return-to-Reference* point, RRp), and the date when equilibrium is achieved (i.e., the *Return-to-Equilibrium* point, REp).

The *Return to pre-fire* class corresponds to situations when an equilibrium state has been reached within the pre-fire reference interval, which is in line with the concept of *engineering resilience*. On the other hand, the *Over-recovery* and *Under-recovery* classes correspond to situations when a new equilibrium state has been reached, outside of the pre-fire reference interval, either with or without having crossed the pre-fire reference interval, respectively. When the post-fire trajectory has crossed the pre-fire reference interval, but no equilibrium was reached, the corresponding post-fire trajectory is classified as *No equilibrium*. Finally, when no recovery has been detected, all these situations are

classified as *(not detected)*, which could correspond to neither RRp nor REp points being identified, neither the inflection point being found within the reference interval (or at all).

4.2.2. Test case

Study area

This study analyzed all areas burned in 2005, in the northwest Iberian Peninsula (NW-IP; **Figure 4.4a,b**). This area has one of the highest densities of ignitions among southern European countries, and one of the highest annual values of burned area in Europe (Catry *et al.* 2009), despite the enormous investments in fire suppression (Moreira *et al.* 2020). The year 2005 was particularly devastating in NW-IP, with over 340 000 ha burned (almost 4% of the total area), coinciding with very severe drought (Bastos *et al.* 2011). This year was chosen for the availability of SITS for more than a decade following the fire occurrences.

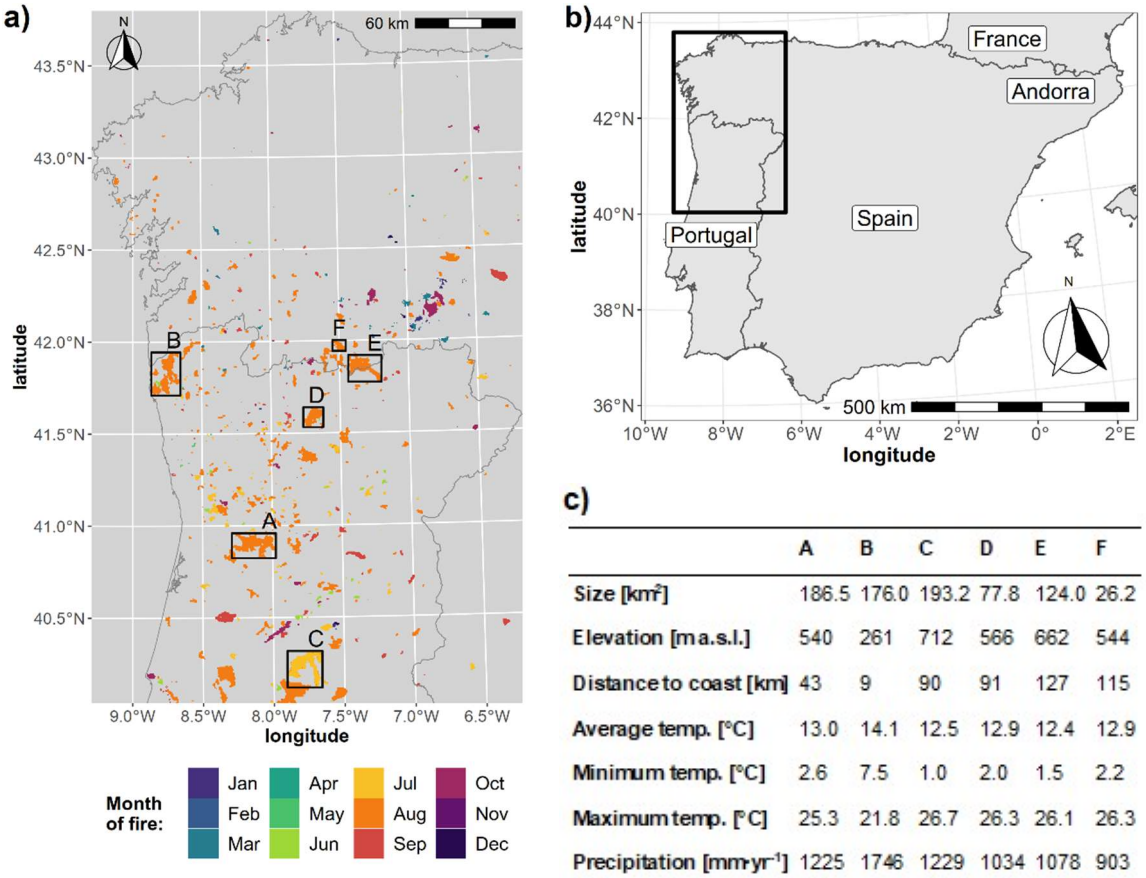

	A	B	C	D	E	F
Size [km²]	186.5	176.0	193.2	77.8	124.0	26.2
Elevation [m a.s.l.]	540	261	712	566	662	544
Distance to coast [km]	43	9	90	91	127	115
Average temp. [°C]	13.0	14.1	12.5	12.9	12.4	12.9
Minimum temp. [°C]	2.6	7.5	1.0	2.0	1.5	2.2
Maximum temp. [°C]	25.3	21.8	26.7	26.3	26.1	26.3
Precipitation [mm·yr⁻¹]	1225	1746	1229	1034	1078	903

Figure 4.4. The burned areas analyzed in this study: (a) burned patches of fires that occurred in 2005, with the corresponding month of occurrence (letters A–F); (b) geographical context within the Iberian Peninsula; and (c) summary table of environmental characteristics of the six individual burned areas (letters A–F).

The NW-IP features a highly diverse set of environmental characteristics, with strong environmental gradients, and a major biogeographic transition, from the Atlantic climate with temperate mixed and deciduous broadleaf forests in the north and west to the Mediterranean climate with evergreen sclerophyllous vegetation towards the southeast. Major land cover classes include shrublands in different successional stages, and plantation forests such as maritime pine, eucalyptus, and mixed stands. Increasing fuel load and continuity, along with historical use of fire for agrosilvopastoral purposes, and extensive abandonment of farming and husbandry, turned this area into a highly fire-prone landscape, and a hotspot in terms of wildfire occurrences, within the European context, in the last decades.

In addition to using all areas burned in 2005 in NW-IP to analyze overall patterns at the regional level, we selected six individual burned areas, within the study area (**Figure 4.4a,c**), with diverse baseline environmental characteristics, to showcase the proposed approach.

Satellite data collection and preprocessing

To illustrate our proposed approach, we extracted satellite image time-series (SITS) of proxy indicators for the four aspects of ecosystem functioning (i.e., primary productivity, vegetation water content, albedo, and sensible heat), from MODIS products MOD09A1 and MOD11A2, for the years between 2000 and 2018.

From the MOD09A1 Terra Surface Reflectance product (8-Day L3 Global 500m, Collection 6; Vermote, 2015), we calculated the *Tasseled Cap Transformation* features of *Greenness* (TCTG), *Wetness* (TCTW), and *Brightness* (TCTB), as proxies for *primary productivity*, *vegetation water content*, and *albedo*, respectively. Specifically, we used the coefficients in Lobser and Cohen (2007) to compute the three TCT features, using the seven bands available in MOD09A1 (see **Table 4.1**). As for the dimension of ecosystem functioning related to sensible heat, we extracted the day *land surface temperatures* (LST) from the MOD11A2 Terra Land Surface Temperature/Emissivity product (8-Day L3 Global 1000m, Collection 6; Wan *et al.*, 2015). Burned areas for fires that occurred in 2005 in NW-IP were extracted from the MCD64A1 Terra+Aqua Burned Area product (monthly L3 Global 500m, Collection 6; Giglio *et al.*, 2018). These burned patches were filtered so that only those with areas above 100 ha were used, following previous work (see Marcos *et al.*, 2019).

Most tasks were undertaken within the *R* statistical programming environment (R Core Team 2021), using mainly the *raster* package (Hijmans 2020), with additional R packages

complemented by other software, for more particular tasks, as specified whenever relevant. All three MODIS products covering the study area (i.e., MODIS tile h17v04) were downloaded and reprojected to the WGS84/UTM29N coordinate system using the *MODIStsp* R package (Busetto and Ranghetti 2016). Rescaling of LST values to degrees Celsius, and the computation of TCT features was done using the *rasterio* Python package (Gillies *et al.* 2013). Finally, to SITS of the three TCT features and LST, a filter based on the *Hampel* identifier (Hampel 1971, 1974) was applied pixel-wise to correct spurious values.

Table 4.1. MODIS-specific coefficients used to calculate the *Tasseled Cap Transformation* (TCT) features of *Brightness*, *Greenness*, and *Wetness*, which result from a rotation of principal component axes so that these are aligned with the biophysical parameters of albedo, amount of photosynthetically active vegetation, and soil/vegetation moisture, respectively (Lobser and Cohen 2007).

Band			Coefficients		
No.	*Name*	*Range [nm]*	*Brightness*	*Greenness*	*Wetness*
1	Red	620 – 670	0.4395	–0.4064	0.1147
2	NIR 1	841 – 876	0.5945	0.5129	0.2489
3	Blue	459 – 479	0.2460	–0.2744	0.2408
4	Green	545 – 565	0.3918	–0.2893	0.3132
5	NIR 2	1230 – 1250	0.3506	0.4882	–0.3122
6	SWIR 1	1628 – 1652	0.2136	–0.0036	–0.6416
7	SWIR 2	2105 – 2155	0.2678	–0.4169	–0.5087

NIR: near-infrared; SWIR: short-wavelength infrared.

Time-series decomposition and normalization

In our illustrative test case, we applied pixel-wise *STL decomposition*, for each of the four SITS, with both the *t.window* and *s.window* parameters equal to 47 (i.e., the nearest odd number above the number of observations in each year, in MODIS products with 8-day temporal resolution). We used this value for both those parameters, as this seemed to allow capturing a wide range of effects at *short-* (i.e., less than one year), *medium-term* (i.e., up to three years), and *long-term* (i.e., above three years) effects, for post-fire analysis. Also, we opted for using robust fitting (i.e., *robust* parameter = *TRUE*) to reduce the effect of occasional unusual observations on the trend and seasonal components. All other parameters of the STL procedure were fixed at their respective default values.

We defined the pre-fire reference intervals (see **Figure 4.2**), for our test case, as one median absolute deviation around the median value (i.e., median ±1 M.A.D.), calculated using all values within three years before the date of the fire occurrence, to reduce the

impact of extreme values in the calculation of the reference intervals. For the calculation of grouped medians, we used a single fixed window size equal to the *t.window* and *s.window* parameters of the STL decomposition, since it approximately corresponds to one year of observations.

Characterization of post-fire trajectories

To analyze the main patterns of resilience to the 2005 wildfires in our study area, in terms of both resistance and recovery, we extracted the S95, I1T, RRT, and RET indicators (see **Figure 4.2**) from the post-fire trajectories of SITS, for each of the four dimensions of ecosystem functioning considered (i.e., primary productivity, vegetation water content, albedo, and sensible heat). We used a threshold of 5% for the maximum change rate between consecutive moving windows after the inflection point to determine the REp point. These 16 indicators (i.e., four indicators for each of four dimensions) allowed for the characterization of post-fire trajectories in the study area in the short-, medium-to-long-, and long-terms. Additionally, we calculated *Spearman* rank correlations to assess potential collinearity among indicators, using all complete pairwise observations.

Identification of potential regime shifts

To identify potential regime shifts in NW-IP due to the 2005 wildfires, post-fire trajectories were classified into the major types of long-term recovery by combining the classified outcomes of the RRT and RET indicators, for each of the four dimensions of ecosystem functioning, for all patches burned in 2005. Next, we compared the relative frequency of each class, obtained from this classification at the regional level, across dimensions. Additionally, we used both the balanced accuracy (BAcc; Brodersen *et al.* 2010) and the multi-class Matthews correlation coefficient (MCC; Chicco and Jurman, 2020; Matthews, 1975) to evaluate the relative pairwise agreement between the classifications obtained for each dimension of ecosystem functioning, as both measures can be used with unbalanced data. To that end, we used the *mlr3measures* (Lang 2021) and *mltools* (Gorman 2018) R packages, respectively. This procedure was applied to evaluate potential redundancies between classifications for each ecosystem functioning dimension. We then mapped the classifications for each dimension of ecosystem functioning, for all of the six individual burned patches identified in **Figure 4.4a**. Finally, we calculated and showcased, for each of the six selected burned patches, the pixel-wise percentages of those four dimensions for which either the class *Under-recovery* or *Over-recovery* was obtained. This can be regarded as a synthetic measure that aims to translate the overall *Strength-of-*

Evidence (SoE) of regime shifts in ecosystem functioning across the four dimensions analyzed.

4.3. Results

4.3.1. General patterns of post-fire indicators

Statistical distributions

The distributions of the four MODIS-derived indicators used to characterize the post-fire trajectories in our study area (i.e., S95, I1T, RRT, and RET), for each of the four aspects of ecosystem functioning considered (i.e., primary productivity, vegetation water content, albedo, and sensible heat), are shown in **Figure 4.5**.

The obtained distributions for the S95 severity indicator (**Figure 4.5a**) showed the overall directionality of the short-term effects of wildfires, for each of the four dimensions of ecosystem functioning. Namely, *Productivity* and *Water* decreased immediately after a fire, while *Heat* increased. On the other hand, *Albedo* exhibited a well-marked multi-modal distribution, with one group corresponding to decreased values, whereas the other corresponded to increased values. The distributions of the I1T short-term recovery indicator (**Figure 4.5b**) obtained for *Productivity*, *Water*, and *Heat* were mainly concentrated within the two first years after a fire, with lower values for *Productivity*, followed by *Water* and *Heat*. As for *Albedo* and the I1T indicator, values were much more dispersed than the other dimensions, with both low and high values within the first year and after two years following the fire, respectively. The RRT *medium-to-long-term recovery* indicator (**Figure 4.5c**) had more tightly concentrated (i.e., less dispersed) distributions for *Productivity* and *Heat* but more dispersed for the *Albedo* and *Water* dimensions. Furthermore, while *Albedo* had more values concentrated in the first year after fire than the other dimensions, *Water* was the dimension with the overall highest values for this indicator (e.g., higher than four years after the fire). Finally, distributions of the RET *long-term recovery indicator* (**Figure 4.5d**) were more dispersed than for RRT. Overall values were higher for *Productivity*, followed by *Water*, and then *Albedo*. On the other hand, values for *Heat* were generally lower than for the other three dimensions.

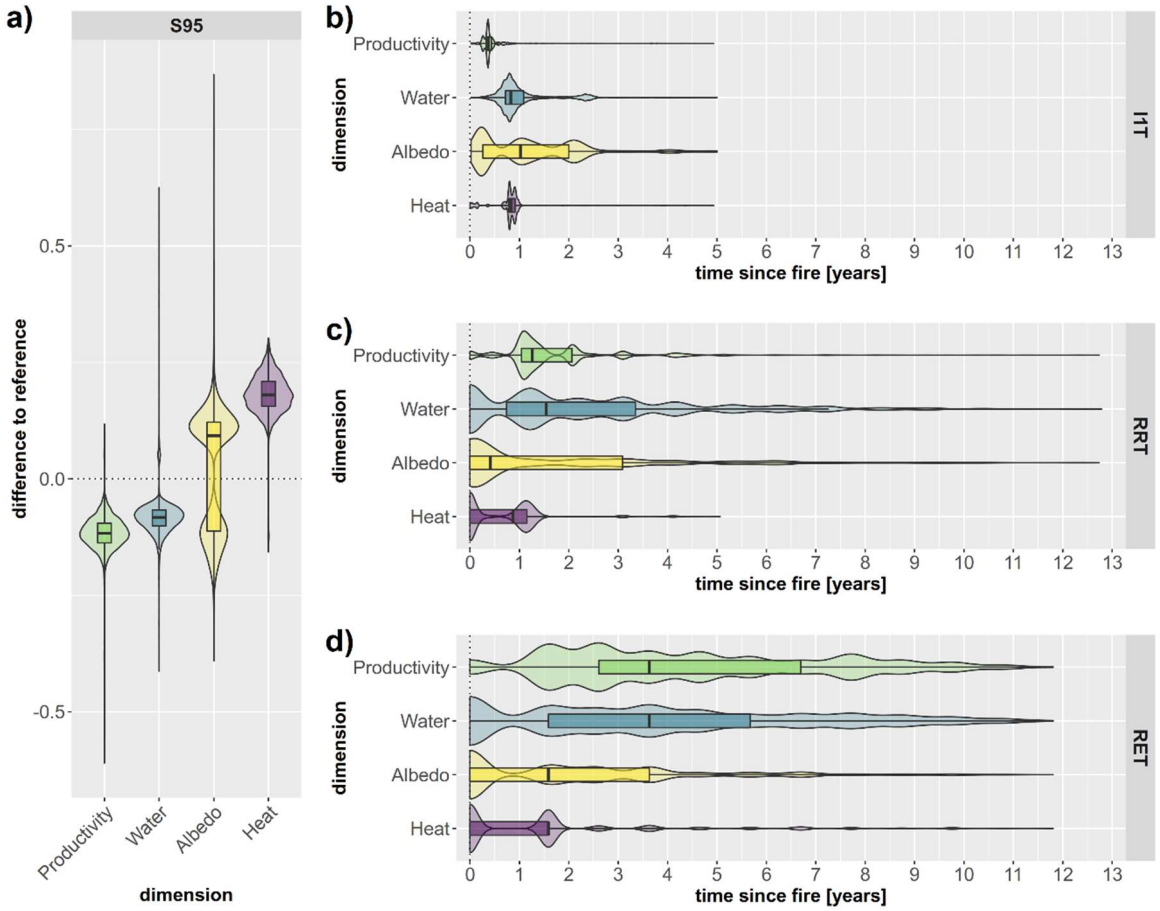

Figure 4.5. Distributions of the four MODIS-derived indicators extracted from post-fire trajectories, represented in combined box-violin plots, for all areas burned in 2005 (identified by the MODIS burned area product), in NW Iberian Peninsula, for each of the four dimensions of ecosystem functioning (i.e., primary productivity, vegetation water content, albedo, and sensible heat). (a) the S95 *fire severity/resistance* indicator, obtained as the difference between the pre-fire median and the 95% percentile of the seasonally adjusted time-series values within the first moving window immediately after a fire (note that the values for the *Heat* dimension presented are scaled by a factor of 0.01, for visual comparability purposes); (b) the *Time to Inflection* (I1T) indicator of *short-term recovery speed*, obtained as the duration of the period between the date of the fire event and the date of the first inflection in the trend component; (c) the *Time to Return-to-Reference* (RRT) indicator of *medium-to-long-term recovery and resilience*, obtained as the duration of the period between the date of the fire event and the date when the values of the trend component achieve the pre-fire reference interval; and (d) the *Time to Return-to-Equilibrium* (RET) indicator of *long-term recovery and resilience*, obtained as the duration of the period between the date of the fire event and the date when the trend component achieves equilibrium or a stable state.

Pairwise correlations

The Spearman rank correlations between each pair of 16 indicators analyzed are presented in **Table 4.2**. The correlations obtained were overall low to moderate (i.e., $|\rho| \leq 0.50$), except for six pairs of indicators. Three of those moderate to high correlations were obtained between RRT and RET, for *Heat* ($\rho = 0.84$), *Albedo* ($\rho = 0.72$), and *Water* ($\rho = 0.57$), with 100% of the pairwise observations with valid values (i.e., n = 13,751; see *Supplementary material—Table S4.1*). The remaining three correlation values above $|\rho| = 0.50$ were obtained between S95 and I1T ($\rho = -0.65$), S95 and RRT ($\rho = 0.68$), and I1T and

RRT (ρ = 0.79), all for *Albedo*. In the case of these last three pairs, the respective correlation values were calculated using only 62% of the total number of observations (i.e., n = 8,529; see *Supplementary material—Table S4.1*), since, in some cases, it is not possible to find either the RRp and REp or both) points in the post-fire trajectory. This situation can happen if, e.g., the values of the trend component never cross the pre-fire reference interval and/or never achieve a relative change between consecutive moving windows below the predefined threshold, in the post-fire period. Furthermore, it should also be noted that all the six values that were considered moderately to highly correlated were found for pairs in which both indicators belonged to the same ecosystem functioning dimension.

Table 4.2. Pairwise correlations between the indicators proposed in this study, for complete pairwise observations (maximum n = 13,751). Numbers in bold highlight values of Spearman rank correlation of | ρ | > 0.50.

		Productivity				**Water**				**Albedo**				**Heat**			
		S95	*I1T*	*RRT*	*RET*	*S95*	*I1T*	*RRT*	*RET*	*S95*	*I1T*	*RRT*	*RET*	*S95*	*I1T*	*RRT*	*RET*
Heat	*RET*	0.26	0.15	0.34	0.15	0.28	-0.02	0.26	0.26	-0.00	-0.08	0.17	0.18	0.00	0.05	**0.84**	1.00
	RRT	0.27	0.18	0.46	0.18	0.31	0.06	0.35	0.30	-0.01	-0.06	0.20	0.18	-0.44	0.46	1.00	
	I1T	-0.01	0.18	0.24	0.15	-0.02	0.31	0.11	0.04	0.15	-0.07	-0.08	-0.08	0.04	1.00		
	S95	-0.32	-0.13	-0.29	-0.05	-0.15	0.03	-0.06	-0.09	-0.07	0.10	-0.09	-0.17	1.00			
Albedo	*RET*	0.25	0.03	0.25	0.09	0.25	-0.06	0.28	0.28	-0.16	0.07	**0.72**	1.00				
	RRT	0.16	0.03	0.26	0.10	0.33	-0.08	0.39	0.28	**-0.68**	**0.79**	1.00					
	I1T	-0.25	-0.05	-0.08	-0.01	0.09	-0.05	0.11	0.01	**-0.65**	1.00						
	S95	0.28	0.10	0.11	0.02	-0.28	0.15	-0.19	-0.12	1.00							
Water	*RET*	0.26	0.12	0.33	0.11	0.21	0.06	**0.57**	1.00								
	RRT	0.20	0.11	0.41	0.16	0.29	0.36	1.00									
	I1T	-0.13	0.06	0.15	0.13	-0.10	1.00										
	S95	0.34	0.12	0.32	0.13	1.00											
Productivity	*RET*	0.04	0.05	0.33	1.00												
	RRT	0.29	0.40	1.00													
	I1T	0.15	1.00														
	S95	1.00															

4.3.2. Classifications of post-fire resilience

Main regional-scale patterns

Overall, pixels corresponding to patches that burned in 2005 in NW-IP were mostly classified under the *Return to pre-fire* class, for three of the four dimensions of ecosystem

functioning considered: primary productivity, vegetation water content, and sensible heat (**Figure 4.6**). The percentage of this class was lowest for *Albedo* and highest for *Productivity*. On the other hand, the percentage of the *(not detected)* class for *Albedo* was slightly higher than that of *Return to pre-fire*. Furthermore, the percentage of the *(not detected)* class was lowest for *Productivity* and highest for *Heat*. The percentages of the *Under-recovery* class were higher for *Water* and *Albedo* than for the remaining two dimensions, while for the *Over-recovery* class percentages were higher for *Productivity* and *Albedo*. Finally, *No equilibrium* class percentages were the lowest for all four dimensions of ecosystem functioning, with the highest percentage of this class obtained for *Albedo*. **Figure 4.6** shows the relative frequency of each class in terms of post-fire resilience for each one of the four dimensions considered (see *Supplementary material—Figure S4.1* for illustrative temporal profiles for each of the five classes of post-fire recovery and resilience). Agreement measures between each pair of the four classifications of post-fire recovery and resilience obtained were all below 0.30 (**Table 4.3**), which can be considered low.

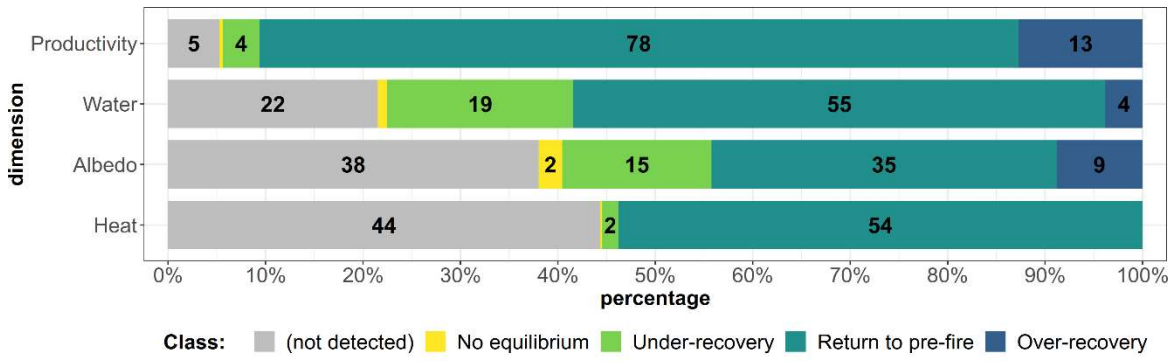

Figure 4.6. Relative frequencies of the obtained classes of long-term post-fire recovery, for each of the four dimensions of ecosystem functioning considered (i.e., primary productivity, vegetation water content, albedo, and sensible heat), across all patches burned in 2005 in NW Iberian Peninsula, using satellite image time-series between 2000 and 2018. Numbers in bold correspond to percentages above 1%.

Table 4.3. Pairwise agreement between the classifications of post-fire recovery and resilience, obtained for each of the four dimensions of ecosystem functioning considered (i.e., primary productivity, vegetation water content, albedo, and sensible heat), across all patches burned in 2005 in NW Iberian Peninsula.

	Productivity		**Water**		**Albedo**		**Heat**	
	BAcc	*MCC*	*BAcc*	*MCC*	*BAcc*	*MCC*	*BAcc*	*MCC*
Heat	0.19	0.06	0.28	0.21	0.29	0.10	–	–
Albedo	0.24	0.09	0.30	0.15	–	–		
Water	0.27	0.12	–	–				
Productivity	–	–						

BAcc: balanced accuracy; MCC: multi-class Matthews correlation coefficient.

Patterns in individual burned areas

Spatial outputs of the classifications into major types of post-fire recovery and resilience, for each of the four dimensions of ecosystem functioning, are shown in **Figure 4.7**, for the six selected burned patches (A–F). In these patches, different local-scale patterns were observed, for specific dimensions, across the six burned patches, which were in line with the results from the regional-scale class compositions, for each of the four dimensions. For instance, areas classified as *Return to pre-fire* were dominant, especially for *Productivity* and *Heat*, across dimensions. Furthermore, most areas classified as *(not detected)* were located in areas either near or adjacent to the periphery of the burned patches, especially for the *Heat* dimension. Within individual burned patches, we also found examples of specific areas for which the class *Under-recovery* for *Water* coincided with the class *Over-recovery* for *Albedo* (e.g., burned patch F), while in other cases, the classification obtained converged between those two dimensions (e.g., burned patch B).

Figure 4.8 illustrates the spatialized results of the synthetic measure of the overall *Strength-of-Evidence* (SoE) of regime shifts, across the four dimensions of ecosystem functioning, for each of the six selected burned patches. Maps such as these maps allow to visually identify (in darker colors) which areas were more likely to have experienced a regime shift, based on higher percentages of key aspects of ecosystem functioning with a post-fire trajectory type that point to such changes (i.e., either the *Under-recovery* or the *Over-recovery* classes).

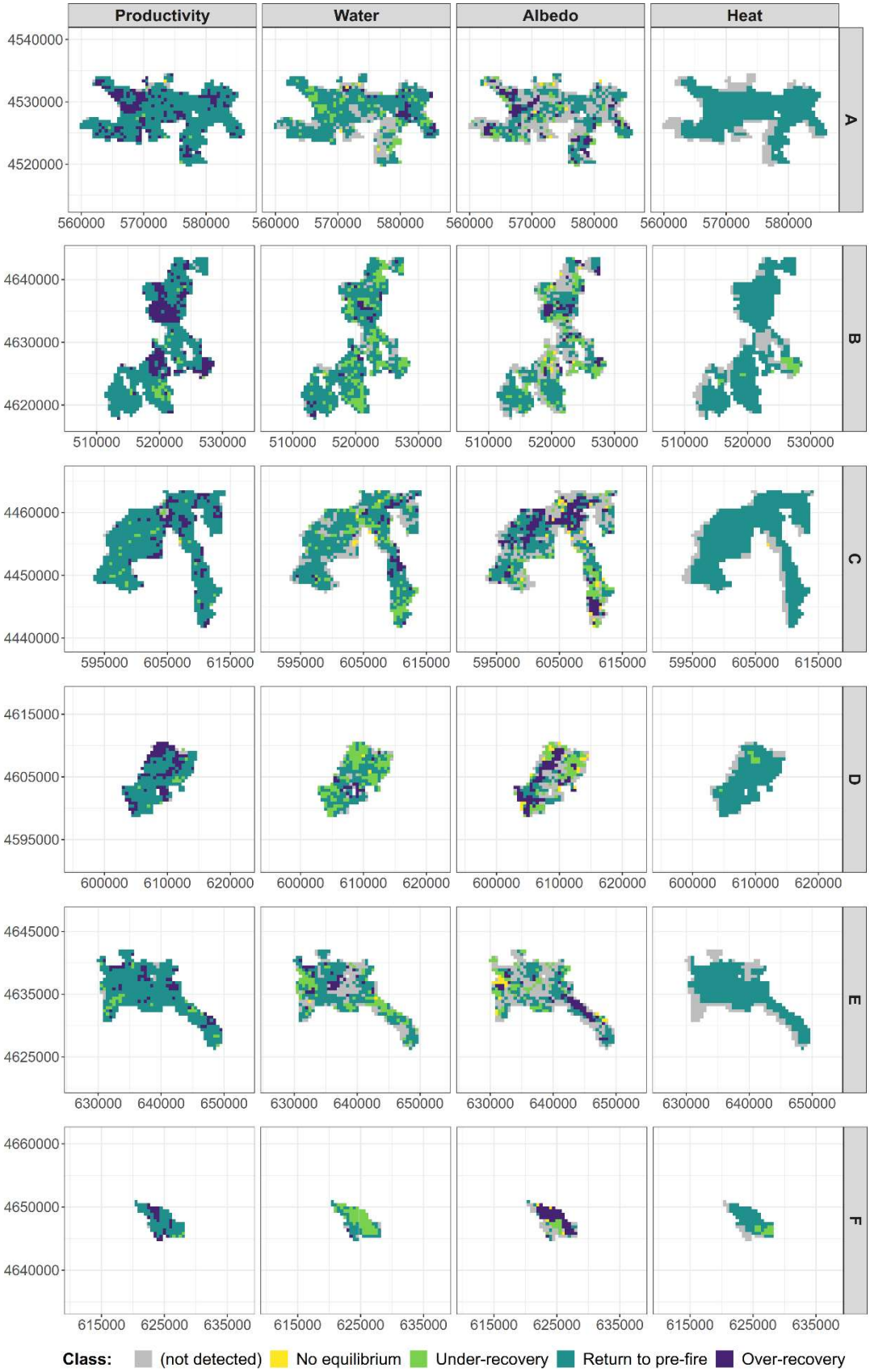

Figure 4.7. Maps of post-fire recovery and resilience classifications, for each of the four dimensions of ecosystem functioning – i.e., primary productivity (*Productivity*), vegetation water content (*Water*), *Albedo*, and sensible heat (*Heat*) – considered for the six selected individual burned areas (A–F).

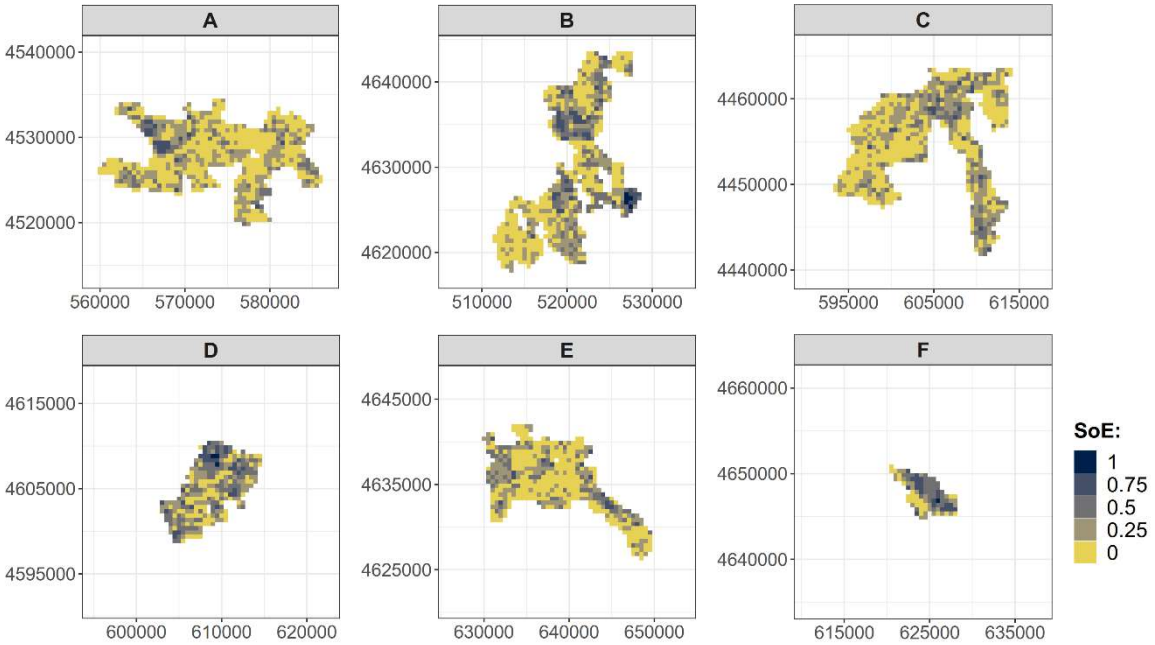

Figure 4.8. Maps of the *Strength-of-Evidence* (SoE) of regime shifts, across the four dimensions of ecosystem functioning considered (i.e., primary productivity, vegetation water content, albedo, and sensible heat), for the six selected individual burned areas (A–F).

4.4. Discussion

4.4.1. Patterns of resilience to wildfire disturbances in NW Iberian Peninsula

Primary productivity

The abrupt breaks that can be observed in the temporal profiles of vegetation indices such as TCTG (e.g., García-Llamas *et al.*, 2019; Sander Veraverbeke *et al.*, 2011), as well as the distribution of values of S95 extracted for NW-IP, suggest that the sudden removal of green vegetation is a major source of short-term variation induced by wildfire disturbances in primary productivity. Leaf shutdown, and consequent death and shedding, within the canopy, leads to a short-term cessation of ecosystem carbon uptake (Beringer *et al.* 2003), and hence to substantial losses in primary productivity and biomass (Leys *et al.* 2016, Pellegrini *et al.* 2018, Sparks *et al.* 2018).

Post-fire recovery of the vegetation in our study area usually started in the first six months after the fire, as suggested by the distribution of the I1T indicator extracted from TCTG. In previous work (João *et al.* 2018), early post-fire responses were found to be highly dependent on both suitable abiotic conditions such as post-fire climate (e.g., precipitation, temperature), as well as biotic factors such as vegetation composition (Prior and Bowman 2020). In turn, post-fire vegetation composition is mediated by fire characteristics of the fire regime, such as frequency and severity (Díaz-Delgado *et al.* 2002, Tiribelli *et al.* 2018). For instance, higher severity and drier conditions have been associated with a higher abundance of seeders, whereas lower severity and wetter conditions have been associated with a higher abundance of resprouters (Day *et al.* 2020), although this may either be region-specific and/or dependent on the abundance and distribution of forest species and other factors. On the other hand, drier post-fire conditions can more negatively affect seeders than resprouters (Parra and Moreno 2018), whereas overall regeneration rates seem to increase when seeders are more abundant in the pre-fire community (Arnan *et al.* 2007). Spatial heterogeneity in fire severity also plays an important role in the early post-fire recovery, since less severely burned or unburned patches (or *islands*) within fire perimeters – such as the ones found in the classification maps (Figure 8) –, can provide ecological refugia, as well as sources for seed recruitment (Kolden *et al.* 2012, Meddens *et al.* 2018).

Overall, post-fire trajectories of primary productivity in NW-IP typically followed a pattern of relatively steep recovery, usually reaching the pre-fire reference interval in the first two years after the fire, with the response speed gradually decreasing into eventual stabilization in the subsequent years, as shown by temporal profiles of TCTG. Together with

the distributions obtained for the RRT and RET indicators extracted from TCTG, this translates into a return to pre-fire levels of primary productivity in most of the cases, which is in line with what was found in other studies (Gouveia *et al.* 2010, Bastos *et al.* 2011, João *et al.* 2018). However, in some cases, high-severity fires can cause increased depletion of the recovery capacity of the vegetation (Díaz-Delgado *et al.* 2002, van Leeuwen *et al.* 2010), leading to regime shifts, whereas rapid recovery often follows low-severity fires, and the highest post-fire recovery rates fires usually correspond to intermediate severity (Meng *et al.* 2018). Therefore, fire severity can have a drastic influence on post-fire recovery in the medium-to-long term, shaping the trajectory of post-fire recovery through vegetation composition (Tiribelli *et al.* 2018, Day *et al.* 2020). Regime shifts to less productive vegetation than in the pre-fire period – classified as *Under-recovery* – can include land-cover conversions such as forest to shrubland, which has been previously reported in our study area, particularly when land abandonment followed the wildfire events (Silva *et al.* 2011). Similar transitions were also observed in other ecosystems, in which increased fire activity has led to new alternative stable states with lower tree density, thus lowering overall primary productivity (e.g., Dwomoh and Wimberly, 2017).

On the other hand, regime shifts to post-fire vegetation that is more productive than in the pre-fire period – classified as *Over-recovery* – can also occur. For instance, as a typical seeder, maritime pine (*Pinus pinaster*) can successfully colonize recently burned areas, leading to fire-driven transitions to conifer forests (Fernandes and Rigolot 2007). Indeed, seeders such as coniferous species may have slower short-time recoveries, but steeper medium-to-long-term recovery times than resprouting species such as broadleaf and scrubland species (Bastos *et al.* 2011, João *et al.* 2018). Notwithstanding, transitions of shrublands to broadleaf forests have also been previously recorded, even if primarily to planted forests of species such as eucalypts (e.g., Silva *et al.*, 2011). Moreover, the effect of species traits and interannual variations in climate tend to be averaged out, eventually reducing the differences between vegetation types in the long term (Johnstone *et al.* 2010). However, in some cases, this kind of transition may also correspond to the replacement of native species or species of economic interest by exotic species with invasive behavior (Nunes *et al.* 2020), – e.g., species of the genus *Acacia*, which can be highly resilient to fire and other disturbances (Lorenzo *et al.* 2010, Silva *et al.* 2011, Hernández *et al.* 2014). Nonetheless, fire can also play a beneficial role in some ecosystems by decreasing the amount of fuel (in the case of low severity fires), creating discontinuities and decreasing the probability of occurrence of *megafires*, or by inducing the regeneration of several species and the replacement of older and drier plants by more productive saplings, thus potentially

leading to increased primary productivity in the post-fire period (Oliveira *et al.* 2012, Semeraro *et al.* 2019).

Vegetation water content

Overall, the negative impacts of the 2005 wildfires in NW-IP on vegetation water content, as observed in the distribution of the S95 indicator extracted from TCT wetness (TCTW), seems to have captured changes in both foliar moisture, leading to leaf shut down due to fire damage (Beringer *et al.* 2003, Senf and Seidl 2020), as well as in vegetation structure (Hansen *et al.* 2001, Nguyen *et al.* 2018). Additionally, TCTW is also sensitive to change in hydrological dynamics, since increased quantities of impervious materials such as ashes, char, and soot can clog soil pores (Ramanathan and Carmichael 2008, Bodí *et al.* 2014), leading to decreased water retention capacity. Both the effects of increased water repellency in soils and the loss of moisture in canopy foliage due to fire-related damage can persist for up to one year after the fire, leading to increases in post-fire runoff and erosion rates (MacDonald and Huffman 2004, Hubbert *et al.* 2012), and vegetation mortality (Lobser and Cohen 2007, Senf and Seidl 2020, Viana-Soto *et al.* 2020). These effects can explain the continued decrease in the temporal profiles of TCTW after a fire, with associated temporal delays between the values of the I1T indicator extracted from TCTW, relative to the ones extracted from TCT greenness (TCTG), as was reported in previous work (Marcos *et al.* 2021).

In the medium-to-long term, TCTW is expected to rise with post-fire regeneration of the vegetation, and the associated increase in canopy structural complexity (Nguyen *et al.* 2018), as well as the decrease of the concentrations of impervious materials in the soil. Temporal profiles of TCTW in NW-IP showed a slower and more gradual post-fire recovery of vegetation water content, compared to that of primary productivity, since values of RRT were generally higher for TCTW than for TCTG, whereas values of RET were slightly lower for TCTW than for TCTG. While this is in line with some studies (e.g., Viana-Soto *et al.*, 2020), the opposite relationship has also been observed in other studies using different spectral indices (e.g., Ryu *et al.*, 2018). This gradual recovery may explain the moderate pairwise correlation found between the RRT and RET indicators extracted from TCTW. Furthermore, TCTW was more frequently classified as *Under-recovery* than TCTG, in our study area, as illustrated in the classification maps for the six individual burned patches. This result points to a decreased ability of vegetation and soils to retain moisture after the fire, even for similar levels between pre- and post-fire primary productivity, leading to increased fuel flammability, and hence to increased fire risk (Pausas and Paula 2012). The

resilience capacity of vegetation water content to wildfire disturbances may thus have been even more depleted than that of primary productivity, especially when accompanied by drought conditions in the post-fire period (Liu *et al.* 2021).

Albedo

Temporal profiles of TCT brightness (TCTB), as well as the distribution of the S95 indicator extracted from this spectral index, showed a duality in the effects of wildfire disturbances on albedo, which mainly link to a directionality shift in the post-fire trajectories of this dimension of ecosystem functioning (Ramanathan and Carmichael 2008, Quintano *et al.* 2019, Marcos *et al.* 2021). This is mostly due to post-fire changes in the relative abundance of surfaces with distinct reflective properties, such as green vegetation, bare soil, as well as ash, char, and soot (Lentile *et al.* 2006). Immediately after the fire, TCTB tends to decrease, leading to a darkening effect due to increased concentration of black carbon in soot and char, which absorbs visible solar radiation (Ramanathan and Carmichael 2008). This effect tends to dissipate before the regeneration of vegetation, leading to a temporary brightening effect one to two years after fire (Quintano *et al.* 2019, Saha *et al.* 2019). Together with the multi-modality of the distribution of I1T extracted from TCTB, our results suggest that either darkening or brightening effects – but not both – were captured in each post-fire trajectory's inflection point (i.e., I1p). This could also justify both the moderate correlation between the values of S95 and I1T extracted from TCTB, as well as that inflection points were found for only approximately 62% of the corresponding post-fire trajectories.

The directionality shifts frequently observed in albedo were also reflected in the medium-to-long-term, as shown by the distribution of values of RRT extracted from TCTB. More specifically, when the inflection point captured the post-fire darkening effect, RRT measured the speed with which TCTB crossed the pre-fire reference interval, corresponding to decreasing concentrations of char and soot, before eventually approaching brightening. On the other hand, with inflection points that captured only the brightening effect, RRT instead measured the speed with which albedo finally transitioned from values above the pre-fire reference interval to pre-fire values, suggesting a corresponding regeneration of vegetation. However, these darkening or brightening effects can sometimes persist for many years after the fire, as suggested by the distribution of the RET indicator and the post-fire trajectories from TCTB classified as either *Under-recovery* or *Over-recovery*. This translates to a potential depletion of the resilience capacity of ecosystems, as reported in other studies (e.g., Gatebe *et al.*, 2014; Saha *et al.*, 2017). Overall, albedo seems to have regime-shifted more often than the other three dimensions of ecosystem functioning, in

response to the 2005 wildfires in NW-IP. Nonetheless, changes in albedo tend to dominate the surface radiative budget in the medium-to-long term (Liu *et al.* 2019). These have even been suggested as potential surrogate retrospective measures of fire intensity (Smith *et al.* 2007), which may explain the moderate-to-high pairwise correlations obtained between the values of RRT and those of S95, I1T, and RET, extracted from TCTB.

Sensible heat

Increases in LST immediately following the fire such as the ones shown by both the temporal profiles and the distribution of the S95 indicator are in line with other studies (e.g., Marcos *et al.*, 2021; Quintano *et al.*, 2015; Zheng *et al.*, 2016). This effect is usually a direct consequence of removing vegetation, which leads to an increased ratio of sensible to latent heat (Vlassova *et al.* 2014) due to a reduction in evapotranspiration (Beringer *et al.* 2003, Liu, Ballantyne, *et al.* 2018). However, this effect tends to be of short duration and start dissipating one year after fire (Liu *et al.* 2019), as shown by the distribution of the I1T indicator extracted from LST for our study area. Furthermore, LST tends to recover to pre-fire levels after one to two years following the fire (Veraverbeke, Verstraeten, *et al.* 2012), as translated by the distributions of both the RRT and RET indicators. The effects of wildfire disturbances on sensible heat are thus more transient than for other dimensions of ecosystem functioning, as reported in other studies (Quintano *et al.* 2015, Marcos *et al.* 2018), which may explain the high similarity correlation obtained between the RRT and RET indicators extracted from LST. In the medium-to-long term, the surface radiative budget tends to be dominated by albedo changes (Liu *et al.* 2019). Based on both the classification outcomes and visual inspection of post-fire trajectories, LST in NW-IP mostly returned to pre-fire levels or had inflection points inside the pre-fire reference interval, with low instances corresponding to potential regime shifts. This suggests overall high resilience of sensible heat to the 2005 wildfires, frequently associated with low severity, particularly in areas located near the boundaries of the burned patches, as illustrated by the maps for the six individual burned areas.

General patterns across dimensions

The four indicators extracted from post-fire trajectories obtained from SITS proposed in this study allowed us to describe the main response patterns of the four dimensions of ecosystem functioning – primary productivity, vegetation water content, albedo, and sensible heat – to the 2005 wildfires in NW-IP. Short-term effects and responses related to fire severity and resistance, as well as to early post-fire recovery, respectively, were characterized using the S95 and I1T indicators, whereas medium-to-long-term post-fire

recovery, either to pre-fire conditions or to equilibrium, were characterized through the RRT and RET indicators. Although some degree of correlation between these four indicators was expected, since they aim to capture different aspects of the same post-fire trajectories, correlations found were mainly low to moderate. This result suggests a higher degree of complementarity than redundancy between these four indicators, highlighting the importance of considering different timeframes for characterizing the main patterns of resistance and recovery from wildfire disturbances on multiple dimensions of ecosystem functioning. Moreover, correlations were low when comparing indicators extracted from different dimensions of ecosystem functioning, which further highlights the added value of using information from multiple dimensions of ecosystem functioning for characterizing post-fire resilience to wildfire disturbances.

Based on our results, most of the areas burned in 2005 in NW-IP seem to have either not been significantly impacted by the wildfires, as partially translated by the *(not detected)* classes – especially in the case of sensible heat –, or returned to pre-fire conditions (i.e., within the pre-fire reference interval) between 2005 and 2018, as translated by the *Return to pre-fire* class (especially for primary productivity). On the other hand, considerable portions of the analyzed burned areas seem to have regime shifted to new stable states, corresponding to either the *Under-recovery* or the *Over-recovery* classes, and translating into changes in ecosystem functioning between pre- and post-fire conditions.

Furthermore, a small portion of the post-fire trajectories in NW-IP, across the four dimensions of ecosystem functioning analyzed, translated incomplete recovery processes, in the sense that no stable state was reached until the end of the period considered in the time-series, which could be re-evaluated once longer time-series are available for the target area. These outcomes, mainly classified as *No equilibrium* if the pre-fire reference interval was crossed after the fire, or as *(not detected)* if otherwise, may have been affected, in some cases, by at least one of two factors: (i) additional wildfire disturbances further in the time-series may have prevented the successful detection of the REp points; and (ii) seasonal effects may still be present in the time-series due to sub-optimal seasonal adjustment since seasonal oscillation patterns can change between the pre- and post-fire periods. Additionally, it cannot be excluded that some of these post-fire trajectories may be exhibiting early-warning signals of imminent regime shifts or even ecosystem collapse, such as *flickering* (i.e., increased variance), which has previously been related to potential critical transitions (Dakos *et al.* 2012). It is also important to note that post-fire trajectories corresponding to those classified as *No equilibrium*, unlike those classified as *(not detected)*, would have been misinterpreted as false recovery under an approach solely based on *engineering resilience*.

The overall low levels of agreement between the classifications obtained from each of the four dimensions of ecosystem functioning suggest low inter-dimensional redundancy, which further showcases the importance of multi-dimensional approaches. However, it is important to note that considerable differences can be observed between individual burned patches, as illustrated by our six examples. This points to the importance of analyzing and mapping patch-specific patterns of ecosystem resilience (including both resistance and recovery aspects) to wildfire disturbances, allowing for the identification and location of, e.g., either *hotspots* of potential regime shifts or *unburned islands*. Together, our results showcase the added value of the proposed approach to characterize the effects and responses of different dimensions of ecosystem functioning to wildfire disturbances, as well as to identify and map potential regime shifts due to those disturbances.

4.4.2. General considerations about the proposed framework

Applicability

Although we targeted a specific study area to showcase our approach, the proposed framework should be sufficiently generic to be applied over diverse geographic and environmental contexts. Moreover, SITS from other platforms can be used in alternative to MODIS, with different spatial, temporal, and spectral resolutions, such as Sentinel, Landsat, and PROBA-V. To that end, image archives should be long enough to establish a pre-fire reference period and evaluate post-fire trajectories in the short, medium, and long terms, which will vary according to factors such as fire regimes, vegetation types, and climate. Furthermore, we argue that SITS of LST and the TCT features of *Brightness*, *Greenness*, and *Wetness* constitute an efficient and transferable option to provide information about the four dimensions of ecosystem functioning analyzed – i.e., sensible heat, albedo, primary productivity, and vegetation water content, respectively –, since these can be computed from a wide range of satellite sensors (e.g., Shi and Xu, 2019). Nonetheless, alternative remotely sensed variables and spectral indices to the ones used in this study, such as the Normalized Difference Vegetation Index (NDVI), the Normalized Difference Water Index (NDWI), and the Normalized Burned Ratio (NBR), could also be used instead.

The proposed framework is highly dependent on the extraction of indicators from post-fire trajectories with prior seasonal adjustment through time-series decomposition techniques. This *deseasonalization* is commonly used (e.g., Sever *et al.*, 2012) to remove seasonal oscillations in the time-series that could potentially be misinterpreted as changes in its overall variation. Consequently, this makes our approach not suitable to address changes in timing or cyclic patterns (e.g., phenology), as this is not its focus. However,

although there are other approaches more suitable for those particular ends, some degree of trade-off seems to usually exist between the ability to assess both cyclic and non-cyclic changes in time-series. Moreover, different time-series decomposition could be used, besides STL, to account for seasonal effects, such as multiplicative approaches, or other additive decomposition methods with a linear, instead of non-linear, trend component. Break-point detection techniques such as BFAST (Verbesselt, Hyndman, Newnham, *et al.* 2010, Verbesselt, Hyndman, Zeileis, *et al.* 2010) can also be valuable for supporting the characterization of overall patterns and trends. However, these methods target generic change detection through time-series segmentation, rather than specifically characterizing aspects of post-fire trajectories extracted from multiple SITS with diverse features.

Future improvements

Based on the results obtained for the presented test case, some minor modifications could be introduced to the proposed framework to enhance its ability to support the characterization of post-fire trajectories. For instance, time-series decomposition procedures could be optimized by automatizing the selection of its parameter values. Furthermore, analysis of post-fire trajectories of albedo through spectral indices such as TCTB could be improved by extracting two separate sets of indicators, each using a different set of time-series decomposition parameters. This procedure would allow tackling both inflection points corresponding to darkening and brightening effects known to frequently characterize post-fire trajectories (Ramanathan and Carmichael 2008, Quintano *et al.* 2019, Marcos *et al.* 2021).

Moreover, additional indicators could be extracted from post-fire trajectories for even more detailed descriptions of post-fire processes. For example, the value of the trend component at the inflection point could be used as a complementary indicator of fire severity that is more conservative than the S95 indicator, since the former is based on the direct value of the overall variation component of the time-series, whereas the latter aims to estimate a value that is closer to the maximum impact of the wildfire disturbance immediately after a fire. Furthermore, these and other indicators extracted from post-fire trajectories could be used to derive more intricate classifications to support more detailed and thorough evaluations of the resilience of ecosystem functioning to wildfire disturbances, as well as to identify additional potential regime shifts. In this regard, the potential of indicators such as I2T, RRT, and RET as early-warning signals of regime shifts, or even imminent ecosystem collapse, should be further explored, since critical slowing down implies that post-fire recovery may become slower as a system approaches a tipping point (Scheffer *et al.* 2015, Verbesselt *et al.* 2016).

On the other hand, regional resilience should be evaluated by analyzing several disturbances in both time and space, since alternative states can be characterized in probabilistic terms based on large numbers of observations (Scheffer *et al.* 2015). This should be complemented, when possible, with well-designed field-based measurements such as in-field spectral/radiometric readings, and UAV-based aerial surveys, following robust sampling designs. Although obtaining this kind of data can sometimes present challenges such as high costs and/or access constraints, it would be crucial not only to validate the information provided by the indicators extracted from SITS, but also to collect additional information that is not easily obtainable remotely, such as management and restoration operations, or other human activities that may influence post-fire ecosystem processes.

Finally, other studies also addressed the characterization and classification of post-fire trajectories using indicators of magnitude, duration, and timing extracted from SITS (e.g., Viana-Soto *et al.*, 2020), although not analyzing multiple dimensions of ecosystem functioning. To provide insights on different aspects of the post-fire processes over multiple dimensions of ecosystem functioning, complementary approaches to the framework proposed here could be used (e.g., Marcos *et al.*, 2021). Indeed, our approach could also be adapted to support the parametrization of different environmental models (e.g., Carvalho-Santos *et al.*, 2019).

4.5. Conclusions

In this study, we described a framework for characterizing and classifying ecosystem resilience to wildfire disturbances, using indicators of resistance and recovery extracted from post-fire trajectories of satellite image time-series related to four key aspects of ecosystem functioning: primary productivity, vegetation water content, albedo, and sensible heat. Since our approach is explicitly compatible with both situations of return to pre-fire conditions, as well as alternative stable states, potential regime shifts can be identified for more in-depth and detailed studies.

To showcase our proposed framework, we used MODIS data for the period between 2000 and 2018, to characterize and classify ecosystem resilience to wildfires that occurred in 2005 in NW Iberian Peninsula. Our results allowed us to analyze the main patterns of both the effects of, as well as the responses to wildfire disturbances, across the four dimensions of ecosystem functioning considered. Moreover, we were able to identify potential regime shifts, which can be patent in some specific dimensions of ecosystem functioning, but not others. Differences between individual burned areas were illustrated for six burned patches within the study area, highlighting the potential of the proposed approach for regional-scale analysis, which could be used for spatially explicit prioritization, and lead to more detailed local-scale assessments to investigate specific patterns.

Overall, our results suggest that the indicators proposed successfully depict key features of the post-fire processes in ecosystem functioning, at different timeframes, with a high degree of complementarity between those indicators, and especially between the different dimensions of ecosystem functioning, which shows the added value of a multi-dimensional approach to analyze ecosystem resilience to wildfire disturbances. We argue that such frameworks can provide enhanced characterization and classification of the resilience of ecosystems to those disturbances, ultimately upholding potential implications for post-fire ecosystem management.

References

Adámek, M., Hadincová, V., and Wild, J., 2016. Long-term effect of wildfires on temperate Pinus sylvestris forests: Vegetation dynamics and ecosystem resilience. *Forest Ecology and Management*, 380, 285–295. DOI: 10.1016/j.foreco.2016.08.051.

Alcaraz-Segura, D., Cabello, J., Paruelo, J.M., and Delibes, M., 2008. Trends in the surface vegetation dynamics of the national parks of Spain as observed by satellite sensors. *Applied Vegetation Science*, 11 (4), 431–440. DOI: 10.3170/2008-7-18522.

Andersen, T., Carstensen, J., Hernández-García, E., and Duarte, C.M., 2009. Ecological thresholds and regime shifts: approaches to identification. *Trends in Ecology and Evolution*, 24 (1), 49–57. DOI: 10.1016/j.tree.2008.07.014.

Arnan, X., Rodrigo, A., and Retana, J., 2007. Post-fire regeneration of Mediterranean plant communities at a regional scale is dependent on vegetation type and dryness. *Journal of Vegetation Science*, 18 (1), 111–122. DOI: 10.1111/j.1654-1103.2007.tb02521.x.

Baho, D.L., Allen, C.R., Garmestani, A., Fried-Petersen, H., Renes, S.E., Gunderson, L., and Angeler, D.G., 2017. A quantitative framework for assessing ecological resilience. *Ecology and Society*, 22 (3), 1. DOI: 10.5751/ES-09427-220317.

Bastos, A., Gouveia, C.M., DaCamara, C.C., and Trigo, R.M., 2011. Modelling post-fire vegetation recovery in Portugal. *Biogeosciences*, 8 (12), 3593–3607. DOI: 10.5194/bg-8-3593-2011.

Beringer, J., Hutley, L.B., Tapper, N.J., Coutts, A., Kerley, A., and O'Grady, A.P., 2003. Fire impacts on surface heat, moisture and carbon fluxes from a tropical savanna in northern Australia. *International Journal of Wildland Fire*, 12 (3–4), 333–340. DOI: 10.1071/wf03023.

Bisson, M., Fornaciai, A., Coli, A., Mazzarini, F., and Pareschi, M.T., 2008. The Vegetation Resilience After Fire (VRAF) index: Development, implementation and an illustration from central Italy. *International Journal of Applied Earth Observation and Geoinformation*, 10 (3), 312–329. DOI: 10.1016/j.jag.2007.12.003.

Bodí, M.B., Martin, D.A., Balfour, V.N., Santín, C., Doerr, S.H., Pereira, P., Cerdà, A., and Mataix-Solera, J., 2014. Wildland fire ash: Production, composition and eco-hydro-geomorphic effects. *Earth-Science Reviews*, 130, 103–127. DOI: 10.1016/j.earscirev.2013.12.007.

Boettiger, C., Ross, N., and Hastings, A., 2013. Early warning signals: The charted and uncharted territories. *Theoretical Ecology*, 6, 255–264. DOI: 10.1007/s12080-013-0192-6.

Bowman, D.M.J.S., Balch, J.K., Artaxo, P., Bond, W.J., Carlson, J.M., Cochrane, M.A., D'Antonio, C.M., DeFries, R.S., Doyle, J.C., Harrison, S.P., Johnston, F.H., Keeley, J.E., Krawchuk, M.A., Kull, C.A., Marston, J.B., Moritz, M.A., Prentice, I.C., Roos, C.I., Scott, A.C., Swetnam, T.W., van der Werf, G.R., and Pyne, S.J., 2009. Fire in the Earth System. *Science*, 324 (5926), 481–484. DOI: 10.1126/science.1163886.

Bowman, D.M.J.S., Perry, G.L.W., and Marston, J.B., 2015. Feedbacks and landscape-level vegetation dynamics. *Trends in Ecology & Evolution*, 30 (5), 255–260. DOI: 10.1016/j.tree.2015.03.005.

Brodersen, K.H., Ong, C.S., Stephan, K.E., and Buhmann, J.M., 2010. The balanced accuracy and its posterior distribution. *In*: *Proceedings - International Conference on Pattern Recognition*. 3121–3124. DOI: 10.1109/ICPR.2010.764.

Busetto, L. and Ranghetti, L., 2016. MODIStsp: An R package for automatic preprocessing of MODIS Land Products time series. *Computers and Geosciences*, 97, 40–48. DOI: 10.1016/j.cageo.2016.08.020.

Caccamo, G., Bradstock, R., Collins, L., Penman, T., and Watson, P., 2015. Using MODIS data to analyse post-fire vegetation recovery in Australian eucalypt forests. *Journal of Spatial Science*, 60 (2), 341–352. DOI: 10.1080/14498596.2015.974227.

Carvalho-Santos, C., Marcos, B., Nunes, J., Regos, A., Palazzi, E., Terzago, S., Monteiro, A., and Honrado, J., 2019. Hydrological Impacts of Large Fires and Future Climate: Modeling Approach Supported by Satellite Data. *Remote Sensing*, 11 (23), 2832. DOI: 10.3390/rs11232832.

Catry, F.X.F., Rego, F.C.F.F.C., Bação, F.L., Moreira, F., 2009. Modeling and mapping wildfire ignition risk in Portugal. *International Journal of Wildland Fire*, 18 (8), 921. DOI: 10.1071/WF07123.

Chicco, D. and Jurman, G., 2020. The advantages of the Matthews correlation coefficient (MCC) over F1 score and accuracy in binary classification evaluation. *BMC Genomics*, 21 (1), 6. DOI: 10.1186/s12864-019-6413-7.

Chuvieco, E., Mouillot, F., van der Werf, G.R., San Miguel, J., Tanase, M., Koutsias, N., García, M., Yebra, M., Padilla, M., Gitas, I., Heil, A., Hawbaker, T.J., and Giglio, L., 2019. Historical background and current developments for mapping burned area from

satellite Earth observation. *Remote Sensing of Environment*, 225, 45–64. DOI: 10.1016/j.rse.2019.02.013.

Cleveland, R.B., Cleveland, W.S., McRae, J.E., and Terpenning, I., 1990. STL: A seasonal-trend decomposition procedure based on loess. *Journal of Official Statistics*, 6 (1), 3–73. DOI: citeulike-article-id:1435502.

Coops, N.C., Wulder, M.A., Duro, D.C., Han, T., and Berry, S., 2008. The development of a Canadian dynamic habitat index using multi-temporal satellite estimates of canopy light absorbance. *Ecological Indicators*, 8 (5), 754–766. DOI: 10.1016/j.ecolind.2008.01.007.

Cui, X., Gibbes, C., Southworth, J., and Waylen, P., 2013. Using Remote Sensing to Quantify Vegetation Change and Ecological Resilience in a Semi-Arid System. *Land*, 2 (2), 108–130. DOI: 10.3390/land2020108.

Dakos, V., Carpenter, S.R., Brock, W.A., Ellison, A.M., Guttal, V., Ives, A.R., Kéfi, S., Livina, V., Seekell, D.A., van Nes, E.H., and Scheffer, M., 2012. Methods for detecting early warnings of critical transitions in time series illustrated using simulated ecological data. *PLoS ONE*, 7 (7), e41010. DOI: 10.1371/journal.pone.0041010.

Day, N.J., White, A.L., Johnstone, J.F., Degré-Timmons, G.É., Cumming, S.G., Mack, M.C., Turetsky, M.R., Walker, X.J., and Baltzer, J.L., 2020. Fire characteristics and environmental conditions shape plant communities via regeneration strategy. *Ecography*, 43 (10), 1464–1474. DOI: 10.1111/ecog.05211.

Delettre, O., 2021. Identity of Ecological Systems and the Meaning of Resilience. *Journal of Ecology*, 1365-2745.13655. DOI: 10.1111/1365-2745.13655.

Díaz-Delgado, R., Lloret, F., Pons, X., and Terradas, J., 2002. Satellite Evidence of Decreasing Resilience in Mediterranean Plant Communities after Recurrent Wildfires. *Ecology*, 83 (8), 2293–2303. DOI: 10.1890/0012-9658(2002)083[2293:SEODRI]2.0.CO;2.

Donohue, I., Hillebrand, H., Montoya, J.M., Petchey, O.L., Pimm, S.L., Fowler, M.S., Healy, K., Jackson, A.L., Lurgi, M., McClean, D., O'Connor, N.E., O'Gorman, E.J., and Yang, Q., 2016. Navigating the complexity of ecological stability. *Ecology Letters*, 19 (9), 1172–1185. DOI: 10.1111/ele.12648.

Donohue, I., Petchey, O.L., Montoya, J.M., Jackson, A.L., McNally, L., Viana, M., Healy, K., Lurgi, M., O'Connor, N.E., and Emmerson, M.C., 2013. On the dimensionality of ecological stability. *Ecology Letters*, 16 (4), 421–429. DOI: 10.1111/ele.12086.

Duan, S.-B., Li, Z.-L., Li, H., Göttsche, F.-M., Wu, H., Zhao, W., Leng, P., Zhang, X., and Coll, C., 2019. Validation of Collection 6 MODIS land surface temperature product using in situ measurements. *Remote Sensing of Environment*, 225, 16–29. DOI: 10.1016/j.rse.2019.02.020.

Dwomoh, F.K. and Wimberly, M.C., 2017. Fire regimes and forest resilience: alternative vegetation states in the West African tropics. *Landscape Ecology*, 32 (9), 1849–1865. DOI: 10.1007/s10980-017-0553-4.

Fan, X., Hao, X., Hao, H., Zhang, J., and Li, Y., 2021. Comprehensive Assessment Indicator of Ecosystem Resilience in Central Asia. *Water*, 13 (2), 124. DOI: 10.3390/w13020124.

Fernandes, P.M. and Rigolot, E., 2007. The fire ecology and management of maritime pine (Pinus pinaster Ait.). *Forest Ecology and Management*, 241 (1–3), 1–13. DOI: 10.1016/j.foreco.2007.01.010.

Fernandez-Manso, A., Quintano, C., and Roberts, D.A., 2016. Burn severity influence on post-fire vegetation cover resilience from Landsat MESMA fraction images time series in Mediterranean forest ecosystems. *Remote Sensing of Environment*, 184, 112–123. DOI: 10.1016/j.rse.2016.06.015.

Folke, C., Carpenter, S., Walker, B., Scheffer, M., Elmqvist, T., Gunderson, L., and Holling, C.S., 2004. Regime Shifts, Resilience, and Biodiversity in Ecosystem Management. *Annual Review of Ecology, Evolution, and Systematics*, 35 (1), 557–581. DOI: 10.1146/annurev.ecolsys.35.021103.105711.

Frazier, A.E., Renschler, C.S., and Miles, S.B., 2013. Evaluating post-disaster ecosystem resilience using MODIS GPP data. *International Journal of Applied Earth Observation and Geoinformation*, 21, 43–52. DOI: 10.1016/j.jag.2012.07.019.

French, N.H.F., Whitley, M.A., and Jenkins, L.K., 2016. Fire disturbance effects on land surface albedo in Alaskan tundra. *Journal of Geophysical Research: Biogeosciences*, 121 (3), 841–854. DOI: 10.1002/2015JG003177.

García-Llamas, P., Suárez-Seoane, S., Fernández-Guisuraga, J.M., Fernández-García, V., Fernández-Manso, A., Quintano, C., Taboada, A., Marcos, E., and Calvo, L., 2019. Evaluation and comparison of Landsat 8, Sentinel-2 and Deimos-1 remote sensing indices for assessing burn severity in Mediterranean fire-prone ecosystems. *International Journal of Applied Earth Observation and Geoinformation*, 80, 137–144. DOI: 10.1016/j.jag.2019.04.006.

Gatebe, C.K.K., Ichoku, C.M.M., Poudyal, R., Román, M.O.O., and Wilcox, E., 2014. Surface albedo darkening from wildfires in northern sub-Saharan Africa. *Environmental Research Letters*, 9 (6), 065003. DOI: 10.1088/1748-9326/9/6/065003.

Giglio, L., Boschetti, L., Roy, D.P., Humber, M.L., and Justice, C.O., 2018. The Collection 6 MODIS burned area mapping algorithm and product. *Remote Sensing of Environment*, 217, 72–85. DOI: 10.1016/j.rse.2018.08.005.

Gillies, S., Ward, B., and Petersen, A.S., 2013. Rasterio: geospatial raster I/O for Python programmers version 0.36.0.

Gorman, B., 2018. mltools: Machine Learning Tools, version 0.3.5.

Gouveia, C., DaCamara, C.C., and Trigo, R.M., 2010. Post-fire vegetation recovery in Portugal based on spot/vegetation data. *Natural Hazards and Earth System Science*, 10 (4), 673–684. DOI: 10.5194/nhess-10-673-2010.

Gunderson, L.H., 2000. Ecological Resilience—In Theory and Application. *Annual Review of Ecology and Systematics*, 31 (1), 425–439. DOI: 10.1146/annurev.ecolsys.31.1.425.

Hampel, F.R., 1971. A General Qualitative Definition of Robustness. *The Annals of Mathematical Statistics*, 42 (6), 1887–1896.

Hampel, F.R., 1974. The Influence Curve and its Role in Robust Estimation. *Journal of the American Statistical Association*, 69 (346), 383–393. DOI: 10.1080/01621459.1974.10482962.

Hansen, M.J., Franklin, S.E., Woudsma, C., and Peterson, M., 2001. Forest structure classification in the North Columbia mountains using the Landsat TM Tasseled Cap wetness component. *Canadian Journal of Remote Sensing*, 27 (1), 20–32. DOI: 10.1080/07038992.2001.10854916.

Harris, A., Carr, A.S.S., and Dash, J., 2014. Remote sensing of vegetation cover dynamics and resilience across southern Africa. *International Journal of Applied Earth Observation and Geoinformation*, 28 (1), 131–139. DOI: 10.1016/j.jag.2013.11.014.

Hernández, L., Martínez- Fernández, J., Cañellas, I., and de la Cueva, A.V., 2014. Assessing spatiotemporal rates, patterns and determinants of biological invasions in forest ecosystems. The case of Acacia species in NW Spain. *Forest Ecology and Management*, 329, 206–213. DOI: 10.1016/j.foreco.2014.05.058.

Hijmans, R.J., 2020. raster: Geographic Data Analysis and Modeling. R package version 3.4-5.

Hirota, M., Holmgren, M., Van Nes, E.H., and Scheffer, M., 2011. Global resilience of tropical forest and savanna to critical transitions. *Science (New York, N.Y.)*, 334 (6053), 232–5. DOI: 10.1126/science.1210657.

Hodgson, D., McDonald, J.L., and Hosken, D.J., 2015. What do you mean, 'resilient'? *Trends in Ecology & Evolution*, 30 (9), 503–506. DOI: 10.1016/j.tree.2015.06.010.

Holling, C.S., 1973. Resilience and Stability of Ecological Systems. *Annual Review of Ecology and Systematics*, 4 (1), 1–23. DOI: 10.1146/annurev.es.04.110173.000245.

Holling, C.S., 1996. Engineering Resilience versus Ecological Resilience. *In*: P.E. Schulze, ed. *Engineering within Ecological Constraints*. Washington, D.C.: National Academies Press, 31–43. DOI: 10.17226/4919.

Hope, A., Albers, N., and Bart, R., 2012. Characterizing post-fire recovery of fynbos vegetation in the Western Cape Region of South Africa using MODIS data. *International Journal of Remote Sensing*, 33 (4), 979–999. DOI: 10.1080/01431161.2010.543184.

Hope, A., Tague, C., and Clark, R., 2007. Characterizing post-fire vegetation recovery of California chaparral using TM/ETM+ time-series data. *International Journal of Remote Sensing*, 28 (6), 1339–1354. DOI: 10.1080/01431160600908924.

Hubbert, K.R., Wohlgemuth, P.M., Beyers, J.L., Narog, M.G., and Gerrard, R., 2012. Post-fire soil water repellency, hydrologic response, and sediment yield compared between grass-converted and chaparral watersheds. *Fire Ecology*, 8 (2), 143–162. DOI: 10.4996/fireecology.0802143.

Hyndman, R.J. and Athanasopoulos, G., 2018. *Forecasting: Principles and Practice*. 2nd ed. Melbourne, Australia: OTexts.

Ingrisch, J. and Bahn, M., 2018. Towards a Comparable Quantification of Resilience. *Trends in Ecology & Evolution*, 33 (4), 251–259. DOI: 10.1016/j.tree.2018.01.013.

João, T., João, G., Bruno, M., and João, H., 2018. Indicator-based assessment of post-fire recovery dynamics using satellite NDVI time-series. *Ecological Indicators*, 89, 199–212. DOI: 10.1016/j.ecolind.2018.02.008.

Johnstone, J.F., Chapin, F.S., Hollingsworth, T.N., Mack, M.C., Romanovsky, V., and Turetsky, M., 2010. Fire, climate change, and forest resilience in interior alaska1. *Canadian Journal of Forest Research*, 40 (7), 1302–1312. DOI: 10.1139/X10-061.

Keeley, J.E., 2009. Fire intensity, fire severity and burn severity: a brief review and suggested usage. *International Journal of Wildland Fire*, 18 (1), 116. DOI: 10.1071/WF07049.

De Keersmaecker, W., Lhermitte, S., Tits, L., Honnay, O., Somers, B., and Coppin, P., 2015. A model quantifying global vegetation resistance and resilience to short-term climate anomalies and their relationship with vegetation cover. *Global Ecology and Biogeography*, 24 (5), 539–548. DOI: 10.1111/geb.12279.

Kolden, C.A., Lutz, J.A., Key, C.H., Kane, J.T., and van Wagtendonk, J.W., 2012. Mapped versus actual burned area within wildfire perimeters: Characterizing the unburned. *Forest Ecology and Management*, 286, 38–47. DOI: 10.1016/j.foreco.2012.08.020.

Lang, M., 2021. mlr3measures: Performance Measures for 'mlr3', version 0.3.1.

van Leeuwen, W.J.D., Casady, G.M., Neary, D.G., Bautista, S., Alloza, J.A., Carmel, Y., Wittenberg, L., Malkinson, D., and Orr, B.J., 2010. Monitoring post-wildfire vegetation response with remotely sensed time-series data in Spain, USA and Israel. *International Journal of Wildland Fire*, 19 (1), 75. DOI: 10.1071/WF08078.

Lentile, L.B., Holden, Z.A., Smith, A.M.S.S., Falkowski, M.J., Hudak, A.T., Morgan, P., Lewis, S.A., Gessler, P.E., Benson, N.C., Lentile, L.B., Holden, Z.A., Smith, A.M.S.S., Falkowski, M.J., Hudak, A.T., Morgan, P., Lewis, S.A., Gessler, P.E., and Benson, N.C., 2006. Remote sensing techniques to assess active fire characteristics and post-fire effects. *International Journal of Wildland Fire*, 15 (3), 319. DOI: 10.1071/WF05097.

Leys, B., Higuera, P.E., McLauchlan, K.K., and Dunnette, P. V., 2016. Wildfires and geochemical change in a subalpine forest over the past six millennia. *Environmental Research Letters*, 11 (12), 125003. DOI: 10.1088/1748-9326/11/12/125003.

Liu, F., Liu, H., Xu, C., Shi, L., Zhu, X., Qi, Y., and He, W., 2021. Old-growth forests show low canopy resilience to droughts at the southern edge of the taiga. *Global Change Biology*, 27 (11), 2392–2402. DOI: 10.1111/gcb.15605.

Liu, H., Zhan, Q., Yang, C., and Wang, J., 2018. Characterizing the Spatiotemporal Pattern of Land Surface Temperature through Time Series Clustering: Based on the Latent Pattern and Morphology. *Remote Sensing*, 10 (4), 654. DOI: 10.3390/rs10040654.

Liu, Z., Ballantyne, A.P., and Cooper, L.A., 2018. Increases in Land Surface Temperature in Response to Fire in Siberian Boreal Forests and Their Attribution to Biophysical Processes. *Geophysical Research Letters*, 45 (13), 6485–6494. DOI: 10.1029/2018GL078283.

Liu, Z., Ballantyne, A.P., and Cooper, L.A., 2019. Biophysical feedback of global forest fires on surface temperature. *Nature Communications*, 10 (1), 1–9. DOI: 10.1038/s41467-018-08237-z.

Lobser, S.E. and Cohen, W.B., 2007. MODIS tasselled cap: land cover characteristics expressed through transformed MODIS data. *International Journal of Remote Sensing*, 28 (22), 5079–5101. DOI: 10.1080/01431160701253303.

Lorenzo, P., González, L., and Reigosa, M.J., 2010. The genus Acacia as invader: The characteristic case of Acacia dealbata Link in Europe. *Annals of Forest Science*, 67 (1), 101–101. DOI: 10.1051/forest/2009082.

MacDonald, L.H. and Huffman, E.L., 2004. Post-fire Soil Water Repellency. *Soil Science Society of America Journal*, 68 (5), 1729–1734. DOI: 10.2136/sssaj2004.1729.

Maffei, C., Alfieri, S.M., Menenti, M., 2018. Relating Spatiotemporal Patterns of Forest Fires Burned Area and Duration to Diurnal Land Surface Temperature Anomalies. *Remote Sensing*, 10 (11), 1777. DOI: 10.3390/rs10111777.

Marcos, B., Gonçalves, J., Alcaraz-Segura, D., Cunha, M., and Honrado, J.P., 2019. Improving the detection of wildfire disturbances in space and time based on indicators extracted from MODIS data: a case study in northern Portugal. *International Journal of Applied Earth Observation and Geoinformation*, 78, 77–85. DOI: 10.1016/j.jag.2018.12.003.

Marcos, B., Gonçalves, J., Alcaraz-Segura, D., Cunha, M., and Honrado, J.P., 2021. A Framework for Multi-Dimensional Assessment of Wildfire Disturbance Severity from Remotely Sensed Ecosystem Functioning Attributes. *Remote Sensing*, 13 (4), 780. DOI: 10.3390/rs13040780.

Marcos, E., Fernández-García, V., Fernández-Manso, A., Quintano, C., Valbuena, L., Tárrega, R., Luis-Calabuig, E., and Calvo, L., 2018. Evaluation of Composite Burn Index and Land Surface Temperature for Assessing Soil Burn Severity in Mediterranean Fire-Prone Pine Ecosystems. *Forests*, 9 (8), 494. DOI: 10.3390/f9080494.

Matthews, B.W., 1975. Comparison of the predicted and observed secondary structure of T4 phage lysozyme. *BBA - Protein Structure*, 405 (2), 442–451. DOI: 10.1016/0005-2795(75)90109-9.

Di Mauro, B., Fava, F., Busetto, L., Crosta, G.F., and Colombo, R., 2014. Post-fire resilience in the Alpine region estimated from MODIS satellite multispectral data. *International*

Journal of Applied Earth Observation and Geoinformation, 32 (1), 163–172. DOI: 10.1016/j.jag.2014.04.010.

Meddens, A.J.H., Kolden, C.A., Lutz, J.A., Abatzoglou, J.T., and Hudak, A.T., 2018. Spatiotemporal patterns of unburned areas within fire perimeters in the northwestern United States from 1984 to 2014. *Ecosphere*, 9 (2), e02029. DOI: 10.1002/ecs2.2029.

Meng, J.-N., Fang, H., and Scavia, D., 2021. Application of ecosystem stability and regime shift theories in ecosystem assessment-calculation variable and practical performance. *Ecological Indicators*, 125, 107529. DOI: 10.1016/j.ecolind.2021.107529.

Meng, R., Wu, J., Zhao, F., Cook, B.D., Hanavan, R.P., and Serbin, S.P., 2018. Measuring short-term post-fire forest recovery across a burn severity gradient in a mixed pine-oak forest using multi-sensor remote sensing techniques. *Remote Sensing of Environment*, 210, 282–296. DOI: 10.1016/J.RSE.2018.03.019.

Moreira, F., Ascoli, D., Safford, H., Adams, M.A., Moreno, J.M., Pereira, J.M.C., Catry, F.X., Armesto, J., Bond, W., González, M.E., Curt, T., Koutsias, N., McCaw, L., Price, O., Pausas, J.G., Rigolot, E., Stephens, S., Tavsanoglu, C., Vallejo, V.R., Van Wilgen, B.W., Xanthopoulos, G., and Fernandes, P.M., 2020. Wildfire management in Mediterranean-type regions: paradigm change needed. *Environmental Research Letters*, 15 (1), 011001. DOI: 10.1088/1748-9326/ab541e.

Mildrexler, D.J., Zhao, M., and Running, S.W., 2009. Testing a MODIS Global Disturbance Index across North America. *Remote Sensing of Environment*, 113 (10), 2103–2117. DOI: 10.1016/j.rse.2009.05.016.

Mouillot, F., Schultz, M.G., Yue, C., Cadule, P., Tansey, K., Ciais, P., and Chuvieco, E., 2014. Ten years of global burned area products from spaceborne remote sensing—A review: Analysis of user needs and recommendations for future developments. *International Journal of Applied Earth Observation and Geoinformation*, 26 (1), 64–79. DOI: 10.1016/j.jag.2013.05.014.

Nguyen, T.H., Jones, S.D., Soto-Berelov, M., Haywood, A., and Hislop, S., 2018. A spatial and temporal analysis of forest dynamics using Landsat time-series. *Remote Sensing of Environment*, 217, 461–475. DOI: 10.1016/J.RSE.2018.08.028.

Nunes, L.J.R., Raposo, M.A.M., Meireles, C.I.R., Pinto Gomes, C.J., and Ribeiro, N.M.C.A., 2020. Fire as a Selection Agent for the Dissemination of Invasive Species: Case Study on the Evolution of Forest Coverage. *Environments*, 7 (8), 57. DOI: 10.3390/environments7080057.

Oliveira, S.L.J., Pereira, J.M.C., Carreiras, 2012. Fire frequency analysis in Portugal (1975 - 2005), using Landsat-based burnt area maps. *International Journal of Wildland Fire*, 21 (1), 48. DOI: 10.1071/WF10131.

Parks, S.A., Holsinger, L.M., Koontz, M.J., Collins, L., Whitman, E., Parisien, M.-A., Loehman, R.A., Barnes, J.L., Bourdon, J.-F., Boucher, J., Boucher, Y., Caprio, A.C., Collingwood, A., Hall, R.J., Park, J., Saperstein, L.B., Smetanka, C., Smith, R.J., Soverel, N., 2019. Giving Ecological Meaning to Satellite-Derived Fire Severity Metrics across North American Forests. *Remote Sensing*, 11 (14), 1735. DOI: 10.3390/rs11141735.

Parra, A. and Moreno, J.M., 2018. Drought differentially affects the post-fire dynamics of seeders and resprouters in a Mediterranean shrubland. *Science of the Total Environment*, 626, 1219–1229. DOI: 10.1016/j.scitotenv.2018.01.174.

Pausas, J.G. and Paula, S., 2012. Fuel shapes the fire-climate relationship: evidence from Mediterranean ecosystems. *Global Ecology and Biogeography*, 21 (11), 1074–1082. DOI: 10.1111/j.1466-8238.2012.00769.x.

Pellegrini, A.F.A., Ahlström, A., Hobbie, S.E., Reich, P.B., Nieradzik, L.P., Staver, A.C., Scharenbroch, B.C., Jumpponen, A., Anderegg, W.R.L., Randerson, J.T., and Jackson, R.B., 2018. Fire frequency drives decadal changes in soil carbon and nitrogen and ecosystem productivity. *Nature*, 553 (7687), 194–198. DOI: 10.1038/nature24668.

Petropoulos, G., Carlson, T.N., Wooster, M.J., and Islam, S., 2009. A review of Ts/VI remote sensing based methods for the retrieval of land surface energy fluxes and soil surface moisture. *Progress in Physical Geography*, 33 (2), 224–250. DOI: 10.1177/0309133309338997.

Prior, L.D. and Bowman, D.M.J.S., 2020. Classification of Post-Fire Responses of Woody Plants to include Pyrophobic Communities. *Fire*, 3 (2), 15. DOI: 10.3390/fire3020015.

Prodon, R. and Diaz-Delgado, R., 2021. Assessing the postfire resilience of a Mediterranean forest from satellite and ground data (NDVI, vegetation profile, avifauna). *Écoscience*, 1–11. DOI: 10.1080/11956860.2021.1871826.

Quintano, C., Fernández-Manso, A., Calvo, L., Marcos, E., and Valbuena, L., 2015. Land surface temperature as potential indicator of burn severity in forest Mediterranean ecosystems. *International Journal of Applied Earth Observation and Geoinformation*, 36, 1–12. DOI: 10.1016/j.jag.2014.10.015.

Quintano, C., Fernandez-Manso, A., Marcos, E., and Calvo, L., 2019. Burn Severity and Post-Fire Land Surface Albedo Relationship in Mediterranean Forest Ecosystems. *Remote Sensing*, 11 (19), 2309. DOI: 10.3390/rs11192309.

R Core Team, 2021. R: A Language and Environment for Statistical Computing version 4.0.4.

Ramanathan, V. and Carmichael, G., 2008. Global and regional climate changes due to black carbon. *Nature Geoscience*, 1 (4), 221–227. DOI: 10.1038/ngeo156.

Roy, D.P., Huang, H., Boschetti, L., Giglio, L., Yan, L., Zhang, H.H., and Li, Z., 2019. Landsat-8 and Sentinel-2 burned area mapping - A combined sensor multi-temporal change detection approach. *Remote Sensing of Environment*, 231, 111254. DOI: 10.1016/j.rse.2019.111254.

Ryu, J.-H., Han, K.-S., Hong, S., Park, N.-W., Lee, Y.-W., and Cho, J., 2018. Satellite-Based Evaluation of the Post-Fire Recovery Process from the Worst Forest Fire Case in South Korea, 10 (6), 918.

Saha, M. V., D'Odorico, P., and Scanlon, T.M., 2017. Albedo changes after fire as an explanation of fire-induced rainfall suppression. *Geophysical Research Letters*, 44 (8), 3916–3923. DOI: 10.1002/2017GL073623.

Saha, M. V., D'Odorico, P., and Scanlon, T.M., 2019. Kalahari Wildfires Drive Continental Post-Fire Brightening in Sub-Saharan Africa. *Remote Sensing*, 11 (9), 1090. DOI: 10.3390/rs11091090.

Samiappan, S., Hathcock, L., Turnage, G., McCraine, C., Pitchford, J., and Moorhead, R., 2019. Remote Sensing of Wildfire Using a Small Unmanned Aerial System: Post-Fire Mapping, Vegetation Recovery and Damage Analysis in Grand Bay, Mississippi/Alabama, USA. *Drones*, 3 (2), 43. DOI: 10.3390/drones3020043.

San-Miguel-Ayanz, J., Moreno, J.M., and Camia, A., 2013. Analysis of large fires in European Mediterranean landscapes: Lessons learned and perspectives. *Forest Ecology and Management*, 294, 11–22. DOI: 10.1016/j.foreco.2012.10.050.

Santos, R.M.B., Sanches Fernandes, L.F., Pereira, M.G., Cortes, R.M.V., and Pacheco, F.A.L., 2015. Water resources planning for a river basin with recurrent wildfires. *Science of the Total Environment*, 526, 1–13. DOI: 10.1016/j.scitotenv.2015.04.058.

Scheffer, M., Bascompte, J., Brock, W.A., Brovkin, V., Carpenter, S.R., Dakos, V., Held, H., van Nes, E.H., Rietkerk, M., and Sugihara, G., 2009. Early-warning signals for critical transitions. *Nature*, 461 (7260), 53–59. DOI: 10.1038/nature08227.

Scheffer, M. and Carpenter, S.R., 2003. Catastrophic regime shifts in ecosystems: linking theory to observation. *Trends in Ecology & Evolution*, 18 (12), 648–656. DOI: 10.1016/j.tree.2003.09.002.

Scheffer, M., Carpenter, S.R., Dakos, V., and van Nes, E.H., 2015. Generic Indicators of Ecological Resilience: Inferring the Chance of a Critical Transition. *Annual Review of Ecology, Evolution, and Systematics*, 46 (1), 145–167. DOI: 10.1146/annurev-ecolsys-112414-054242.

Scheffer, M., Carpenter, S.R., Lenton, T.M., Bascompte, J., Brock, W., Dakos, V., van de Koppel, J., van de Leemput, I.A., Levin, S.A., van Nes, E.H., Pascual, M., and Vandermeer, J., 2012. Anticipating Critical Transitions. *Science*, 338 (6105), 344–348. DOI: 10.1126/science.1225244.

Selles, O.A. and Rissman, A.R., 2020. Content analysis of resilience in forest fire science and management. *Land Use Policy*, 94, 104483. DOI: 10.1016/j.landusepol.2020.104483.

Semeraro, T., Vacchiano, G., Aretano, R., and Ascoli, D., 2019. Application of vegetation index time series to value fire effect on primary production in a Southern European rare wetland. *Ecological Engineering*, 134, 9–17. DOI: 10.1016/j.ecoleng.2019.04.004.

Senf, C. and Seidl, R., 2020. Mapping the forest disturbance regimes of Europe. *Nature Sustainability*, 4 (1). DOI: 10.1038/s41893-020-00609-y.

Sever, L., Leach, J., and Bren, L., 2012. Remote sensing of post-fire vegetation recovery; a study using Landsat 5 TM imagery and NDVI in North-East Victoria. *Journal of Spatial Science*, 57 (2), 175–191. DOI: 10.1080/14498596.2012.733618.

Shi, T. and Xu, H., 2019. Derivation of Tasseled Cap Transformation Coefficients for Sentinel-2 MSI At-Sensor Reflectance Data. *IEEE Journal of Selected Topics in Applied Earth Observations and Remote Sensing*, 12 (10), 4038–4048. DOI: 10.1109/JSTARS.2019.2938388.

Silva, J.S., Vaz, P., Moreira, F., Catry, F., and Rego, F.C., 2011. Wildfires as a major driver of landscape dynamics in three fire-prone areas of Portugal. *Landscape and Urban Planning*, 101 (4), 349–358. DOI: 10.1016/j.landurbplan.2011.03.001.

Smith, A.M.S., Lentile, L.B., Hudak, A.T., and Morgan, P., 2007. Evaluation of linear spectral unmixing and ΔNBR for predicting post-fire recovery in a North American ponderosa pine forest. *International Journal of Remote Sensing*, 28 (22), 5159–5166. DOI: 10.1080/01431160701395161.

Smith, A.M.S.S., Kolden, C.A., Tinkham, W.T., Talhelm, A.F., Marshall, J.D., Hudak, A.T., Boschetti, L., Falkowski, M.J., Greenberg, J.A., Anderson, J.W., Kliskey, A., Alessa, L., Keefe, R.F., and Gosz, J.R., 2014. Remote sensing the vulnerability of vegetation in natural terrestrial ecosystems. *Remote Sensing of Environment*, 154, 322–337. DOI: 10.1016/j.rse.2014.03.038.

Smith, H.G., Sheridan, G.J., Lane, P.N.J., Nyman, P., and Haydon, S., 2011. Wildfire effects on water quality in forest catchments: A review with implications for water supply. *Journal of Hydrology*, 396 (1–2), 170–192. DOI: 10.1016/j.jhydrol.2010.10.043.

Sparks, A.M., Kolden, C.A., Smith, A.M.S., Boschetti, L., Johnson, D.M., and Cochrane, M.A., 2018. Fire intensity impacts on post-fire temperate coniferous forest net primary productivity. *Biogeosciences*, 15 (4), 1173–1183. DOI: 10.5194/bg-15-1173-2018.

Spasojevic, M.J., Bahlai, C.A., Bradley, B.A., Butterfield, B.J., Tuanmu, M.-N., Sistla, S., Wiederholt, R., and Suding, K.N., 2016. Scaling up the diversity-resilience relationship with trait databases and remote sensing data: the recovery of productivity after wildfire. *Global Change Biology*, 22 (4), 1421–1432. DOI: 10.1111/gcb.13174.

Staal, A., van Nes, E.H., Hantson, S., Holmgren, M., Dekker, S.C., Pueyo, S., Xu, C., and Scheffer, M., 2018. Resilience of tropical tree cover: The roles of climate, fire, and herbivory. *Global Change Biology*, 24 (11), 5096–5109. DOI: 10.1111/gcb.14408.

Sun, X., Zou, C.B., Wilcox, B., and Stebler, E., 2019. Effect of Vegetation on the Energy Balance and Evapotranspiration in Tallgrass Prairie: A Paired Study Using the Eddy-Covariance Method. *Boundary-Layer Meteorology*, 170 (1), 127–160. DOI: 10.1007/s10546-018-0388-9.

Tedim, F., Remelgado, R., Borges, C., Carvalho, S., and Martins, J., 2013. Exploring the occurrence of mega-fires in Portugal. *Forest Ecology and Management*, 294, 86–96. DOI: 10.1016/j.foreco.2012.07.031.

Tiribelli, F., Kitzberger, T., and Morales, J.M., 2018. Changes in vegetation structure and fuel characteristics along post-fire succession promote alternative stable states and positive fire-vegetation feedbacks. *Journal of Vegetation Science*, 29 (2), 147–156. DOI: 10.1111/jvs.12620.

Veraverbeke, S., Gitas, I., Katagis, T., Polychronaki, A., Somers, B., and Goossens, R., 2012. Assessing post-fire vegetation recovery using red–near infrared vegetation indices: Accounting for background and vegetation variability. *ISPRS Journal of Photogrammetry and Remote Sensing*, 68 (1), 28–39. DOI: 10.1016/j.isprsjprs.2011.12.007.

Veraverbeke, S., Lhermitte, S., Verstraeten, W.W., and Goossens, R., 2011a. A time-integrated MODIS burn severity assessment using the multi-temporal differenced normalized burn ratio (dNBRMT). *International Journal of Applied Earth Observation and Geoinformation*, 13 (1), 52–58. DOI: 10.1016/j.jag.2010.06.006.

Veraverbeke, S., Lhermitte, S., Verstraeten, W.W., and Goossens, R., 2011b. Evaluation of pre/post-fire differenced spectral indices for assessing burn severity in a Mediterranean environment with Landsat Thematic Mapper. *International Journal of Remote Sensing*, 32 (12), 3521–3537. DOI: 10.1080/01431161003752430.

Veraverbeke, S., Verstraeten, W.W., Lhermitte, S., Van De Kerchove, R., and Goossens, R., 2012. Assessment of post-fire changes in land surface temperature and surface albedo, and their relation with fire - burn severity using multitemporal MODIS imagery. *International Journal of Wildland Fire*, 21 (3), 243. DOI: 10.1071/WF10075.

Verbesselt, J., Hyndman, R., Newnham, G., and Culvenor, D., 2010. Detecting trend and seasonal changes in satellite image time series. *Remote Sensing of Environment*, 114 (1), 106–115. DOI: 10.1016/j.rse.2009.08.014.

Verbesselt, J., Hyndman, R., Zeileis, A., and Culvenor, D., 2010. Phenological change detection while accounting for abrupt and gradual trends in satellite image time series. *Remote Sensing of Environment*, 114 (12), 2970–2980. DOI: 10.1016/j.rse.2010.08.003.

Verbesselt, J., Umlauf, N., Hirota, M., Holmgren, M., Van Nes, E.H., Herold, M., Zeileis, A., and Scheffer, M., 2016. Remotely sensed resilience of tropical forests. *Nature Climate Change*, 6 (11), 1028–1031. DOI: 10.1038/nclimate3108.

Vermote, E., 2015. MOD09A1 MODIS/Terra Surface Reflectance 8-Day L3 Global 500m SIN Grid V006. *NASA EOSDIS Land Processes DAAC.*

Viana-Soto, A., Aguado, I., Salas, J., and García, M., 2020. Identifying post-fire recovery trajectories and driving factors using landsat time series in fire-prone mediterranean pine forests. *Remote Sensing*, 12 (9), 1499. DOI: 10.3390/RS12091499.

Vlassova, L., Pérez-Cabello, F., Mimbrero, M., Llovería, R., and García-Martín, A., 2014. Analysis of the Relationship between Land Surface Temperature and Wildfire Severity in a Series of Landsat Images. *Remote Sensing*, 6 (7), 6136–6162. DOI: 10.3390/rs6076136.

Wan, Z., Hook, S., and Hulley, G., 2015. MOD11A2 MODIS/Terra Land Surface Temperature/Emissivity 8-Day L3 Global 1km SIN Grid V006. *NASA EOSDIS Land Processes DAAC*.

Wei, X., Hayes, D.J., Fraver, S., and Chen, G., 2018. Global Pyrogenic Carbon Production During Recent Decades Has Created the Potential for a Large, Long-Term Sink of Atmospheric CO2. *Journal of Geophysical Research: Biogeosciences*, 123 (12), 3682–3696. DOI: 10.1029/2018JG004490.

Willis, K.J., Jeffers, E.S., and Tovar, C., 2018. What makes a terrestrial ecosystem resilient? *Science*, 359 (6379), 988–989. DOI: 10.1126/science.aar5439.

Zheng, Z., Zeng, Y., Li, S., and Huang, W., 2016. A new burn severity index based on land surface temperature and enhanced vegetation index. *International Journal of Applied Earth Observation and Geoinformation*, 45, 84–94. DOI: 10.1016/j.jag.2015.11.002.

Supplementary material

Table S4.1. Percentages of complete pairwise observations (maximum *n* = 13,751) for the indicators proposed in this study.

		Productivity				**Water**				**Albedo**				**Heat**			
		S95	*I1T*	*RRT*	*RET*	*S95*	*I1T*	*RRT*	*RET*	*S95*	*I1T*	*RRT*	*RET*	*S95*	*I1T*	*RRT*	*RET*
Heat	*RET*	95%	95%	100%	100%	79%	79%	100%	100%	62%	62%	100%	100%	56%	56%	100%	100%
	RRT	95%	95%	100%	100%	79%	79%	100%	100%	62%	62%	100%	100%	56%	56%	100%	
	I1T	55%	55%	56%	56%	49%	49%	56%	56%	39%	39%	56%	56%	56%	56%		
	S95	55%	55%	56%	56%	49%	49%	56%	56%	39%	39%	56%	56%	56%			
Albedo	*RET*	95%	95%	100%	100%	79%	79%	100%	100%	62%	62%	100%	100%				
	RRT	95%	95%	100%	100%	79%	79%	100%	100%	62%	62%	100%					
	I1T	61%	61%	62%	62%	55%	55%	62%	62%	62%	62%						
	S95	61%	61%	62%	62%	55%	55%	62%	62%	62%							
Water	*RET*	95%	95%	100%	100%	79%	79%	100%	100%								
	RRT	95%	95%	100%	100%	79%	79%	100%									
	I1T	77%	77%	79%	79%	79%	79%										
	S95	77%	77%	79%	79%	79%											
Productivit	*RET*	95%	95%	100%	100%												
	RRT	95%	95%	100%													
	I1T	95%	95%														
	S95	95%															

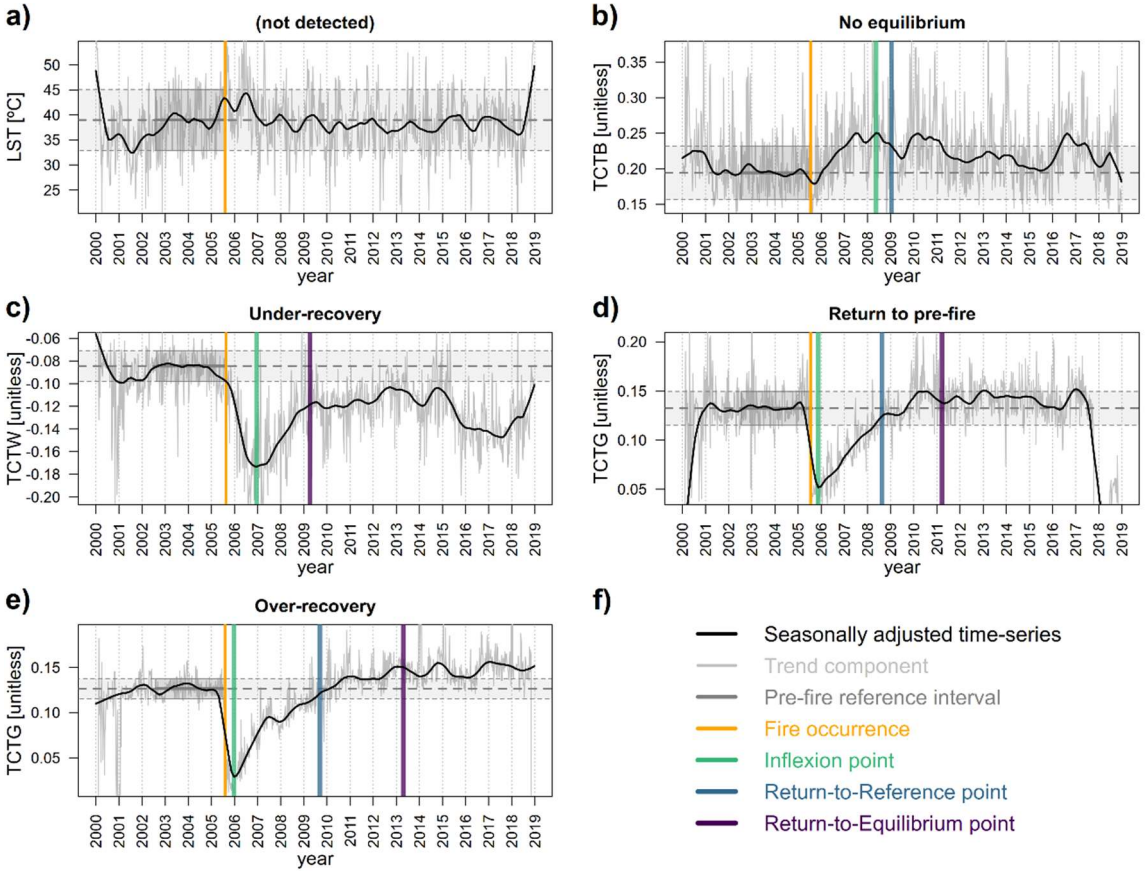

Figure S4.1. Examples of pixel-wise post-fire trajectory profiles (a–e), each corresponding to one of the classes of post-fire recovery and resilience obtained: *(not detected)* (a), *No equilibrium* (b), *Under-recovery* (c), *Return to pre-fire* (d), and *Over-recovery* (e); as well as the respective legend (f).

CHAPTER 5. General discussion and conclusions

Preamble

This final chapter aims to provide an integrative view of the research developed for this thesis, and the main conclusions and future directions towards further improvements. It is therefore organized in two main sections: (i) a synthesis of the rationale, implementation, and main findings and contributions of the conceptual and experimental framework for the multi-dimensional assessment of wildfire disturbances developed and proposed in this thesis; and (ii) a summary of future research and development pathways – as well as challenges – for further testing and improvement of the proposed framework, and a set of concluding remarks of the thesis.

5.1. Synthesis: a framework for the multi-dimensional assessment of wildfire disturbances

5.1.1. Rationale

In an intrinsically flammable planet, wildfire disturbances are an integral part of the natural dynamics of ecosystems in several biomes (San-Miguel-Ayanz *et al.* 2013, Adámek *et al.* 2016). As a biological filter that shapes biodiversity, wildfires constitute a major driver of ecological change, modifying the composition, structure, and functioning of ecosystems and, consequently, the provision of ecosystem services to humankind (João *et al.* 2018). Notwithstanding, wildfire events can pose a major threat to a wide range of social, economic, and environmental assets. Since wildfire events have been generally increasing in recent decades, both in terms of frequency and intensity (Bowman *et al.* 2009) – which has been exacerbated by global climate change and by shifts in land use and forest management (Tedim *et al.* 2013) –, there is an increasing need for methods to assess and monitor the ecological consequences of such disturbances.

Fire can cause rapid and profound modifications on many key aspects of the flows of matter and energy (Petropoulos *et al.* 2009) – such as those related to the biogeochemical cycles of carbon (e.g., primary productivity, biomass), and water (e.g., vegetation water content, soil moisture), as well as to energy balances (e.g., albedo, latent heat, sensible heat). For this reason, approaches based on ecosystem functioning offer advantages over structural or compositional ones since functional attributes have a quicker response to disturbances and are more directly connected to ecosystem services (Alcaraz-Segura *et al.* 2008). Furthermore, wildfires can contribute to eroding the resilience of terrestrial ecosystems (Johnstone *et al.* 2010, Scheffer *et al.* 2015) –, decreasing their ability to persist in the face of disturbances and their self-repairing capacity, and increasing the risk of sudden collapse or regime shifts (Folke *et al.* 2004). However, most resilience assessments do not account for ecosystem functioning after disturbance events (Frazier *et al.* 2013), and multi-dimensional evaluations of the environmental impacts of wildfires on ecosystem functioning are still scarce. Therefore, since both wildfire disturbances and resilience are multi-dimensional (Donohue *et al.* 2013, 2016), and post-fire trajectories of each dimension of ecosystem functioning are different (Ryu *et al.* 2018), more comprehensive indicators are still needed to better understand post-fire ecological processes.

In this regard, over the last decades, remote sensing has revolutionized the way environmental changes are monitored (Kwok 2018). It provides valuable data at

increasingly higher temporal, spatial, and spectral resolutions, due to lower costs and improved technology for providing up-to-date information on the status of ecosystem resources. Moreover, remote sensing techniques have been increasingly used in fire-related applications (Szpakowski and Jensen 2019), namely to derive indicators of different aspects of the post-fire period (Lentile *et al.* 2006), enabling in-depth and integrative characterizations of post-fire recovery and resilience (João *et al.* 2018). Nevertheless, to fully understand the effects of wildfire disturbances on multiple dimensions of ecosystems, a better translation of spectral indices into informative ecosystem variables is needed. Therefore, there is a need to devise consistent conceptual and experimental frameworks capable of linking ecological theory to remotely sensed data through essential ecological concepts such as resistance and resilience, and essential biodiversity variables related to ecosystem function(ing). Developing operational frameworks based on remotely-sensed sources would enhance and accelerate the assessment and mapping of the spatiotemporal heterogeneous effects of wildfires on ecosystem functioning, as well as the responses and resilience of ecosystems to those disturbances. Such operational frameworks represent a major asset for risk assessment and governance, and post-fire management and restoration (Keeley 2009, Tedim *et al.* 2013, Smith *et al.* 2014, Parks *et al.* 2019).

5.1.2. Implementation

Theoretical foundations: the multi-dimensionality of ecosystem functioning

With the broad overarching goal of **improving the assessment of wildfire disturbances**, this thesis developed, described, and showcased an integrative conceptual and experimental framework to evaluate the effects of wildfire disturbance on multiple dimensions of ecosystem functioning. To that end, four essential variables of the flows of matter (i.e., carbon and water dynamics) and energy (i.e., radiation and heat balances) in ecosystems were addressed: *primary productivity*, *vegetation water content*, *albedo*, and *sensible heat*. Together, these four variables summarize ecosystem processes that govern several crucial aspects of ecosystem functioning, which can all be strongly impacted by wildfires (Petropoulos *et al.* 2009).

Primary productivity (i.e., the amount of biomass produced by an ecosystem within a defined period; Leys *et al.* 2016) can be expressed as the amount of carbon assimilated by photosynthesis since plant biomass has a fairly constant carbon content (Geller *et al.* 2017). Wildfires play an important role in primary productivity, as a focal component of the carbon cycle in terrestrial ecosystems (Wei *et al.* 2018). Vegetation water content is a proxy of

water availability for plants and other organisms and related to canopy and soil moisture, which have a direct influence on ecosystem functioning (Lozano-Parra *et al.* 2018). Conversely, wildfire disturbances can have a direct or indirect effect on water content (Senf and Seidl 2020). Land surface albedo (i.e., the ratio of irradiance reflected to the irradiance received by the land surface) is a primary controlling factor for the surface energy budget. Since it depends on both the atmospheric conditions and surface reflective properties (Zhao *et al.* 2018), it can also be linked to changes in climate (Yu *et al.* 2017), and land degradation and desertification (Zhao *et al.* 2018). Finally, sensible heat, which can also be profoundly altered by wildfires (Liu *et al.* 2018, Maffei *et al.* 2018), is crucial for drought monitoring, soil moisture estimation, and evapotranspiration estimates (e.g., Anderson *et al.* 2012, Semmens *et al.* 2016). Along with albedo, sensible heat plays an important role in determining the radiative energy budget of the Earth's surface, both being important climate system variables (Hulley *et al.* 2019).

Input data: satellite image time-series

Throughout this thesis, freely available data from the Moderate Resolution Imaging Spectroradiometer (MODIS) sensors onboard the Terra and Aqua satellites was used to derive different fire-related indicators extracted from several well-known remotely-sensed variables related to the four dimensions of ecosystem functioning (see **Table 2.1** in Chapter 2). This approach addressed the important strategic objective of contributing to clarifying and mainstreaming the links between ecological processes, wildfire disturbances, and remotely-sensed observations, under the remote sensing paradigm shift in terrestrial ecosystems monitoring (Kwok 2018).

Space-borne multispectral sensors – such as MODIS – are the most commonly used remote sensing systems for fire ecology research (Szpakowski and Jensen 2019). Furthermore, MODIS time-series are well-suited to measure functional aspects of ecosystems (e.g., Alcaraz-Segura *et al.* 2008, Neumann *et al.* 2016), and it has indeed been broadly used for fire-related applications (e.g., Veraverbeke *et al.* 2012, João *et al.* 2018). Despite its moderate to coarse spatial resolutions (i.e., between 250m and 1km), MODIS data can provide valuable tools for monitoring, mainly at regional scales. Indeed, MODIS data features high coverage and temporal resolution, wide availability of the datasets, and a data archive spanning two decades, providing data with spectral bands appropriate for wildfire applications (Giglio *et al.* 2018). Its high temporal resolution, in particular, is a key aspect towards operational monitoring systems since it translates into higher robustness against unfavorable weather conditions such as cloud cover, which can hinder remotely-

sensed time-series. Ranging from yearly or monthly products and 16- or 8-day composites, up to four observations per day, it allows for near real-time monitoring capabilities (e.g., Xin *et al.* 2013, Briones-Herrera *et al.* 2020).

Test case: regional-scale study area

The framework presented in this thesis was applied and tested for a specific regional-scale study area – the northwest Iberian Peninsula (NW-IP) –, and illustrated for several local-scale areas within that main area. This region is a hotspot in terms of wildfire occurrences within the European context, being one of the regions with both the highest annual values of burnt area in Europe (San-Miguel-Ayanz *et al.* 2017) and the highest density of ignitions among southern European countries (Catry *et al.* 2009, Barros and Pereira 2014). It also features a strong climatic gradient, a major biogeographic transition, and a large diversity of environmental conditions, and well-diversified and highly heterogeneous land cover and land use types (Vicente *et al.* 2013, Carvalho-Santos *et al.* 2014), which, together with socio-economic drivers, contribute to a highly fire-prone landscape (Oliveira *et al.* 2012, João *et al.* 2018).

The use of a common base in terms of both regional-scale study area and input data sources, as well as their processing, allowed for optimization of both computational resources and time allocated to the execution of the necessary tasks. Nevertheless, it should be noted that the methodologies employed in the framework proposed in this thesis should apply to other areas with diverse geographical contexts, baseline environmental conditions, and fire disturbance regimes. The applicability of the principles underlying the framework developed for this thesis is related to the general tendency of the remotely-sensed variables used to hold overall similar behavior patterns in response to wildfire disturbances, across different biomes, vegetation types, and climatic regimes (Hope *et al.* 2012, Leon *et al.* 2012, Lanorte *et al.* 2014).

Technical implementation: open code-based workflows

The framework developed in this thesis aimed to contribute to the important strategic objective of improving the comprehensiveness and cost-efficiency of monitoring systems, underlying the development and implementation of regional monitoring programs supported by land observation systems. This goal was achieved by showcasing the opportunities enabled by using cost-free data derived from remote sensing, which was processed and analyzed within highly reproducible, code-based workflows developed in free and open-source software environments. Namely, all processing and analytical tasks undertaken

throughout this thesis were implemented mainly using the *R* and *Python* programming languages, as well as shell scripts, with appropriate source code management and versions control. Indeed, the concepts of *Free and Open Source Software* (FOSS; Söderberg 2015) and data, and *open science* principles (Woelfle *et al.* 2011, Vicente-Saez and Martinez-Fuentes 2018) are becoming increasingly popular in the fields of ecology, conservation, and ecosystem monitoring using remote sensing (Rocchini *et al.* 2017). Moreover, this approach contributes to fulfilling the requirements of monitoring systems to ensure high data quality, accessibility, and cost-effectiveness (Lovett *et al.* 2007).

5.1.3. Summary of main findings and contributions

The rationale and the theoretical foundations established above supported the implementation of the conceptual and experimental framework developed in this thesis, which was demonstrated by addressing the overarching goals of the thesis and three research hypotheses (H1–H3) throughout the three individual studies presented in Chapters 2–4.

Improving the detection of wildfire disturbances

The first study, presented in Chapter 2, addressed **Research Hypothesis 1** (H1) – *"The location, extension, and date of occurrence of wildfire disturbance events can be identified using indicators of multiple dimensions of ecosystem functioning, related to matter and energy exchanges, to enhance existing burned area maps and fill important gaps in fire databases"*.

This study provided support for confirming H1 by successfully using indicators of wildfire occurrence extracted from several well-known remotely-sensed variables, which were then compared, ranked, and selected for mapping annually burned area and estimating dates of fire occurrence. Among these indicators, those derived from the *Tasseled Cap* features of *Greenness* (TCTG), *Wetness* (TCTW), and *Brightness* (TCTB) – as proxies of primary productivity, vegetation water content, and albedo, respectively –, and *Land Surface Temperature* (LST) – as a proxy of sensible heat – performed particularly well. These four remotely-sensed variables have all been used for disturbance detection purposes in previous studies (e.g., Mildrexler *et al.* 2009). However, to our knowledge, they have not been previously compared and combined, in a multi-indicator consensus approach, for detecting wildfire disturbances in space and time. Moreover, these variables have relatively low requirements both in terms of input data and computation since they are often available for the major satellite data sources (e.g., Shi and Xu 2019), and the three

Tasseled Cap features are extracted from common data sources and a set of transformation coefficients. Besides, these are well-known and widely used remotely-sensed variables that integrate information from several wavelengths of the visible and infrared regions of the electromagnetic spectrum, allowing for capturing different aspects of the Earth's surface (Lobser and Cohen 2007). Based on the results of this study, those four remotely-sensed variables were selected as input data for the two subsequent studies.

Expanding the assessment of wildfire disturbance severity

The second study, presented in Chapter 3, partially addressed **Research Hypothesis 2** (H2) – *"The short-, medium-, and long-term effects of wildfires on ecosystem functioning, and ecosystem responses to those disturbances can be better estimated with the synergistic use of multiple indicators, enabling in-depth multi-dimensional and synoptic assessments of wildfire disturbance severity and post-fire recovery"*.

In this study, indicators of wildfire severity were derived from inter-annual anomalies (i.e., deviations from the normal inter-annual variability) of a large set of descriptors of the intra-annual dynamics – called *Ecosystem Functioning Attributes* (EFAs) – of TCTG, TCTW, TCTB, and LST, as proxies of the four dimensions of ecosystem functioning of primary productivity, vegetation water content, albedo, and sensible heat, respectively. These indicators were computed, at the regional scale, and then compared at both *short-* (i.e., the year of the fire) and *medium-term* (i.e., up to the second year after the fire). These analyses allowed for important effects of wildfire disturbances to be observed on all four dimensions of ecosystem functioning, with quantity metrics of primary productivity performing the best, which can be associated with the removal of vegetation (e.g., Pellegrini *et al.* 2018). Other observed post-fire effects of wildfire disturbances included lagged effects in vegetation water content, potentially related to canopy damage and mortality (e.g., Senf and Seidl 2020), and brightening and darkening effects in albedo, related to the concentrations of radiation-absorbing materials (e.g., Ramanathan and Carmichael 2008), which also contributed to hydrological changes. On the other hand, observed effects on land surface temperature were generally transient (e.g., Quintano *et al.* 2015). These effects had all been previously reported, except – to our knowledge – for the lagged effects on vegetation water content. The approach employed in this study also allowed the selection of a parsimonious set of indicators to illustrate the main effects of wildfire disturbances on ecosystem functioning at the scale of individual burned patches. Together, the results highlighted the importance and added value of multi-dimensional and multi-timeframe approaches for improved satellite-based wildfire severity assessment, mapping, and monitoring, providing support to partially confirm H2.

Characterizing post-fire recovery and resilience

Finally, the third and final study, presented in Chapter 4, partially addressed H2 but mainly addressed **Research Hypothesis 3** (H3) – *"Indicators extracted from post-fire trajectories of remotely-sensed variables of ecosystem functioning allow for the identification and characterization of potential regime shifts after wildfires and, consequently, the assessment of (changes in) ecological resilience to those disturbances"*.

In this study, indicators of both wildfire severity and post-fire recovery were extracted from post-fire trajectories of TCTG, TCTW, TCTB, and LST, as proxies of the four dimensions of ecosystem functioning of primary productivity, vegetation water content, albedo, and sensible heat, respectively. These indicators were used for characterizing those post-fire trajectories in the *short-term*, and also in the *medium* and *long terms*, linking the effects of wildfire disturbances on, respectively, ecosystem resistance and resilience. Similarly to what was observed in the previous study (Chapter 3), results showed effects on all four dimensions of ecosystem functioning, especially on primary productivity and sensible heat – due to the removal of vegetation –, although those effects were mostly transient in the case of sensible heat (e.g., Quintano *et al.* 2015, Pellegrini *et al.* 2018). Effects such as lagged and slow recovery on vegetation water content – due to canopy damage and mortality induced by fire (e.g., Senf and Seidl 2020) –, and brightening and darkening effects in albedo – related to the concentrations of radiation-absorbing materials (e.g., Ramanathan and Carmichael 2008) – were also observed. Then, indicators of post-fire recovery in the medium and long terms were used for establishing a resilience-based classification of post-fire trajectories. This approach allowed for identifying potential regime shifts, for each dimension of ecosystem functioning, based on the establishment (or not) of equilibrium states in the post-fire period, and their relative distance to the pre-fire reference conditions, as suggested, e.g., by Boettiger *et al.* (2013). The results of the classification procedure for each dimension of ecosystem functioning were then combined to illustrate a multi-dimensional assessment of the strength-of-evidence for regime shifts, at the scale of individual burned patches. Together, the results of this study highlighted the high degree of complementarity between indicators and their ability to depict key features of the underlying post-fire processes, at different timeframes. Furthermore, the added value of the proposed multi-dimensional approach for analyzing ecosystem resistance and ecological resilience (*sensu* Holling 1973, 1996) to wildfire disturbances was also demonstrated. The results of this study contributed to complement the previous study in confirming H2 and provided support to confirm H3, by highlighting the potential of post-fire trajectories to derive information on multiple aspects of the post-fire period (Viana-Soto *et al.* 2020).

Post-fire assessments at multiple timeframes

Throughout the work developed in this thesis, indicators related to multiple aspects of matter and energy fluxes, derived from satellite image time-series, were able to provide detailed insights into different aspects of the interactions between wildfire disturbances and ecosystem functioning. Furthermore, those indicators were useful for both characterizing baseline (i.e., pre-fire reference) conditions, and for assessing the ecological effects of wildfires and the responses of ecosystems to those events, at multiple timeframes. Indeed, assessing different timeframes within the post-fire period allowed for a more complete, comprehensive, and synoptic view of the effects of wildfire disturbances on ecosystem functioning and the underlying processes.

Firstly, the very short-term effects of wildfire disturbances – used in Chapter 2 – that can be observed immediately, and up to one year, after the fire are useful for detecting such disturbances in both space and time, and thus for mapping burned areas and estimating the dates of fire occurrences (Benali *et al.* 2016). Fire date estimation is also key for extracting information with precise timing – such as the indicators of post-fire severity, recovery, and resilience presented in Chapter 4. Second, the *short-* to *medium-term* effects of wildfire disturbances (i.e., between the year of the fire and up to the second year after) are crucial for evaluating fire severity and ecosystem resistance to those disturbances (e.g., De Keersmaecker *et al.* 2015). In that regard, Chapter 3 presented indicators of fire severity with an annual basis – since those indicators were based on EFAs, which also have an annual basis. Although approaches at annual basis are not as appropriate for applications that need more precise timing as approaches at a more continuous time basis, annual-scale assessments can be simpler to communicate and they also can be more useful for applications that are inherently delivered at an annual frequency (e.g., annual reports from official authorities). Finally, indicators of the *medium-* (i.e., typically between the second and fifth year following the fire) to *long-term* (i.e., after the fifth year following the fire) effects of wildfires on ecosystems, and their responses to those disturbances – such as the ones used in Chapter 4 – are key to evaluating and monitoring the post-fire recovery of ecosystems and their resilience to wildfire disturbances (Meng *et al.* 2021). Overall, these aspects contributed to support the confirmation of all three research hypotheses (i.e., H1–H3), particularly in what concerns the importance of assessing multiple stages of the post-fire period (e.g., Bartels *et al.* 2016).

5.2. General conclusions and outlook

5.2.1. General concluding remarks

The key messages and overarching remarks from the research developed in this thesis (presented in Chapters 2–4) to address the research goals and hypotheses are summarized and briefly highlighted in the following 17 points, organized under four main topics: (i) *multi-dimensional and multi-timeframe approach*; (ii) *wildfire occurrence detection and severity assessment*; (iii) *post-fire recovery and resilience evaluation and monitoring*; and (iv) *cost-efficiency and open principles*.

Wildfire occurrence detection and severity assessment

1) Indicators of multiple dimensions of ecosystem functioning were used to improve the identification and characterization of the location, extension, and date of occurrence of wildfire disturbance events;

2) Ranking and selection procedures were used to compare different indicators of wildfire occurrence, maximizing the ability to detect wildfire disturbances in both space and time;

3) Multi-indicator consensus approaches showed enhanced capabilities for improving existing burned area maps and filling important information gaps in fire databases;

4) The dominant effects of wildfire disturbances on ecosystem functioning were observed mainly in primary productivity and sensible heat – although with mostly transient effects in the latter case –, associated with the removal of vegetation; and

5) Other important effects observed included lagged effects on vegetation water content due to canopy damage and mortality induced by fire, and post-fire darkening and/or brightening effects on albedo related to the relative concentrations of radiation-absorbing materials, also contributing to hydrological changes.

Post-fire recovery and resilience evaluation and monitoring

6) The proposed framework contributed to enhancing monitoring of post-fire effects and trajectories, ultimately contributing to improved risk assessment and governance, and post-fire management and restoration;

7) Remotely-sensed indicators facilitated the characterization and classification of the post-fire period, ultimately upholding promising implications for post-fire ecosystem management;

8) Post-fire trajectories of remotely-sensed ecosystem functioning variables allowed for the identification of potential regime shifts after wildfires and, consequently, the assessment of (changes in) ecosystem resilience to those disturbances;

9) Resilience theory provided a basis for more ecologically supported assessments of wildfire disturbances, ultimately upholding promising implications for post-fire ecosystem management; and

10) The developed indicators seemed to have a high degree of inter-complementarity, highlighting the added value of the approach for analyzing post-fire severity, recovery, and resilience.

Multi-dimensional and multi-timeframe approach

11) Multiple dimensions of ecosystem functioning depicted different patterns in crucial features of the interactions between wildfires and ecosystem functioning, providing valuable insights and a more comprehensive picture of the underlying post-fire processes;

12) The four remotely-sensed variables of the *Tasseled Cap* features of *Greenness*, *Wetness*, and *Brightness*, as well as *Land Surface Temperature*, were able to provide indicators strongly related to the key aspects of ecosystem functioning of primary productivity, vegetation water content, albedo, and sensible heat, respectively;

13) Establishing baseline conditions based on a pre-fire reference period was essential for evaluating and comparing indicators of post-fire severity, recovery and, resilience, related to multiple aspects of ecosystem functioning derived from satellite image time-series; and

14) The synergistic use of indicators from multiple dimensions of ecosystem functioning, at multiple timeframes, enabled in-depth and synoptic assessments of wildfire disturbances and improved the estimation of the short-, medium-, and long-term effects of wildfire disturbances on ecosystems and their responses to those disturbances.

Cost-efficiency and open principles

15) The use of freely available data and software led to improved cost-efficiency of monitoring systems;

16) The reproducibility and transparency of wildfire disturbance assessments was enhanced by the adoption of open science principles, particularly in what concerned data and its processing using code-based workflows supported by free and open-source software; and

17) The framework proposed in this thesis provided a comprehensive, cost-effective, and coherent tool to assess and monitor the impacts of wildfires.

In summary, the framework developed, implemented, and presented in this thesis allowed for successfully testing the research hypotheses outlined, and achieving all its main research goals. Indeed, these outcomes provide strong support to the added value of the proposed framework combining resilience theory and remote sensing of ecosystem functioning for an integrative assessment of fire patterns and impacts. Ultimately, the research developed for this thesis contributed to the advancement of scientific knowledge in fire ecology, ecosystem functioning, and ecological resilience.

5.2.2. Future directions

Additional input satellite data

In the future, the generic framework proposed in this thesis could take advantage of additional sources of input data, capitalizing on a more diverse set of characteristics in terms of temporal, spatial, and spectral resolutions, as well as the length of the historical archive available. Several other current or upcoming platform-sensor systems can provide data from Earth observations with different characteristics (**Table 5.1**). Indeed, data with high temporal resolution (i.e., revisit times between six hours and eight days) and moderate spatial resolution (250m–1km) could be used to complement and expand on the capabilities of the MODIS sensors in applications such as active fire and burnt area monitoring. Remote sensing systems capable of delivering such data include the *Visible Infrared Imaging Radiometer Suite* (VIIRS) sensor onboard the Suomi-National Polar-orbiting Partnership (S-NPP) satellite (e.g., Schroeder *et al.* 2014), and the *Sea and Land Surface Temperature Radiometer* (SLSTR) sensor onboard the Sentinel-3 satellites (e.g., Xu *et al.* 2020). Moreover, data with very high temporal resolutions (i.e., less than 1 hour) holds great

potential for observation of disastrous events, due to their near real-time monitoring capabilities. Examples of such sensors are the *Flexible Combined Imager* (FCI) onboard the third generation of Meteosat (MTG) satellites (Chuvieco *et al.* 2020), and the *Advanced Himawari Imager* (AHI) onboard the Himawari-8/9 geostationary satellites (e.g., Xu and Zhong 2017).

In the last two decades, remote sensing instruments providing data at high spatial resolutions (i.e., 10–100m) have also been improving in terms of their temporal resolutions, increasing their potential for post-fire applications such as finer-scale burned area and fire severity mapping. Such sensors include the *Advanced Spaceborne Thermal Emission and Reflection Radiometer* (ASTER) onboard the Terra satellite (e.g., Giglio *et al.* 2008), the *Operational Land Imager* (OLI), and *Thermal InfraRed Sensor* (TIRS) onboard the Landsat-8 satellite (e.g., Schroeder *et al.* 2016), and the *Multi-Spectral Instrument* (MSI) onboard the Sentinel-2 satellites (e.g., García-Llamas *et al.* 2019). Furthermore, hyperspectral (i.e., above 200 spectral bands) data could also help to improve the establishment of links between ecosystem functioning, wildfire disturbances, and remotely-sensed observations. Recent and upcoming hyperspectral sensors include the *Precursore IperSpectrale della Missione Applicativa* (PRISMA) satellites (Vangi *et al.* 2021), and the *Hyperspectral Imager* (HSI) onboard the Environmental Mapping and Analysis (EnMAP) satellite (Guanter *et al.* 2015). Additionally, data from *Synthetic Aperture Radio Detection and Ranging* (SAR) instruments – such as the *C-band Synthetic-Aperture Radar* (C-SAR) onboard the Sentinel-1 satellites – can be useful to overcome limitations in terms of cloud cover or insufficient light (e.g., Czuchlewski and Weissel 2005). Finally, it is important to note that multiple sources of satellite data can be combined through advanced data fusion techniques (e.g., Xin *et al.* 2013, Zhu *et al.* 2016).

Other types of input data and validation

Besides remotely-sensed data, other types of data can be either combined in consensus-based approaches (e.g., Marcos *et al.* 2012), assimilated, or integrated to complement and/or to validate the information provided by the satellite image time-series. For instance, *Unoccupied Aerial Vehicles* (UAVs) provide the means for rapid and cost-effective data acquisition necessary for fire ecology research by providing timely multispectral measurements and 3D models of terrain and vegetation structure (Szpakowski and Jensen 2019). Equipped with capable sensors, UAVs can deliver fine spatial resolution data at temporal resolutions defined by the end-user, thus potentially revolutionizing spatial ecology (Anderson and Gaston 2013). Indeed, although UAV-based research is an

emerging technology, the data have been used for fire detection (Umar and De Silva 2018), fire severity assessment (Carvajal-Ramírez *et al.* 2019), and post-fire recovery monitoring (Aicardi *et al.* 2016).

Table 5.1. Some of the current and upcoming platform-sensor systems that could potentially be used in the future for post-fire monitoring. "MODIS" = Moderate Resolution Imaging Spectroradiometer; "ASTER" = Advanced Spaceborne Thermal Emission and Reflection Radiometer; "VIIRS" = Visible Infrared Imaging Radiometer Suite; "S-NPP" = Suomi-National Polar-orbiting Partnership; "OLI" = Operational Land Imager; "TIRS" = Thermal InfraRed Sensor; "C-SAR" = C-band Synthetic-Aperture Radar; "MSI" = Multi-Spectral Instrument; "AHI" = Advanced Himawari Imager; "SLSTR" = Sea and Land Surface Temperature Radiometer; "PRISMA" = Precursore IperSpettrale della Missione Applicativa; "HSI" = Hyperspectral Imager; "EnMAP" = Environmental Mapping and Analysis; "FCI" = Flexible Combined Imager; and "MTG" = Meteosat Third Generation.

Sensor(s)	**Platform(s)**	**Launch date**	**Resolutions**		
			Temporal	*Spatial*	*Spectral*
MODIS	Terra/Aqua	1999-12-18	1 day	250–1000m	36 bands
ASTER	Terra	1999-12-18	16 days	15–90m	14 bands
VIIRS	S-NPP	2011-10-28	12 hours	375–750m	22 bands
OLI/TIRS	Landsat-8	2013-02-11	16 days	15–100m	11 bands
C-SAR	Sentinel-1	2014-04-03	12 days	5–100m	dual polarization
MSI	Sentinel-2	2015-06-23	10 days	10–60m	13 bands
AHI	Himawari-8/9	2015-10-07	10 minutes	500–2000m	16 bands
SLSTR	Sentinel-3	2016-02-16	1 day	500–1000m	11 bands
PRISMA-I	PRISMA	2019-03-22	29 days	5–30m	250 bands
HSI	EnMAP	? 2022 ?	4–27 days	30m	230 bands
FCI	MTG-I	? 2022 ?	10 minutes	1000m	21 bands

In addition to aerial photography and photogrammetry collected by sensors onboard UAVs, non-remotely-sensed data collected either through preexisting sensor networks or well-designed field-based measurements can be used to validate the information provided by satellite-based observations, further enhancing the proposed approach. For instance, spectral readings from handheld instruments such as spectroradiometers can be used for validation purposes or inter-calibration with satellite-based observations. Observational data collected in-field using either already existing and commonly-used protocols or newly-developed ones for more comprehensive fire severity assessment, and post-fire recovery evaluation. Examples of preexisting protocols for in-field post-fire assessment include the *Composite Burn Index* (CBI; e.g., Cardil *et al.* 2019) and the improved *Geometrically structured Composite Burn Index* (GeoCBI; e.g., De Santis and Chuvieco 2009), for burn severity assessment. However, multi-dimensional approaches such as the one proposed in this thesis could go further and beyond the most common approaches. For instance, the

multi-dimensional approach based on ecosystem functioning described in this thesis could support more comprehensive and complete post-fire assessments than the widely-used burn severity assessments based on the *Differenced Normalized Burn Ratio* (∆NBR; e.g., Escuin *et al.* 2008), or any of its enhanced forms, such as the *Relative Normalized Burn Ratio* (R∆NBR; Miller and Thode 2007) and the *Relativized Burn Ratio* (RBR; Parks *et al.* 2014). Further sources of information can be used for validation purposes, such as, e.g., eddy covariance data for point-scale validation (e.g., Ueyama *et al.* 2014), and land-surface ecohydrological models for validating results at the watershed scale (e.g., Xiang *et al.* 2014).

Methodological improvements and dissemination of outputs

Advanced technologies, as well as methodological improvements and automatization procedures, could facilitate the overall improvement of the proposed framework, contributing to fulfilling the requirements of monitoring systems to ensure high data quality, accessibility, and cost-effectiveness (Lovett *et al.* 2007). These improvements include the use of cloud-based processing resources, such as *Google Earth Engine* (GEE; e.g., Parks *et al.* 2018, Ermida *et al.* 2020, Seydi *et al.* 2021, Swetnam *et al.* 2021) and the employment of *Big Data* routines and procedures (e.g., Hampton *et al.* 2013, Liu 2015, Chi *et al.* 2016, Farley *et al.* 2018), supported by modern *Data Science* principles and techniques, to up-scale the proposed framework. Moreover, the use of advanced techniques such as *Deep Learning* algorithms (e.g., Ma *et al.* 2019, Pelletier *et al.* 2019, Jia *et al.* 2020), and the application of statistical time-series analysis and forecasting methods to remote sensing data (e.g., Kesavan *et al.* 2021), could help to leverage the full potential of such data for applications related to both fire ecology and ecosystem functioning. Additionally, automated workflows and processing pipelines could be invaluable to support the development of more ecologically-based fire data products, as well as web-based services, at regional and national scales.

On the other hand, the application of such technologies may also present several challenges, such as those related to implementing customized and detailed routines in radically different architectures, the inherent complexity of those methods, or the uncertainty in the future availability, stability, and accessibility of some of those resources. To help mitigate those challenges, additional steps can be taken towards cost-effectiveness and more reproducible and open science, through increased use of free (i.e., both cost-free, as well as free to run for any purpose, inspect, modify, and (re)distribute) and open data, software, and standards, as well as open access scientific publication of results and other outputs (Rocchini *et al.* 2017). In this regard, both *Free and Open Source Software* (FOSS;

Söderberg 2015) and data, and *open science* principles (Woelfle *et al.* 2011, Vicente-Saez and Martinez-Fuentes 2018) are becoming increasingly popular in the fields of ecology, conservation, and ecosystem monitoring using remote sensing (Rocchini *et al.* 2017). Indeed, in addition to publishing scientific results in international peer-reviewed journals, output datasets and related metadata (e.g., Pôças *et al.* 2014), and software routines developed for the implementation of the framework described in this thesis could be published and made openly available through the appropriate platforms (e.g., data repositories and software packages, respectively).

Applications and contributions at the global scale

Although the framework presented in this thesis was only tested at the regional and the individual burned area scales, further testing within different geographical and environmental contexts, and diverse fire regimes should be carried out in the future, to optimize and fine-tune the framework for the widest set of situations possible.

Conversely, global-scale assessments of the post-fire impacts and the ecological consequences of wildfire disturbances on ecosystem functioning could also benefit from its up-scaling, adaptation, and application to such types of contexts. Frameworks for post-fire assessment such as the one described and proposed in this thesis could also provide valuable contributions towards achieving the goals of international initiatives. For instance, the set of remotely-sensed variables informing on the biological effects of wildfire disturbances – such as their direction, duration, abruptness, magnitude, extent, and frequency –, was considered the top priority remote sensing biodiversity product within the *Essential Biodiversity Variables* (EBVs; Skidmore *et al.* 2021). Furthermore, the four remotely-sensed variables used in this thesis – i.e., primary productivity, vegetation water content, albedo, and sensible heat – point to four essential dimensions of ecosystem function(ing), which is one of the EBV classes (Pereira *et al.* 2013, Geller *et al.* 2017).

In effect, the strong ecological bases underlying the framework proposed in this thesis, as well as the importance of evaluating and monitoring the impacts of wildfires, could lead to potential contributions of this framework towards the *U.N. Sustainable Goals for 2030* (Reddy 2021). Namely, it could contribute to Goal number 15, i.e., *"Life on Land – protect, restore and promote sustainable use of terrestrial ecosystems, sustainably manage forests, combat desertification and halt and reverse land degradation and halt biodiversity loss"*. Also, it could contribute to Goal number 13, i.e., *"Climate Action – exhort humankind to take urgent action to combat climate change and its impacts"*.

References

Adámek, M., Hadincová, V., and Wild, J., 2016. Long-term effect of wildfires on temperate Pinus sylvestris forests: Vegetation dynamics and ecosystem resilience. Forest Ecology and Management, 380, 285–295. DOI: 10.1016/j.foreco.2016.08.051.

Aicardi, I., Garbarino, M., Lingua, A., Lingua, E., Marzano, R., and Piras, M., 2016. Monitoring post-fire forest recovery using multi-temporal Digital Surface Models generated from different platforms. In: I. Gitas and R. Reuter, eds. EARSeL eProceedings 15(1). EARSeL, 1–8. DOI: 10.12760/01-2016-1-01.

Alcaraz-Segura, D., Cabello, J., Paruelo, J.M., and Delibes, M., 2008. Trends in the surface vegetation dynamics of the national parks of Spain as observed by satellite sensors. Applied Vegetation Science, 11 (4), 431–440. DOI: 10.3170/2008-7-18522.

Anderson, K. and Gaston, K.J., 2013. Lightweight unmanned aerial vehicles will revolutionize spatial ecology. Frontiers in Ecology and the Environment, 11 (3), 138–146. DOI: 10.1890/120150.

Anderson, M.C., Allen, R.G., Morse, A., and Kustas, W.P., 2012. Use of Landsat thermal imagery in monitoring evapotranspiration and managing water resources. Remote Sensing of Environment, 122, 50–65. DOI: 10.1016/j.rse.2011.08.025.

Barros, A.M.G. and Pereira, J.M.C., 2014. Wildfire selectivity for land cover type: does size matter? PloS one, 9 (1), e84760. DOI: 10.1371/journal.pone.0084760.

Bartels, S.F., Chen, H.Y.H., Wulder, M.A., and White, J.C., 2016. Trends in post-disturbance recovery rates of Canada's forests following wildfire and harvest. Forest Ecology and Management, 361, 194–207. DOI: 10.1016/j.foreco.2015.11.015.

Benali, A., Russo, A., Sá, A., Pinto, R., Price, O., Koutsias, N., and Pereira, J., 2016. Determining Fire Dates and Locating Ignition Points With Satellite Data. Remote Sensing, 8 (4), 326. DOI: 10.3390/rs8040326.

Boettiger, C., Ross, N., and Hastings, A., 2013. Early warning signals: The charted and uncharted territories. Theoretical Ecology, 6, 255–264. DOI: 10.1007/s12080-013-0192-6.

Bowman, D.M.J.S., Balch, J.K., Artaxo, P., Bond, W.J., Carlson, J.M., Cochrane, M.A., D'Antonio, C.M., DeFries, R.S., Doyle, J.C., Harrison, S.P., Johnston, F.H., Keeley, J.E., Krawchuk, M.A., Kull, C.A., Marston, J.B., Moritz, M.A., Prentice, I.C., Roos, C.I., Scott, A.C., Swetnam, T.W., van der Werf, G.R., and Pyne, S.J., 2009. Fire in the Earth System. Science, 324 (5926), 481–484. DOI: 10.1126/science.1163886.

Briones-Herrera, C.I., Vega-Nieva, D.J., Monjarás-Vega, N.A., Briseño-Reyes, J., López-Serrano, P.M., Corral-Rivas, J.J., Alvarado-Celestino, E., Arellano-Pérez, S., Álvarez-González, J.G., Ruiz-González, A.D., Jolly, W.M., and Parks, S.A., 2020. Near Real-Time Automated Early Mapping of the Perimeter of Large Forest Fires from the Aggregation of VIIRS and MODIS Active Fires in Mexico. Remote Sensing, 12 (12), 2061. DOI: 10.3390/rs12122061.

Cardil, A., Mola-Yudego, B., Blázquez-Casado, Á., and González-Olabarria, J.R., 2019. Fire and burn severity assessment: Calibration of Relative Differenced Normalized Burn Ratio (RdNBR) with field data. Journal of Environmental Management, 235, 342–349.

Carvajal-Ramírez, F., Marques da Silva, J.R., Agüera-Vega, F., Martínez-Carricondo, P., Serrano, J., Moral, F.J., Carvajal-Ramírez, F., Marques da Silva, J.R., Agüera-Vega, F., Martínez-Carricondo, P., Serrano, J., and Moral, F.J., 2019. Evaluation of Fire Severity Indices Based on Pre- and Post-Fire Multispectral Imagery Sensed from UAV. Remote Sensing, 11 (9), 993. DOI: 10.3390/rs11090993.

Carvalho-Santos, C., Honrado, J.P., and Hein, L., 2014. Hydrological services and the role of forests: Conceptualization and indicator-based analysis with an illustration at a regional scale. Ecological Complexity, 20, 69–80. DOI: 10.1016/j.ecocom.2014.09.001.

Catry, F.X.F., Rego, F.C.F.F.C., Bação, F.L., Moreira, 2009. Modeling and mapping wildfire ignition risk in Portugal. International Journal of Wildland Fire, 18 (8), 921. DOI: 10.1071/WF07123.

Chi, M., Plaza, A., Benediktsson, J.A., Sun, Z., Shen, J., and Zhu, Y., 2016. Big Data for Remote Sensing: Challenges and Opportunities. Proceedings of the IEEE, 104 (11), 2207–2219. DOI: 10.1109/JPROC.2016.2598228.

Chuvieco, E., Aguado, I., Salas, J., García, M., Yebra, M., and Oliva, P., 2020. Satellite Remote Sensing Contributions to Wildland Fire Science and Management. Current Forestry Reports, 6 (2), 81–96. DOI: 10.1007/s40725-020-00116-5.

Czuchlewski, K.R. and Weissel, J.K., 2005. Synthetic Aperture Radar (SAR)-based mapping of wildfire burn severity and recovery. In: International Geoscience and Remote Sensing Symposium (IGARSS). 55–58. DOI: 10.1109/IGARSS.2005.1526102.

Donohue, I., Hillebrand, H., Montoya, J.M., Petchey, O.L., Pimm, S.L., Fowler, M.S., Healy, K., Jackson, A.L., Lurgi, M., McClean, D., O'Connor, N.E., O'Gorman, E.J., and Yang,

Q., 2016. Navigating the complexity of ecological stability. Ecology Letters, 19 (9), 1172–1185. DOI: 10.1111/ele.12648.

Donohue, I., Petchey, O.L., Montoya, J.M., Jackson, A.L., McNally, L., Viana, M., Healy, K., Lurgi, M., O'Connor, N.E., and Emmerson, M.C., 2013. On the dimensionality of ecological stability. Ecology Letters, 16 (4), 421–429. DOI: 10.1111/ele.12086.

Ermida, S.L., Soares, P., Mantas, V., Göttsche, F.-M., and Trigo, I.F., 2020. Google Earth Engine Open-Source Code for Land Surface Temperature Estimation from the Landsat Series. Remote Sensing, 12 (9), 1471. DOI: 10.3390/rs12091471.

Escuin, S., Navarro, R., and Fernández, P., 2008. Fire severity assessment by using NBR (Normalized Burn Ratio) and NDVI (Normalized Difference Vegetation Index) derived from LANDSAT TM/ETM images. International Journal of Remote Sensing, 29 (4), 1053–1073. DOI: 10.1080/01431160701281072.

Farley, S.S., Dawson, A., Goring, S.J., and Williams, J.W., 2018. Situating ecology as a big-data science: Current advances, challenges, and solutions. BioScience, 68 (8), 563–576. DOI: 10.1093/biosci/biy068.

Folke, C., Carpenter, S., Walker, B., Scheffer, M., Elmqvist, T., Gunderson, L., and Holling, C.S., 2004. Regime Shifts, Resilience, and Biodiversity in Ecosystem Management. Annual Review of Ecology, Evolution, and Systematics, 35 (1), 557–581. DOI: 10.1146/annurev.ecolsys.35.021103.105711.

Frazier, A.E., Renschler, C.S., and Miles, S.B., 2013. Evaluating post-disaster ecosystem resilience using MODIS GPP data. International Journal of Applied Earth Observation and Geoinformation, 21, 43–52. DOI: 10.1016/j.jag.2012.07.019.

García-Llamas, P., Suárez-Seoane, S., Taboada, A., Fernández-Manso, A., Quintano, C., Fernández-García, V., Fernández-Guisuraga, J.M., Marcos, E., and Calvo, L., 2019. Environmental drivers of fire severity in extreme fire events that affect Mediterranean pine forest ecosystems. Forest Ecology and Management, 433, 24–32. DOI: 10.1016/j.foreco.2018.10.051.

Geller, G.N., Halpin, P.N., Helmuth, B., Hestir, E.L., Skidmore, A., Abrams, M.J., Aguirre, N., Blair, M., Botha, E., Colloff, M., Dawson, T., Franklin, J., Horning, N., James, C., Magnusson, W., Santos, M.J., Schill, S.R., and Williams, K., 2017. Remote Sensing for Biodiversity. In: The GEO Handbook on Biodiversity Observation Networks. Cham: Springer International Publishing, 187–210. DOI: 10.1007/978-3-319-27288-7_8.

Giglio, L., Boschetti, L., Roy, D.P., Humber, M.L., and Justice, C.O., 2018. The Collection 6 MODIS burned area mapping algorithm and product. Remote Sensing of Environment, 217, 72–85. DOI: 10.1016/j.rse.2018.08.005.

Giglio, L., Csiszar, I., Restás, Á., Morisette, J.T., Schroeder, W., Morton, D., and Justice, C.O., 2008. Active fire detection and characterization with the advanced spaceborne thermal emission and reflection radiometer (ASTER). Remote Sensing of Environment, 112 (6), 3055–3063. DOI: 10.1016/j.rse.2008.03.003.

Guanter, L., Kaufmann, H., Segl, K., Foerster, S., Rogass, C., Chabrillat, S., Kuester, T., Hollstein, A., Rossner, G., Chlebek, C., Straif, C., Fischer, S., Schrader, S., Storch, T., Heiden, U., Mueller, A., Bachmann, M., Mühle, H., Müller, R., Habermeyer, M., Ohndorf, A., Hill, J., Buddenbaum, H., Hostert, P., van der Linden, S., Leitão, P., Rabe, A., Doerffer, R., Krasemann, H., Xi, H., Mauser, W., Hank, T., Locherer, M., Rast, M., Staenz, K., and Sang, B., 2015. The EnMAP Spaceborne Imaging Spectroscopy Mission for Earth Observation. Remote Sensing, 7 (7), 8830–8857. DOI: 10.3390/rs70708830.

Hampton, S.E., Strasser, C.A., Tewksbury, J.J., Gram, W.K., Budden, A.E., Batcheller, A.L., Duke, C.S., and Porter, J.H., 2013. Big data and the future of ecology. Frontiers in Ecology and the Environment. DOI: 10.1890/120103.

Holling, C.S., 1973. Resilience and Stability of Ecological Systems. Annual Review of Ecology and Systematics, 4 (1), 1–23. DOI: 10.1146/annurev.es.04.110173.000245.

Holling, C.S., 1996. Engineering Resilience versus Ecological Resilience. In: P.E. Schulze, ed. Engineering within Ecological Constraints. Washington, D.C.: National Academies Press, 31–43. DOI: 10.17226/4919.

Hope, A., Albers, N., and Bart, R., 2012. Characterizing post-fire recovery of fynbos vegetation in the Western Cape Region of South Africa using MODIS data. International Journal of Remote Sensing, 33 (4), 979–999. DOI: 10.1080/01431161.2010.543184.

Hulley, G.C., Ghent, D., Göttsche, F.M., Guillevic, P.C., Mildrexler, D.J., and Coll, C., 2019. Land Surface Temperature. Taking the Temperature of the Earth, 57–127. DOI: 10.1016/B978-0-12-814458-9.00003-4.

Jia, D., Song, C., Cheng, C., Shen, S., Ning, L., and Hui, C., 2020. A Novel Deep Learning-Based Spatiotemporal Fusion Method for Combining Satellite Images with Different Resolutions Using a Two-Stream Convolutional Neural Network. Remote Sensing 2020, Vol. 12, Page 698, 12 (4), 698. DOI: 10.3390/RS12040698.

João, T., João, G., Bruno, M., and João, H., 2018. Indicator-based assessment of post-fire recovery dynamics using satellite NDVI time-series. Ecological Indicators, 89, 199–212. DOI: 10.1016/j.ecolind.2018.02.008.

Johnstone, J.F., Chapin, F.S., Hollingsworth, T.N., Mack, M.C., Romanovsky, V., and Turetsky, M., 2010. Fire, climate change, and forest resilience in interior alaska1. Canadian Journal of Forest Research, 40 (7), 1302–1312. DOI: 10.1139/X10-061.

Keeley, J.E., 2009. Fire intensity, fire severity and burn severity: a brief review and suggested usage. International Journal of Wildland Fire, 18 (1), 116. DOI: 10.1071/WF07049.

De Keersmaecker, W., Lhermitte, S., Tits, L., Honnay, O., Somers, B., and Coppin, P., 2015. A model quantifying global vegetation resistance and resilience to short-term climate anomalies and their relationship with vegetation cover. Global Ecology and Biogeography, 24 (5), 539–548. DOI: 10.1111/geb.12279.

Kesavan, R., Muthian, M., Sudalaimuthu, K., Sundarsingh, S., and Krishnan, S., 2021. ARIMA modeling for forecasting land surface temperature and determination of urban heat island using remote sensing techniques for Chennai city, India. Arabian Journal of Geosciences 2021 14:11, 14 (11), 1–14. DOI: 10.1007/S12517-021-07351-5.

Kwok, R., 2018. Ecology's remote-sensing revolution. Nature, 556 (7699), 137–138. DOI: 10.1038/d41586-018-03924-9.

Lanorte, A., Lasaponara, R., Lovallo, M., and Telesca, L., 2014. Fisher–Shannon information plane analysis of SPOT/VEGETATION Normalized Difference Vegetation Index (NDVI) time series to characterize vegetation recovery after fire disturbance. International Journal of Applied Earth Observation and Geoinformation, 26, 441–446. DOI: 10.1016/J.JAG.2013.05.008.

Lentile, L.B., Holden, Z.A., Smith, A.M.S.S., Falkowski, M.J., Hudak, A.T., Morgan, P., Lewis, S.A., Gessler, P.E., Benson, N.C., Lentile, L.B., Holden, Z.A., Smith, A.M.S.S., Falkowski, M.J., Hudak, A.T., Morgan, P., Lewis, S.A., Gessler, P.E., and Benson, N.C., 2006. Remote sensing techniques to assess active fire characteristics and post-fire effects. International Journal of Wildland Fire, 15 (3), 319. DOI: 10.1071/WF05097.

Leon, J.R.R., van Leeuwen, W.J.D., Casady, G.M., Leon, J.R.R., van Leeuwen, W.J.D., and Casady, G.M., 2012. Using MODIS-NDVI for the Modeling of Post-Wildfire Vegetation Response as a Function of Environmental Conditions and Pre-Fire Restoration Treatments. Remote Sensing, 4 (3), 598–621. DOI: 10.3390/rs4030598.

Leys, B., Higuera, P.E., McLauchlan, K.K., and Dunnette, P. V., 2016. Wildfires and geochemical change in a subalpine forest over the past six millennia. Environmental Research Letters, 11 (12), 125003. DOI: 10.1088/1748-9326/11/12/125003.

Liu, H., Zhan, Q., Yang, C., and Wang, J., 2018. Characterizing the Spatiotemporal Pattern of Land Surface Temperature through Time Series Clustering: Based on the Latent Pattern and Morphology. Remote Sensing, 10 (4), 654. DOI: 10.3390/rs10040654.

Liu, P., 2015. A Survey of Remote-sensing Big Data. Frontiers in Environmental Science, 3. DOI: 10.3389/fenvs.2015.00045.

Lobser, S.E. and Cohen, W.B., 2007. MODIS tasselled cap: land cover characteristics expressed through transformed MODIS data. International Journal of Remote Sensing, 28 (22), 5079–5101. DOI: 10.1080/01431160701253303.

Lovett, G.M., Burns, D.A., Driscoll, C.T., Jenkins, J.C., Mitchell, M.J., Rustad, L., Shanley, J.B., Likens, G.E., and Haeuber, R., 2007. Who needs environmental monitoring? Frontiers in Ecology and the Environment, 5 (5), 253–260. DOI: 10.1890/1540-9295(2007)5[253:WNEM]2.0.CO;2.

Lozano-Parra, J., Schnabel, S., Pulido, M., Gómez-Gutiérrez, Á., and Lavado-Contador, F., 2018. Effects of soil moisture and vegetation cover on biomass growth in water-limited environments. Land Degradation & Development, 29 (12), 4405–4414. DOI: 10.1002/LDR.3193.

Ma, L., Liu, Y., Zhang, X., Ye, Y., Yin, G., and Johnson, B.A., 2019. Deep learning in remote sensing applications: A meta-analysis and review. ISPRS Journal of Photogrammetry and Remote Sensing. DOI: 10.1016/j.isprsjprs.2019.04.015.

Maffei, C., Alfieri, S.M., Menenti, M., 2018. Relating Spatiotemporal Patterns of Forest Fires Burned Area and Duration to Diurnal Land Surface Temperature Anomalies. Remote Sensing, 10 (11), 1777. DOI: 10.3390/rs10111777.

Marcos, B., Pôças, I., Gonçalves, J., and Honrado, J.P., 2012. Multi-sensor assessment of trends in attributes of vegetation dynamics and ecosystem functioning derived from NDVI time series. In: Workshop Proceedings 1st EARSeL Workshop on Temporal Analysis of Satellite Images. Mykonos, Greece, 254–268.

Meng, J.-N., Fang, H., and Scavia, D., 2021. Application of ecosystem stability and regime shift theories in ecosystem assessment-calculation variable and practical performance. Ecological Indicators, 125, 107529. DOI: 10.1016/j.ecolind.2021.107529.

Mildrexler, D.J., Zhao, M., and Running, S.W., 2009. Testing a MODIS Global Disturbance Index across North America. Remote Sensing of Environment, 113 (10), 2103–2117. DOI: 10.1016/j.rse.2009.05.016.

Miller, J.D. and Thode, A.E., 2007. Quantifying burn severity in a heterogeneous landscape with a relative version of the delta Normalized Burn Ratio (dNBR). Remote Sensing of Environment, 109 (1), 66–80.

Neumann, M., Moreno, A., Thurnher, C., Mues, V., Härkönen, S., Mura, M., Bouriaud, O., Lang, M., Cardellini, G., Thivolle-Cazat, A., Bronisz, K., Merganic, J., Alberdi, I., Astrup, R., Mohren, F., Zhao, M., and Hasenauer, H., 2016. Creating a Regional MODIS Satellite-Driven Net Primary Production Dataset for European Forests. Remote Sensing, 8 (7), 554. DOI: 10.3390/rs8070554.

Oliveira, S.L.J., Pereira, J.M.C., Carreiras, 2012. Fire frequency analysis in Portugal (1975 - 2005), using Landsat-based burnt area maps. International Journal of Wildland Fire, 21 (1), 48. DOI: 10.1071/WF10131.

Parks, S.A., Holsinger, L.M., Koontz, M.J., Collins, L., Whitman, E., Parisien, M.-A., Loehman, R.A., Barnes, J.L., Bourdon, J.-F., Boucher, J., Boucher, Y., Caprio, A.C., Collingwood, A., Hall, R.J., Park, J., Saperstein, L.B., Smetanka, C., Smith, R.J., Soverel, N., 2019. Giving Ecological Meaning to Satellite-Derived Fire Severity Metrics across North American Forests. Remote Sensing, 11 (14), 1735. DOI: 10.3390/rs11141735.

Parks, S., Holsinger, L., Voss, M., Loehman, R., and Robinson, N., 2018. Mean Composite Fire Severity Metrics Computed with Google Earth Engine Offer Improved Accuracy and Expanded Mapping Potential. Remote Sensing, 10 (6), 879. DOI: 10.3390/rs10060879.

Parks, S.A., Dillon, G.K., and Miller, C., 2014. A New Metric for Quantifying Burn Severity: The Relativized Burn Ratio. Remote Sensing. Multidisciplinary Digital Publishing Institute. DOI: 10.3390/rs6031827.

Pellegrini, A.F.A., Ahlström, A., Hobbie, S.E., Reich, P.B., Nieradzik, L.P., Staver, A.C., Scharenbroch, B.C., Jumpponen, A., Anderegg, W.R.L., Randerson, J.T., and Jackson, R.B., 2018. Fire frequency drives decadal changes in soil carbon and nitrogen and ecosystem productivity. Nature, 553 (7687), 194–198. DOI: 10.1038/nature24668.

Pelletier, C., Webb, G., Petitjean, F., Pelletier, C., Webb, G.I., and Petitjean, F., 2019. Temporal Convolutional Neural Network for the Classification of Satellite Image Time Series. Remote Sensing, 11 (5), 523. DOI: 10.3390/rs11050523.

Pereira, H.M., Ferrier, S., Walters, M., Geller, G.N., Jongman, R.H.G., Scholes, R.J., Bruford, M.W., Brummitt, N., Butchart, S.H.M., Cardoso, A.C., Coops, N.C., Dulloo, E., Faith, D.P., Freyhof, J., Gregory, R.D., Heip, C., Hoft, R., Hurtt, G., Jetz, W., Karp, D.S., McGeoch, M.A., Obura, D., Onoda, Y., Pettorelli, N., Reyers, B., Sayre, R., Scharlemann, J.P.W., Stuart, S.N., Turak, E., Walpole, M., and Wegmann, M., 2013. Essential Biodiversity Variables. Science, 339 (6117), 277–278. DOI: 10.1126/science.1229931.

Petropoulos, G., Carlson, T.N., Wooster, M.J., and Islam, S., 2009. A review of Ts/VI remote sensing based methods for the retrieval of land surface energy fluxes and soil surface moisture. Progress in Physical Geography, 33 (2), 224–250. DOI: 10.1177/0309133309338997.

Pôças, I., Gonçalves, J., Marcos, B., Alonso, J., Castro, P., and Honrado, J.P., 2014. Evaluating the fitness for use of spatial data sets to promote quality in ecological assessment and monitoring. International Journal of Geographical Information Science, 28 (11). DOI: 10.1080/13658816.2014.924627.

Quintano, C., Fernández-Manso, A., Calvo, L., Marcos, E., and Valbuena, L., 2015. Land surface temperature as potential indicator of burn severity in forest Mediterranean ecosystems. International Journal of Applied Earth Observation and Geoinformation, 36, 1–12. DOI: 10.1016/j.jag.2014.10.015.

Ramanathan, V. and Carmichael, G., 2008. Global and regional climate changes due to black carbon. Nature Geoscience, 1 (4), 221–227. DOI: 10.1038/ngeo156.

Reddy, C.S., 2021. Remote sensing of biodiversity: what to measure and monitor from space to species? Biodiversity and Conservation, 1–15. DOI: 10.1007/s10531-021-02216-5.

Rocchini, D., Petras, V., Petrasova, A., Horning, N., Furtkevicova, L., Neteler, M., Leutner, B., and Wegmann, M., 2017. Open data and open source for remote sensing training in ecology. Ecological Informatics, 40, 57–61. DOI: 10.1016/j.ecoinf.2017.05.004.

Ryu, J.-H., Han, K.-S., Hong, S., Park, N.-W., Lee, Y.-W., and Cho, J., 2018. Satellite-Based Evaluation of the Post-Fire Recovery Process from the Worst Forest Fire Case in South Korea, 10 (6), 918.

San-Miguel-Ayanz, J., Durrant, T., Boca, R., Libertà, G., Branco, A., de Rigo, D., Ferrari, D., Maianti, P., Vivancos, T.A., Schulte, E., and Loffler, P., 2017. Forest Fires in Europe, Middle East and North Africa 2016. Luxembourg. DOI: 10.2760/66820.

San-Miguel-Ayanz, J., Moreno, J.M., and Camia, A., 2013. Analysis of large fires in European Mediterranean landscapes: Lessons learned and perspectives. Forest Ecology and Management, 294, 11–22. DOI: 10.1016/j.foreco.2012.10.050.

De Santis, A. and Chuvieco, E., 2009. GeoCBI: A modified version of the Composite Burn Index for the initial assessment of the short-term burn severity from remotely sensed data. Remote Sensing of Environment, 113 (3), 554–562. DOI: 10.1016/j.rse.2008.10.011.

Scheffer, M., Carpenter, S.R., Dakos, V., and van Nes, E.H., 2015. Generic Indicators of Ecological Resilience: Inferring the Chance of a Critical Transition. Annual Review of Ecology, Evolution, and Systematics, 46 (1), 145–167. DOI: 10.1146/annurev-ecolsys-112414-054242.

Schroeder, W., Oliva, P., Giglio, L., and Csiszar, I.A., 2014. The New VIIRS 375m active fire detection data product: Algorithm description and initial assessment. Remote Sensing of Environment, 143, 85–96. DOI: 10.1016/j.rse.2013.12.008.

Schroeder, W., Oliva, P., Giglio, L., Quayle, B., Lorenz, E., and Morelli, F., 2016. Active fire detection using Landsat-8/OLI data. Remote Sensing of Environment, 185, 210–220. DOI: 10.1016/j.rse.2015.08.032.

Semmens, K.A., Anderson, M.C., Kustas, W.P., Gao, F., Alfieri, J.G., McKee, L., Prueger, J.H., Hain, C.R., Cammalleri, C., Yang, Y., Xia, T., Sanchez, L., Mar Alsina, M., and Vélez, M., 2016. Monitoring daily evapotranspiration over two California vineyards using Landsat 8 in a multi-sensor data fusion approach. Remote Sensing of Environment, 185, 155–170. DOI: 10.1016/j.rse.2015.10.025.

Senf, C. and Seidl, R., 2020. Mapping the forest disturbance regimes of Europe. Nature Sustainability, 4 (1). DOI: 10.1038/s41893-020-00609-y.

Seydi, S.T., Akhoondzadeh, M., Amani, M., and Mahdavi, S., 2021. Wildfire damage assessment over australia using sentinel-2 imagery and modis land cover product within the google earth engine cloud platform. Remote Sensing, 13 (2), 1–30. DOI: 10.3390/rs13020220.

Shi, T. and Xu, H., 2019. Derivation of Tasseled Cap Transformation Coefficients for Sentinel-2 MSI At-Sensor Reflectance Data. IEEE Journal of Selected Topics in

Applied Earth Observations and Remote Sensing, 12 (10), 4038–4048. DOI: 10.1109/JSTARS.2019.2938388.

Skidmore, A.K., Coops, N.C., Neinavaz, E., Ali, A., Schaepman, M.E., Paganini, M., Kissling, W.D., Vihervaara, P., Darvishzadeh, R., Feilhauer, H., Fernandez, M., Fernández, N., Gorelick, N., Geizendorffer, I., Heiden, U., Heurich, M., Hobern, D., Holzwarth, S., Muller-Karger, F.E., Van De Kerchove, R., Lausch, A., Leitãu, P.J., Lock, M.C., Mücher, C.A., O'Connor, B., Rocchini, D., Turner, W., Vis, J.K., Wang, T., Wegmann, M., and Wingate, V., 2021. Priority list of biodiversity metrics to observe from space. Nature Ecology & Evolution, 1–11. DOI: 10.1038/s41559-021-01451-x.

Smith, A.M.S.S., Kolden, C.A., Tinkham, W.T., Talhelm, A.F., Marshall, J.D., Hudak, A.T., Boschetti, L., Falkowski, M.J., Greenberg, J.A., Anderson, J.W., Kliskey, A., Alessa, L., Keefe, R.F., and Gosz, J.R., 2014. Remote sensing the vulnerability of vegetation in natural terrestrial ecosystems. Remote Sensing of Environment, 154, 322–337. DOI: 10.1016/j.rse.2014.03.038.

Söderberg, J., 2015. Hacking Capitalism. 1st ed. New Yoork: Routledge. DOI: 10.4324/9780203937853.

Swetnam, T.L., Yool, S.R., Roy, S., and Falk, D.A., 2021. On the Use of Standardized Multi-Temporal Indices for Monitoring Disturbance and Ecosystem Moisture Stress across Multiple Earth Observation Systems in the Google Earth Engine. Remote Sensing, 13 (8), 1448. DOI: 10.3390/rs13081448.

Szpakowski, D.M. and Jensen, J.L.R., 2019. A Review of the Applications of Remote Sensing in Fire Ecology. Remote Sensing, 11 (22), 2638. DOI: 10.3390/rs11222638.

Tedim, F., Remelgado, R., Borges, C., Carvalho, S., and Martins, J., 2013. Exploring the occurrence of mega-fires in Portugal. Forest Ecology and Management, 294, 86–96. DOI: 10.1016/j.foreco.2012.07.031.

Ueyama, M., Ichii, K., Iwata, H., Euskirchen, E.S., Zona, D., Rocha, A. V., Harazono, Y., Iwama, C., Nakai, T., and Oechel, W.C., 2014. Change in surface energy balance in Alaska due to fire and spring warming, based on upscaling eddy covariance measurements. Journal of Geophysical Research: Biogeosciences, 119 (10), 1947–1969. DOI: 10.1002/2014JG002717.

Umar, M.M. and De Silva, L.C., 2018. Onset fire detection in video sequences using region based structure from motion for nonrigid bodies algorithm. In: IET Conference Publications. Institution of Engineering and Technology. DOI: 10.1049/cp.2018.1533.

Vangi, E., D'Amico, G., Francini, S., Giannetti, F., Lasserre, B., Marchetti, M., and Chirici, G., 2021. The New Hyperspectral Satellite PRISMA: Imagery for Forest Types Discrimination. Sensors, 21 (4), 1182. DOI: 10.3390/s21041182.

Veraverbeke, S., Verstraeten, W.W., Lhermitte, S., Van De Kerchove, R., and Goossens, R., 2012. Assessment of post-fire changes in land surface temperature and surface albedo, and their relation with fire - burn severity using multitemporal MODIS imagery. International Journal of Wildland Fire, 21 (3), 243. DOI: 10.1071/WF10075.

Viana-Soto, A., Aguado, I., Salas, J., and García, M., 2020. Identifying post-fire recovery trajectories and driving factors using landsat time series in fire-prone mediterranean pine forests. Remote Sensing, 12 (9), 1499. DOI: 10.3390/RS12091499.

Vicente-Saez, R. and Martinez-Fuentes, C., 2018. Open Science now: A systematic literature review for an integrated definition. Journal of Business Research, 88, 428–436. DOI: 10.1016/J.JBUSRES.2017.12.043.

Vicente, J.R., Fernandes, R.F., Randin, C.F., Broennimann, O., Gonçalves, J., Marcos, B., Pôças, I., Alves, P., Guisan, A., and Honrado, J.P., 2013. Will climate change drive alien invasive plants into areas of high protection value? An improved model-based regional assessment to prioritise the management of invasions. Journal of Environmental Management, 131, 185–195. DOI: 10.1016/j.jenvman.2013.09.032.

Wei, X., Hayes, D.J., Fraver, S., and Chen, G., 2018. Global Pyrogenic Carbon Production During Recent Decades Has Created the Potential for a Large, Long-Term Sink of Atmospheric CO2. Journal of Geophysical Research: Biogeosciences, 123 (12), 3682–3696. DOI: 10.1029/2018JG004490.

Woelfle, M., Olliaro, P., and Todd, M.H., 2011. Open science is a research accelerator. Nature Chemistry 2011 3:10, 3 (10), 745–748. DOI: 10.1038/nchem.1149.

Xiang, T., Vivoni, E.R., and Gochis, D.J., 2014. Seasonal evolution of ecohydrological controls on land surface temperature over complex terrain. Water Resources Research, 50 (5), 3852–3874. DOI: 10.1002/2013WR014787.

Xin, Q., Olofsson, P., Zhu, Z., Tan, B., and Woodcock, C.E., 2013. Toward near real-time monitoring of forest disturbance by fusion of MODIS and Landsat data. Remote Sensing of Environment, 135 (null), 234–247. DOI: 10.1016/j.rse.2013.04.002.

Xu, G. and Zhong, X., 2017. Real-time wildfire detection and tracking in Australia using geostationary satellite: Himawari-8. Remote Sensing Letters, 8 (11), 1052–1061. DOI: 10.1080/2150704X.2017.1350303.

Xu, W., Wooster, M.J., He, J., and Zhang, T., 2020. First study of Sentinel-3 SLSTR active fire detection and FRP retrieval: Night-time algorithm enhancements and global intercomparison to MODIS and VIIRS AF products. Remote Sensing of Environment, 248, 111947. DOI: 10.1016/J.RSE.2020.111947.

Yu, Y., Notaro, M., Wang, F., Mao, J., Shi, X., and Wei, Y., 2017. Observed positive vegetation-rainfall feedbacks in the Sahel dominated by a moisture recycling mechanism. Nature Communications 2017 8:1, 8 (1), 1–9. DOI: 10.1038/s41467-017-02021-1.

Zhao, Y., Wang, X., Novillo, C.J., Arrogante-Funes, P., Vázquez-Jiménez, R., and Maestre, F.T., 2018. Albedo estimated from remote sensing correlates with ecosystem multifunctionality in global drylands. Journal of Arid Environments, 157, 116–123. DOI: 10.1016/j.jaridenv.2018.05.010.

Zhu, X., Helmer, E.H., Gao, F., Liu, D., Chen, J., and Lefsky, M.A., 2016. A flexible spatiotemporal method for fusing satellite images with different resolutions. Remote Sensing of Environment, 172, 165–177. DOI: 10.1016/j.rse.2015.11.016.

Appendix

About the Author

Biosketch

Bruno Marcos was born in Matosinhos, Portugal, on the 27th of January, 1984. He received a B.Sc. degree in *Environmental Science and Technology* from the *Faculty of Sciences, University of Porto* (FCUP), Portugal in 2007, with a final scientific internship report entitled *"Remote Sensing applications to ecological and biogeographical studies"*. Next, he received an M.Sc. degree in *Environmental Science and Technology – Specialization in Ecology and Natural Resources Management* – from the same institution in 2008, with a dissertation entitled: *"Spatiotemporal analysis of primary production in Northern Portugal from the MODIS GPP product"*.

Since then, Bruno has worked in different projects within the *Research Center in Biodiversity and Genetic Resources – Research Network in Biodiversity and Evolutionary Biology, Associate Laboratory* (CIBIO-InBIO), and FCUP, always related to geospatial (including remote sensing) data management and its use for environmental analysis. In this regard, the topic of wildfires was addressed in several of those projects. During this time, he collaborated with several researchers and technicians, participating in numerous scientific and technical-scientific publications, ranging from peer-reviewed articles in international journals, to oral and poster communications, a book chapter, and project reports. He presented his work in international forums such as the 1st and 2nd Workshops on *Temporal Analysis of Satellite Images* – organized by the *European Association of Remote Sensing Laboratories* (EARSeL) – in 2012 in Greece, and 2015 in Sweden, respectively, and a *Land Training Course* – organized by the *European Space Agency* (ESA) – in 2015 in Romania.

In October 2015, Bruno started working on his Ph.D. within the *Doctoral Program in Biodiversity, Genetics, and Evolution* in CIBIO-InBIO and FCUP, under the topic of remotely-sensed monitoring of the effects of wildfire disturbances on ecosystem functioning, which he is presenting in this thesis. As an environmental scientist, he is interested in

environmental monitoring, particularly ecological disturbances, as well as in ecological theory, namely within the fields of disturbance and fire ecology, ecosystem functioning, and ecological resilience. On the other hand, he is also interested in more technical and technological aspects of Environmental Science, such as Earth Observation, GIS, and remote sensing. Additionally, he also likes to incorporate elements of Computer Science in his research, such as Data Science and Big Data methods and techniques, as well as Free and Open Source Software and data, and Open and Reproducible Science principles.

Selected works

- **Marcos B**, Gonçalves J, Alcaraz-Segura D, Cunha M, and Honrado JP (2021). *"A Framework for Multi-Dimensional Assessment of Wildfire Disturbance Severity from Remotely Sensed Ecosystem Functioning Attributes"*. Remote Sensing, Special Issue "Advances in Remote Sensing of Post-fire Environmental Damage and Recovery Dynamics", 13(4): 780. URL: https://doi.org/10.3390/rs13040780;
- **Marcos B**, Gonçalves J, Alcaraz-Segura D, Cunha M, and Honrado JP (2019). *"Improving the detection of wildfire disturbances in space and time based on indicators extracted from MODIS data: a case study in northern Portugal"*. International Journal of Applied Earth Observation and Geoinformation, 78; 77–85. URL: https://doi.org/10.1016/j.jag.2018.12.003;
- João T, João G, **Bruno M**, and João PH (2018). *"Indicator-based assessment of post-fire recovery dynamics using satellite NDVI time-series"*. Ecological Indicators, 89: 199–212. URL: https://doi.org/10.1016/j.ecolind.2018.02.008 (Note that the author names were wrongly published and should instead have been published as follows: Torres J, Gonçalves J, **Marcos B**, and Honrado JP.);
- Carvalho-Santos C, **Marcos B**, Nunes JP, Regos A, Palazzi E, Terzago S, Monteiro AT, and Honrado JP (2019). *"Hydrological impacts of large fires and future climate: modelling approach supported by satellite data"*. Remote Sensing, Special Issue "Remote Sensing in Ecosystem Modelling", 11(23): 2832. URL: https://doi.org/10.3390/rs11232832;
- **Marcos B**, Gonçalves J, Monteiro A, Alcaraz-Segura D, Cunha M, and Honrado JP (2015). *"Comparison of indicators of wildfire impacts on ecosystem functional attributes derived from MODIS"*. ESA Land Training Course, Bucharest, Romania, September 14–18. URL: https://www.researchgate.net/publication/283486285_Comparison_of_indicators_of_wildfire_impacts_on_ecosystem_functional_attributes_derived_from_MODIS;

- **Marcos B**, Gonçalves J, Monteiro A, Alcaraz-Segura D, Cunha M, and Honrado JP (2015). *"Remote sensing indicators of changes in ecosystem functioning related to wildfire disturbances"*. 2nd EARSeL Workshop on Temporal Analysis of Satellite Images. Stockholm, Sweden, June 17–19. URL: https://www.researchgate.net/publication/279848212_Remote_sensing_indicators_of_changes_in_ecosystem_functioning_related_to_wildfire_disturbances;
- Carvalho-Santos C, **Marcos B**, Marques JE, and Honrado JP. *"Evaluation of hydrological ecosystem services through remote sensing"*. in: Alcaraz-Segura D, Di Bella CM, and Straschnoy JV (Eds.). *"Earth Observation of Ecosystem Services"*. CRC Press, 464 pp., ISBN: 978146650588. URL: https://www.researchgate.net/publication/257940752_Evaluation_of_Hydrological_Ecosystem_Services_through_Remote_Sensing;
- **Marcos B**, Pôças I, Gonçalves J, and Honrado JP (2012). *"Multi-sensor assessment of trends in attributes of vegetation dynamics and ecosystem functioning derived from NDVI time series"*. 1st EARSeL Workshop on Temporal Analysis of Satellite Images. Mykonos, Greece, May 23–25, URL: https://doi.org/10.13140/2.1.2157.1524.